Convergent patterns suggest parallel processes of insular anuran diversification between oceanic archipelagos of the Southwest Pacific and the sky islands of the continental Western Ghats

By

Robin Kurian Abraham
M.Sc., National Centre for Biological Sciences, 2008
B.Sc., Mahatma Gandhi University, 2006

Submitted to the graduate degree program in Ecology & Evolutionary Biology and the Graduate Faculty of the University of Kansas in partial fulfillment of the requirements for the degree of Doctor of Philosophy.

Chair: Rafe M. Brown

W. Leo Smith

Jorge L. Soberón

Mark Mort

Jennifer A. Roberts

Date Defended: 19 November 2020

The dissertation committee for Robin Kurian Abraham
certifies that this is the approved version of the following dissertation:

Convergent patterns suggest parallel processes of insular anuran diversification between oceanic archipelagos of the Southwest Pacific and the sky islands of the continental Western Ghats

Chair: Rafe M. Brown

Date Approved: 19 November 2020

Abstract

The unprecedented surge in frog species descriptions over the last two decades has been attributed to increasing access to remote regions, more advanced technology and techniques, and greater interest in these groups. The advent of genetic methods had been welcomed by practitioners as a boon in identifying species and their relationships. Suggestions were made that significant diversity was yet unrecognized and that the genetic tools would help uncover "cryptic" species that are not obvious. This notion, however, is contentious, and has been debated. As part of my dissertation thesis, I re-evaluate groups of frogs from two highly biodiverse tropical regions in the Western Ghats of India and the Philippines Archipelago of the Western Pacific. In my first chapter, I revisit a clade of *Nyctibatrachus* Nightfrogs in the Southern Western Ghats with an integrative approach utilizing morphologic, molecular, bioacoustic, developmental and life history data and reveal that species diversity may likely be inflated in that group (the *Nyctibatrachus aliciae* group). In my second chapter, I similarly reevaluate a clade of Philippine *Limnonectes* Fanged Frogs and find evidence to reconfigure species boundaries in the *Limnonectes magnus* clade. The third chapter addressed the same *Limnonectes* clade, but with genomic data using the newly developed FrogCap protocol, and finds geneflow between some groups identified in the previous chapter, but not so in other groups, reinforcing some species boundaries while questioning others. My fourth chapter evaluates a species complex of Philippine endemic *Pulchrana* Spotted Frogs in the eastern islands of the archipelago with genomic data. The results show that *Pulchrana grandocula* and *P. similis* cluster together as a group with the remaining Philippine species of *Pulchrana* forming another. I also find that two formerly recognized rare species represented by singleton specimens

have highly admixed genotypes calling into question whether these are indeed unique taxa. My final chapter explores a higher-level genomic dataset of frogs of the superfamily Ranoidea with the inclusion of the three paleoendemic Indian ranoid families of Nyctibatrachidae, Micrixalidae and Ranixalidae. My results show for the first time that these three families form a single clade representing an Indian subcontinent-wide ancient in-situ radiation. Additionally, preliminary biogeography results based on this dataset support of a "ferry India" model that suggests that several non-African crown groups of ranoids may have evolved on an insular India during its transit from Gondwana to become Eurasia.

Acknowledgements

To the world; I am most grateful to simply exist and for being able to have water to drink, food to eat, shelter to rest, and great friends and family for companionship. I start with Dr. Anil Zachariah, my good friend and well-wisher, without whose unfading support, I would be less inspired. His constant provision of emotional, intellectual and logistic support throughout the duration of my doctoral degree is far more than laudable.

In helping me accomplish this thesis, I am obliged to, and would like to express my sincere gratitude to my advisor, Dr. Rafe Brown, who provided his support, patience and knowledge from my day one in Kansas till now, and most importantly, for inviting me to join the lab and department at the University of Kansas, which has among the most wonderful set of people I have been fortunate to meet and become acquainted with. My appreciation extends to the emeriti professors Dr. Bill Duellman and Dr. Linda Trueb, who encouraged me during their time here.

The support from Ramprasad Rao, whose patient and diligent support in the field is by no means trivial, and one that I am greatly thankful for. And to Jobin Mathew who has supported me with considerable hospitality and logistics. Many thanks to Dr. Arun Zachariah who helped make the labwork in India possible, and Mr. Sam Santhosh, who helped me greatly during times of distress.

I am most indebted to my colleagues (who are also great friends) Carl Hutter, Chan Kin Onn, Jeffrey Weinell, Pietro de Mello, Walter Tapondjou, Perry L. Wood Jr., Kaitlyn Allen

Tapondjou, Mark Herr, Yong-Chao Su and Kerry Cobb all of who have provided methodological guidance and shared considerable time explaining tools and techniques at various stages of my time here. Most of my learning here has been from my colleagues in the department. I also acknowledge help in the lab by Rayanna Otterholt, Viktoria Sterkhova and Tatiana Doroskin.

This project was supported by several sources of funding by the National Geographic (EC-58048R-19), IdeaWild, the KU Panorama grants (courtesy of the University of Kansas Biodiversity Institute and the Department of Ecology and Evolutionary Biology, thanks to Leonard Kristalka and Chis Haufler), and the KU Research Excellence Initiative. I would also like to extend my thanks to the Kerala Forests & Wildlife Department for having sanctioned permits in the past to access protected areas and collect range restricted taxa in the Western Ghats for my research. Similarly, I am most grateful to Jason Fernandez, Renato Fernandez and David Montallana. for support in the field in the Philippines. Last, but not least, I wish to acknowledge my parents for their love and support, especially during my long jaunts in India on account of fieldwork.

Contents

Introduction

At the onset of our earliest stages of evolutionary thinking (Darwin, 1859; Wallace, 1881; Carlquist, 1974), islands archipelagos have been widely recognized as vital landscape systems, crucial to the accrual of evidence needed for demonstrating processes of speciation (Mayr, 1949; Simpson, 1949, 1951; Losos & Ricklefs, 2009; Brown 2009, 2016; Whittaker et al., 2017). Many independent, unrelated lineages have diversified as spectacular evolutionary radiations entirely within island systems, providing key insights for understanding processes of diversification (e.g., adaptive radiation; Goldschmidt, 1996; Petren et al., 2005) and evolutionary responses of organisms to shared geological, geographical, and/or climatic histories (Schluter 2000; Brown et al., 2013). Although islands are conceptually understood be isolated blocks or fragments of land in water bodies ranging from lakes to oceans, isolated and far-removed mountain peaks and terrestrial outcrops on lands have been recently recognized as sharing properties with marine islands (Huges & Eastwood, 2006; Martinelli, 2007). Such terrestrial islands isolated by elevational gradients, known as "sky islands," (Fave et al., 2015; McLaughlin, 1995; Warshall, 1994) have more been noted for their ecological and evolutionary significance by many recent biological studies (McCormack et al., 2009; Robin & Nandini, 2010; Robin et al., 2010).

In this work, my colleagues and I investigate two disparate insular systems, one terrestrial and the other marine (Kitayama, 1996), to explore evolutionary and speciation processes using different radiations of frogs as models. Patterns of species diversity in an oceanic/marine archipelago, versus a continental series of isolate, "insular" mountains, can be compared in parallel, to relate patterns and, ultimately, test hypotheses related to mechanisms of species diversification.

One system is the endemic Nightfrog radiation (genus *Nyctibatrachus*) in the Western Ghats mountain range of peninsular India. The other involves two groups of frogs; Fanged frogs (genus *Limnonectes*) and Spotted frogs (genus *Pulchrana*) of the Philippine archipelago straddling the Pacific Ocean. Both these systems have been well recognized as natural laboratories that maintain among the highest levels of biodiversity (Brown & Guttman, 2002; Emerson et al., 2000; Evans et al., 2003; Garg et al., 2017; Setiadi et al., 2011; Van Boxlaer et al., 2012), and have complex geodynamic histories (Campanile, 2007; Hall, 2002; Santhosh, 2020; Yumul et al., 2009). The geologic and climatic settings of both these regions are elaborated in the following sections.

The Western Ghats: a geomorphological and climatic background

The Western Ghats is today recognized as one of the most important Biodiversity Hotspots, a status that heralds it as a significant reservoir of unique organisms in irreplaceable habitats (Mittermeier et al., 1999; Myers et al., 2000). Detailed explorations and inventorying continue to produce numerous surprising biological discoveries. Foremost among these are the amphibians, of which anuran families yield among the highest number of novelties in recent times (Dinesh et al., 2019). To better understand drivers of this diversity, a preliminary knowledge of the geologic and climatic background of these mountains is useful.

Landscape and Geology

The Western Ghats is often described as a narrow mountain chain that straddles the western coastal plains of peninsular India. Technically though, the Ghats are the passive western margin of a massive elevated peneplain (generally labeled as the Deccan Plateau), occurring as a precipitous edge and spanning almost the entirety of the Indian Peninsula. The southernmost

parts of this geomorphological feature are clusters of hilly massifs that jut out over the southwestern margin of the peninsula. The Western Ghats can be geologically separated into three broad regions: the southern granulite Proterozoic mobile belts (2.5–2.6 Ga*) of Kerala and Tamil Nadu; the Archeaen granite-greenstone Dharwar craton (2.9–3.4 Ga) of Goa and Karnataka; and the Cretaceous/Paleocene Deccan volcanic province (~66 Ma*) of Maharashtra and Gujarat (Campanile, 2007; Richards et al., 2016). Its lengthwise extent is almost 1500km, stretching from the state of Gujarat in the north to Tamil Nadu in the south (21°16'24"—08°19'08"N to 72°56'24"—78°19'40"E), interrupted thrice, by the smaller two Goa and Shencottah Gaps, and the more pronounced Palghat Gap. The Ghats have a minimum width of 48 km and maximum width of 210 km; they cover a total area of 136,800 km^2 (CEPF, 2007) (see Fig. 1).

The geology of this prominent landscape feature of peninsular India is testimony to long and complex orogenic processes from Precambrian times, with the current structure and configuration of these mountains forming as a result of the rifting apart from Madagascar, followed by events during the Deccan volcanism (Drury et al., 1984; Gunnell & Fleitout, 1998; Torsvik et al., 2000; Gupta et al., 2003; Rajesh & Santosh; 2004; Rao et al., 2020; Campanile, 2007; Clark et al., 2020; Collins et al., 2007a; Collins et al., 2007b; Santosh, 2020). This history has given the northern parts of the Ghats a relatively uniform relief and for the central and southern parts a much more heterogenetic profile (Nair, 1991). The northern parts - known as the Sahyadris - are a relatively younger layer of the range, resulting from the Deccan volcanic events ~66 million years ago. The Sahyadris comprise mainly of young igneous basalts and are relatively uniform throughout in elevation range. This formation ends abruptly at the Goa Gap, from where it is replaced with far older Archaean and Proterozoic metamorphic granites,

gneisses and schists. The altitudinal range is also relatively uniform, apart from the Kodachadri, Kudremukh and Bababudangiri Hills (which comprise greenstone belts), where the mountains climb above 1500m above sea level (ASL). These central parts of the range are infused with several other rock formations as well. Further south, the range enters a plateaued region in the Kodagu (Coorg) and Wayanad regions, where these plateaux are fortified on the west by monadnocks such as the Talacauveri Brahmagiri, Bhagmandala, Nishanimotte, Thadiyandamol and Brahmagiri Hills, and the higher Banasura, Kurichiyarmala and the Camel's Hump Hills, which tower up at around and just over 2000m ASL. After a brief disruption southward by the Gudalur/Sigur Plateau, the mountains tower again at the Nilgiris, a high massif with an area of 2480Km^2 and an average elevation of ~2000m ASL. The Nilgiris descends to the coastal plains of the west via a steep escarpment into the Nilambur Embayment. The summit of the Nilgiris can be divided into a western Upper Nilgiris and an eastern Lower Nilgiris. Immediately south of the Nilgiris, across the Attappady Valley, is the more isolated, curved ridge of the Siruvani (Palakkad) Hills, which mark the northern boundary of the 30km Palghat Gap. The Palghat Gap is a low mountain pass with an average elevation of 145m ASL.

South of the Palghat Gap, the hilly profile resumes again with the Nelliyampathy Hills and the Anamalais. The Anamalais extend southward into the higher Eravikulam plateau and the Devikulam Plateau (together known as the High Ranges), which are high massifs that drain westward through the Chalakudy, Idamalayar and Pooyamkutty valleys. The High Ranges are drained eastward by the Amaravati River in the Marayur Valley, which roughly disrupts the Anamalai-High Range complex from the eastern Palnis, an equally high massif. To the south of the Devikulam Plateau, lies the Cardamom Hills, a broad expanse of hilly terrain at an average of 700m ASL, further extending south into the slightly higher Pandalam Hills which mark the

headwater drainage of the Periyar, Vaigai and Pamba rivers. This entire region is bordered by a higher hill range to the east, which rises up to almost 1900m ASL in places. East of the Cardamom-Pandalam Hills junction is the High Wavy Hills (otherwise known as the Varushanad Hills), which descend into the Andipatti Hills in the Tamil Nadu plains. The Achankovil and Ariyankavu valleys to the south of the Pandalam Hills mark another gap in the Western Ghats, namely the Shencottah Gap. This gap corresponds with the Achankovil Shear Zone, a major geological boundary. The rock in the section between the Palghat Gap and the Shencottah Gap is dominantly represented by metamorphic Proterozoic *Charnokite*. The Agasthyamalai Hill Range south of the Shencottah Gap, is the southernmost hill cluster of the Western Ghats and is predominately of the *Khondalite* rock type.

Thus, it is inferred that the Western Ghats is a relatively stable geomorphological feature that has remained in relative stasis since the northward drift of the Indian plate. This is the physical setting in which the amphibian communities of the Western Ghats have developed through various processes, and where this study was carried out, with our focus largely being restricted to the members of Nyctibatrachidae in the region broadly south of the Goa Gap.

Paleoclimate and Historical Phytogeography

A brief overview of Cenozoic climate is necessary to attempt reconstruction of historic phytogeographic patterns (Maury-Lechon & Curtet, 1998) in the Western Ghats, and Peninsular India in general, which in turn would help in reconstructing the evolutionary dynamics leading to the contemporary amphibian diversity here. Thus, in the following account, we review global and regional literature and attempt to recreate the phytogeographic trends in the Western Ghats region during a period of glacial maxima (typified here by the LGM at ~19 Ka) and compare it to the current interglacial. Though several attempts have been made in India to also correlate soil

properties with local forest formations, it is now known that the phytogeographic and botanical subdivisions are primarily bioclimatic (Blasco et al., 1996, 2020).

Globally, while the Cenozoic era was largely a cooler and drier period than the previous Mesozoic, it was punctuated in the Paleogene by very warm intervals like the Paleocene–Eocene Thermal Maximum (PETM; 55.8 Ma), the Early Eocene Climatic Optimum (EECO; 53.5 Ma) and Late Oligocene warming (27–26 Ma) (Zachos et al., 2001). However, the Neogene was dominated by a predominantly wet climate especially during the Miocene Climatic Optimum (17–15 Ma) and the Mid-Pliocene warm period (3.3–3.0 Ma) (Axelrod, 1979). This wet Neogene period subsequently shifted to the unusually dry and cool Quaternary, as a result of a combination of factors such as the cessation of the circum-equatorial ocean current, the ongoing circum-Antarctic current (otherwise known as the West Wind Drift, which had initiated during the Oligocene), changes in the Earth's orbit (Milankovitch cycles), snow–temperature feedback from albedo effects and reduced volcanic activity (Budyko, 1969; Bush & Philander, 1999; Lawver & Gahagan, 2003; Smith & Pickering, 2003). Beginning with this global cooling in the late Pliocene Epoch (Zachos et al., 2001), and following into the Pleistocene Epoch, the Earth witnessed at least 22 episodic cycles of glacial-interglacials, of which the Last Glacial Maximum (LGM) peaked at 22 Ka and ended by 19 Ka* (Yokoyama et al., 2000). The glacial-interglacial cycles of the Quaternary resulted in the greatest decline in global temperatures of the Cenozoic and also had a significant influence on global sea levels (Miller et al., 2020). But since ~12.5 Ka, a warmer and wetter climate regime was maintained, especially during the Holocene Climatic Optimum (~9–6 Ka) (Morrill et al., 2003), albeit punctuated by a brief but relatively dryer period between ~5–3 Ka (Naidu and Malmgren, 1996; Staubwasser et al., 2003).

The Cenozoic climatic trends of peninsular India largely reflected global patterns of the time. Fossil pollen from one of the warm intervals of the Late Paleocene–Early Eocene in lignite and coal deposits in northwestern and northeastern India signifies the widespread presence of equatorial rain forests in the Indian subcontinent (Prasad et al., 2009; Shukla & Mehrotra, 2013) at the time. These same lignite deposits have also yielded fossils of amphibians such as tropical Bombinatorids, Ranids and the suspected Rhacophorid *Indorana prasadi* (Folie et al. 2012). Thus, potentially diverse assemblages of tropical amphibians too were once widespread across the subcontinent during the warmer and humid climatic regimes of the Tertiary (Paleogene + Neogene). However, the development of the Himalayan-Tibetan orogen led to the initiation of a monsoonal system and the transition from an equatorial climatic regime to a seasonal type (Bonnefille et al., 1999; Aravind et al. 2013). Additionally, following the advancement of the orogen in the Oligocene, northern India underwent gradual aridification with the expansion of deserts, grasslands and scrublands, as a result of a combination of increasing glaciation in the northern latitudes and the Himalayan-Tibetan plateau and intermediate suppression of the monsoon (Quade et al., 1995; Behrensmeyer, 2007; Molnar & Rajagopalan, 2012; Zhang et al., 2015). The grassland expansion, in particular, was brought on by a decline in atmospheric CO_2, which continued into the late Miocene, whereby the drastic climate change created a fire climate capable of replacing woodlands with C4 grasslands (Keeley & Rundel, 2005). Paleovegetation studies and fungal spores collected from southern India confirm the presence of a tropical-subtropical warm humid climate with high precipitation at the same time during the Miocene, which supported a rich floral community in southern parts of peninsular India (Kumar, 1990; Mandaokar & Mukherjee, 2012; Kern et al., 2013; Rao & Verma, 2014).

The Quaternary climate in India, like most other tropical regions at the time, was greatly influenced by repeated glacial and interglacial cycles, and had a significant effect on the vegetation dynamics of the region. The cyclical waxing and waning of glaciers and ice-sheets during the late Pliocene and Pleistocene controlled a corresponding expansion and contraction of humid forests in the landmass, up until the end of the LGM. Congruently, during episodes of glacial maxima, global sea-level falls also lowered coastlines, exposing a considerable portion of the coastal shelf, in particular the western margin of the subcontinent (Field et al., 2007). It is now known that much of the vegetation in peninsular India during the glacial maxima was dominated by C4 plants, mostly as dry grasslands and savannahs, which correspond to increasing aridity (Sukumar et al., 1993; Adams & Faure, 1997; Bera & Farooqui, 2000; Chabangborn et al., 2014). However, such widespread arid conditions would have extended even much later, since the summer monsoon was much weaker than present up until ~11 Ka, notably due to brief stadials (little ice ages) including the Older and Younger Dryas (Williams, 1975; Hashimi & Nair, 1986; Zonneveld et al. 1997; Williams et al., 2006). Meanwhile, vegetation representatives of the once widespread tropical rain forest that existed during the early-Palaeogene up until the early Miocene, survived as 'refugia', without undergoing much change to the overall floristic makeup (Prabhu et al., 2004; Prasad et al., 2009), even though there was a regional reduction in taxonomic diversity (e.g. the extinction of the Dipterocarp genera *Anisoptera* and *Dryobalanops* from India) (Maury-Lechon & Curtet, 1998; Shukla et al., 2013). These refugia survived till today through the different episodes of glacial maxima. But during the inter-glacial periods, with the Indian summer monsoon increasing in intensities (Zhisheng et al. 2011), humid forest cover expanded on a northward transect along the Western Ghats as demonstrated for the inter-glacials 44 Ka by Kumaran et al. (2013). It is possible that once a rainforest conducive climate appeared

in the northern parts of the Ghats, SE Asian elements could have dispersed into the Ghats via the central Indian Hills (Meher-Homji, 1972 & 1974), as there is an abundance of several taxa with Malayan affinities (Mani, 1974). Correspondingly, during glacial maxima, when reduced atmospheric carbon dioxide and lower ambient temperatures prevailed in the lowlands, montane forest belts now confined to higher elevations occupied lower reaches in the late Quaternary (Colinvaux, 1998). This was followed by an upward altitudinal migration of the forest line during the warmer inter-glacials, including now during the Holocene (Hooghiemstra & van der Hammen, 2004).

In the Western Ghats, the Palghat gap would have served not only as an important physical barrier, but also as a climatic frontier. Pollen studies from the Nilgiris have suggested that montane grasslands persisted and dominated this massif from 40-23 Ka indicating a prolonged cold and dry climate (Sukumar et al., 1993; Rajagopalan et al. 1997; Bera & Farooqui, 2000). But, during the inter-glacial periods, many high elevation areas with C_4 plants were replaced with C_3 plants. Sedimentary profiles from the Palni Hills, south of the Palghat gap, also suggest cycles of cold & dry and warm & moist climates, with vegetation swinging between C_4 and C_3 dominant plant communities (Bera et al., 1997). However, this study also shows an absence of pollen records from some sequences, which possibly indicates a lack of vegetation in those zones as a result of increasingly permanent frosty conditions (Bera et al., 1997) and the cooler climate that did not support vegetation in the highest elevations. A sequence, dated between 30–25 Ka by the authors, though not conforming to the dating of glacial maxima globally (Yokoyama et al., 2000), is evidence of the influence of a long cooling interval in the Western Ghats. It is more likely that the effects of global cooling on the Western Ghats occurred between 22–19 Ka, as demonstrated for other parts of the world by several studies (e.g. Yokoyama et al., 2000; Zachos

et al., 2001). As illustrated for the similar north-south trending Andes in South America by Colinvaux (1998), the montane vegetation belt of the Western Ghats in the late Quaternary would have occurred at lower elevations than as at present. Likewise, the montane grasslands now occupying the highest reaches of the Ghats today (Ashton & Gunatilleke, 1987), would also have occurred more widespread at lower elevations during the Quaternary. It has been suggested that in tropical mountain ecosystems, the replacement of forest by open alpine biomes during the LGM could be to a considerable part forced by low $pC0_2$ and not only by temperature as previously thought (Street-Perrott, 1994). But, the lower reaches of the southernmost regions of the Ghats would have been occupied by tropical humid forests that survived as refugia even in xeric quaternary periods (i) as several independent patches formed on mountain-tops (Robin et al., 2010), (ii) as riparian vegetation due to soil moisture availability (Farooqui et al., 2010), and (iii) as larger blocks in the southern-most parts of the Western Ghats [being closer to the equator] (Mayr & O'Hara, 1986; Ramesh et al., 1997; Prasad et al., 2009). At the turn of the Holocene (~11.5 cal. Ka), when monsoon precipitation intensified dramatically (Morrill et al., 2003), the resulting wetter climate prompted a latitudinal and altitudinal expansion of evergreen forests from refugia (Adams & Faure, 1997), even though the tempo of expansion went down since ~3.5 Ka (Caratini et al., 1994). But also, this forest expansion was restricted and maintained only along the coastal plains and hill slopes of the western part of the Indian peninsula, since much of the rest of India underwent another bout of aridification more recently (5.4-3.5 Ka) in the late Holocene (Ponton et al., 2012; Prasad & Enzel, 2006). The overall climatic pattern has, since then, remained relatively stable until very recently. Conclusively, we do acknowledge that there are considerable uncertainties regarding the Cenozoic climatic trends

that prevailed in peninsular India and that further information, direct or proxy, needs to be gathered to present a more accurate picture.

The Philippines Archipelago: a geomorphological and climatic background

With over 7,100 islands, a landmass of 300,000 km^2, and very high species diversity per unit land, the Philippines is a global biodiversity hotspot (Brown et al., 2013; Mittermeier et al., 1999). Explorations and inventorying in the Philippines archipelago continue to produce numerous faunal and floral discoveries (Brown et al., 2014; Weinell & Brown, 2017; Welton et al., 2010). A preliminary knowledge of the geologic and climatic background of this archipelago is vital to better understand the archipelago setting (a highly fragmented geographic template), the nested series of islands and island banks (Brown & Diesmos, 2009) which undoubtedly has played an important role in generating, maintaining and partitioning this tremendous land vertebrate diversity.

Landscape and Geology

The Philippines Archipelago system is at the periphery of Southeast Asia with the Pacific Ocean to its east and the South China Sea to the west. Underneath, in the ocean, this archipelago is bound by a pair of subduction zones that includes the Manila Trench to the west and the proto-East Luzon Trough to the east (Yumul et al., 2008). The NW-SE oriented Philippine Mobile Belt is a series of tectonically and volcanically active island arcs, ophiolite suites (uplifted exposed sections of crust and underlying mantle), and exposed terranes of continental origin (Hall 1996, 1998; Yumul et al., 2008). The archipelago is essentially severed along its northwest-southeast axis by the Philippine fault (Yumul et al. 2008). Yumul et al. (2008) had described the mobile belt landmasses moving great distances as they were pushed up and exposed above sea level by

collision between the Philippine Sea Plate and Sundaic or Eurasian continental fragments (the Palawan Microcontinent Block, the Zambales Block, the Zamboanga Peninsula and the southern Mindanao Daguma Range Block) (Fig. 3).

Several geologic processes such as block migration, collision, subduction and island emergence and submergence have likely played vital roles in opening opportunities for land vertebrates to colonize the Philippines over geologic time (Inger, 1954; Brown & Alcala, 1970; Leviton, 1963; Heaney, 1985; Diamond & Gilpin, 1983). Despite these inferences remaining speculative based on reconstructions, notable cases of highly diverse and/or ancient, paleoendemic clades originating in the archipelago via geologic mechanisms have been inferred (e.g., Blackburn et al. 2010, Siler et al. 2012; Chan & Brown, 2017).

We have increasing evidence that the Philippines has been relatively stable over the past 5 Ma, and this stability in geologic configuration has been postulated to explain more recent colonization of the archipelago (Diamond & Gilpin, 1983; Heaney 1985). Diamond & Gilpin (1983) identified four major colonization routes, or biogeographic umbilici, as entryways to portions of the archipelago that have never been connected to a mainland (Inger, 1954; Brown & Guttman, 2002). These corridors include two 800-km-long island chains that may have allowed "stepping stone" dispersal events into the archipelago from Borneo, which comprises the edge of the Sunda Shelf (Inger, 1954; Heaney, 1985; Voris, 2000). These two very widely suggested colonization routes include western [Borneo+Palawan+Mindoro+ Luzon] and eastern island arcs [Sulu Archipelago+Mindanao+Leyte–Samar+Luzon] (Everett, 1889; Dickerson, 1928; Huxley, 1868; Mayr, 1944).

Paleoclimate and Inter-Island Dynamics

Within the Philippines archipelago, a hierarchical temporal structure of landmass connectivity during the Pleistocene gave rise to a simple model of diversification, which was based on observations that species distributions were organized into biogeographic sub-provinces (Inger, 1954; Leviton, 1963; Brown & Alcala, 1970; Heaney, 1985). These sub-provinces have been recognized to corresponded to Pleistocene land connections (Kloss, 1929; Inger, 1954; Heaney ,1985; Voris ,2000) (Fig. 4). Formally defined by Inger (1954) and Heaney (1985), the seven Pleistocene Aggregate Island Complexes or PAICs (Brown & Diesmos, 2009) formed repeatedly (perhaps ten times during the late Pleistocene) due to the oscillating sea levels (Voris, 2000) associated with Pleistocene glacial cycles (Siddal et al., 2003). Five large PAICs are recognized as primary biogeographic regions: the Luzon,Mindanao, Mindoro, Negros-Panay (or West Visayan), and Palawan faunal regions (Brown & Diesmos, 2009; Lomolino et al., 2010).

Paleoclimate and Intra-Island Dynamics

Among others, a set of key factors recognized for the diversification of Philippine biodiversity are elevationally structured ecological gradients (Heaney & Regalado, 1998; Brown et al 2013). Finer-scale differentiation may also be important mechanisms of diversification in taxa with specialized ecological requirements or limited dispersal abilities. In such cases, isolation of populations among mountain ranges, valleys, rivers, etc. could be typical on islands with heterogeneous geographic configurations, allowing further accrual of vertebrate diversity at repeated sites across large islands (Balete et al. 2011; Brown and Diesmos 2009; Brown et al. 2015). Our knowledge of the impact of the hypothesized geographical/geological processes on generation of biodiversity is still unfolding (Esselstyn et al. 2009; Oaks et al. 2013 2019; Weinell et al 2020), but derives predominantly from recent comprehensive faunal inventories, molecular phylogeographic studies (Heaney 2001, 2007; Brown & Diesmos, 2009; Brown et al 2012,

2013), and application of genomic data to reconsiderations of a well-developed tradition of biogeographical studies (Barley et al. 2015; Oaks et al. 2019; Brown et al. 2016; in review; Chan et al in review; Abraham, chapters 3 and 4).

References:

Adams, J. M. & Faure, H. (1997) Preliminary vegetation maps of the world since the last glacial maximum: an aid to archaeological understanding. *Journal of Archaeological Science*, 24(7), 623–647.

Aman, M. A., Yunus, A. P., & Javed, A. (2020) Fluvial knickpoint identification and their characterizations in the drainage basins of Western Ghats, India. Spatial Information Research, 1-10.

Aravind, N. A., Ganeshaiah, K. N. & Shaanker, R. U. (2013) Indian monsoons shape dispersal phenology of plants. *Biology letters*, 9(6), 20130675.

Ashton, P. S. & Gunatilleke, C. V. S. (1987) New light on the plant geography of Ceylon. I. Historical plant geography. *Journal of Biogeography*, 14, 249–285.

Axelrod, D. I. (1979) Age and origin of Sonoran Desert vegetation. *Occasional Papers of the California Academy of Sciences*, 132, 1–74.

Balete, D. S., Alviola, P. A., Duya, M. R. M., Duya, M. V., Heaney, L. R., & Rickart, E. A. (2011). The mammals of the Mingan Mountains, Luzon: evidence for a new center of mammalian endemism. Fieldiana Life and Earth Sciences, 2011(2), 75-87.

Barley, A. J., Monnahan, P. J., Thomson, R. C., Grismer, L. L., & Brown, R. M. (2015). Sun skink landscape genomics: assessing the roles of microevolutionary processes in shaping

genetic and phenotypic diversity across a heterogeneous and fragmented landscape. Molecular Ecology, 24(8), 1696-1712.

Bera, S. K. Farooqui, A., & Gupta, H. P. (1997) Late Pleistocene/Holocene vegetation and environment in and around Marian shola, Palni hills, Tamil Nadu. *Paleobotanist*, 46 (1–2), 191–195.

Bera, S. K. & Farooqui, A. N. J. U. M. (2000) Mid-Holocene vegetation and climate of south Indian Montane. *Journal Paleontological Society of India*, 45, 49–56.

Behrensmeyer, A. K., Quade, J., Cerling, T. E., Kappelman, J., Khan, I. A., Copeland, P., Roe, L., Hicks, J., Stubblefield, P., Wills, B.J. & Latorre, C. (2007) The structure and rate of late Miocene expansion of C4 plants: Evidence from lateral variation in stable isotopes in paleosols of the Siwalik Group, northern Pakistan. *Geological Society of America Bulletin*, 119(11–12), 1486–1505.

Blackburn, D. C., Bickford, D. P., Diesmos, A. C., Iskandar, D. T., & Brown, R. M. (2010). An ancient origin for the enigmatic flat-headed frogs (Bombinatoridae: *Barbourula*) from the islands of Southeast Asia. PLoS One, 5(8), e12090.

Blasco, F., Bellan, M. F. & Aizpuru, M. (1996) A vegetation map of tropical continental Asia at scale 1: 5 million. *Journal of Vegetation Science*, 7(5), 623–634.

Blasco, F., Whitmore, T. C., & Gers, C. (2000). A framework for the worldwide comparison of tropical woody vegetation types. Biological Conservation, 95(2), 175-189.

Bonnefille, R., Anupama, K., Barboni, D., Pascal, J., Prasad, S. & Sutra, J. P. (1999) Modern pollen spectra from tropical South India and Sri Lanka: altitudinal distribution. *Journal of Biogeography*, 26(6), 1255–1280.

Brown, R. M. (2009). Frogs in Island Archipelagos. Pp. 347–351 In: Gillespie, R., and D. Clague (Eds.). Encyclopedia of Islands. University of California Press, Berkeley.

Brown, R.M. & Diesmos, A.C. (2009). Philippines, biology. In: Gillespie, R., Clague, D. (Eds.), Encyclopedia of Islands. University of California Press, Berkeley, pp. 723– 732.

Brown, R. M., Diesmos, A. C., Sanguila, M. B., Siler, C. D., Diesmos, M. L. D., & Alcala, A. C. (2012). Amphibian conservation in the Philippines. FrogLog, 104, 40-43.

Brown, R. M., Siler, C. D., Oliveros, C. H., Esselstyn, J. A., Diesmos, A. C., Hosner, P. A., Linkem, C.W., Barley, A.J., Oaks, J.R., Sanguila, M.B., & Welton, L. J. (2013). Evolutionary processes of diversification in a model island archipelago. Annual Review of Ecology, Evolution, and Systematics, 44, 411-435.

Brown, R. M., Weghorst, J. A., Olson, K. V., Duya, M. R., Barley, A. J., Duya, M. V., Shekelle, M., Neri-Arboleda, I., Esselstyn, J.A., Dominy, N.J., & Ong, P. S. (2014). Conservation genetics of the Philippine tarsier: Cryptic genetic variation restructures conservation priorities for an island archipelago primate. PLoS One, 9(8), e104340.

Brown, R. M., Siler, C. D., Richards, S. J., Diesmos, A. C., & Cannatella, D. C. (2015). Multilocus phylogeny and a new classification for Southeast Asian and Melanesian forest frogs (family Ceratobatrachidae). Zoological Journal of the Linnean Society, 174(1), 130-168.

Brown, R. M. (2016). Biogeography of Land Vertebrates. 2016. In: Kliman, R.M. (ed.), The Encyclopedia of Evolutionary Biology. Vol. 1, pp. 211–220. Oxford: Academic Press/Elsevier Inc.

Brown, R. M., C. R. Hutter, P. L. Wood, Jr., R. K. Abraham, J. G. Vallejos, M. W. Herr, & C. K. Onn. (in prep) Comprehensive, archipelago-wide, sequence-capture phylogenomic inference for species discovery in Philippine Fanged Frogs. Biology Letters.

Brown, W. C., & Alcala, A. C. (1970). The zoogeography of the herpetofauna of the Philippine Islands, a fringing archipelago. California Academy of Sciences.

Budyko, M. I. (1969) The effect of solar radiation variations on the climate of the earth. *Tellus*, 21(5), 611–619.

Bush, A. B. & Philander, S. G. H. (1999) The climate of the Last Glacial Maximum: Results from a coupled atmosphere-ocean general circulation model. *Journal of Geophysical Research: Atmospheres (1984–2012)*, 104(D20), 24509–24525.

Campanile, D. J. (2007) The post-breakup evolution of the western Indian high-elevation passive margin (Doctoral dissertation, University of Glasgow).

Caratini, C., Bentaleb, I., Fontugne, M., Morzadec-Kerfourn, M. T., Pascal, J. P. & Tissot, C. (1994) A less humid climate since ca. 3500 yr BP from marine cores off Karwar, western India. *Palaeogeography, Palaeoclimatology, Palaeoecology*, 109(2), 371–384.

Carlquist, S. J. (1974). Island Biology. Columbia University Press.

CEPF (2007) Ecosystem Profile Western Ghats & Sri Lanka Biodiversity Hotspot, Western Ghats Region. Critical Ecosystem Partnership Fund, Washington, DC.

Chabangborn, A., Brandefelt, J. & Wohlfarth, B. (2014) Asian monsoon climate during the Last Glacial Maximum: palaeo-data–model comparisons. *Boreas*, 43(1), 220–242.

Chan, K. O., & Brown, R. M. (2017). Did true frogs 'dispersify'?. Biology Letters, 13(8), 20170299.

Chan, K. O., C. R. Hutter, P. L. Wood, Jr., Y.-C. Su, & R. M. Brown. (in review). Admixture underlies cryptic diversity in Philippine Puddle-frogs (*Occidozyga laevis*). Systematic Biology.

Clark, C., Collins, A. S., Taylor, R. J., & Hand, M. (2020). isotopic systematics of zircon indicate an African affinity for the rocks of southernmost India. Scientific Reports, 10(1), 1-12.

Colinvaux, P. A. (1998) A new vicariance model for Amazonian endemics. *Global Ecology and Biogeography Letters*, 7, 95–96.

Collins, A. S., Santosh, M., Braun, I., & Clark, C. (2007a). Age and sedimentary provenance of the Southern Granulites, South India: U-Th-Pb SHRIMP secondary ion mass spectrometry. Precambrian Research, 155(1-2), 125-138.

Collins, A. S., Clark, C., Sajeev, K., Santosh, M., Kelsey, D. E., & Hand, M. (2007b). Passage through India: The Mozambique Ocean suture, high-pressure granulites and the Palghat-Cauvery shear zone system. Terra Nova, 19(2), 141-147.

Darwin, C. (1859). On the Origin of Species by Means of Natural Selection. London: John Murray.

Diamond, J. M., & Gilpin, M. E. (1983). Biogeographic umbilici and the origin of the Philippine avifauna. Oikos, 307-321.

Dickerson, R. E. (1928). Distribution of Life in the Philippines: 1-322.

Dinesh, K. P., Radhakrishnan, C., Channakeshavamurthy, B. H., Deepak, P., & Kulkarni, N. U. (2019) A checklist of amphibians of India with IUCN conservation status. Version (2.0). Online publication is available at www. zsi. gov. in.

Drury, S.A., Harris, N.B.W., Holt, R.W., Reeves-Smith, G.J., Wightman, R.T. (1984) Precambrian tectonics and crustal evolution in south India. Journal of the Geological Society of India, v.92, pp.3–20.

Esselstyn, J. A., Timm, R. M., & Brown, R. M. (2009). Do geological or climatic processes drive speciation in dynamic archipelagos? The tempo and mode of diversification in Southeast Asian shrews. Evolution: International Journal of Organic Evolution, 63(10), 2595-2610.

Everett, A. H. (1889, March). Remarks on the Zoo-geographical Relationships of the Island of Palawan and some adjacent Islands. In Proceedings of the Zoological Society of London (Vol. 57, No. 2, pp. 220-228). Oxford, UK: Blackwell Publishing Ltd.

Farooqui, A., Ray, J. G., Farooqui, S. A., Tiwari, R. K. & Khan, Z. A. (2010) Tropical rainforest vegetation, climate and sea level during the Pleistocene in Kerala, India. *Quaternary International*, 213(1), 2–11.

Favé, M. J., Johnson, R. A., Cover, S., Handschuh, S., Metscher, B. D., Müller, G. B., Gopalan, S., & Abouheif, E. (2015). Past climate change on Sky Islands drives novelty in a core developmental gene network and its phenotype. BMC Evolutionary Biology, 15(1), 183.

Field, J. S., Petraglia, M. D. & Lahr, M. M. (2007) The southern dispersal hypothesis and the South Asian archaeological record: examination of dispersal routes through GIS analysis. *Journal of Anthropological Archaeology*, 26(1), 88–108.

Folie, A., Rana, R. S., Rose, K. D., Sahni, A., Kumar, K., Singh, L. & Smith, T. (2012) Early Eocene frogs from Vastan Lignite Mine, Gujarat, India. *Acta Palaeontologica Polonica*, 58 (3), 511–524.

Goldschmidt, T. (1996). Darwin's Dreampond: Drama in Lake Victoria. Cambridge, MA: The MIT Press

Guha, S., & Jain, V. (2020) Role of inherent geological and climatic characteristics on landscape variability in the tectonically passive Western Ghat, India. Geomorphology, 350, 106840.

Gunnell, Y. & Fleitout, L., (1998) Shoulder uplift of the Western Ghats passive margin, India: A denudational model. *Earth Surface Processes and Landforms*, 23, 391–404.

Gupta, S., Rai, S. S., Prakasam, K. S., Srinagesh, D., Bansal, B. K., Chadha, R. K., Priestley, K., & Gaur, V. K. (2003) The nature of the crust in southern India: implications for Precambrian crustal evolution. *Geophysical Research Letters*, 30(8).

Hall, R. (1996). Reconstructing Cenozoic SE Asia. Geological Society, London, Special Publications, 106(1), 153-184.

Hall, R. (1998). The plate tectonics of Cenozoic SE Asia and the distribution of land and sea. Biogeography and geological evolution of SE Asia, 99-131.

Hashimi, N. H. & Nair, R. R. (1986) Climatic aridity over India 11,000 years ago: evidence from feldspar distribution in shelf sediments. *Palaeogeography, Palaeoclimatology, Palaeoecology*, 53(2), 309–319.

Heaney, L. R. (1985). Zoogeographic evidence for middle and late Pleistocene land bridges to the Philippine Islands. Modern Quaternary Research in Southeast Asia, 9, 127-144.

Heaney, L. R., & Regalado Jr, J. C. (1998). Vanishing treasures of the Philippine rain forest. The Field Museum.

Hooghiemstra, H. & Van der Hammen, T. (2004) Quaternary Ice-Age dynamics in the Colombian Andes: developing an understanding of our legacy. *Philosophical*

Transactions of the Royal Society of London. Series B: Biological Sciences, 359(1442), 173–181.

Hughes, C., & Eastwood, R. (2006). Island radiation on a continental scale: exceptional rates of plant diversification after uplift of the Andes. Proceedings of the National Academy of Sciences, 103(27), 10334-10339.

Huxley, T. H. (1868). On the classification and distribution of the Alectoromorphae and Heteromorphae. Royal Institution.

Inger, R. F. (1954). Systematics and zoogeography of Philippine Amphibia. Fieldiana Zoology, 33, 181-531.

Keeley, J. E. & Rundel, P. W. (2005) Fire and the Miocene expansion of C_4 grasslands. *Ecology Letters*, 8(7), 683–690.

Kern, A. K., Harzhauser, M., Reuter, M., Kroh, A. & Piller, W. E. (2013) The Miocene coastal vegetation of southwestern India and its climatic significance. *Palaeoworld*. v.22, pp.119-132.

Kloss, B. 1929. The zoo-geographical boundaries between Asia and Australia and some Oriental sub-regions. Bulletin of the Raffles Museum, 2, 1–10.

Kumar, P. (1990) Fungal remains from the Miocene Quilon Beds of Kerala State, South India. *Review of Palaeobotany and Palynology*, 62: 13–28.

Lawver, L. A. & Gahagan, L. M. (2003) Evolution of Cenozoic seaways in the circum-Antarctic region. *Palaeogeography, Palaeoclimatology, Palaeoecology*, 198(1), 11–37.

Leviton, A. E. (1963). Remarks on the zoogeography of Philippine terrestrial snakes. Proceedings of the California Academy of Sciences, 42 (1963), 112-145.

Lomolino, M. V., Brown, J. H., & Sax, D. F. (2010). Island biogeography theory. The theory of island biogeography revisited, 13.

Losos, J. B., & Ricklefs, R. E. (2009). Adaptation and diversification on islands. Nature, 457(7231), 830-836.

Mandaokar, B. D. & Mukherjee, D. (2012) Palynological investigation of early Miocene sediments exposed at Panruti, Cuddalore district, Tamil Nadu, India. International Journal of Geology, Earth and Environmental Sciences, 2(3): 157–175.

Mani, M. S. (1974). Biogeographical evolution in India. In Ecology and biogeography in India (pp. 698-724). Springer, Dordrecht.

Martinelli, G. (2007). Mountain biodiversity in Brazil. Brazilian Journal of Botany, 30(4), 587-597.

Maury-Lechon, G. & Curtet, L. (1998) Biogeography and evolutionary systematics of Dipterocarpaceae. A review of dipterocarps taxonomy, ecology and silviculture. CIFOR, Jakarta, 5–44.

Mayr, E. (1944). Wallace's line in the light of recent zoogeographic studies. The Quarterly Review of Biology, 19(1), 1-14.

Mayr, E. (1949). The species concept: semantics versus semantics. Evolution, 3(4), 371-372.

Mayr, E., & O'Hara, R. J. (1986). The biogeographic evidence supporting the Pleistocene forest refuge hypothesis. Evolution, 40(1), 55–67.

McCormack, J. E., Huang, H., Knowles, L. L., Gillespie, R., & Clague, D. (2009). Sky Islands. Encyclopedia of Islands, 4, 841-843.

Miller, K. G., Browning, J. V., Schmelz, W. J., Kopp, R. E., Mountain, G. S., & Wright, J. D. (2020). Cenozoic sea-level and cryospheric evolution from deep-sea geochemical and continental margin records. Science Advances, 6(20), eaaz1346.

Mittermeier, R. A., Gil, P., Hoffman, M., Pilgrim, J., Brooks, T., & Mittermeier, C. G. (1999) Earth's biologically richest and most endangered terrestrial ecoregions. México: CEMEX.

Meher-Homji, V. M. (1972) Himalayan plants on South Indian Hills: role of Pleistocene glaciation vs. long distance dispersal. *Science and Culture*, 38, 8–12.

Meher-Homji V. M. (1974) Disjunct distributions in the plant kingdom. *Science and Culture*, 40(6), 217–227.

Molnar, P.H. & Rajagopalan, B. (2012) Late Miocene upward and outward growth of eastern Tibet and decreasing monsoon rainfall over the northwestern Indian subcontinent since~ 10 Ma, *Geophysics Research Letters*, 39, 2–5.

Morrill, C., Overpeck, J. T. & Cole, J. E. (2003) A synthesis of abrupt changes in the Asian summer monsoon since the last deglaciation. *The Holocene*, 13(4), 465–476.

Naidu, P. D. & Malmgren, B. A. (1996) A high resolution record of late Quaternary upwelling along the Oman Margin, Arabian Sea based on planktonic foraminifera. *Palaeoceanography*, 11, 129–140.

Maury-Lechon, G., & Curtet, L. (1998). Biogeography and evolutionary systematics of Dipterocarpaceae. A Review of Dipterocarps: Taxonomy, Ecology and Silviculture. Center for International Forestry Research, Indonesia, 5-44.

McLaughlin, S. P. (1995). An overview of the flora of the Sky Islands, southeastern Arizona: Diversity, affinities, and insularity. Biodiversity and management of the Madrean

Archipelago: the Sky Islands of southwestern United States and northwestern Mexico, 60-70.

Myers, N., Mittermeier, R. A., Mittermeier, C. G., Da Fonseca, G. A., & Kent, J. (2000) Biodiversity hotspots for conservation priorities. *Nature*, 403(6772), 853-858.

Nair, S. C. (1991). The Southern Western Ghats: A Biodiversity Conservation Plan (Studies in Ecology and Sustainable Development). New Delhi: INTACH. Lodi Estate Indraprastha press, New Delhi (92 pp).

Oaks, J. R., Siler, C. D., & Brown, R. M. (2019). The comparative biogeography of Philippine geckos challenges predictions from a paradigm of climate-driven vicariant diversification across an island archipelago. Evolution, 73(6), 1151-1167.

Petren, K. Grant, P. R. Grant, B. R., & Keller, L. F. (2005). Comparative landscape genetics and the adaptive radiation of Darwin's finches: the role of peripheral isolation. Molecular Ecology. 14 (10): 2943–2957.

Ponton, C., Giosan, L., Eglinton, T. I., Fuller, D. Q., Johnson, J. E., Kumar, P. & Collett, T. S. (2012) Holocene aridification of India. *Geophysical Research Letters*, 39(3), L03704.

Prabhu, C. N., Shankar, R., Anupama, K., Taieb, M., Bonnefille, R., Vidal, L. & Prasad, S. (2004) A 200-ka pollen and oxygen-isotopic record from two sediment cores from the eastern Arabian Sea. *Palaeogeography, Palaeoclimatology, Palaeoecology*, 214(4), 309–321.

Prasad, S. & Enzel, Y. (2006) Holocene paleoclimates of India. *Quaternary Research*, 66(3), 442–453.

Prasad, V., Farooqui, A., Tripathi, S. K. M., Garg, R. & Thakur, B. (2009) Evidence of Late Palaeocene-Early Eocene equatorial rain forest refugia in southern Western Ghats, India. *Journal of Biosciences*, 34(5), 777–797.

Quade, J., Cater, J. M., Ojha, T. P., Adam, J. & Harrison, T. M. (1995) Late Miocene environmental change in Nepal and the northern Indian subcontinent: Stable isotopic evidence from paleosols. *Geological Society of America Bulletin*, 107(12), 1381–1397.

Rajagopalan, G., Sukumar, R., Ramesh, R. & Pant, R. K. (1997) Late Quaternary vegetational and climatic changes from tropical peats in southern India-An extended record up to 40,000 years BP. *Current Science*, 73(3), 60–63.

Rajesh, H. M., & Santosh, M. (2004) Charnockitic magmatism in southern India. *Journal of Earth System Science*, 113(4), 565-585.

Ramesh, B. R., Menon, S. & Bawa, K. S. (1997) A vegetation based approach to biodiversity gap analysis in the Agastyamalai region, Western Ghats, India. *Ambio*, 26(8), 529–536.

Rao, M. R., & Verma, P. (2014). Miocene palynology in India: present status and future prospect. Special Publication of the Palaeontological Society of India, 5, 145-160.

Rao, Y. B., Kumar, T. V., Sreenivas, B., & Babu, E. V. S. S. K. (2020). A Review of Paleo-to Neoarchean crustal evolution in the Dharwar craton, Southern India and the transition towards a Plate Tectonic regime. *Episodes Journal of International Geoscience*, 43(1), 51-68.

Richards, F. D., Hoggard, M. J., & White, N. J. (2016) Cenozoic epeirogeny of the Indian peninsula. *Geochemistry, Geophysics, Geosystems*, 17(12), 4920-4954.

Robin, V. V., Sinha, A. & Ramakrishnan, U. (2010) Ancient geographical gaps and paleo-climate shape the phylogeography of an endemic bird in the sky islands of southern India. *PloS One*, 5(10), e13321.

Robin, V. V., & Nandini, R. (2012). Shola habitats on sky islands: status of research on montane forests and grasslands in southern India. Current Science, 1427-1437.

Santosh, M. (2020). The Southern Granulite Terrane: A synopsis. Episodes Journal of International Geoscience, 43(1), 109-123.

Schluter, D. (2000). The Ecology of Adaptive Radiation. Oxford University Press.

Shukla, A. & Mehrotra, R. C. (2013) Paleoequatorial rain forest of western India during the EECO: evidence from Uvaria L. fossil and its geological distribution pattern. *Historical Biology*, (ahead-of-print), 1–6.

Shukla, A., Mehrotra, R.C. & Gulleria, J.S. (2013) Emergence and extinction of Dipterocarpaceae in western India with reference to climate change: Fossil wood evidences. *Journal of Earth System Science*, 122(5): 1373–1386.

Siddall, M., Rohling, E. J., Almogi-Labin, A., Hemleben, C., Meischner, D., Schmelzer, I., & Smeed, D. A. (2003). Sea-level fluctuations during the last glacial cycle. Nature, 423(6942), 853-858.

Siler, C. D., Oaks, J. R., Welton, L. J., Linkem, C. W., Swab, J. C., Diesmos, A. C., & Brown, R. M. (2012). Did geckos ride the Palawan raft to the Philippines?. Journal of Biogeography, 39(7), 1217-1234.

Simpson, G (1949). Tempo and Mode in Evolution. New York: Columbia University Press.

Simpson, G. G. (1951). The species concept. Evolution, 5(4), 285-298.

Street-Perrott, F. A. (1994) Palaeo-perspectives: changes in terrestrial ecosystems. *Ambio*, 23, 37–43.

Smith, A. G. & Pickering, K. T. (2003) Oceanic gateways as a critical factor to initiate icehouse Earth. *Journal of the Geological Society*, 160(3), 337–340.

Staubwasser, M., Sirocko, F., Grootes, P. M. & Segl, M. (2003) Climate change at the 4.2 ka BP termination of the Indus valley civilization and Holocene south Asian monsoon variability. *Geophysical Research Letters*, 30(8).

Sukumar, R., Ramesh, R., Pant, R.K. & Rajagopalan, G. (1993) A δ13C record of late Quaternary climate change from tropical peats in southern India. *Nature*, 364, 703–706.

Torsvik, T. H., Tucker, R. D., Ashwal, L. D., Carter, L. M., Jamtveit, B., Vidyadharan, K. T., Venkataramana, P., (2000) Late Cretaceous India-Madagascar fit and timing of break-up related magmatism, *Terra Nova*, 12, 220-224.

Voris, H. K. (2000). Maps of Pleistocene sea levels in Southeast Asia: shorelines, river systems and time durations. Journal of Biogeography, 27(5), 1153-1167.

Wallace, A. R. (1881). Island life or the phenomena and causes of insular faunas and floras including a revision and attempted solution of the problem of geological climates. Macmillan, London.

Warshall, P. (1995). The Madrean sky-island archipelago. Biodiversity and Management of the Madrean Archipelago: the Sky-islands of Southwestern United States and Northwestern Mexico. (LF DeBano, PF Folliott, A. Ortega-Rubio, GJ Gottfried, RH Hamre & CB Edminster, eds.). USDA Forest Service Rocky Mountain Forest and Range Experiment Station, Fort Collins, Colorado, 6-18.

Weinell, J. L., & Brown, R. M. (2018). Discovery of an old, archipelago-wide, endemic radiation of Philippine snakes. Molecular Phylogenetics and Evolution, 119, 144-150.

Weinell, J. L., Barley, A. J., Siler, C. D., Orlov, N. L., Ananjeva, N. B., Oaks, J. R., Burbrink, F.T., & Brown, R. M. (2020). Phylogenetic relationships and biogeographic range evolution in cat-eyed snakes, *Boiga* (Serpentes: Colubridae). Zoological Journal of the Linnean Society.

Welton, L. J., Siler, C. D., Bennett, D., Diesmos, A., Duya, M. R., Dugay, R., Rico, E.L.B., Van Weerd, M., & Brown, R. M. (2010). A spectacular new Philippine monitor lizard reveals a hidden biogeographic boundary and a novel flagship species for conservation. Biology Letters, 6(5), 654-658.

Whittaker, R. J., Fernández-Palacios, J. M., Matthews, T. J., Borregaard, M. K., & Triantis, K. A. (2017). Island biogeography: Taking the long view of nature's laboratories. Science, 357(6354).

Williams, M. A. J. (1975) Late Pleistocene tropical aridity synchronous in both hemispheres? *Nature*, 243, 617–618.

Williams, M. A. J., Pal, J. N., Jaiswal, M., & Singhvi, A. K. (2006) River response to Quaternary climatic fluctuations: evidence from the Son and Belan valleys, north-central India. *Quaternary Science Reviews*, 25(19), 2619–2631.

Yokoyama, Y., Lambeck, K., De Deckker, P., Johnston, P., & Fifield, L. K. (2000) Timing of the Last Glacial Maximum from observed sea-level minima. *Nature*, 406(6797), 713–716.

Yumul, G. P., Dimalanta, C. B., Maglambayan, V. B., & Marquez, E. J. (2008). Tectonic setting of a composite terrane: A review of the Philippine island arc system. Geosciences Journal, 12(1), 7.

Zachos, J., Pagani, M., Sloan, L., Thomas, E., & Billups, K. (2001) Trends, rhythms, and aberrations in global climate 65 Ma to present. *Science*, 292 (5517), 686–693.

Zhang, R., Jiang, D., Zhang, Z., & Yu, E. (2015). The impact of regional uplift of the Tibetan Plateau on the Asian monsoon climate. Palaeogeography, Palaeoclimatology, Palaeoecology, 417, 137-150.

Zhisheng, A., Clemens, S. C., Shen, J., Qiang, X., Jin, Z., Sun, Y., & Lu, F. (2011) Glacial-interglacial Indian summer monsoon dynamics. *Science*, 333(6043), 719–723.

Zonneveld, K. A., Ganssen, G., Troelstra, S., Versteegh, G. J. & Visscher, H. (1997) Mechanisms forcing abrupt fluctuations of the Indian Ocean summer monsoon during the last deglaciation. *Quaternary Science Reviews*, 16(2), 187–201.

Figures

Fig. 1. Topographical map of the Western Ghats Mountain Range with sub ranges marked out.

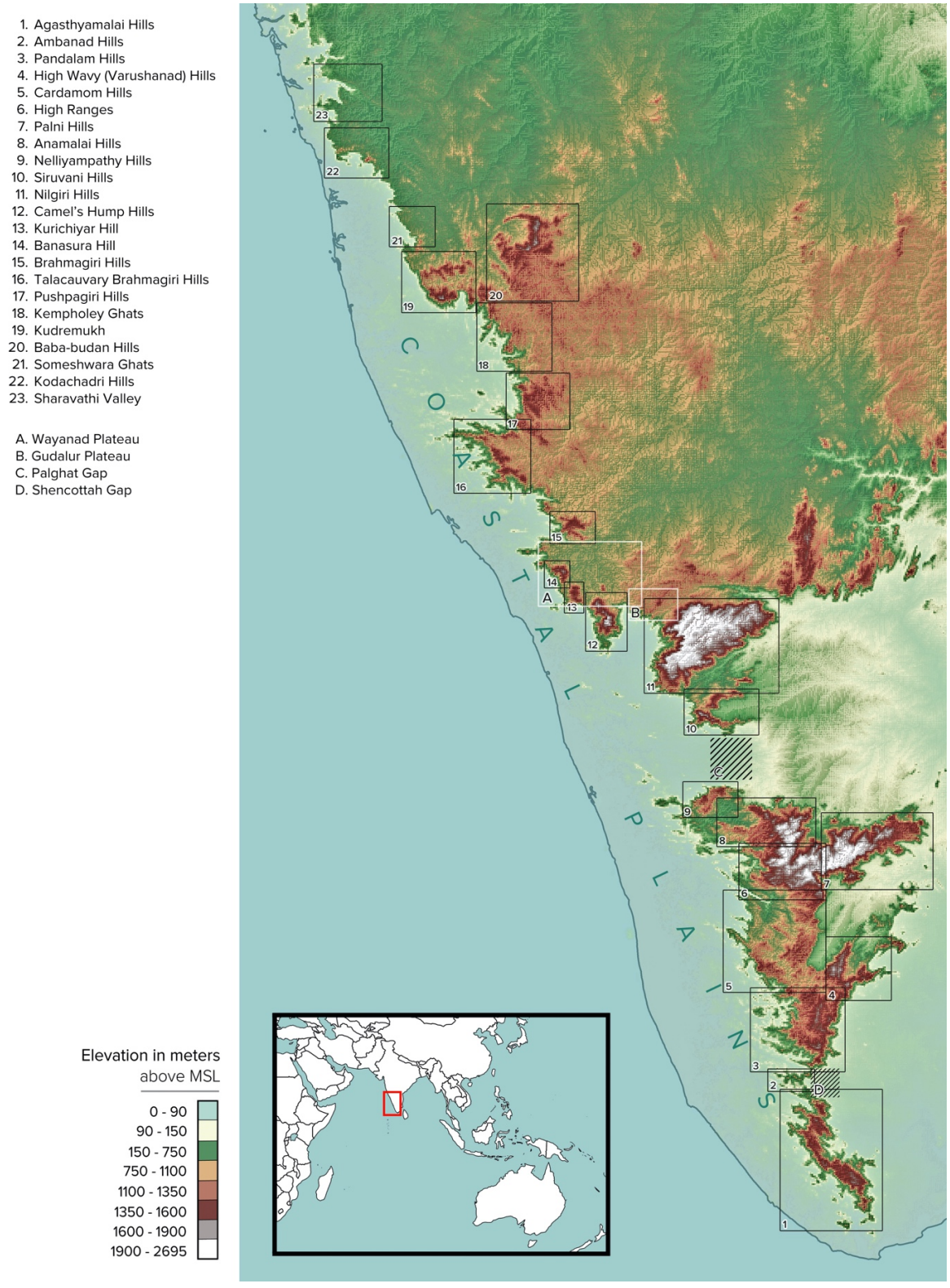

Fig. 2. Schematic vegetation map of the central and southern Western Ghats of the Last Glacial Maxima (LGM) and now: **A. & B.** Physical profile; **C. & D.** Vegetation profile. We depict the LGM at 22,000Ya here, as it was the most recent and is the best known of any of the ice age maxima.

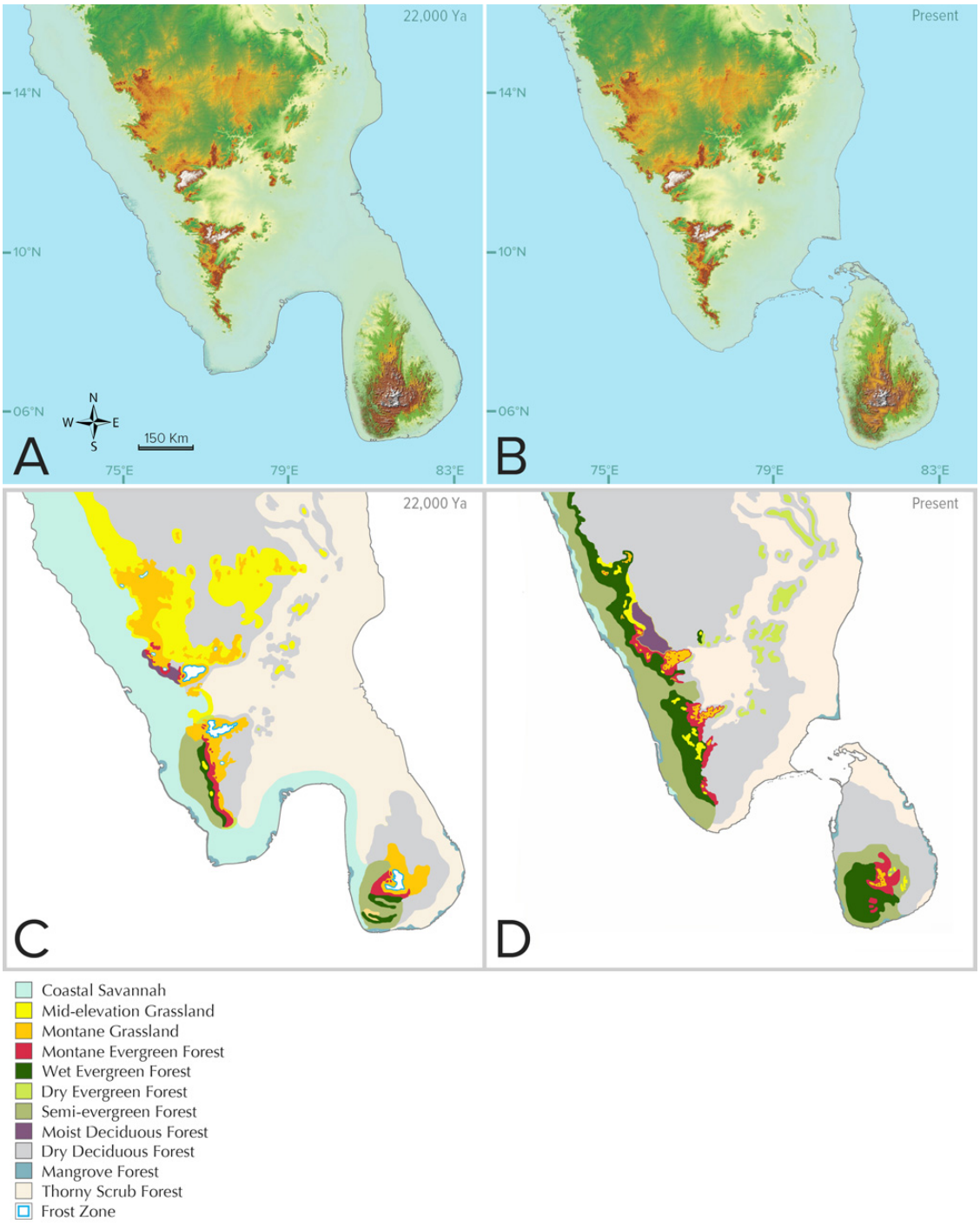

Fig. 3. Major geological features and approximate tectonic evolution of the Philippines archipelago. Both maps of the Philippines (including Fig. 4) from Brown et al., (2013).

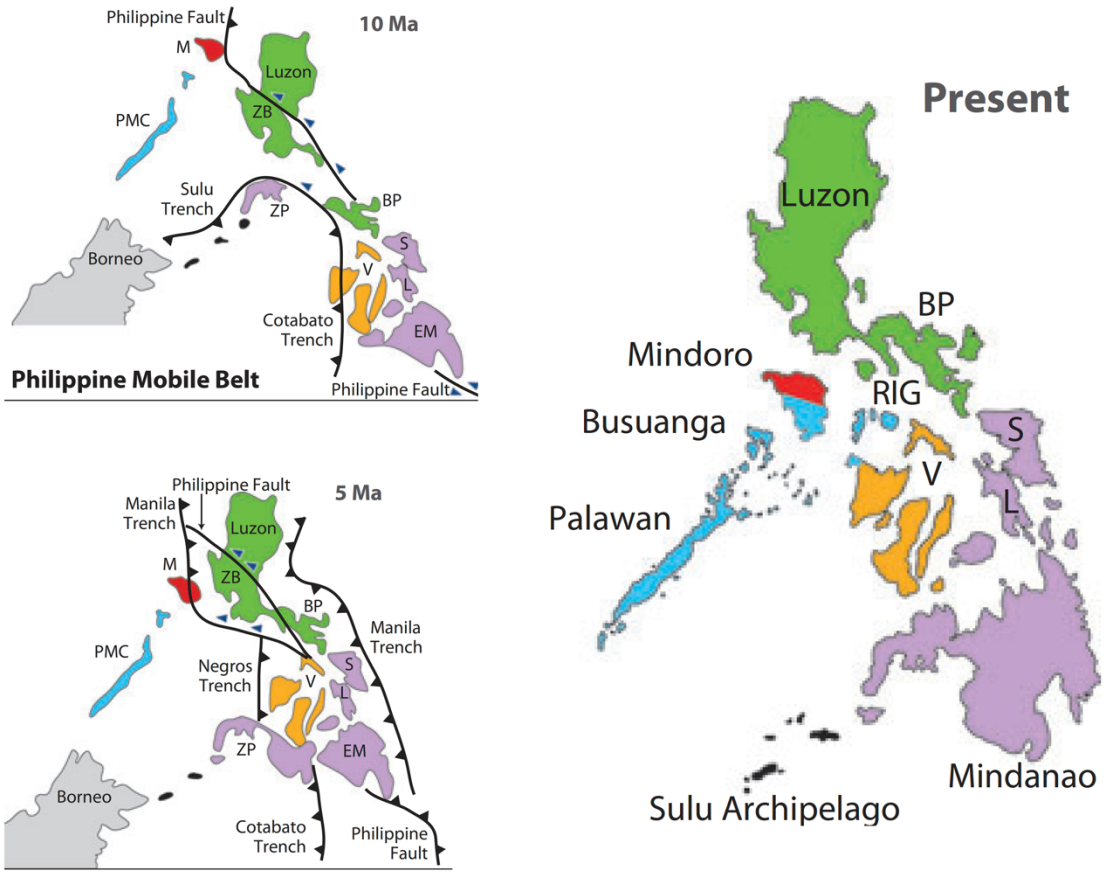

Fig. 4. Pleistocene Aggregate Island Complex (PAIC) diversification model and estimates of the extremes of land connectivity and habitat connectivity during glacial-interglacial cycles.

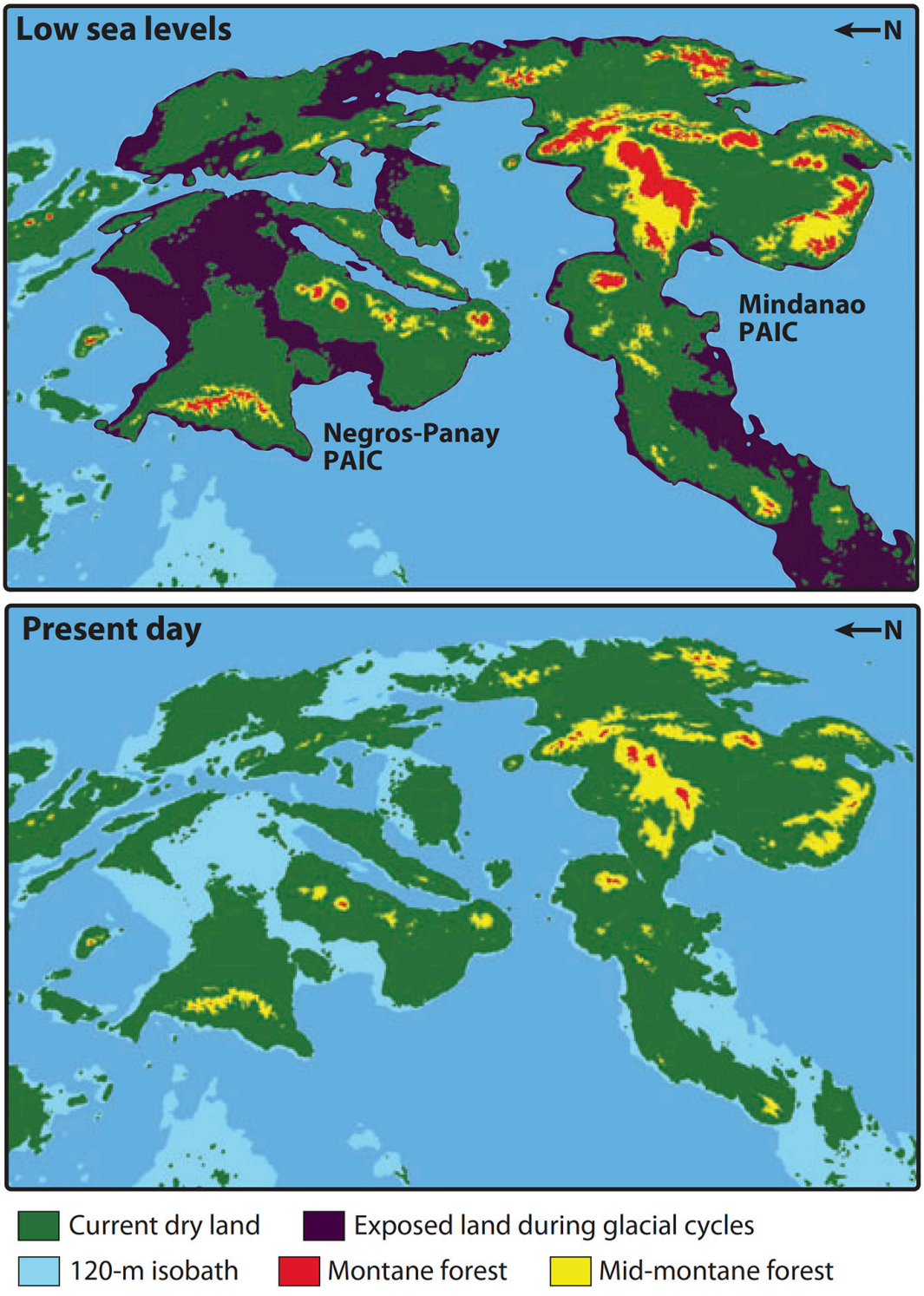

CHAPTER 1

Integration of ecology, larval phenotypes, and mate-recognition signals with molecular and morphological data hint at possible taxonomic inflation in *Nyctibatrachus* (Anura: Nyctibatrachidae)

Robin Kurian Abraham[1,4], Ramprasad Rao[2], Anil Zachariah[3], and Rafe M. Brown[1]

***Key words not in title*:** endemic species, species delineation, reproductive biology, acoustics, tadpoles, Western Ghats.

***Manuscript category*:** Major article.

***Suggested Copeia section*:** General Herpetology.

***Number of text pages*:** 54

***Suggested running head*:** Abraham et al.— Integrative taxonomy of *Nyctibatrachus*

***Line art figures*:** 4.

***Photographic figures*:** 5.

***Tables*:** 3.

[1] Biodiversity Institute, and Department of Ecology and Evolutionary Biology, The University of Kansas, 1345 Jayhawk Boulevard, Lawrence, KS 66045-7561, U.S.A.; Email: (RKA) robinabrahamf50@gmail.com, (RMB) rafe@ku.edu.

[2] Chathurthi, Mudradi, Udupi, Karnataka 576112, India; Email: (RR) rammugudu@gmail.com

[3] Beagle, Chandakunnu, Wayanad, Kerala 673121, India; Email: (AZ) anil.macri@gmail.com

[4] Correspondence: reprint requests to RKA

Taxonomic reappraisals over the past decade, of the endemic Night Frog genus *Nyctibatrachus* (originally described in 1882), of Peninsular India, has more than tripled, from 11 at the turn of this century to 36 by 2017. Despite these revisionary contributions, it is still challenging for field biologists to identify night frog species reliably, due to a near-complete absence of diagnostic, discrete (non-overlapping) characters states or trait values. Worse, many questionably-diagnosed night frog species' status has ostensibly been "supported" by sparsely-sampled single-locus gene-trees, or topologies estimated, from only a handful of markers—with genetic data used primarily to support new species descriptions, on arbitrary genetic distance thresholds of 3–6%. We sought to re-evaluate this conservation-relevant study system by employing an integrative taxonomic approach that integrates classical taxonomy, molecular species delimitation analysis, statistical analysis of morphological characters of adults and larvae, analyses of bioacoustics, natural history information, relationships of genetic versus geographical distance, and environmental variables. Our simultaneous reanalysis of molecular phylogenetic reconstructions, based on mitochondrial DNA sequences and multiple independent data streams, indicated that recent descriptions of *Nyctibatrachus deveni*, *N. periyar* and *N. pillaii* may represent cases of taxonomic inflation (over-splitting), because the evidence cited in support of their recognition is irreproducible, subjective, and devoid statistical support. We demonstrate the need for multidimensional species delimitation approaches in the celebrated Western Ghats biodiversity hotspot paleo-endemic genus *Nyctibatrachus* and suspect that this concerning trend of over-splitting amphibian species based on limited data may generalize to other amphibian groups.

OVER the last decade, systematic biology has undergone major advances in the numbers, and kinds, of methods available for delimiting species boundaries (Carstens et al., 2013). Criteria for

species delimitation typically involve methods employed to translate species concepts into a nominal, Linnaean nomenclatural arrangement (Genus–species name pairs) "logically" consistent with modern species concepts (de Queiroz, 1997; de Queiroz, 1998; de Queiroz, 2007; Frost and Hillis, 1990; Wiley, 1978). With over 7,200 species, anuran amphibians (frogs and toads) are among the most diverse of terrestrial vertebrates; moreover, their numbers are steadily increasing (AmphibiaWeb, 2020; Frost, 2020). With the advent of molecular data and advanced statistical phylogenetics, the past two decades have witnessed a surge in new amphibian taxonomic descriptions, especially in the tropics, which have been noted for harboring markedly high species diversity (Brown, 2014; Pyron and Wiens, 2013; Scott, 1976; Wiens and Donoghue, 2004; Wiens et al., 2009). However, the last decade's indiscriminately-accepted assumption, that a significant portion of that diversity must be phenotypically-cryptic (Bickford et al., 2007; Stuart et al., 2006) has gone largely untested with independent sources of data (Padial et al., 2010).

Molecular sequence data and statistical methods for distance-based analyses of DNA sequences (predominantly relying on one or, at most, a handful of genetic markers) have been pivotal in species delimitation, but have fallen under increased levels of criticism, particularly when evaluating the expectation of the presence of morphologically-cryptic species hidden within widespread or allopatrically-distributed taxa (Collins and Cruickshank, 2013; Taylor and Harris, 2012; Will et al., 2005). Subsequently, this debate recently has focused on approaches for distinguishing speciation-level processes of diversification, from population-level geographic structure, typified by divergent lineages, typically inferred empirically across geographical boundaries (Avise, 2000; Coates et al., 2018; Pfenninger and Schwenk, 2007). However, most recent investigations utilize only a limited number of available procedures (Carstens et al., 2013;

Esselstyn et al., 2012), lack a unified general analytical framework, and have fallen short of fundamental hypothesis-testing analytical procedures (Leache et al., 2009; Vieites et al., 2009; Chan et al., 2017).

One frequent artifact of proposed, but unvalidated, units putatively considered real, biological species is "taxonomic inflation," a relatively recent phenomenon, resulting in diversity estimates of taxonomic groups which may be overestimates of real species diversity (Isaac et al., 2004; Robuchon et al., 2019; Sites and Crandall, 1997). Nevertheless, integrative taxonomic approaches that combine multiple, independent, data or character sets (such as external morphological, internal anatomical, ecological, acoustic, and larval traits; apart from geographic considerations, sympatry versus allopatry, and inference of biogeographical range evolution), and rigorous statistical procedures, have become industry-standard (Dayrat, 2005; Padial et al., 2010).

For any standard, two-step (A) proposition of hypothesized species boundaries ("Discovery stage"), and subsequent (B) testing of hypothesized species boundaries ("Validation stage") procedure, it is the data-driven, statistically-defensible species delimitation (Chan et al. 2017; Freudenstein et al., 2016; Sites Jr and Marshall, 2003; Welton et al., 2013) and analytically-reproduceable framework (Fujita et al., 2012; Leaché et al., 2014), that has the potential to withstanding healthy scientific skepticism. Such objective, statistically robust empirical approaches have replaced taxonomic "authority" (subjectivity) and opinion-based classification of 1–4 centuries ago (Boulenger, 1882; Cope, 1889; Duméril and Bibron, 1841; Günther, 1868). To aid the standardization of integrated taxonomy, three categories of variably-characterized candidate species have been adopted: Unconfirmed Candidate Species, Confirmed Candidate Species and Deep Conspecific Lineages (Vieites et al., 2009).

Analytical advances in statistical species delimitation in recent years have relied increasingly on genetic data, especially in groups for which additional data streams are unlikely to become available (Leavitt et al., 2016; Chan et al., 2020). Recent studies have concluded that barcoding approaches, that may adequately serve as a "discovery" stage in two-step species delimitation procedures, may not actually hold much promise for delineating closely related species in subsequent "validation" stages of species delimitation (Brown et al. 2012; Meyer and Paulay, 2005; Welton et al. 2013). However, the perils of basing inferences of species delimitation (and resulting taxonomic changes) solely on mitochondrial marker barcoding approaches have been recognized (Ahrens et al., 2016; Padial et al., 2010). Also, failure rates of using exclusively morphological data or single-marker barcoding confrm that neither should be used as a single information source (Hillis, 1987; Smith and Carstens, 2019). This awareness has resulted in a cultural change in the practice of revisionary taxonomy, which now places an objective burden of proof on authors, necessitates statistical analyses of multiple data streams, with simultaneous (as opposed to iterative) evaluation of multiple, independent sources of information has become the industry standard in final "validation" stage analyses, before taxonomic changes are implemented (Chan et al., 2017, 2018, 2020; Fujita et al., 2012; Jackson et al., 2017; Oliver et al., 2018; Eliades et al. in press).

The tropical frog genus *Nyctibatrachus* Boulenger, 1882 (commonly called Wrinkled- or Night Frogs) currently contains 36 named species-level entities endemic to the Western Ghats mountains of the Indian Peninsula (Biju et al., 2011a; Garg et al., 2017; Krutha et al., 2017). They are the most diverse group in the family Nyctibatrachidae, which is comprised of two other genera *Astrobatrachus* (1 species) and *Lankanectes* (2 species). Until the last decade, 16 species of *Nyctibatrachus* were recognized; but Biju et al. (2011a) named 12 additional new species,

purportedly on the basis of one or more adult morphologically "diagnostic" traits, and set the precedent for Gururaja et al. (2014), Garg et al. (2017) and Krutha, Dahanukar and Molur (2017) to since name an additional nine new species based on the 2011 taxonomy. In addition, Van Bocxlaer et al. (2012) published a molecular phylogeny that confirmed the taxonomic changes by Biju et al. (2011) and delineated different clades of *Nyctibatrachus.* One particularly interesting clade comprises of *N. aliciae* Inger, Shaffer, Koshy, and Bakde, 1984, *Nyctibatrachus deveni* Biju, Van Bocxlaer, Mahony, Dinesh, Radhakrishnan, Zachariah, Giri, and Bossuyt, 2011, *N. periyar* Biju, Van Bocxlaer, Mahony, Dinesh, Radhakrishnan, Zachariah, Giri, and Bossuyt, 2011 and *N. pillaii* Biju, Van Bocxlaer, Mahony, Dinesh, Radhakrishnan, Zachariah, Giri, and Bossuyt, 2011); which we will henceforth refer to as the ***aliciae*** group [= Van Bocxlaer et al.'s (2012) *aliciae* group], and which were all included in their phylogenetic estimate, based on three mtDNA fragments (16S, ND1, $tRNA^{LEU}$) and one nuclear (Tyrosinase) gene. The type localities of these four species are geographically separated; the greatest aerial distance between such localities (*N. deveni* and *N. pillaii*) is ~230 km (see Fig. 1A).

As members of the ***aliciae*** group, these four species form a clade sister to *N. vasanthi* and *N. poocha* (Garg et al., 2017), and are all restricted to the mountain sub-ranges south of the Palakkad Gap, the most prominent geological discontinuity in the otherwise linear and continuous Western Ghats (Fig. 1A). *Nyctibatrachus aliciae*, the earliest described species in this clade, was described from Ponmudi, a spur hill in the southernmost Agasthyamala Hill Range (Inger et al., 1984). The type localities of the other five species in this clade are summarized in Fig. 1.

In this study, we attempted to replicate the ***aliciae*** group classification (i.e., consisting of four demonstrably distinct species) by statistically characterizing multiple axes of variation and

simultaneously assessing them for geographical and taxonomic points of intersection (e.g., by evaluating if geographic ranges and taxonomic characters overlap) and characterizing both for the presence/absence of discrete differences (non-overlapping ranges of trait values) in character states of acoustics (male vocalizations: the primary anural mate-recognition signal), ecological, and larval/developmental morphological variation. Together with new data on adult morphology, reproductive behavior, habitat preferences, molecular genetic information, and greatly improved biogeographic range/occurrence data, we re-evaluate the taxonomy of Night Frogs. Here we present the results of our comprehensive study of the ***aliciae*** group + *N. vasanthi* + *N. poocha* clade as a first step in reconsidering the degree to which the last century's typological approach has resulted (or not) in defensible, demonstrably diagnostic units of species-level diversity.

MATERIALS AND METHODS

We consider the Biju et al. (2011), Gururaja et al. (2014), Garg et al. (2017) and Krutha, Dahanukar and Molur (2017) studies as having accomplished the first stage of an industry-standard two-stage species delimitation analysis (Chan et al. 2017; Freudenstein et al., 2016; Fujita et al., 2012). These studies have used Sanger data, consisting of one or two gene regions, and identified genetically divergent individuals, purportedly justified to represent new species by genetic cut-offs of 7–9%, as measured by uncorrected p-distances of mtDNA. This "discovery" step was used to identify and justify describing putative species in the ***aliciae*** group + *N. vasanthi* + *N. poocha* clade. Because we consider these entities unconfirmed candidate species (Vietes et al. 2008), which have not yet been confirmed via discrete character state differences or other independent data stream, we implemented the following multi-step species validation process.

Fieldwork and sampling.—We conducted field studies in intervening areas, separating the type localities (Fig. 1A) of all six species of Night Frogs (of the ***aliciae*** group + *N. vasanthi* + *N. poocha* clade) and collected two adult specimens of each named taxon, from each type locality (except for *N. pillaii*, for which we collected individuals from adjacent sites outside the protected area network). Additionally, we observed and collected adult and larval specimens from intermediate sites between pairs of type localities, from elevational ranges of 140–1450 m above sea level (Appendix 1). We photographed tadpoles and adults in life, then staged the tadpoles (Gosner, 1960), euthanized both tadpoles and adults in 5% lidocaine, preserved their tissues for genetic material, and fixed voucher specimens in 10% neutral-buffered formalin. After two days in formalin, adult specimens were transferred to 70% ethanol.

Phenotypic data collection.—Definitions of measurements (rounded to nearest 0.1 mm) and terminology for adult frogs follow Biju et al. (2011b), after independently reviewing their mensural characters. Specimens were vouchered and deposited in the Natural History Museum, Trivandrum (TNHM), India (Appendix 1). We also measured all original type specimens of all six purported species in the museum of the Zoological Survey of India, Western Ghats Field Research Station, Kozhikode, India (ZSI/WGFRS). We recorded larval morphological measurements (see Appendix 3 for list of characters) [to the nearest 0.1 mm, with Mitutoyo calipers, following Altig and McDiarmid (1999)] from preserved specimens. Characters such as skin texture, shape of the tips of terminal phalanges, and extent of interdigital webbing of the foot were critically reconsidered for all specimens, with a goal of quantitatively describing variation in proportions, shape, and presence/absence of distinct structures.

Phenotypic data analyses.—Raw morphological measurements were obtained both from individuals documented in Biju et al. (2011; table 2) and our collection (Appendix 2). Due to differences in body size and to eliminate bias caused by ontogenetic variation, each character (except SVL) was scaled to the same size by adjusting their shape according to allometry (Thorpe, 1983; Lleonart et al., 2000). Measurements were adjusted for allometric growth using the following equation: $X_{adj} = \log (X) - \beta [\log (SVL) - \log (SVL_{mean})]$, where X_{adj} = adjusted value; X = measured value; β = unstandardised regression coefficient for each population; SVL = measured snout-vent length; SVL_{mean} = overall average SVL of all samples. All downstream analyses were performed on the adjusted values in the statistical software environment R v.3.5.2 (Team, 2019). We then performed principal component analysis (PCA) to find the best minimum-dimensional representation of external phenotypic variation in the data and to further determine whether continuous morphological variation could form the basis of statistically detectable group structure. Principal components with eigenvalues of 1.0 or more were retained in accordance to Kaiser's criterion (Kaiser, 1960). The R package "hypervolume" (Blonder et al., 2014) was used to construct hypervolumes using Gaussian kernel density estimation to estimate the probability density function of the retained principal components. An ANOVA was performed on the same dataset to determine whether the means of morphological characters differed significantly among populations, followed by a Tukey HSD test to determine specifically, which population pair of character means differed after adjusting for multiple comparisons (Abdi and Williams, 2010). These morphological analyses were performed and visualized in R (Team RDC 2019).

Molecular data collection and analyses.—We extracted total genomic DNA from five *Nyctibatrachus* specimens (four *N.* cf. *aliciae* samples included previously unsampled intermediate locations, as was a single *N. poocha*) with Qiagen DNeasy extractions. A ~570-bp segment of mitochondrial DNA, corresponding to a portion of the ribosomal subunit (16S rRNA) (Frost et al., 2006), was amplified with standard polymerase chain reaction (PCR) (Palumbi, 1996). Raw reads were quality trimmed, filtered, error corrected, and aligned using default parameters of the MAFFT algorithm (Katoh and Standley, 2013), implemented in Geneious Prime® version 2019.1.3 (Kearse et al., 2012). Resulting alignments were subsequently refined (adjusting ambiguous sites to conservatively reduce or eliminate parsimony-informative positional information) by eye in the Geneious program and new sequences were deposited in GenBank under accession numbers MN496458–MN496462. A combined/concatenated dataset of 2172 bp was assembled from Biju et al.'s (2011) original dataset, augmented with our newly-collected data. We also included three samples of *Lankanectes* (the endemic Sri Lankan sister genus of *Nyctibatrachus*) and *Astrobatrachus* (another Western Ghats endemic nyctibatrachid) as outgroups and consisted of 570 bp 16S fragments generated in our study, and single exemplar sequences from GenBank with complete 16S, ND1, and TYR (Tyrosinase) data from all described species of *Nyctibatrachus.*

A heuristic Maximum Likelihood (ML) point-estimate of phylogeny was estimated from the 16S mtDNA dataset, using RAxMLv7.2.8 (Stamatakis, 2006) (substitution model: GTR + G; 200 independent best-tree searches; rapid-bootstrapping algorithm with 500 replicates). To obtain an overview of intra- vs. interspecific genetic variation, pairwise uncorrected 16S *p*-distances were calculated in PAUP* 4.0b10 (Swofford, 2001) and visualized as a sequence of ridgeline plots using R (for individual values, see Table S3).

Our uncorrected *p*-distance matrix of the 16S gene include apart from the ***aliciae*** group + *N. vasanthi* + *N. poocha* clade, *Nyctibatrachus minimus* (a miniature species outside of the ***aliciae*** group + *N. vasanthi* + *N. poocha* clade), *Lankanectes* (the sole sister genus within the subfamily Nyctibatrachinae) and *Astrobatrachus* (the sole sister subfamily in the family Nyctibatrachidae).

Molecular species delimitation.—We delimited operational taxonomic units by implementing the tree-based program mPTP ver. 0.2.4 [multi-rate Poisson Tree Processes (Kapli et al., 2017)] for single-locus species delimitation. In order to obtain more robust and comprehensive estimates of intra- versus interspecific divergences, we performed this analysis on a larger phylogeny that included our sequences and representative species of other clades in *Nyctibatrachus*. 16S rRNA sequences for the additional species that were obtained from GenBank (Biju et al., 2011, table 4.) and a ML phylogeny was estimated using IQ-TREE v.1.6.8 (Nguyen et al., 2014). The minimum branch length was first calculated from the aligned sequences, followed by the mPTP analysis using the IQ-TREE phylogeny. Two independent MCMC chains were executed (10,000,000 generations each), with sampling done every 50,000 generations. Convergence between MCMC runs was assessed by examining the combined likelihood values of each run. We present, however, only results pertinent to this study, the ***aliciae*** group + *N. vasanthi* + *N. poocha* clade.

Acoustic data and analyses.—We recorded advertisement calls (Bee et al., 2013) of males from all sites visited with a Roland Edirol R-09HR portable stereo recorder, in uncompressed .wav format at a sampling rate of 44.1 kHz and 16-bit resolution. Recording segments varied from 5 to 15 calls (depending on logistics and safety) and was made from a distance of 50–150 cm. We then visualized recordings using the SEEWAVE R package (Sueur et al., 2008; Team, 2019),

and temporal and spectral properties were analyzed in Raven©Pro 1.5 (Bioacoustics Research Group, Cornell Lab of Ornithology 2012). Call analyses included generating audiospectrograms, oscillograms and a standardized Fast Fourier transformation (FFT), with a frame length of 512 Hz, a time-grid overlap of 99%, and Hann windows. We adopted a common, simple definition of a call and defined calls as an entire assemblage of acoustic signals produced in a given sequence (Duellman and Trueb, 1986). Ambient temperature was noted during call recordings, and temperature around the frog was measured using a Fluke 62 MAX InfraRed Thermometer. Calls are deposited in Cornell University's Macaulay Library of Animal Sounds under accession numbers ML237488– ML237496.

Isolation by distance versus by environment?.—To determine whether observed genetic structure in the ***aliciae*** group could be associated with spatial or environmental processes, we followed Guayasamin et al. (2017) in testing the following hypotheses: (a) Isolation by Distance (IBD), where patterns of genetic differentiation are explained solely by geographic distance, or (b) Isolation by Environment (IBE), where genetic differentiation is explained by environmental isolation (Wang and Summers, 2010).

To test these hypotheses, we used uncorrected *p*-distances of the ***aliciae*** group calculated from 16S sequences (because we had wider sampling across multiple geographic populations only for this gene) as our measure of genetic distance among individuals. Recent studies suggest that Mantel tests generate biases (i.e., low p-values) in systems with autocorrelated variables (Guillot and Rousset, 2013). Hence, we used Multiple Matrix Regression with Randomization (MMRR) to estimate the independent effects on genetic differentiation from geographic distance and environmental dissimilarity among different species from across their range (Wang, 2013).

Next, we used the WorldClim dataset and extracted data from 19 climatic variables for each of the seven study sites, at 30 second resolution (Hijmans et al., 2005). We then performed a principal component analysis (PCA) on the 19 BioClim (bioclimatic) variables to reduce the dimensionality of the data (to eliminate correlation among variables), and selected the first three principal components, which represented 97.1% of the total variation in our dataset. We calculated environmental dissimilarity matrices among sites using Euclidean distances (the distances between any two points) among three PC axes. To estimate geographic distance (i.e. straight-line distance between points in km), we calculated a Euclidean distance matrix in kilometers among study sites. Finally, we used Wang's (2013) MMRR code to quantify how genetic distances respond to changes in geographic and environmental distances (regression coefficients), the overall fit of the model (coefficient of determination), and the significance of each variable (P-values) using 10,000 permutations (i.e. random permutations of a set of distance matrices, which calculates the regression coefficients and coefficient of determination to estimate significance values for all parameters). For this analysis, we used the following R packages: RASTER [for geographic analyses; (Hijmans and van Etten, 2014)], DISMO [for analyses of BioClim variables; (Hijmans and Elith, 2013)], and APE [for calculating genetic distances; (Paradis et al., 2004)].

We follow the Generalized Lineage Species Concept (de Queiroz, 2007) to evaluate the hypothesis of speciation-level divergence (species boundaries reflected by taxonomy) between all pairs of proposed/named species, by attempting to reject the null hypothesis of conspecificity, potentially in favor of accepting an alternate hypothesis of independent species-level lineage status, following *a priori* designated group assignment from Biju et al. (2011)'s taxonomy.

RESULTS

Adult morphology: traditional character state "differences".—Our critical reevaluation of Biju et al.'s (2011) morphological descriptions of the four species in the ***aliciae*** group, plus *N. poocha* and *N. vasanthi* revealed that minimal variation in any quantified dimension can be reproduced and even none can be reproduced using their non-diagnostic character state comparisons, which constituted the diagnoses of newly named taxa (Table 1). In contrast to the purportedly "diagnostic" (= discrete, or non-overlapping, fixed differences among nominal taxa) character "states" that could not be reproduced, little, or no, differences among populations named as *N. aliciae*, *N. pillaii*, *N. periyar* or *N. deveni* (Biju et al., 2011) is evident to us using either solely their specimens (these species' type material) or their specimens together with our additional specimens from the same localities. We present our assessment of each reported "diagnostic" character difference originally reported by Biju et al. (2011), below:

(1) Adult male SVL upper limit for the first three species was reported to be ~25 mm, whereas we find a marginally smaller maximum SVL of 24.2 mm in *N. deveni*. Biju et al. (2011) categorized *N. periyar* as a "medium-sized" species and categorized the other three species as "small-sized" even though all four groups of specimens' maximum SVL falls within a range of 24–25 mm (see Table 1). Given the < 1 mm difference in body size and clear pitfalls inherent in inference of the evolutionary process of speciation based solely on one tail end of a continuously-distributed trait such as body size, we disregard the allegedly "diagnostic" character state difference of "medium-sized" versus "small-sized."

(2) We find major discrepancies in accuracy of Biju et al.'s (2011) morphological description of *N. pillaii*, its phylogenetic placement, reporting of type specimens, and diagnostic

traits, depicted in their photographic figures. We have identified the holotype ZSI/WGRC/V/A/808 from Kakachi to be a subadult of *N. vasanthi* (identified by the species' characteristic linear-ridge skin structure on the limbs and reticulated lateral skin folds; see species diagnosis below; Fig. 2B), which is found sympatric with the purported *N. pillaii*. Photographs of both live and preserved specimens (Biju et al., 2011; figures 47 and 48) are actually of *N. vasanthi*. Thus, we removed the measurements/values from the holotype specimen from our PCA analysis because including these data would clearly confound analysis of morphological data with interspecific variation. We note that Biju et al. (2011) reported the GenBank sequence JF274074 as *N. pillaii* derived from specimen voucher SDB 40286 from Sengalthery, Tamil Nadu, (Biju et al., 2011; tables 2 & 4) on the eastern slopes of the Agasthyamala Hills (this sequence falls sister to the *N. aliciae* population from Ponmudi in the ND1 gene tree; not shown), and is, thus, a member of the ***aliciae*** group. We conclude that it is possible Biju et al. (2011) sequenced tissues from eastern populations of *N. aliciae*, but mistakenly designated a verifiably distinct subadult *N. vasanthi* as the holotype [whose sequence evidently has not been included in the Van Bocxlaer et al. (2012) phylogeny]. We thus find no data support for the distinctiveness or taxonomic validity of *N. pillaii* due to the erroneously unique combination of phylogenetic placement of *N. pillaii* and its conflicting morphological characteristics.

(3) Biju et al.'s (2011) "*finger and toe disc*" characters correspond to no reproducible variation. The character combination of "*third finger disc with dorso-terminal groove, cover notched distally, fourth toe disc with dorso-terminal groove, cover bifurcating distally*" is entirely subjective, cannot be qualitatively confirmed, using the same original specimens, or quantitatively characterized with expanded sampling. We find these

structures to be uniform in all four species of the ***aliciae*** group (Supporting Information, Fig. S2). Additionally, Biju et al. (2011), having mistakenly designated a subadult *N. vasanthi* as the holotype for *N. pillaii*, provided the *finger and toe disc* character of *N. vasanthi* in their description of *N. pillaii*: "*third finger and fourth toe discs with dorso-terminal groove, cover bifurcate distally*." Our study of both the paratype specimens of *N. pillaii* and individuals of the ***aliciae*** group from our own collection (collected from the various type localities), including those from unprotected areas near the type locality show that all four described species possess the same *finger and toe disc* character state, which we document here (Supporting Information, Fig. S2) to provide final correction of these compounded errors. Given that neither the species "Diagnoses" presented in the original Biju et al. (2011) paper, nor our confirmation of (the absence of) variation among all type series show no differences, we find that *N. aliciae*, *N. pillaii*, *N. periyar* and *N. deveni* have the same "*finger and toe disc*" character "state" (Supporting Information, Fig. S2).

(4) The character combination of "*well developed ridge extending from the lip over the tip of the snout to between the nostrils, at which point it bifurcates, producing an inverted 'Y'* are minimally variable. This is not a characteristic trait for any specific species or clade of *Nyctibatrachus*, but a common character in all species in the genus (see Biju et al., 2011). Thus, the *inverted 'Y'* ridge character on the snout being common for all species of *Nyctibatrachus*, it cannot be considered a valid diagnostic character in the sense that its presence/absence varies among species or can be used to distinguish one unconfirmed candidate species from another.

(5) The only skin texture diagnosis offered by Biju et al. (2011) is for *N. aliciae* and *N. deveni* which have the "*dorsal skin with prominent granular projections.*" Our observations of the museum type material and of specimens from our collections reveal that this trait is shared by all individuals of all four purported species of the ***aliciae*** group (Fig. 2I) and, as such, cannot be used to distinguish any one species from any/all others.

(6) Interdigital webbing of the foot is a highly variable character among individuals of the same population (at a single locality), as well as between left and right feet of the same individual in some instances, and so qualitative characterizations (e.g., one specimen more or less webbed than another) of degree of webbing are unreliable for distinguishing species (or populations). We find that interdigital webbing attachment of the right foot differs from that of the left on a single individual of *N. periyar* from Uppukunnu (Fig. 3A; TNHM (H) NY5), where the webbing reaches only up to the third subarticular tubercle on either side of the right Toe IV, while it reaches the base of the toe disc on both sides of the left Toe IV. We also find two individuals of *N. aliciae* from the same population in Ponmudi, with complete webbing (i.e. webbing reaching just below the toe disc on either side of toe IV; Fig. 3B; TNHM (H) NY6) and medium webbing (i.e. webbing reaching just beyond the third subarticular tubercle on one side, and just above the same on the other side of toe IV; Fig. 3C; TNHM (H) NY3). Considering the high levels of intraspecific, and within-individual variation in interdigital webbing of the foot (thus its unreliability as a discrete interspecific diagnostic/taxonomic character in the ***aliciae*** group), we are again forced to disregard the comparative account in Biju et al.'s (2011) description of *N. deveni*'s variation in interdigital webbing of the foot as "diagnostic," of the species. The authors stated that webbing reaches above the third

subarticular tubercle on either side of Toe IV (vs. *N. periyar*'s extent of webbing 'up to the third subarticular tubercle on either side of Toe IV').

(7) Biju et al. (2011) described the canthus rostralis as "indistinct" in *N. deveni*, versus "rounded" in *N. periyar*, but provided no detail on this character for *N. pillaii*. This character was not reported for *N. vasanthi*, but was characterized as "indistinct" in *N. poocha*. Our observation of the series including the types and our own fixed specimens for all species in the ***aliciae*** group + *N. vasanthi* + *N. poocha* show the canthus rostralis as being rounded and the loreal region as concave and downward facing. Lacking any perceivable difference, we consider the dichotomy of Biju et al. (2011) ("indistinct" [degree of prominence] versus "rounded" [shape or degree of angularity between dorsal and lateral surfaces]) to be subjective, non-diagnostic, and of no use for distinguishing any populations/species in this complex.

In conclusion, all seven of the purportedly diagnostic character states for one or more species are found to not vary (uniform across all species), to vary intraspecifically, and/or form continous ranges of variation, with overlapping and subjective "ranges" (e.g., "medium," versus "small") assigned to individual species, but with no discrete gaps in states among proposed species. We conclude that none of the reported discrete, or "fixed," purportedly species-specific, character states are actually correlated with proposed "boundaries" among Biju et al.'s (2011) unconfirmed candidate species.

Tadpole morphology.—We measured tadpoles from different sites of *Nyctibatrachus aliciae* (Ponmudi), *N. deveni* (Nelliyampathy), *N. poocha* (Valparai and Munnar) and *N vasanthi*

(Pandipath and Pandimotta). We use 16S data to genetically confirm the identity of tadpoles to these four described species/populations. We describe the tadpole of *N. aliciae* and *N. deveni* as a single population/taxonomic entity because the larvae of these proposed unconfirmed candidate species are morphologically identical and our traditional, character-based comparisons ("diagnoses") and multivariate analyses of mensural variation in adults demonstrate no discernable differences between these populations.

Nyctibatrachus aliciae: This description is based on two specimens (one from Ponmudi and the other from Nelliyampathy) in Stage 27 (Fig. 4A; Appendix 3). At this stage, larvae of this species have a pale brown body and an off-white tail that has off-white caudal fins. Dorsal surfaces of body with few scattered dark-brown spots; tail covered with irregular dark brown speckles, which extend into caudal fins, albeit at a smaller size. Both ventral and ventrolateral body surfaces with golden or silver iridocytes, in irregularly-spaced clustered rows. Eyes black and gold, of moderate size, positioned dorsolaterally, not visible in ventral view. In lateral view, the body is slightly depressed, with snout rounded. Narial openings closer to tip of snout than distance from eye. Spiracle sinistral, ventrolaterally positioned at midbody; lateral line nonevident. Dorsal caudal fin larger than lower. Oral disc small (Fig. 4D), consisting of anterior and posterior labia, anteroventrally positioned, floral shaped, its periphery framed by large marginal papillae; small submarginal papillae cover entire inner rim of oral disc. Large, finger-like papillae cover entirety of posterior labium and its fringes, forming a single row on inner margin of the anterior labium. Labial tooth rows absent, keratinized jaw sheaths serrated and saw toothed. Upper jaw sheath wide, U-shaped; lower jaw sheath V-shaped. Measurements (mm) of two specimens: total length 53.9, 53.7, body length 15.1, 16, tail length 37, 37.9, body width 9.9, 10.8, body height 6, 7, maximum tail length 6.4, 7.5, lower tail fin height 1.3, 1.8, upper tail fin

height 2.1, 2.7, eye-snout distance 3.6, 5, snout-spiracle distance 7.9, 7.9, internarial distance 1.2, 2.3, interorbital distance 4.2, 4.5, and eye diameter 2, 2.2. Advanced metamorphic stages of the tadpole are shown in Fig. 9.

Nyctibatrachus vasanthi: This description is based on one specimen in Stage 27 (Fig. 4B; Appendix 3). Tadpole body blackish-brown with rusty shades due to presence of copper-colored iridocytes on lateral body surfaces. Tail off-white, paler, with off-white caudal fins and black horizontal band, formed from series of vertically barred, broken bands, extending from central caudal musculature, dorsally and ventrally, partially into caudal fins. Tail with irregular horizontal stripe on anterior half of tail, extending from body posterior portion of body; posterior (caudal) portion of with irregular horizontal stripe formed from prominent black vertical barred blotches, extending throughout both dorsal and ventral fin structures, with few copper-colored iridocytes, organized into irregularly-spaced but clustered lines on ventrolateral body surface. Lateral line system evident in two series of minute golden spots: one on dorsolateral body surface, straight, continuing into the tail; second series circular, incomplete, encircling spiracle. Eyes moderate, black and gold, positioned dorsolaterally, not visible in ventral view. In lateral view, body dorsoventrally depressed; snout rounded. Narial openings located closer to eye than tip of snout. Spiracle sinistral, positioned ventrolaterally at midbody. Caudal fin rounded at tip; upper fin larger than lower. Oral disc small (Fig. 4E), consisting of anterior and posterior labia, anteroventrally positioned, floral shaped, its periphery framed by large marginal papillae; small submarginal papillae cover entire inner rim of oral disc. Large, finger-like papillae cover entirety of posterior labium and its fringes, forming a single row on inner margin of the anterior labium. Labial tooth rows absent, keratinized jaw sheaths serrated and saw toothed. Upper jaw sheath wide, U-shaped; lower jaw sheath V-shaped. Measurements (mm) of one specimen: total length

60.7, body length 16.3, tail length 43.9, body width 9.9, body height 8.1, maximum tail length 8.9, lower tail fin height 1.5, upper tail fin height 2.4, eye-snout distance 4.1, snout-spiracle distance 8.4, internarial distance 2.9, interorbital distance 5.4, and eye diameter 1.5.

Nyctibatrachus poocha: This description is based on two specimens (one from Munnar and the other from Valparai) preserved at Stage 27 (Fig. 4C; Appendix 3), at which this species' larvae have bronze-brown bodies with paler brown tails (pinkish-white in some individuals; observed in the wild, but not collected) off-white caudal fins. Dorsal body surfaces covered in black spots; tail with large black broken bands, extending from central tail musculature dorsally and ventrally into fin structures. Body covered in silver iridocytes, which become more prominent on caudal fins. Silver iridocytes on ventrolateral body surfaces arranged into irregularly-spaced clusters. Lateral line system evident as straight line, running dorsolaterally, continuing onto tail. Eyes, moderate, black and gold, with reddish hue on outer pupil margin, positioned dorsolaterally; not visible in ventral view. In lateral view, body dorsoventrally depressed; snout rounded. Narial openings located at a midpoint between tip of snout and eye. Spiracle sinistral, ventrolaterally positioned at midbody. Upper caudal fin larger than lower. Oral disc small (Fig. 4F), consisting of anterior and posterior labia, anteroventrally positioned, floral shaped, its periphery framed by large marginal papillae; small submarginal papillae cover entire inner rim of oral disc. Large, finger-like papillae cover entirety of posterior labium and its fringes, forming a single row on inner margin of the anterior labium. Labial tooth rows absent, keratinized jaw sheaths serrated and saw toothed. Upper jaw sheath wide, U-shaped; lower jaw sheath V-shaped. Measurements (mm) of three specimens: total length 66, body length 20.3, tail length 45.9, body width 11.5, body height 9, maximum tail length 9.8, lower tail fin height 2.6,

upper tail fin height 2.7, eye-snout distance 3.2, snout-spiracle distance 9.6, internarial distance 3, interorbital distance 5.9, and eye diameter 2.

Adult morphology; multivariate analyses of continuous variation.—We also observe considerable color variation in the ***aliciae*** group both among individuals from the same population, and across populations with no clear association (Fig. 2C–H). Base body color in individuals ranges from ochre brown to rusty brown to dark chocolate brown, with a variety of black or grey mottled patterns on dorsal surfaces and banded patterns on the limbs. In some individuals, a brighter version of the base body color extends as longitudinal dorsal bands from the back of the eyelids to the middle of dorsum. In all individuals, the dorsal surface immediately behind all finger and toe discs sports a bright white bar. The edge of the subocular gland is either bright white or grey color in all individuals.

Results of our PCA analysis of adults show that the first four principal components have eigenvalues of more than 1.0 and together accounts for 75% of the total variance (Supporting Information, Table S1). The first principal component (PC1) has the highest loadings for SL, HL, FL, FAL and EL, indicating that these characters explains most of the variation along the PC1 axis. The second component (PC2) possesses the highest loadings for EL, SVL, SHL and TL. Ordination of the first two principal components shows overlap of all four species in the ***aliciae*** group along both axes (Fig. 5). Results from the PCA analysis indicate significant overlaps in morphological variation among *Nyctibatrachus aliciae*, *N. pillaii*, *N. periyar* and *N. deveni* and that these putative species show no distinct separation in adult morphospace.

Tadpole morphology; multivariate analyses of continuous variation.—In our PCA analysis of the tadpoles of the ***aliciae*** group + *N. poocha* + *N. vasanthi* clade, we could include only five specimens of *N. aliciae* and three of *N. deveni*. The first seven principal components have eigenvalues ≥ 1.0, together accounting for 88% of the total variance (Supporting Information, Table S2). Principal component 1 exhibits loadings for TL, TAL, ED, ODW and TMH, indicating that these characters explain most of the variation along the PC1 axis. Principal component 2 possessed loadings for BL, BH, TMW, ES and SN. Ordination of the first two principal components show non-overlap among *N. aliciae*, *N. poocha,* and *N. vasanthi* along both axes, which leads us to interpret this variation as evidence in favor of three potentially diagnosable species (Fig. 5). In conclusion, and in contrast to adult morphology, we observe distinct separation in larval morphospace in *N. aliciae*, *N. poocha*, and *N. vasanthi*.

Phylogeny and genetic distance.—The results of our ML phylogenetic analysis (for which only the results of the ***aliciae*** group + *N. vasanthi* + *N. poocha* clade are shown here) corroborate previous studies defining this clade, as a monophyletic group consisting of *Nyctibatrachus aliciae*, *N. pillaii*, *N. periyar* and *N. deveni*, along with sister species *N. poocha* and *N. vasanthi*. The placement of *N. vasanthi* in our tree agree with results of Garg et al. (2017) but not those of Van Bocxlaer et al. (2012) with regards to this species' relationship with *N. poocha* (Fig. 1B). Both former studies contained only a single representative tip per proposed species in phylogenetic analyses, so we improve upon this singleton sampling with five additional tissue samples, representing previously unsampled intermediate geographic localities (Fig. 1A; a–d).

The average inter-subfamilial 16SrRNA pairwise divergence in Nyctibatrachidae (between Nyctibatrachinae and Astrobatrachinae) is 18.6% (Fig. 6). Within the subfamily

Nyctibatrachinae, the average intergeneric divergence between *Nyctibatrachus* and *Lankanactes* is 14.6%. Within the ***aliciae*** group + *N. vasanthi* + *N. poocha* clade, the average interspecific divergences between *N. vasanthi* and *N. poocha* is 8.3% and 8.7% among *N. poocha* + *N. vasanthi* and other samples of the ***aliciae*** group.

Within the ***aliciae*** group, the lowest interspecific divergence is 1.3% (between *N. deveni* and *N. periyar*) and the highest is 4.2% (between *N. pillaii* and *N. periyar*). The intraspecific divergence between individuals of *N.* cf. *deveni* in Kadalar in the High Ranges (55 km aerial distance from the type locality) and Uppukkunu in the Cardamom Hills [680 m above sea level (ASL); 78 km aerial distance from the type locality] is 0%, even though the type locality of *N. periyar* is also on the Cardamom Hills (815 m ASL; 44 km aerial distance from Uppukunnu); these localities include no significant shifts, perceivable breaks, or detectable gradients in habitat types, temperature, precipitation, or elevation.

Our exploration of uncorrected *p*-distances of the other two genes [TYR and ND1 (table 1 of Biju et al., 2011)] used in this study has yielded a similarly continuous range of divergences, smoothly scaling from intraspecific to "interspecific" [interpreted by Biju et al. (2011) and cited as support for taxonomic changes and new "species" descriptions (Supporting Information, Fig. S1)].

Molecular species delimitation.—Our mPTP analysis inferred a total of five species in the ***aliciae*** group (with three species) + *N. vasanthi* + *N. poocha* clade (Fig. 1C). The topology was similar to the concatenated ML topology (Fig. 1B), even with the inclusion of two additional 16S rRNA GenBank samples from different individuals. The first species (Sp.1) comprises all the *N. poocha* samples, while the second species (Sp. 2) is *N. vasanthi*. The third species identified by

the analysis includes all the species of the ***aliciae*** group, including Biju et al.'s (2011) proposed species: *N. aliciae*, *N. periyar*, *N. pillaii* and *N. deveni* (Fig. 1C).

Bioacoustic analysis of male mate-recognition signals.—Males of all species belonging to the ***aliciae*** group + *N. poocha* + *N. vasanthi* have paired lateral vocal sacs (Fig. 8A & 8I). Advertisement calls of all four species of the ***aliciae*** group are recorded from a range of elevations, and all species make the same repertoire of two call variants, which we call Type 1a and Type 1b. In *N. aliciae* from the type locality on the slopes of Ponmudi (all calls recorded at ambient temperatures of 28.2 ± 0.5 ºC), the Type 1a call consists of a rapid 'twoi' with a dominant frequency of 1,550 Hz and call duration averaging 0.31s (mean = 0.31, range = 0.26–0.41, SD = 0.05, n = 7; Fig. 7B). The Type 1b call is an extended 'shirrrr,' which seems like a drawn-out variant of Type 1a, with spectral modulation and a dominant frequency of 1,378 Hz and call duration of 1.04 s (n = 2; Fig. 7A). The Type 1a call of *N. periyar* (recorded at 21.7 ºC) at the type locality of Vallakadavu is also a fast 'twoi,' with a dominant frequency of 1,550 Hz and call duration averaged 0.35 s (mean = 0.35, range = 0.15–0.33, SD = 0.05, n = 23; Fig. 7C), and the Type 1b call has a dominant frequency of 1,550 Hz and call duration of 0.94 s (mean = 0.94, range = 0.86–0.98, SD = 0.06, n = 4). For *N. deveni*, we could make recordings of only the Type 1a call of individuals, but from two sites; one at the type locality of Nelliyampathy and the other at Kadalar. The Nelliyampathy call (recorded at 25.9 ºC) has a dominant frequency of 1,875 Hz and call duration of 0.2 s (n = 1; Fig. 7D), while the Kadalar call (recorded at 21 ºC) has a dominant frequency of 2,625 Hz and call duration of 0.22 s (mean = 0.22, range = 0.20–0.26, SD = 0.02, n = 9; Fig. 7E). Type 1a calls for *N. pillaii* (recorded between 24.4 ± 0.5 ºC)

from Kakachi near the type locality of Sengaltheri has a dominant frequency of 3,375 Hz and call duration of 0.14 s (mean = 0.14, range = 0.13–0.16, SD = 0.01; n = 4).

Nyctibatrachus poocha (recorded at Kadalar at an ambient temperature of 18.5 ºC) produces only one type of advertisement call, a kitten-like 'paow,' with a dominant frequency of 1,875 Hz and average call duration of 0.28 s (mean = 0.28, range = 0.11–0.56, SD = 0.11; n = 50; Fig. 7F). The call of *N. vasanthi* (recorded both at Pandimotta in Shendurney Wildlife Sanctuary, and at the type locality in Kakachi, at an ambient temperature of 22.3 ± 1.5 ºC) is typically a long 'shtrrrreeew,' with a dominant frequency of 2,437 Hz and an average call duration of 1.04 s (mean = 1.04, range = 0.89–1.25, SD = 0.15; n = 7; Fig. 7G).

Elevational Stratification.—We have never succeeded in documenting, nor are we aware of any records for *Nyctibatrachus vasanthi* or *N. poocha*, below 700m ASL. Thus, both species apparently are elevationally/ecologically isolated from one another by the Shencottah Gap, which divides the Agasthyamala Range from the Nelliyampathy Hills-High Ranges-Cardamom Hills-Pandalam Hills complex. However, we observe species of the ***aliciae*** group across elevations of 80–1450m ASL, with continuous populations from Nelliyampathy Hills in the north to Mahendragiri in the south spanning 270 km north to south, with populations even in the Shencottah Gap at 80m ASL (Fig. 1).

Isolation by Distance versus by Environment.—Our MMRR analysis shows that geographic (measured as straight-line distance in km) and environmental dissimilarity (measured using the first three axes from the PCA of 19 BioClim variables) within the geographic range of the ***aliciae*** group do not explain genetic differentiation among populations (Supporting Information, Table

S4; Fig. S1). PC loadings and alternative results using a subset of uncorrelated BioClim variables can be found in Supporting Information, Table S4. Temperature and precipitation variables were strongly associated with these PC axes. An alternative analysis that selects uncorrelated raw climatic variables is also not significant and is therefore consistent with the PCA results (see Table 2 for details). We consider this lack of support for isolation by environment (quantified genetic variation unrelated to environmental variables), as supportive of the interpretation that the various populations of the ***aliciae*** group form a continuous range of intra-populational variation, which cannot be characterized as different species, demonstrably adapted to (or "specialized" on), distinct microhabitats.

Natural History and Breeding Behavior.—*Nyctibatrachus aliciae* is found among rocky substrates along forested streams, with males typically vocalizing upside down from the undersides of boulders; males also call from crevices and cracks along seepages. All three unconfirmed candidate species of the ***aliciae*** group occur in the same sets of habitats (and precisely same microhabitats) throughout the 270 km-long geographical range of this group (= single species). Our IBE analysis corroborates these results, with the principal loading (PC1) axis of the correlation of bioclimatic variables with species of the ***aliciae*** group clustering together (Supporting Information, Table S5), which suggests no significant difference among habitat types of the four putative species of the ***aliciae*** group.

We find no differences in the breeding behavior of *N. aliciae*, *N. periyar* or *N. deveni* for which we made detailed observations. This account of breeding behavior of *N. aliciae* is made at Ponmudi at an elevation of 820 m ASL. At 21:32 on 20 June 2018, a male was making the Type 1b calls continuously from under an overhanging boulder on the stream's edge, directly above

the water column. The male stopped calling briefly when a female approached him. At 21:37, he resumed making calls after the female moved towards the potential oviposition spot (Fig. 8A), stopped calling and mounted her from her rear quarters, clasping her dorsally on her back in what is not truly inguinal amplexus. Then they remained in that posture till 22:02, when he slowly moved his hands towards the female's pectoral region (Fig. 8B). At 22:05, the female began depositing pigmented eggs on the roof of the boulder, soon after making a quivering gesture and with the male separating backwards from the female (Fig. 8C). At 22:16, with oviposition of 17 eggs completed, the female rested adjacent to the clutch. At 22:18, the male climbed onto the clutch and moved in a spinning manner over it (Fig. 8D), where the femoral glands came in contact with most of the eggs, but we are uncertain if this has any bearing on fertilization or larval development. By 22:30, the female moved away from the vicinity, leaving the male and the egg clutch. We have observed males guarding clutches (egg jelly is always clear and never covered with any substrate) at various developmental stages (Fig. 8E, 8F & 8G) deposited as a result of amplexus with different females, at similar habitats throughout the distribution range of *N. aliciae*, *N. pillaii*, *N. periyar* and *N. deveni*. Clutch sizes observed in different pairs ranged from 11 to 19.

We observed several *Nyctibatrachus poocha* males calling from moss-covered or bare slopes along stream banks. We noted males guarding egg clutches, deposited at a height of 1.5 to 2 m from the flowing stream, the jelly layer of which was covered in either dust from decaying vegetative debris or mud depending on the oviposition site chosen (Fig. 8H). At all sites where egg clutches were observed, we noted guarding males close beside them (Fig. 8H), many of them vocalizing. Clutch sizes ranged from 6 to 17.

Our observations of *Nyctibatrachus vasanthi* reveals that the males call from the openings of either small crevices between rocks or crab tunnels on sandy banks along hill streams, unless in antagonistic interactions when they call and engage in combat in the open (Fig. 8I). We also observed sand-covered egg clutches on a dried and fallen *Ochlandra* reed above the stream near a burrow with a vocalizing male that we suspect the male was guarding, but this needs to be further verified.

Taxonomic revision.—Based on the evidence provided, we place *N. pillaii* syn.n. in synonymy with *N. vasanthi* (the holotype of *N. pillaii* [ZSI/WGRC/V/A/808] is a subadult of *N. vasanthi*).

***Nyctibatrachus vasanthi* Ravichandran, 1997**

Nyctibatrachus pillaii Biju, Van Bocxlaer, Mahony, Dinesh, Radhakrishnan, Zachariah, Giri, and Bossuyt, 2011 syn.n.

Diagnosis.—*Nyctibatrachus vasanthi* can be distinguished from known congeners by the following combination of characters: (1) small to medium male adult size (SVL 24.5–29.8 mm, N = 6); (2) skin on dorsal surfaces of the body and appendages with fine sinewy linear ridges running parallel to each other, and the lateral surface of body with fine reticulated ridges (Fig. 2K); (3) advertisement call comprising of a 'shtrrrreeew' call; (4) large tadpole with large black blotches over a coppery brown to pale pinkish-brown body and tail; with black vertical bars and; (5) eggs laid in clutches covered with decomposed vegetation or sand/mud typically on mossy/rocky or vegetative substrate above streams.

Distribution.— Restricted to the Agasthyamala Range along an elevational range of 800–1700m ASL.

Although we have presented adult morphology and bioacoustic lines of evidence for little variation between *Nyctibatrachus aliciae*, *N. deveni* and *N. periyar*, we refrain here from undertaking formal taxonomic revision for the ***aliciae*** group, considering the limitations of currently-available molecular analyses (ours and that of Biju et al., 2011), all of which are based on one or two Sanger loci and all of which require confirmation and additional statistical delimitation procedures, based on current-generation, industry standard genomic data, which represents a clear challenge for future studies.

DISCUSSION

Our results derived from revisiting the relationships between described species in the *Nyctibatrachus* ***aliciae*** group + *N. vasanthi* + *N. poocha* clade, in conjunction with our natural history observations, ecological/microhabitat preferences, morphometric analyses of adults and larvae, and new data from name-bearing type specimens of all proposed, but unconfirmed candidate species in this clade fail to replicate past results, purportedly justifying the recognition of several past ***aliciae*** group species, which have been unquestioningly recognized for the last decade (Biju et al., 2011). Our mPTP analysis delimited only three species with the ***aliciae*** clade (lumping three proposed taxa as a single species); along with *N. vasanthi* and *N. poocha*, we are only able to reproduce support for three putative species, albeit with moderate support. Nevertheless, the zero values associated with the ***aliciae*** group provide statistical evidence to the contrary—namely that branches within this clade are associated with the coalescent as opposed

to speciation processes. The moderate support delimiting *N. poocha*, *N. vasanthi*, and the ***aliciae*** group could relate to the sampling available for *N. poocha* and *N. vasanthi*; or, alternatively these too may require taxonomic reconsideration.

It is also understood that populations that are geographically distant from each other also tend to be more genetically divergent (and vice versa), a phenomenon known as 'Isolation by Distance' or IBD (Sexton et al., 2014; Wright, 1943). Consequently, high genetic divergence among geographically distant populations may be an artefact of IBD, as opposed to underlying evolutionary processes that result in reproductive isolation. Therefore, the presence of IBD would indicate that genetic structure is spatially autocorrelated as opposed to being associated with species divergence. In contrast, 'Isolation by Environment' or IBE is an association between genetic distance and environmental variables, which can be an indication of adaptive divergence in response to differing environmental parameters, potentially contributing to speciation (Wang and Bradburd, 2014). The results from our MMRR analysis demonstrated that any environmental dissimilarity within the range of the ***aliciae*** group is not correlated with (and, thus, cannot explain) observed genetic differentiation among populations; thus, the interpretation of different species, residing in isolated patches of distinct habitats or microhabitats is unsupported. Although we did not detect IBD (as would be anticipated in metapopulation lineages that are autocorrelated), to date, limitations in available data and incomplete sampling may, in part, explain our results, which are not negated by mPTP of genetic data, which failed to reject the hypothesis of conspecificity of named entities within the ***aliciae*** group. We hypothesize that the absence of IBD could be due to (a) conspecific populations not necessarily having to be spatially autocorrelated, (b) limitations of our analysis (which featured only few sampled populations), and (c) other evolutionary processes (such as gene flow, non-linear

historical migration routes, etc.). Resolution of these questions, the irreproducibility and subjectivity of *N.* ***aliciae*** group taxonomy, and formal taxonomic resolution of the suspected taxonomic inflation of this clade will require modern statistical species delimitation analyses with genomic-level data sampled from throughout the genomic (Chan et al. 2017, 2020).

We identified a serious mix-up of type series specimens of *N. pillaii*, in which the species' holotype is assignable to another valid, sympatric species *N. vasanthi* [Biju et al. (2011: figure 48A)], whereas genetic material ascribed to it was sampled from a *N. aliciae* individual from Sengaltheri, all of which has caused significant confusion, and which may have allowed for such an egregious lapsus taxonomy to persist in the form of formal taxonomy, unchallenged, until now.

Another error involves a photograph of a live specimen of *N. periyar* [Biju et al. (2011: figure 44A)], which is wrongly attributed to the holotype. In fact, the individual in this figure with reticulated dorsal skin surface (as opposed to a granular one) unquestionably depicts a subadult *N. poocha* (RA, personal observations; Biju et al. 2011; Fig. 50A). Finally, we also found misleading discrepancies in the tadpole descriptions by Biju et al. (2011). Although Biju et al. (2011) provided the purportedly first documentation of tadpole development (from egg to metamorph stage) of *N. aliciae*; we have unequivocally identified larvae in these images as *N. major* (Biju et al. 2011; figure 5C) and *N. beddomii* (Biju et al. 2011; figure 5D, 5E, 5F & 5G) based on a combination of color patterns and size; we are convinced that the confusion resulting from these simple mis-labeling errors and/or inadvertent figure legend switches is to blame for the lengthy period of time that it took the community to identify these mistakes. In this paper, we have provided accurate and revised descriptions of *N.* ***aliciae*** group tadpoles (Fig. 4A and 9); descriptions of *N. major* and *N. beddomii* tadpoles represent an important next step (RA,

unpublished data). Together, all of these examples demonstrate how dependence on traditional, qualitative morphology, even when combined with molecular data encompassing a handful of markers, can result in confusing and misleading taxonomy when the subjectivity of character "states" such as "small," "medium," and "large" are not reinforced with quantitative characterizations of variation, and phenotypic data are not critically evaluated for discrete variation—all of which is crucial for formulation of taxonomic diagnoses that are actually diagnostic (Welton et al., 2013).

Our surveys of mate-recognition vocalizations of males show limited regional variation, yet calls are overwhelmingly similar in harmonic and temporal structure (call types) for all unconfirmed candidate species throughout the range of the cohesive taxonomic unit we refer to as the ***aliciae*** group. However, our acoustic comparisons were affected by limited sample sizes of calling individuals, that corresponded to specimens, due primarily collecting restrictions (permit limitations). Thus, we cannot refute the possibility that our inability to correct for body size, upon which the dominant frequency is dependent, may be associated with variation among populations (Hoskin, James and Grigg, 2009). A comparison of intra- and interspecies *p*-distances demonstrated that mitochondrial genetic variation among four unconfirmed candidate species pairs is inconsistent with levels of interspecific levels of divergence between uncontroversial, clearly diagnosable species pairs *N. poocha* and *N. vasanthi* (Fig. 6; Fig. S1).

Our analyses also demonstrate that geographic and environmental variation do not explain genetic variation among populations of the ***aliciae*** group, rejecting a fundamental tenant of the hypothesis that habitat/microhabitat specialization (or physiological tolerance limits) may have given rise to multiple, isolated "sky island" species (Table 3; Fig. 1).

Finally, our natural history observations show that the different populations of the ***aliciae*** group are unified by life-history strategies and offspring care features such as egg clutches that are never covered up by debris, whereas *N. poocha* and *N. vasanthi* (albeit, based on a single observation of a clutch of sand-covered eggs near a vocalizing male's territory) cover their egg clutches with sand, mud or vegetative debris; this parental care behavioral dichotomy may be a diagnostic trait that separates both these species from *N. aliciae*. Similar egg protection behavior has been noted in other *Nyctibatrachus* clades (Gururaja et al., 2014), and our observations demonstrate that such behaviors are more widespread in the genus.

Our re-evaluation of the taxonomic status of six unconfirmed candidate species belonging to the ***aliciae*** group + *N. vasanthi* + *N. poocha* clade demonstrates an underlying problem manifest in recent and current taxonomic descriptions from the region (Biju et al., 2011; Biju et al., 2014a; Biju et al., 2014b). Utilizing data from adult morphology, habitat preferences, molecular/genetic information, improved biogeographic range/occurrence data, and previously unreported tadpole descriptions, we reveal a case of suspected taxonomic inflation (over-splitting). Every tip (all of which were named as separate species) in the focal clade studied here has been inadequately justified for taxonomic recognition by Biju et al. (2011). All were subsequently included in the phylogeny of Van Bocxlaer et al. (2012), uncritically, as full species. Finding no support for the recognition of three species in Biju et al.'s (2011) and Van Bocxlaer et al.'s (2012) *aliciae* clade, we recommend the collection of genomic data, statistical species delimitation analyses, and reconsideration of the possibility that *N. deveni* and *N. periyar* may need to be placed in synonymy with *N. aliciae*. However, we place *N. pillaii* in synonymy with *N. vasanthi* after our inspection of the holotypes of both published species revealed the serious mix-up explained in our results. Despite having conclusive adult and larval morphological and bioacoustics evidence,

until we have genome-scale data from sampling including intermediate geographic localities, formal taxonomic actions should be held in abeyance to avoid further subjectivity and opinion-based changes to the already convoluted synonymies of the taxa considered here.

It has not escaped our attention that many Asian amphibian groups that have been the focus of recent taxonomic revisionary work, predicated on the accepted assumption of widespread "cryptic" species complexes (Bickford et al. 2007; Chan et al. 2020). Many of these may now warrant additional scrutiny, using integrative taxonomy, modern two-step (discovery/validation) species delimitation procedures, genomic data, and/or robust statistical analyses subjected to multiple independent sources of data (Hillis, 2019). Given the subjectivity and inconsistent, non-diagnostic patterns of character state presentation in past treatments of the ***aliciae*** group + *N. poocha* + *N. vasanthi* clade, we question whether the remaining clades in this genus may be composed of "species" that have the same underlying problems of irreproducibility and possible taxonomic inflation as well. Thus, *Nyctibatrachus* species descriptions following Biju et al.'s (2011) taxonomic procedures—those of Gururaja et al. (2014), Garg et al. (2017) and Krutha, Dahanukar and Molur (2017)—may need to be revisited in this context, in the same way that we have begun the process of revisiting species-level taxonomy of the ***aliciae*** group + *N. vasanthi* + *N. poocha* here. Although the proposed but unconfirmed increase in species numbers may reinforce the conservation status and perceived "importance" of a proposed biodiversity conservation hotspot, amphibian taxonomists must be conservative, hypothesis-based, data driven, and impervious to the criticism of taxonomic inflation (Conix, 2019). To be relevant to conservation biology, amphibian taxonomy must be minimally, or demonstrably, representative of biological diversity, perhaps particularly when involving the inference of microendemism limited to global biodiversity hotspots (Chan et al. 2020; Lawson, 2013; Vietes et al., 2009).

LITERATURE CITED

Abdi, H., & Williams, L. J. 2010. Tukey's honestly significant difference (HSD) test. Encyclopedia of Research Design 3:583–585.

Ahrens, D., T. Fujisawa, H. J. Krammer, J. Eberle, S. Fabrizi, and A. P. Vogler. 2016. Rarity and Incomplete Sampling in DNA-Based Species Delimitation. Systematic Biology 65:478–494.

Altig, R., and R. W. McDiarmid. 1999. Tadpoles: The Biology of Anuran Larvae. University of Chicago Press, Chicago.

Avise, J. C. 2000. Phylogeography: the history and formation of species. Harvard University Press, Cambridge, MA.

Bee, M. A., R. Suyesh, and S. Biju. 2013. Vocal behavior of the Ponmudi Bush Frog (*Raorchestes graminirupes*): repertoire and individual variation. Herpetologica 69:22–35.

Bickford, D., D. J. Lohman, N. S. Sodhi, P. K. Ng, R. Meier, K. Winker, K. K. Ingram, and I. Das. 2007. Cryptic species as a window on diversity and conservation. Trends in Ecology & Evolution 22:148–155.

Biju, S. D., I. Van Bocxlaer, S. Mahony, K. P. Dinesh, C. Radhakrishnan, A. Zachariah, V. Giri, and F. Bossuyt. 2011. A taxonomic review of the Night Frog genus *Nyctibatrachus* Boulenger, 1882 in the Western Ghats, India (Anura: Nyctibatrachidae) with description of twelve new species. Zootaxa 3029:1–96.

Biju, S. D., Garg, S., Gururaja, K. V., Shouche, Y., & Walujkar, S. A. 2014a. DNA barcoding reveals unprecedented diversity in Dancing Frogs of India (Micrixalidae,

Micrixalus): a taxonomic revision with description of 14 new species. Ceylon Journal of Science (Biological Sciences) 43:37–123.

Biju, S. D., Garg, S., Mahony, S., Wijayathilaka, N., Senevirathne, G., & Meegaskumbura, M. 2014b. DNA barcoding, phylogeny and systematics of Golden-backed frogs (*Hylarana*, Ranidae) of the Western Ghats-Sri Lanka biodiversity hotspot, with the description of seven new species. Contributions to Zoology, 83:269–335.

Blonder, B., C. Lamanna, C. Violle, and B. J. Enquist. 2014. The n-dimensional hypervolume. Global Ecology and Biogeography 23:595–609.

Boulenger, G. A. 1882. Catalogue of the Batrachia Salientia s. Ecaudata in the collection of the British Museum. London: British Museum (Natural History).

Brown, J. H. 2014. Why are there so many species in the tropics? Journal of Biogeography 41:8–22.

Carstens, B. C., T. A. Pelletier, N. M. Reid, and J. D. Satler. 2013. How to fail at species delimitation. Molecular Ecology 22:4369–4383.

Chan, K. O., R. K. Abraham, J. L. Grismer, and L. L. Grismer. 2018. Elevational size variation and two new species of torrent frogs from Peninsular Malaysia (Anura: Ranidae: *Amolops* Cope). Zootaxa 4434:250–264.

Chan, K. O., A. M. Alexander, L. L. Grismer, Y. C. Su, J. L. Grismer, E. S. H. Quah, and R. M. Brown. 2017. Species delimitation with gene flow: A methodological comparison and population genomics approach to elucidate cryptic species boundaries in Malaysian Torrent Frogs. Molecular Ecology 26:5435–5450.

Coates, D. J., M. Byrne, and C. Moritz. 2018. Genetic diversity and conservation units: Dealing with the species-population continuum in the age of genomics. Frontiers in Ecology and Evolution 6:165.

Collins, R. A., and R. H. Cruickshank. 2013. The seven deadly sins of DNA barcoding. Molecular Ecology Resources 13:969–975.

Conix, S. 2019. Taxonomy and conservation science: interdependent and value-laden. History and Philosophy of the Life Sciences 41:15.

Cope, E. D. 1889. The Batrachia of North America. US Government Printing Office.

Dayrat, B. 2005. Towards integrative taxonomy. Biological Journal of the Linnean Society 85:407–417.

de Queiroz, K. 1997. The Linnaean hierarchy and the evolutionization of taxonomy, with emphasis on the problem of nomenclature. Aliso 15:125–144.

de Queiroz, K. 1998. The general lineage concept of species, species criteria, and the process of speciation. Endless forms: species and speciation.

de Queiroz, K. 2007. Species concepts and species delimitation. Systematic Biology 56:879–886.

Duellman, W. E., and L. Trueb. 1986. Biology of Amphibians. John Hopkins University Press, Baltimore.

Duméril, C., and G. Bibron. 1841. Erpétologie générale ou histoire naturelle complète des reptiles: comprenant l'histoire génerale des batraciens, et la description des cinquante-deux genres et des cent soixante-trois espèces des deux premiers sous-ordres: les péroméles. Roret.

Freudenstein, J. V., M. B. Broe, R. A. Folk, and B. T. Sinn. 2016. Biodiversity and the species concept—lineages are not enough. Systematic Biology 66:644–656.

Frost, D. R. 2019. Amphibian Species of the World: an Online Reference. Version 6.0. American Museum of Natural History, New York, USA., Electronic Database accessible at http://research.amnh.org/herpetology/amphibia/index.html

Frost, D. R., T. Grant, J. Faivovich, R. H. Bain, A. Haas, C. F. B. Haddad, R. O. De Sa, A. Channing, M. Wilkinson, and S. C. Donnellan. 2006. The Amphibian Tree of Life. Bulletin of the American Museum of Natural History 2006:1–291.

Frost, D. R., and D. M. Hillis. 1990. Species in concept and practice: herpetological applications. Herpetologica 46:86–104.

Fujita, M. K., A. D. Leache, F. T. Burbrink, J. A. McGuire, and C. Moritz. 2012. Coalescent-based species delimitation in an integrative taxonomy. Trends in Ecology & Evolution 27:480-488.

Garg, S., R. Suyesh, S. Sukesan, and S. D. Biju. 2017. Seven new species of Night Frogs (Anura, Nyctibatrachidae) from the Western Ghats Biodiversity Hotspot of India, with remarkably high diversity of diminutive forms. PeerJ 5:e3007.

Gosner, K. L. 1960. A simplified table for staging anuran embryos and larvae with notes on identification. Herpetologica 16:183-190.

Guayasamin, J. M., C. R. Hutter, E. E. Tapia, J. Culebras, N. Penafiel, R. A. Pyron, C. Morochz, W. C. Funk, and A. Arteaga. 2017. Diversification of the rainfrog *Pristimantis ornatissimus* in the lowlands and Andean foothills of Ecuador. PLoS One 12:e0172615.

Guillot, G., and F. Rousset. 2013. Dismantling the Mantel tests. Methods in Ecology and Evolution 4:336–344.

Günther, A. C. L. G. 1868. First account of species of tailless batrachians added to the collection of the British Museum, p. 478-499. *In:* Proceedings of the Zoological Society of London. Vol. 1868.

Hijmans, R. J., S. E. Cameron, J. L. Parra, P. G. Jones, and A. Jarvis. 2005. Very high resolution interpolated climate surfaces for global land areas. International Journal of Climatology 25:1965–1978.

Hijmans, R. J., and J. Elith. 2013. Species distribution modeling with R. R CRAN Project.

Hijmans, R. J., and J. van Etten. 2014. raster: Geographic data analysis and modeling. R package version. 2.

Hillis, D. M. 1987. Molecular Versus Morphological Approaches to Systematics. Annual Review of Ecology and Systematics 18:23–42.

Hillis, D. M. 2019. Species Delimitation in Herpetology. Journal of Herpetology 53:3–12.

ICZN. 1999. International Code of Zoological Nomenclature. Fourth edition, p. 306. International Commission on Zoological Nomenclature, The Natural History Museum, London, United Kingdom [available online at http://www.iczn.org/iczn/index.jsp].

Inger, R. F., H. B. Shaffer, M. Koshy, and R. Bakde. 1984. A report on a collection of amphibians and reptiles from the Ponmudi, Kerala, South India. Journal of the Bombay Natural History Society 81:406–427.

Isaac, N. J., J. Mallet, and G. M. Mace. 2004. Taxonomic inflation: its influence on macroecology and conservation. Trends in Ecology and Evolution 19:464–469.

Jackson, N. D., B. C. Carstens, A. E. Morales, and B. C. O'Meara. 2017. Species delimitation with gene flow. Systematic Biology 66:799–812.

Kaiser, H. F. 1960. The Application of Electronic-Computers to Factor-Analysis. Educational and Psychological Measurement 20:141–151.

Kapli, P., S. Lutteropp, J. Zhang, K. Kobert, P. Pavlidis, A. Stamatakis, and T. Flouri. 2017. Multi-rate Poisson tree processes for single-locus species delimitation under maximum likelihood and Markov chain Monte Carlo. Bioinformatics 33:1630–1638.

Katoh, K., and D. M. Standley. 2013. MAFFT multiple sequence alignment software version 7: improvements in performance and usability. Molecular Biology and Evolution 30:772–780.

Kearse, M., R. Moir, A. Wilson, S. Stones-Havas, M. Cheung, S. Sturrock, S. Buxton, A. Cooper, S. Markowitz, C. Duran, T. Thierer, B. Ashton, P. Meintjes, and A. Drummond. 2012. Geneious Basic: an integrated and extendable desktop software platform for the organization and analysis of sequence data. Bioinformatics 28:1647–1649.

Krutha, K., N. Dahanukar, and S. Molur. 2017. *Nyctibatrachus mewasinghi*, a new species of night frog (Amphibia: Nyctibatrachidae) from Western Ghats of Kerala, India. Journal of Threatened Taxa 9:10985–10997.

Lawson, L. P. 2013. Diversification in a biodiversity hot spot: landscape correlates of phylogeographic patterns in the African spotted reed frog. Molecular Ecology 22: 1947–1960.

Leaché, A. D., M. K. Fujita, V. N. Minin, and R. R. Bouckaert. 2014. Species delimitation using genome-wide SNP data. Systematic Biology 63:534–542.

Leache, A. D., M. S. Koo, C. L. Spencer, T. J. Papenfuss, R. N. Fisher, and J. A. McGuire. 2009. Quantifying ecological, morphological, and genetic variation to delimit species in the coast horned lizard species complex (*Phrynosoma*). Proceedings of the National Academy of Sciences 106:12418–12423.

Leavitt, S. D., P. K. Divakar, A. Crespo, and H. T. Lumbsch. 2016. A matter of time - understanding the limits of the power of molecular data for delimiting species boundaries. Herzogia 29:479–492.

Lleonart, J., J. Salat, and G. J. Torres. 2000. Removing allometric effects of body size in morphological analysis. Journal of Theoretical Biology 205:85–93.

Meyer, C. P., and G. Paulay. 2005. DNA barcoding: error rates based on comprehensive sampling. PLoS Biology 3: 2229–2238.

Oliver, P. M., R. M. Brown, F. Kraus, E. Rittmeyer, S. L. Travers, and C. D. Siler. 2018. Lizards of the lost arcs: mid-Cenozoic diversification, persistence and ecological marginalization in the West Pacific. Proceedings of the Royal Society B: Biological Sciences 285:20171760.

Padial, J. M., A. Miralles, I. De la Riva, and M. Vences. 2010. The integrative future of taxonomy. Frontiers in Zoology 7:16.

Palumbi, S. R. 1996. PCR and molecular systematics. Molecular Systematics 2:205–247.

Paradis, E., J. Claude, and K. Strimmer. 2004. APE: Analyses of Phylogenetics and Evolution in R language. Bioinformatics 20:289–290.

Pfenninger, M., and K. Schwenk. 2007. Cryptic animal species are homogeneously distributed among taxa and biogeographical regions. BMC Evolutionary Biology 7:121.

Pyron, R. A., and J. J. Wiens. 2013. Large-scale phylogenetic analyses reveal the causes of high tropical amphibian diversity. Proceedings of the Royal Society B: Biological Sciences 280:20131622.

Robuchon, M., D. P. Faith, R. Julliard, B. Leroy, R. Pellens, A. Robert, C. Thevenin, S. Veron, and S. Pavoine. 2019. Species splitting increases estimates of evolutionary history at risk. Biological Conservation 235:27–35.

Schlick-Steiner, B. C., F. M. Steiner, B. Seifert, C. Stauffer, E. Christian, and R. H. Crozier. 2010. Integrative taxonomy: a multisource approach to exploring biodiversity. Annual Review of Entomology 55:421–438.

Scott Jr, N. J. 1976. The abundance and diversity of the herpetofaunas of tropical forest litter. Biotropica 8:41–58.

Sexton, J. P., S. B. Hangartner, and A. A. Hoffmann. 2014. Genetic isolation by environment or distance: which pattern of gene flow is most common? Evolution 68:1–15.

Sites Jr, J. W., and J. C. Marshall. 2003. Delimiting species: a renaissance issue in systematic biology. Trends in Ecology & Evolution 18:462–470.

Sites, J. W., and K. A. Crandall. 1997. Testing species boundaries in biodiversity studies. Conservation Biology 11:1289–1297.

Smith, M. L., and B. C. Carstens. 2019. Process-based species delimitation leads to identification of more biologically relevant species. Evolution 74:216–229.

Stamatakis, A. 2006. RAxML-VI-HPC: maximum likelihood-based phylogenetic analyses with thousands of taxa and mixed models. Bioinformatics 22:2688–2690.

Stuart, B. L., R. F. Inger, and H. K. Voris. 2006. High level of cryptic species diversity revealed by sympatric lineages of Southeast Asian forest frogs. Biology Letters 2:470–474.

Sueur, J., T. Aubin, and C. Simonis. 2008. Seewave, a free modular tool for sound analysis and synthesis. Bioacoustics 18:213-226.

Swofford, D. L. 2001. Paup*: Phylogenetic analysis using parsimony (and other methods) 4.0. B5.

Taylor, H. R., and W. E. Harris. 2012. An emergent science on the brink of irrelevance: a review of the past 8 years of DNA barcoding. Molecular Ecology Resources 12:377–388.

Team, R. D. C. 2019. R: A Language and Environment for Statistical Computing. R Foundation for Statistical Computing, Vienna, Austria.

Thorpe, R.S. 1983. A review of the numerical methods for recognising and analysing racial differentiation, p. 404–423. *In*: Numerical Taxonomy: Proceedings of a NATO Advanced Studies Institute NATO ASI series J. Felsenstein, (ed.). Springer Verlag, Berlin, Heidelberg.

Van Bocxlaer, I., S. D. Biju, B. Willaert, V. B. Giri, Y. S. Shouche, and F. Bossuyt. 2012. Mountain-associated clade endemism in an ancient frog family (Nyctibatrachidae) on the Indian subcontinent. Molecular Phylogenetics and Evolution 62:839–847.

Vieites, D. R., K. C. Wollenberg, F. Andreone, J. Kohler, F. Glaw, and M. Vences. 2009. Vast underestimation of Madagascar's biodiversity evidenced by an integrative amphibian inventory. Proceedings of the National Academy of Sciences 106:8267–8272.

Wang, I. J. 2013. Examining the full effects of landscape heterogeneity on spatial genetic variation: a multiple matrix regression approach for quantifying geographic and ecological isolation. Evolution 67:3403–3411.

Welton, L. J., C. D. Siler, J. R. Oaks, A. C. Diesmos, and R. M. Brown. 2013. Multilocus phylogeny and Bayesian estimates of species boundaries reveal hidden evolutionary relationships and cryptic diversity in Southeast Asian monitor lizards. Molecular Ecology 22, 3495–3510.

Wang, I. J., and G. S. Bradburd. 2014. Isolation by Environment. Molecular Ecology 23:5649–5662.

Wang, I. J., and K. Summers. 2010. Genetic structure is correlated with phenotypic divergence rather than geographic isolation in the highly polymorphic strawberry poison-dart frog. Molecular Ecology 19:447–458.

Wiens, J. J., and M. J. Donoghue. 2004. Historical biogeography, ecology and species richness. Trends in Ecology & Evolution 19:639–644.

Wiens, J. J., J. Sukumaran, R. A. Pyron, and R. M. Brown. 2009. Evolutionary and biogeographic origins of high tropical diversity in old world frogs (Ranidae). Evolution 63:1217–1231.

Wiley, E. O. 1978. The evolutionary species concept reconsidered. Systematic Zoology 27:17–26.

Will, K. W., B. D. Mishler, and Q. D. Wheeler. 2005. The perils of DNA barcoding and the need for integrative taxonomy. Systematic Biology 54:844–851.

Wright, S. 1943. Isolation by Distance. Genetics 28:114–138.

Yang, Z. H. 2015. The BPP program for species tree estimation and species delimitation. Current Zoology 61:854–865.

FIGURE CAPTIONS

Fig. 1. (A) map of the southern Western Ghats of India showing estimated distributional range, collection and observation localities of *Nyctibatrachus* species belonging to Left: the ***aliciae*** group (circles); and Right: *N. poocha* (squares) and *N. vasanthi* (polygons). Legend: red = type locality for which genetic samples are available on GenBank; blue = collection locality of specimens and tissues used in this study. Collection localities from previous and current studies: a. Mahendragiri, b. Shendurney, c. Uppukunnu, d. & e. Kadalar, 1. Ponmudi, 2. Sengaltheri, 3. Vallakadavu, 4. Nelliyampathy, 5. Valparai, 6. Kakachi. Samples downloaded from GenBank have respective accession numbers provided respectively. *Nyctibatrachus aliciae* and *N. pillaii* were described from the Agasthymala Hill Range but the former from the western slopes and the latter from the east in Kakachi, whereas *N. periyar* and *N. deveni* were described from Periyar Tiger Reserve in the Pandalam Hills and Kaikatti in the Nelliyampathy Hills respectively (Biju et al., 2011). *Nyctibatrachus vasanthi* was described from Kakachi in the Agasthyamala Hill Range (Ravichandran, 1997) whereas *N. poocha*'s type locality is Munnar in the High Ranges of the southern Western Ghats (Biju et al., 2011). (B) Maximum Likelihood phylogeny of the ***aliciae*** group + *N. poocha* + *N. vasanthi* derived from 2172 bp comprising two mitochondrial (16S and ND1) and one nuclear gene (TYR); newly sequenced individuals from intermediate populations used in this study marked in bold. (C) Species delimitation using mPTP analysis, based on a 16S rRNA ML phylogeny, for which support values at nodes indicate the fraction of sampled delimitations in which a node was part of the speciation process. The analysis strongly supported

the “discovery” step delimitation of Sp. 1 (= *N. poocha*), Sp. 2 (= *N. vasanthi*) and Sp. 3 (= *N. aliciae* + *N. periyar* + *N. deveni* + *N. pillaii*) as distinct species.

Fig. 2. Live adult males of (A) *Nyctibatrachus poocha*; (B) N. vasanthi; (C) N. aliciae from Ponmudi (type locality); (D) *N. pillaii* from Kakachi (type locality); (E) *N.* cf. *aliciae* from Konni; (F) *N. periyar* from Gavi (photograph inverted for comparison); (G) *N. deveni* from Kadalar; (H) *N. deveni* from Nelliyampathy (type locality). Dorsolateral skin texture respectively of (I) *N. aliciae*; (J) *N. poocha*; (K) *N. vasanthi*.

Fig. 3. Variability in foot webbing in the ***aliciae*** group; (A) webbing attachment on the right foot (left) reaches up to the third subarticular tubercle on either side of toe IV of the right foot, while webbing attachments touch intercalary tubercle on either side of toe IV of the left foot; (B) complete webbing, where webbing attachments touch the intercalary tubercle on either side of toe IV of the left foot and; (C) medium webbing, where webbing attachment from toe V reaches up to intercalary tubercle below the toe disc of toe IV and the webbing attachment from toe IV to toe III begins at the third subarticular tubercle of toe IV of the left foot. (A) is a male *N. periyar* from Uppukunnu; (B) and (C) are two individual *N. aliciae* males from the same population in Ponmudi.

Fig. 4. Tadpoles in Stage 27 of (A) *Nyctibatrachus aliciae* (from type locality); (B) *N. vasanthi* (from Pandipath, Kerala); and (C) *N. poocha* (from Valparai, Tamil Nadu). Scale bar = 10 mm. Oral disc structure of (D) *N. aliciae*; (E) *N. vasanthi*; and (F) *N. poocha*, for which there is little variation among the three species.

Fig. 5. PCA plots of morphological variables for adults of the ***aliciae*** group alone (left) and ***aliciae*** group + *N. poocha* + *N. vasanthi* (center) and tadpoles (right) in 2D (top) and 3D (bottom). The principal components are visualized as hypervolumes constructed using kernel density estimation. Geometry of hypervolumes correspond to a minimum convex hull (polytopes) that minimally encloses the data. Axes show the first three principal components and their proportion of variance. Note: The hypervolumes for *N. deveni* and *N. periyar* overlap perfectly, suggesting minimal morphological divergence.

Fig. 6. Comparative uncorrected p-distances at the 16S rRNA gene for different taxonomic ranks in the family Nyctibatrachidae. For each particular rank comparison, the peak in each histogram represent the number of samples included, and the breadth represents range of genetic distances.

Fig. 7. Comparative spectrograms and corresponding oscillograms of advertisement calls of male *Nyctibatrachus* of the ***aliciae*** group + *N. poocha* + *N. vasanthi*. Top: (A) call type 1b of *N. aliciae* from Ponmudi; call type 1a of (B) *N. aliciae* from Ponmudi; (C) *N. periyar* from Vallakadavu; (D) *N.* cf. *deveni* of Kadalar, and; (E) *N. deveni* from Nelliyampathy. Bottom: advertisement call of (F) *N. poocha*, and (G) *N. vasanthi*.

Fig. 8. Breeding behavior of *Nyctibatrachus aliciae*. (A) Male calling with female beside him; (B) male mounting female in loose amplexus; (C) male withdraws backwards off the female, while she lays eggs simultaneously; (D) male sits on freshly laid clutch and rotates over it; (E) freshly laid egg clutch with exposed jelly layer, attached upside down to boulder; (F) egg clutch

with embryos at Stage 10, and; (G) clutch of Stage 19 embryos. Egg clutch protection in *Nyctibatrachus poocha*. (H) Male guarding clutch on a mossy rock overlooking a forest stream; arrow = egg clutch covered with rotting vegetative debris; (I) vocalizing male *Nyctibatrachus vasanthi*.

Fig. 9. Advanced metamorphic stages of *Nyctibatrachus aliciae*. (A) Stage 42; (B) Stage 43; (C) Stage 46.

Supplemental Fig. 1. Top: Isolation-by-distance among sequenced individuals (marked in bold in the 16S heatmap below); Bottom: heatmap of pairwise uncorrected p-distances, calculated from the mtDNA locus (16S, left; ND1, right) in *Nyctibatrachus* species of the ***aliciae*** group + *N. poocha* + *N. vasanthi* clade.

Supplemental Fig. 2. Invariant structure and shape of terminal digital discs (right third finger and left fourth toe) of *Nyctibatrachus* species of the ***aliciae*** group of specimens collected in this study, following Biju et al. (2011). Individuals in each horizontal row belong to continuous populations; across the geographic range of *N. aliciae* [which encompasses all three unconfirmed candidate species described by Biju et al. (2011)]. These specimens are deposited in the TNHM, Trivandrum, Kerala.

APPENDICES

Appendix 1.

Species	Locality	Latitude	Longitude	Elevation (m ASL)	Museum No.	GenBank Acc. No.
N. aliciae	Shendurney	8.868495	77.160821	855	TNHM (H) NY1	MN496458
N. cf. *aliciae*	Uppukunnu	9.824912	76.885721	798	TNHM (H) NY2	MN496459
N. cf. *aliciae*	Mahendragiri	8.417102	77.514027	200	TNHM (H) NY3	MN496460
N. cf. *aliciae*	Kadalar	10.13371	76.999774	1445	TNHM (H) NY4	MN496461
N. cf. *aliciae*	Uppukunnu	9.824912	76.885721	798	TNHM (H) NY5	NA
N. aliciae	Ponmudi	8.763569	77.113989	1025	TNHM (H) NY6	NA
N. aliciae	Konni	9.170126	76.91039	88	TNHM (H) NY7	NA
N. aliciae	Ambanad	9.015081	77.0867	388	TNHM (H) NY8	NA
N. aliciae	Ambanad	9.015081	77.0867	388	TNHM (H) NY9	NA
N. aliciae	Ambanad	9.015081	77.0867	388	TNHM (H) NY10	NA
N. cf. *aliciae*	Uppukunnu	9.824912	76.885721	798	TNHM (H) NY11	NA
N. aliciae	Ponmudi	8.738322	77.122826	455	TNHM (H) NY12	NA
N. aliciae	Ponmudi	8.738322	77.122826	455	TNHM (H) NY13	NA
N. aliciae	Ponmudi	8.728735	77.127618	315	TNHM (H) NY14	NA
N. aliciae	Konni	9.170126	76.91039	88	TNHM (H) NY15	NA
N. periyar	Vallakadavu	9.529731	77.116639	845	TNHM (H) NY16	NA
N. deveni	Nelliyampathy	10.536229	76.676882	955	TNHM (H) NY17	NA
N. poocha	Kadalar	10.127152	76.998083	1328	TNHM (H) NY18	MN496462
N. poocha	Kadalar	10.13371	76.999774	1445	TNHM (H) NY19	NA
N. poocha	Nelliyampathy	10.527134	76.718787	1288	TNHM (H) NY20	NA
N. vasanthi	Pandimotta	8.827011	77.218463	1218	TNHM (H) NY21	NA
N. vasanthi	Pandipath	8.677385	77.193875	1332	TNHM (H) NY22	NA

Appendix 2. Measurements of adult specimens from type and intermediate localities. SVL snout-vent length; HW head width, at the angle of jaws; HL head length, from the rear of the mandible to tip of snout; MN distance from rear mandible to nostril; SL snout length, from tip of snout to anterior orbital border; EL eye length, horizontal distance between bony orbital borders; FAL forearm length, from flexed elbow to base of the outer palmar tubercle; HAL hand length, from base of outer palmar tubercle to tip of third finger, FDI disc width of finger1; FDII disc width of finger II; FDIII disc width of finger III; FDIV disc width of finger IV; SHL shank length; TL thigh length; FOL foot length, from the base of the inner metatarsal tubercle to tip of the fourth toe; TD1 disc width of toe I; TDII disc width of Toe II; TDIII disc width of Toe III; TDIV disc width of toe IV; TDV disc width of toe V.

Species	Specimen No	SVL	HW
N. aliciae	TNHM (H) NY1	21.78	8.97
N. cf. *aliciae*	TNHM (H) NY2	23.98	10.05
N. cf. *aliciae*	TNHM (H) NY3	23.48	9.72
N. cf. *aliciae*	TNHM (H) NY4	26.5	10.06
N. cf. *aliciae*	TNHM (H) NY5	25.03	10.75
N. aliciae	TNHM (H) NY7	23.98	9.77
N. aliciae	TNHM (H) NY8	30.31	12.62
N. aliciae	TNHM (H) NY9	20.16	8.06
N. aliciae	TNHM (H) NY10	21.49	9.25
N. aliciae	TNHM (H) NY11	23.98	10.21
N. cf. *aliciae*	TNHM (H) NY12	21.64	8.76
N. aliciae	TNHM (H) NY13	29.02	11.49
N. aliciae	TNHM (H) NY14	26.5	9.85
N. aliciae	TNHM (H) NY15	18.59	7.57
N. periyar	TNHM (H) NY16	26.5	11.32
N. deveni	TNHM (H) NY17	26.49	11.06
N. poocha	TNHM (H) NY18	30.75	13.07
N. poocha	TNHM (H) NY19	21.6	10.22
N. poocha	TNHM (H) NY20	28.29	12.87
N. vasanthi	TNHM (H) NY21	36.38	14.92
N. vasanthi	TNHM (H) NY22	31.74	14.18

HL	MN	SL	EL	FAL	HAL	TL	SHL
7.42	5.08	3.77	3.26	5.24	5.15	11.51	11.63
7.72	5.45	3.08	4.07	5.45	6.27	11.55	12
7.66	5.3	4.3	3.14	5.45	5.76	12.68	12.21
8.42	6.88	4.63	3.75	6.01	7.28	12.63	11.01
7.05	6.91	4.07	4.35	5.4	6.18	12.91	12.1
7.68	7.28	4.37	3.96	4.89	4.94	11.45	11.65
9.42	7.64	6.22	3.78	6.08	7.17	15.63	13.77
6.95	4.49	3.29	3.53	3.56	4.9	9.49	9.44
7.7	6.16	5.57	5.03	5.15	5.65	11.33	10.93
7.88	5.7	3.56	3.72	5.22	6.48	12.89	11.91
6.97	5.6	4.52	3.73	4.88	5.44	10.72	10.12
8.5	7.01	4.2	4.23	6.16	6.66	14.89	13.99
7.98	6.48	5.38	3.4	4.93	6.32	12.11	12.68
6.62	4.59	3.59	3.57	3.58	4.4	8.83	8.36
7.47	7.57	4.71	3.51	6.09	7.07	14.53	12.7
8.75	6.71	5.21	4.18	6.8	6.73	13.5	12.66
10.71	7.76	5.26	4.85	7.22	6.92	16.24	15.58
6.96	5.38	3.39	3.84	4.83	5.43	12.03	10.8
9.07	8.66	4.79	4.42	5.89	6.7	14.05	13.32
11.4	8.7	5.36	4.89	8.56	8.93	19.98	18.69
8.82	8.9	3.41	4.55	6.99	7.98	16.78	15.94

FOL	FD (Right hand)				TD (Right leg)			
	I	II	III	IV	I	II	III	IV
10.3	0.48	0.42	0.5	0.45	0.77	0.76	0.9	0.7
11.47	0.47	0.46	0.53	0.5	0.75	0.96	0.94	0.72
10.87	0.3	0.46	0.52	0.53	0.9	1.05	0.81	0.73
10.37	0.72	0.85	0.82	0.77	1.05	1.01	1.03	1.09
11.43	0.64	0.6	0.62	0.5	0.9	0.89	1.04	0.99
10.83	0.5	55	0.58	0.59	0.72	0.91	0.86	0.6
13.64	0.61	0.67	0.42	0.4	0.86	1.08	1.02	1.2
7.87	0.31	0.32	0.45	0.34	0.67	0.49	0.45	0.38
10.46	0.55	0.62	0.54	0.66	1.01	1.12	1.08	0.88
11.81	0.47	0.45	0.41	0.39	0.76	0.85	0.75	0.7
10.38	0.42	0.39	0.36	0.37	0.62	0.72	0.64	0.42
12.66	0.6	0.76	0.77	0.7	1	1.01	1.03	0.83
12	0.4	0.54	0.48	0.43	0.76	1	0.85	0.74
7.44	0.22	0.28	0.26	0.22	0.56	0.7	0.55	0.59
12.08	0.74	0.88	0.57	0.57	0.92	1.06	0.9	1.02
11.74	0.49	0.64	0.55	0.38	0.97	0.95	0.82	0.66
15.19	0.53	0.55	0.47	0.49	0.64	0.47	0.7	0.8
10.42	0.38	0.36	0.43	0.3	0.35	0.5	0.49	0.43
13.42	0.41	0.43	0.5	0.53	0.57	0.69	0.65	0.7
16.88	0.75	0.7	0.66	0.83	0.88	1.08	1.14	1.01
13.62	0.59	0.67	0.55	0.53	0.56	0.9	0.84	0.86

V
0.64
0.91
0.3
0.9
0.65
0
0.83
0.37
0.5
0.69
0.51
0.8
0.64
0.51
0.77
0.48
0.66
0.38
0.4
0.78
0.4

Appendix 3. Morphometric measurements (in mm) of 20 meristic characters for *Nyctibatrachus* tadpole specimens (Stages 26–38) of the ***aliciae*** group + *N. vasanthi* + *N. poocha* clade. Measurements are as follows: TTL = total length; BL = body length, i.e., length from snout to body terminus; BH = body height; BW = maximum body width; ED = eye diameter; ES = eye-snout distance; IND = inter-narial distance; IOD = inter-orbital distance; MTH = maximum tail height; LFH = lower fin height (at MTH), UFH = Upper Fin Height (at MTH); NE = distance from center of naris to center of eye; ODW = oral disc width; SN= distance of naris (center) from snout; SS =distance of snout to center of spiracle; TAL = tail length, i.e. length from body terminus to tail tip; TMH = tail muscle height at body-tail junction; TMW = tail muscle width at body-tail junction.

Species	**TTL**	**BL**	**BH**
N. vasanthi	60.68	16.34	8.11
N. vasanthi	51.05	15.88	7.45
N. vasanthi	43.31	12.12	5.67
N. vasanthi	20.05	6.7	3.75
N. vasanthi	24.88	7.09	3.9
N. poocha	39.97	13.98	5.89
N. poocha	59.16	19.04	8.21
N. poocha	69.75	23.11	10.09
N. poocha	48.55	17.39	7.2
N. poocha	66.79	19.7	8.22
N. poocha	61.52	18.17	8.68
N. aliciae	39.65	9.8	5.15
N. aliciae	27.19	8.08	3.71
N. aliciae	53.94	15.11	6.01
N. deveni	53.67	16.03	7.05
N. deveni	32.01	10.09	4.5
N. deveni	29.18	9.71	5.03

BW	ED	ES	IND	IOD	MTH	LFH
9.9	1.48	4.05	2.85	5.42	8.99	1.49
9.88	2.2	3.91	2.7	4.7	7.66	1.22
7.01	1.32	3.04	2.91	4.22	6.45	1.9
3.4	0.99	1.1	1.9	1.87	3.99	1.71
4.22	0.81	1.54	1.66	1.55	3.71	1.08
7	1.01	1.98	1.69	3.22	4.22	1.16
10.78	2.1	3.85	2.87	5.26	8.4	1.57
12.99	2.9	3.11	3.61	7.3	10.51	2.52
8.22	1.89	2.89	2.38	3.59	7.85	2.15
10.28	1.66	3.34	2.84	5.18	9.68	2.91
11.22	1.57	3.29	2.44	5.17	9.08	2.49
5.15	1.41	1.6	1.21	3.89	5.7	1.09
4.41	0.78	1.74	1.69	2.87	3.51	1.19
9.91	1.98	4.98	2.32	4.18	6.44	1.27
10.8	2.17	3.61	1.19	4.51	7.48	1.8
6.01	1.19	2.8	1.99	3.01	4.18	1.1
5.18	0.98	2.19	1.67	2.81	4.9	1.29

UFH	NE	ODW	SN	SS	TAL	TMH	TMW
2.4	2.8	3.88	1.11	8.38	43.99	6.11	5.88
2.11	3	4	1.45	8.09	33.87	5.88	6
2.9	1.5	3.01	3.28	6.99	29.42	4.6	3.12
1.27	1.05	1.5	0.3	4.15	14.81	1.28	1.77
1.91	1.15	1.59	0.39	4.01	16.09	2.77	1.5
1.17	1.11	1.9	0.5	5.99	28.59	3.18	3.55
2.55	2.57	3.43	1.29	9.42	41.91	6.51	6.38
3.1	3.81	5	1.97	11.6	48.79	8.1	7.1
2.56	2.05	3.29	1.06	8.9	31.99	5.28	4.9
2.41	2.9	3.99	1.08	9.95	45.41	5.45	6.88
2.58	2.61	3.37	1.21	7.35	43.37	4.3	6.08
1.1	2	2.91	0.91	6.51	28.19	3.1	3.71
0.9	1.09	1.59	0.98	4.56	19.17	2.98	2.21
2.17	2.1	2.76	1.71	7.9	37.93	3.11	4.23
2.7	2.49	3.8	1.19	7.91	36.97	4.18	3.91
1.81	1.78	2.11	1.4	5.17	21.16	3.76	3.15
1.08	1.04	1.91	1.88	4.99	20.69	2.77	1.4

ACKNOWLEDGMENTS

Our project in the Western Ghats was generously supported by the National Geographic Society (Grant No. EC-58048R-19), the Biodiversity Institute of the University of Kansas and IdeaWild. We are most grateful to K. Vaishnav, E. S. Ganeshan, Geethu Ganesh, K. Shinad, Jobin Mathew, Aravind Anil, Mohammed Ismail, Daniel Raju, David Raju, K. Shiju and Chinnapan for assistance with fieldwork. We are also very thankful to Dr. Arun Zachariah and M. Jishnu for help with DNA extractions, to AgriGenome Labs for sequencing our samples, and to Jafer Palot of ZSI Kozhikode for permitting a study of the type series. Finally, our gratitude extends to the Kerala Forest Department (KFD) for providing access and collection permits to the first and penultimate authors, respectively (WL10-1965/2012 and WL10-38972/2016), and to K. K. Sunil and M. Vimal (ACFs) of the KFD and Dr. Anoop Jayakumar (manager) KLD Bull Station and Farm, Kulathupuzha for logistic support.

Table 1. Morphological diagnoses by Biju et al. (2011) of the different unconfirmed candidate species (named but unvalidated) of *Nyctibatrachus* in the ***aliciae*** group + *N. vasanthi* + *N. poocha* clade.

N. aliciae	***N. deveni***	***N. periyar***	***N. pillaii***	***N. vasanthi***	***N. poocha***
It can be distinguished from known congeners by the following combination of characters:	It can be distinguished from known congeners by the following combination of characters:	It can be distinguished from known congeners by the following combination of characters:	It can be distinguished from known congeners by the following combination of characters:	It can be distinguished from known congeners by the following combination of characters:	It can be distinguished from known congeners by the following combination of characters:
(1) small male adult size (SVL **20.5–25.6** mm);	**(1) small male adult size** (SVL **23.5 ± 0.7** mm, N = 5);	**(1) medium adult size** (male SVL **24.2–25.2** mm, N = 2, female SVL 29.9 mm, N = 1);	**(1) small adult male size** (SVL **20.0–25.4** mm, N = 9);	**(1) small to medium male adult size** (SVL **21.9–27.6** mm, N = 7);	**(1) medium adult male size** (SVL **25.3–32.2** mm, N = 7);
(2) finger and toe discs well	**(2) finger and toe discs well**	**(2) finger and toe discs well**	**(2) finger and toe discs well**	**(2) finger and toe discs well**	**(2) finger and toe discs well**

developed (FDIII 0.6 ± 0.1 mm, FWIII 0.3 ± 0.1 mm, N = 8; TDIV 0.9 ± 0.1 mm, TWIV 0.4 ± 0.1 mm, N = 8);	**developed** (FDIII 0.6 ± 0.0 mm, FWIII 0.3 ± 0.0 mm, N = 5; TDIV 0.7 ± 0.0 mm, TWIV 0.3 ± 0.3 mm, N = 5);	**developed** (FDIII 0.8 ± 0.0 mm, FWIII 0.4 ± 0.0 mm, N =2; TDIV 0.8 ± 0.0 mm, TWIII 0.1 ± 0.0 mm, N = 2);	**developed** (FDIII 0.6 ± 0.1 mm, FWIII 0.3 ± 0.1 mm, N = 9; TDIV 0.8 ± 0.1 mm, TWIV 0.3 ± 0.1 mm, N = 9);	**developed** (FDIII 0.6 ± 0.1 mm, FWIII 0.3 ± 0.0 mm, N = 7; TDIV 0.8 ± 0.1 mm, TWIV 0.4 ± 0.1 mm, N = 7);	**developed** (FDIII 0.7 ± 0.1 mm, FWIII 0.3 ± 0.1 mm, N = 7; TDIV 1.0 ± 0.1 mm, TWIV 0.3 ± 0.0 mm, N = 7);
(3) third finger disc with dorso-terminal groove, cover notched distally, fourth toe disc with dorso-terminal groove,	**(3) third finger disc with dorso-terminal groove, cover notched distally, fourth toe disc with dorso-terminal groove,**	**(3) third finger disc with dorso-terminal groove, cover notched distally, fourth toe disc with dorso-terminal groove,**	**(3) third finger and fourth toe discs with dorso-terminal groove, cover bifurcate distally;**	**(3) third finger and fourth toe discs with dorso-terminal groove, cover bifurcate distally;**	**(3) third finger and fourth toe discs with dorso-terminal groove, cover bifurcate distally**;

cover bifurcate distally;	**cover bifurcate distally**;	**cover bifurcate distally**;			
(4) weakly wrinkled dorsal skin with prominent granular projections;	**(4)** dorsal skin with prominent granular projections;	(4) N/A	(4) N/A	(4) N/A	(4) N/A
(5) well developed ridge extending from the lip over the tip of the snout to between the nostrils, at which point it bifurcates, producing	**(5) well developed ridge extending from the lip over the tip of the snout to between the nostrils, at which point it bifurcates, producing**	**(5) well developed ridge extending from the lip over the tip of the snout to between the nostrils, at which point it bifurcates, producing**	**(5) well developed ridge extending from the lip over the tip of the snout to between the nostrils, at which point it bifurcates, producing**	**(5) well developed ridge extending from the lip over the tip of the snout to between the nostrils, at which point it bifurcates, producing**	**(5) well developed ridge extending from the lip over the tip of the snout to between the nostrils, at which point it bifurcates, producing**

an inverted ‘Y’;	**an inverted ‘Y’**;	**an inverted ‘Y’**;	**an inverted ‘Y’;**	**an inverted ‘Y’**;	**an inverted ‘Y’**;
(6) webbing medium, reaching before the third subarticular tubercle on either side of toe IV.	**(6) webbing medium, reaching above the third subarticular tubercle on either side of toe IV**.	**(6) webbing medium, reaching just above the third subarticular tubercle on either side of toe IV**.	**(6) webbing medium, reaching beyond the third subarticular tubercle on either side of toe IV**.	**(6) webbing medium, reaching before the third subarticular tubercle on either side of toe IV.**	**(6) webbing medium, reaching the third subarticular tubercle on either side of toe IV.**

Table 2. Results of MMRR analysis, based on 16S mtDNA genetic distances and tests of geographic distance vs environmental dissimilarity influence on genetic differentiation among *Nyctibatrachus* populations. This alternative analysis uses the raw climatic variables rather than the axes from a PCA analysis. We assessed the 19 bioclimatic variables for multicollinearity by constructing a Pearson-product correlation matrix from the climatic data. Each variable selected represents one variable from a group of strongly correlated variables (using an arbitrary $p > 0.75$ as the threshold). The results are consistent with those using the first three axes from the PCA and were not significant.

Variable	Coefficient	T statistic	T P-value	F statistic	F p-value
BIO7	0	1.621	0.083	0.609	0.616
BIO6	0	-1.249	0.169		
Geographic	-0.002	-1.215	0.22		
Intercept	0.03	3.005	0.382		
BIO3	0	-0.417	0.659		
BIO9	0	-0.433	0.679		
BIO5	0	0.238	0.784		

Fig. 1

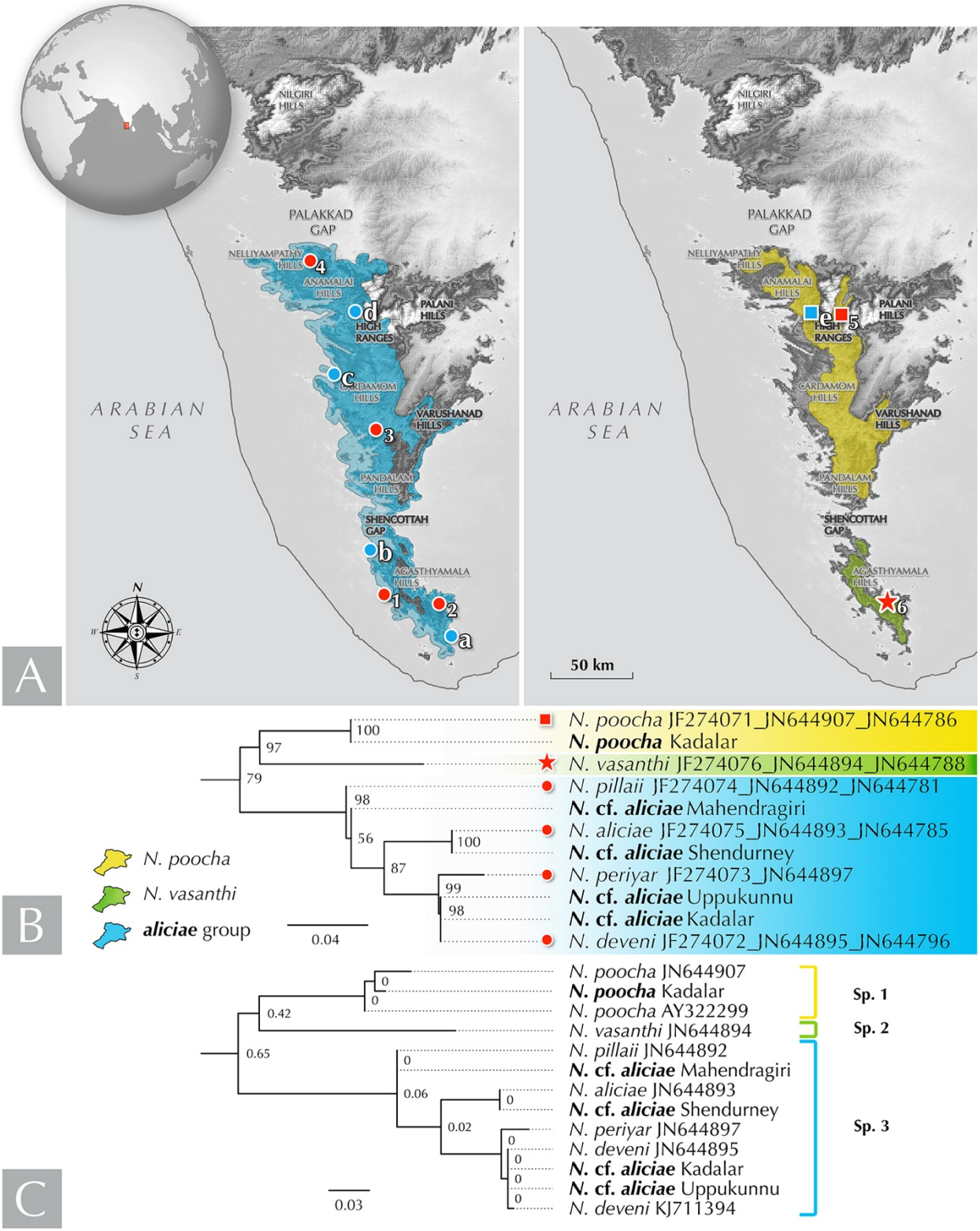
A
NILGIRI HILLS
PALAKKAD GAP
NELLIYAMPATHY HILLS
ANAMALAI HILLS
PALANI HILLS
HIGH RANGES
CARDAMOM HILLS
VARUSHANAD HILLS
PANDALAM HILLS
SHENCOTTAH GAP
AGASTHYAMALA HILLS
ARABIAN SEA
50 km
B
N. poocha
N. vasanthi
aliciae group
0.04
N. poocha JF274071_JN644907_JN644786
N. poocha Kadalar
N. vasanthi JF274076_JN644894_JN644788
N. pillaii JF274074_JN644892_JN644781
N. cf. aliciae Mahendragiri
N. aliciae JF274075_JN644893_JN644785
N. cf. aliciae Shendurney
N. periyar JF274073_JN644897
N. cf. aliciae Uppukunnu
N. cf. aliciae Kadalar
N. deveni JF274072_JN644895_JN644796
C
0.42
0.65
0.06
0.02
0.03
N. poocha JN644907
N. poocha Kadalar
N. poocha AY322299
N. vasanthi JN644894
N. pillaii JN644892
N. cf. aliciae Mahendragiri
N. aliciae JN644893
N. cf. aliciae Shendurney
N. periyar JN644897
N. deveni JN644895
N. cf. aliciae Kadalar
N. cf. aliciae Uppukunnu
N. deveni KJ711394
Sp. 1
Sp. 2
Sp. 3

Fig. 2

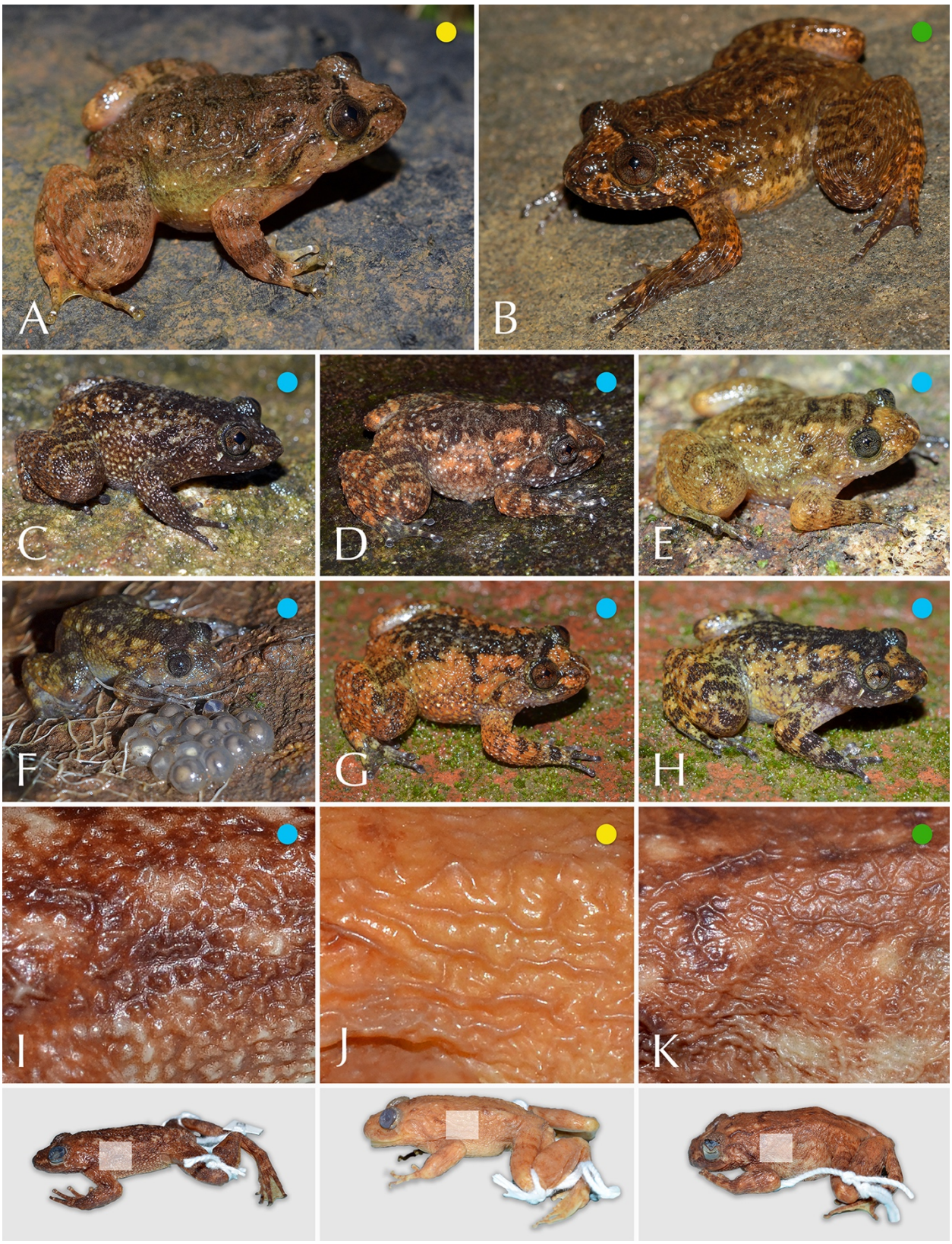

Fig. 3

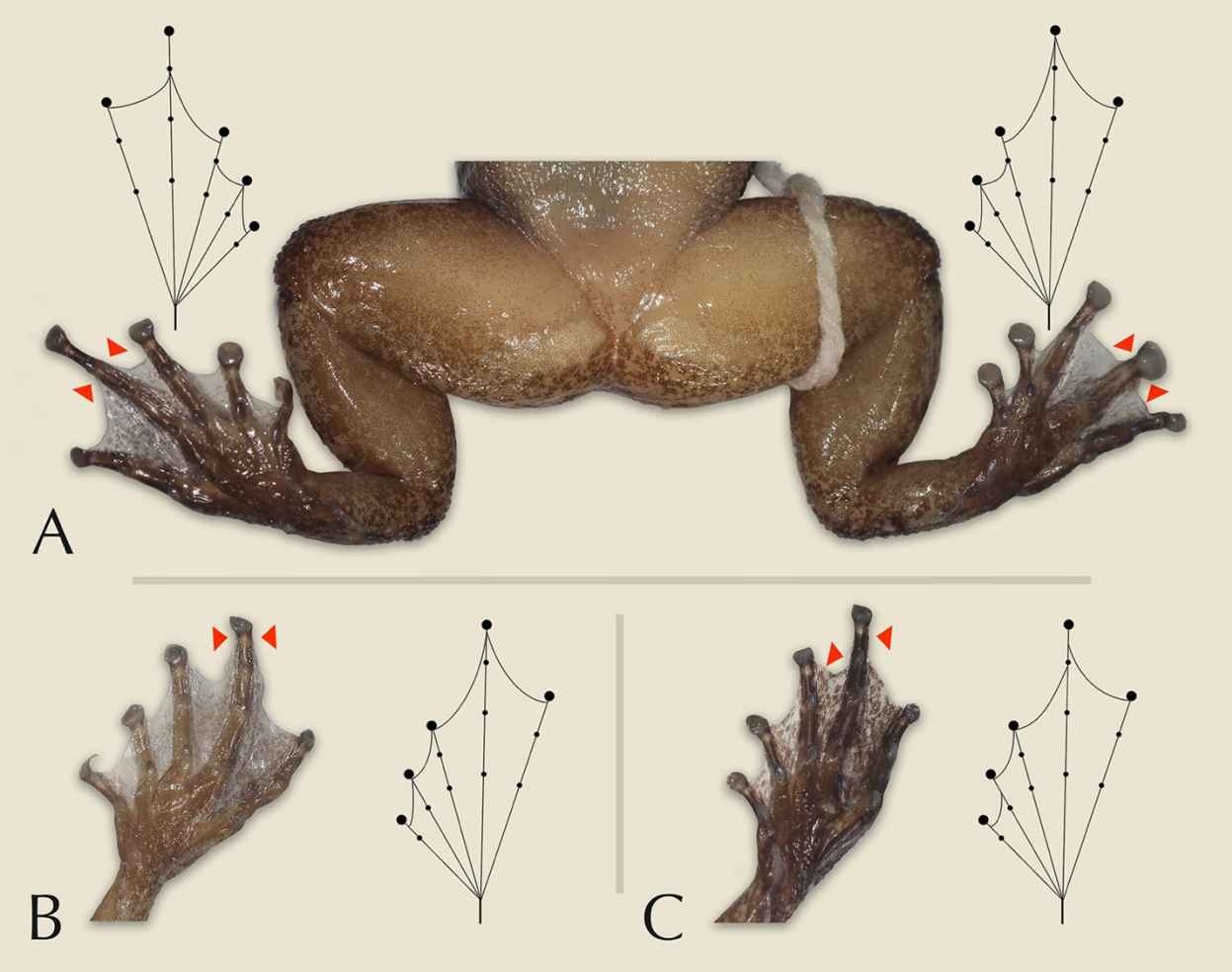

Fig. 4

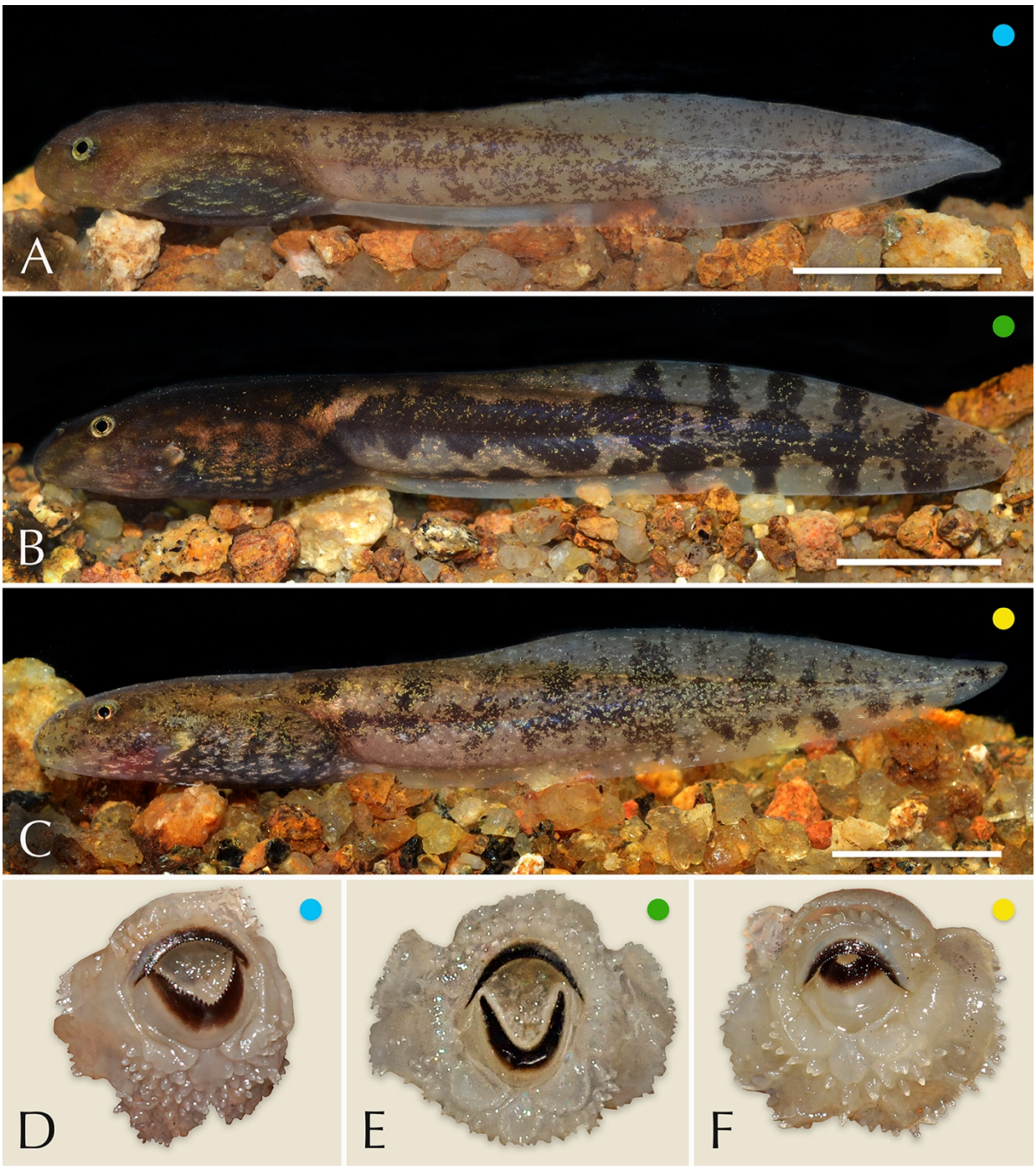

Fig. 5

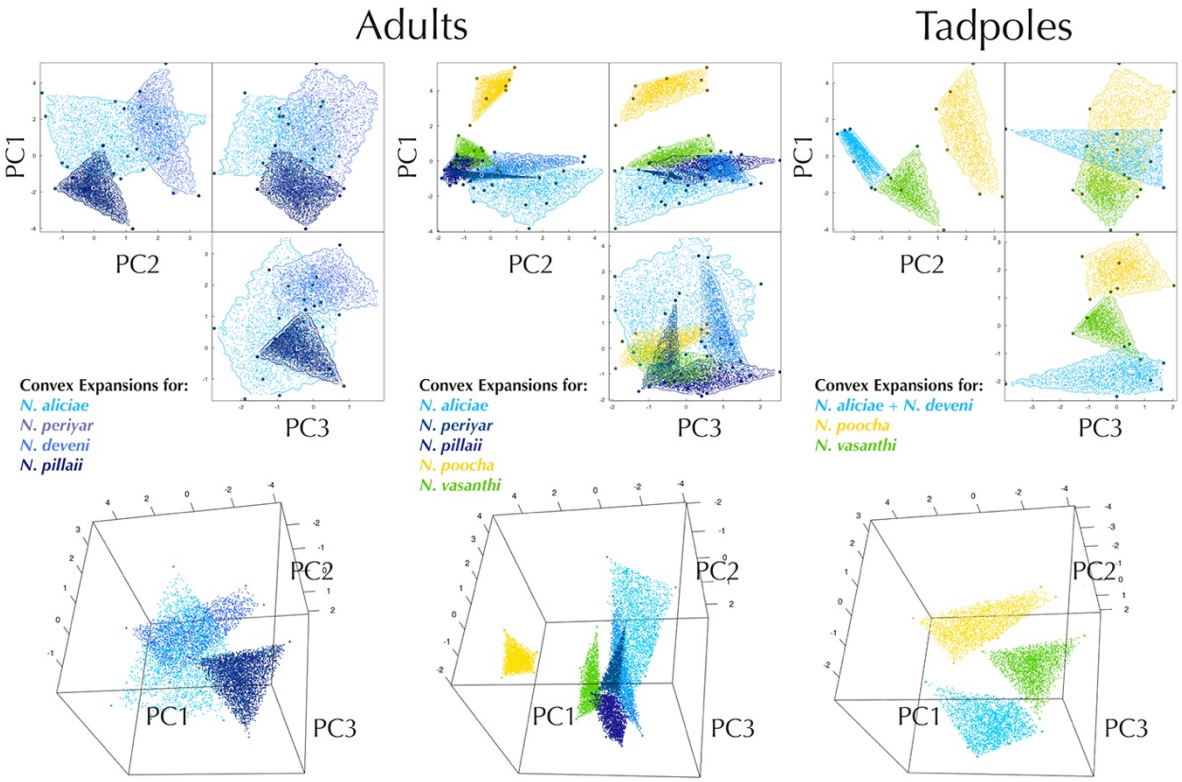
Adults
Tadpoles
PC1
PC2
PC3
Convex Expansions for:
N. aliciae
N. periyar
N. deveni
N. pillaii
Convex Expansions for:
N. aliciae
N. periyar
N. pillaii
N. poocha
N. vasanthi
Convex Expansions for:
N. aliciae + N. deveni
N. poocha
N. vasanthi

Fig. 6

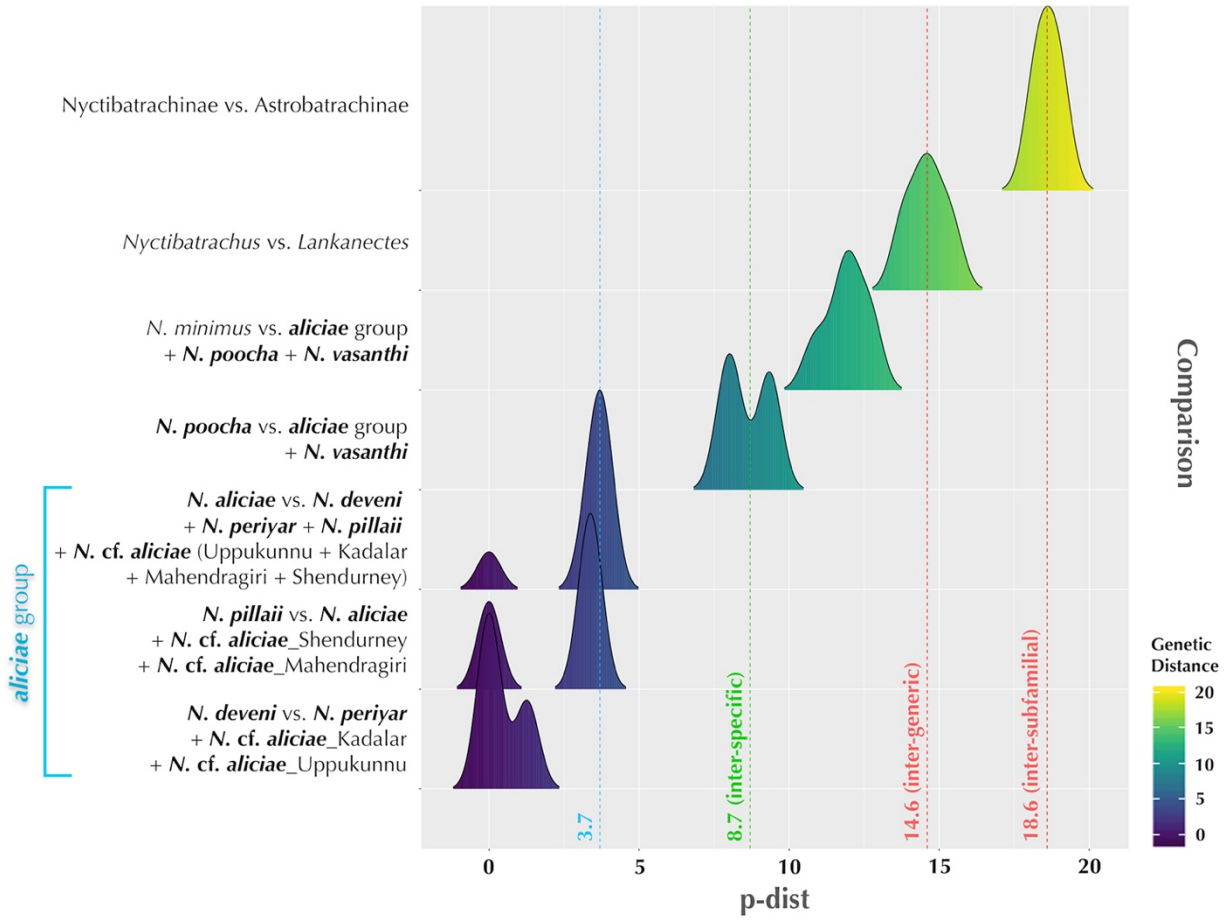
Nyctibatrachinae vs. Astrobatrachinae
Nyctibatrachus vs. Lankanectes
N. minimus vs. aliciae group + N. poocha + N. vasanthi
N. poocha vs. aliciae group + N. vasanthi
N. aliciae vs. N. deveni + N. periyar + N. pillaii + N. cf. aliciae (Uppukunnu + Kadalar + Mahendragiri + Shendurney)
N. pillaii vs. N. aliciae + N. cf. aliciae_Shendurney + N. cf. aliciae_Mahendragiri
N. deveni vs. N. periyar + N. cf. aliciae_Kadalar + N. cf. aliciae_Uppukunnu
aliciae group
3.7
8.7 (inter-specific)
14.6 (inter-generic)
18.6 (inter-subfamilial)
0
5
10
15
20
p-dist
Comparison
Genetic Distance
20
15
10
5
0

Fig. 7

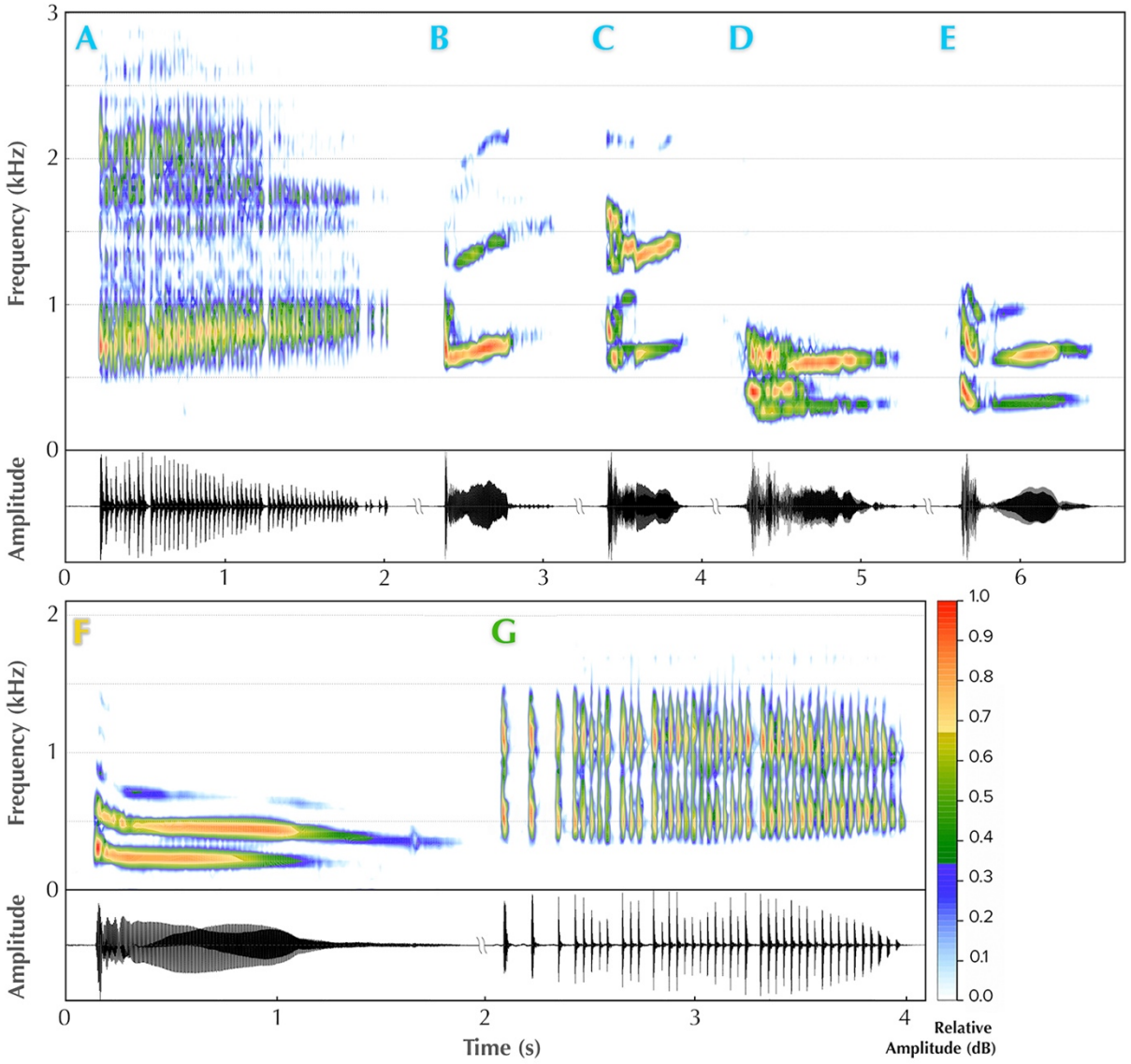
A
B
C
D
E
F
G
Frequency (kHz)
Amplitude
Time (s)
Relative Amplitude (dB)
1.0
0.9
0.8
0.7
0.6
0.5
0.4
0.3
0.2
0.1
0.0

Fig. 8

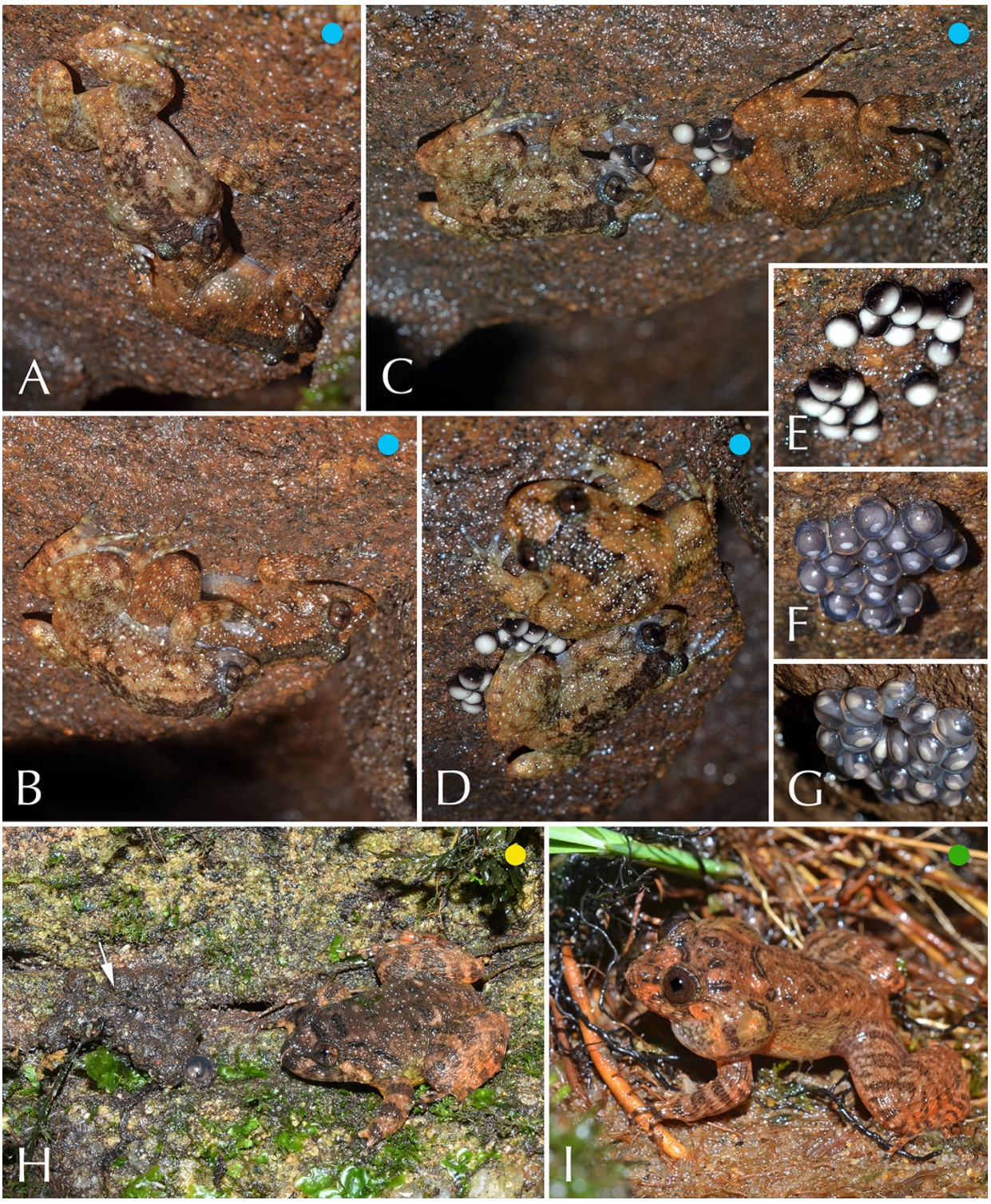

Fig. 9

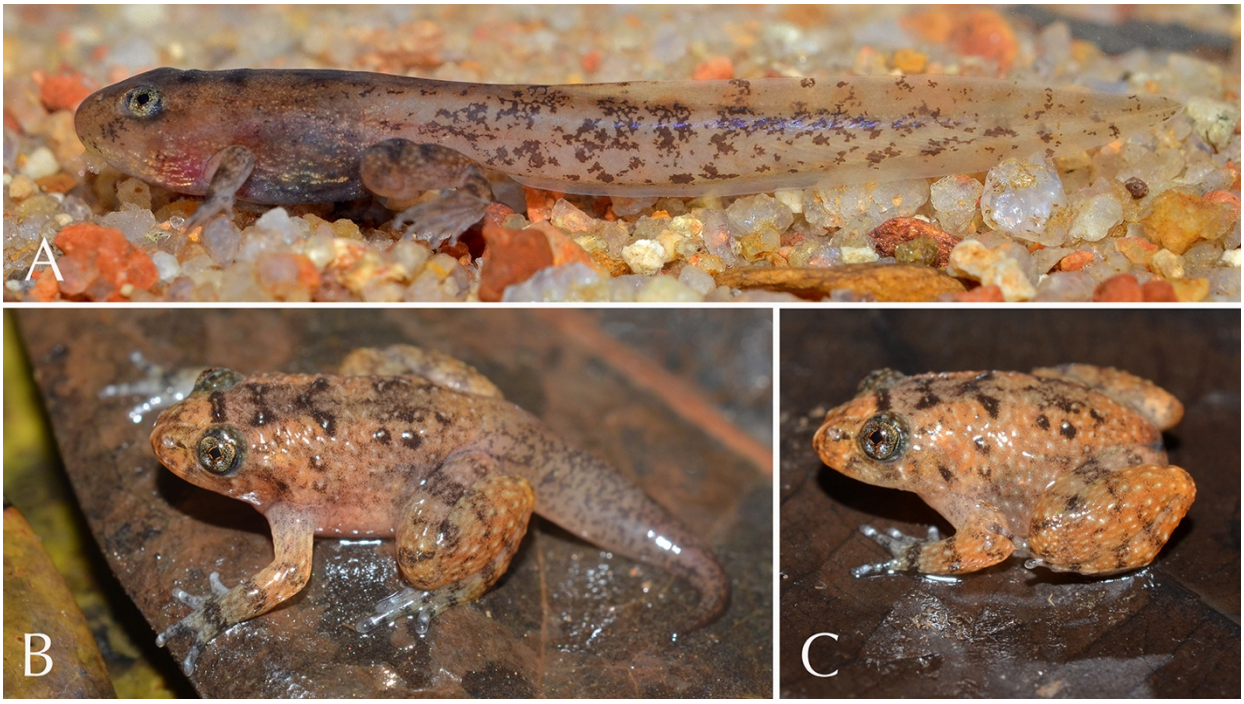

Fig. S1

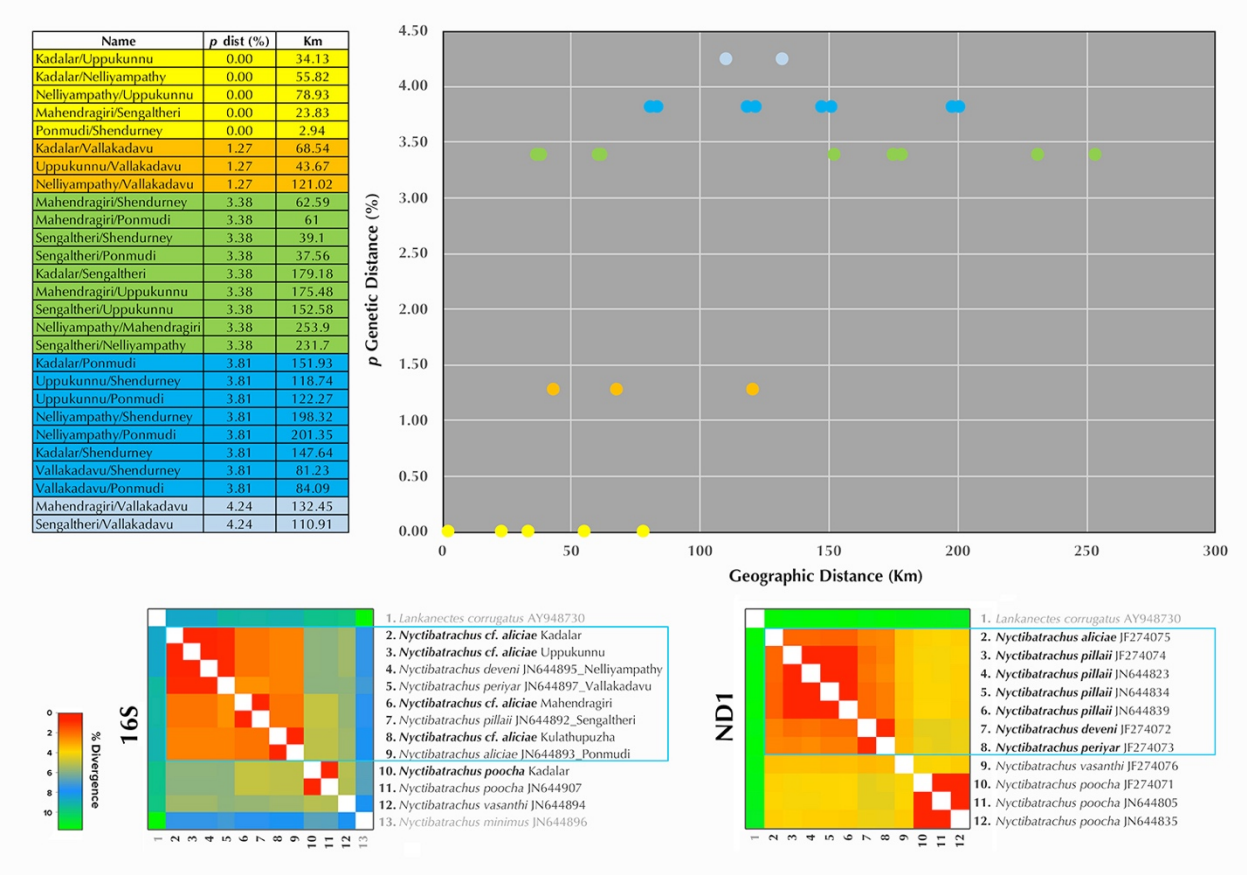
Name | p dist (%) | Km
Kadalar/Uppukunnu | 0.00 | 34.13
Kadalar/Nelliyampathy | 0.00 | 55.82
Nelliyampathy/Uppukunnu | 0.00 | 78.93
Mahendragiri/Sengaltheri | 0.00 | 23.83
Ponmudi/Shendurney | 0.00 | 2.94
Kadalar/Vallakadavu | 1.27 | 68.54
Uppukunnu/Vallakadavu | 1.27 | 43.67
Nelliyampathy/Vallakadavu | 1.27 | 121.02
Mahendragiri/Shendurney | 3.38 | 62.59
Mahendragiri/Ponmudi | 3.38 | 61
Sengaltheri/Shendurney | 3.38 | 39.1
Sengaltheri/Ponmudi | 3.38 | 37.56
Kadalar/Sengaltheri | 3.38 | 179.18
Mahendragiri/Uppukunnu | 3.38 | 175.48
Sengaltheri/Uppukunnu | 3.38 | 152.58
Nelliyampathy/Mahendragiri | 3.38 | 253.9
Sengaltheri/Nelliyampathy | 3.38 | 231.7
Kadalar/Ponmudi | 3.81 | 151.93
Uppukunnu/Shendurney | 3.81 | 118.74
Uppukunnu/Ponmudi | 3.81 | 122.27
Nelliyampathy/Shendurney | 3.81 | 198.32
Nelliyampathy/Ponmudi | 3.81 | 201.35
Kadalar/Shendurney | 3.81 | 147.64
Vallakadavu/Shendurney | 3.81 | 81.23
Vallakadavu/Ponmudi | 3.81 | 84.09
Mahendragiri/Vallakadavu | 4.24 | 132.45
Sengaltheri/Vallakadavu | 4.24 | 110.91
p Genetic Distance (%)
Geographic Distance (Km)
16S
% Divergence
1. Lankanectes corrugatus AY948730
2. Nyctibatrachus cf. aliciae Kadalar
3. Nyctibatrachus cf. aliciae Uppukunnu
4. Nyctibatrachus deveni JN644895_Nelliyampathy
5. Nyctibatrachus periyar JN644897_Vallakadavu
6. Nyctibatrachus cf. aliciae Mahendragiri
7. Nyctibatrachus pillaii JN644892_Sengaltheri
8. Nyctibatrachus cf. aliciae Kulathupuzha
9. Nyctibatrachus aliciae JN644893_Ponmudi
10. Nyctibatrachus poocha Kadalar
11. Nyctibatrachus poocha JN644907
12. Nyctibatrachus vasanthi JN644894
13. Nyctibatrachus minimus JN644896
ND1
1. Lankanectes corrugatus AY948730
2. Nyctibatrachus aliciae JF274075
3. Nyctibatrachus pillaii JF274074
4. Nyctibatrachus pillaii JN644823
5. Nyctibatrachus pillaii JN644834
6. Nyctibatrachus pillaii JN644839
7. Nyctibatrachus deveni JF274072
8. Nyctibatrachus periyar JF274073
9. Nyctibatrachus vasanthi JF274076
10. Nyctibatrachus poocha JF274071
11. Nyctibatrachus poocha JN644805
12. Nyctibatrachus poocha JN644835

Fig. S2

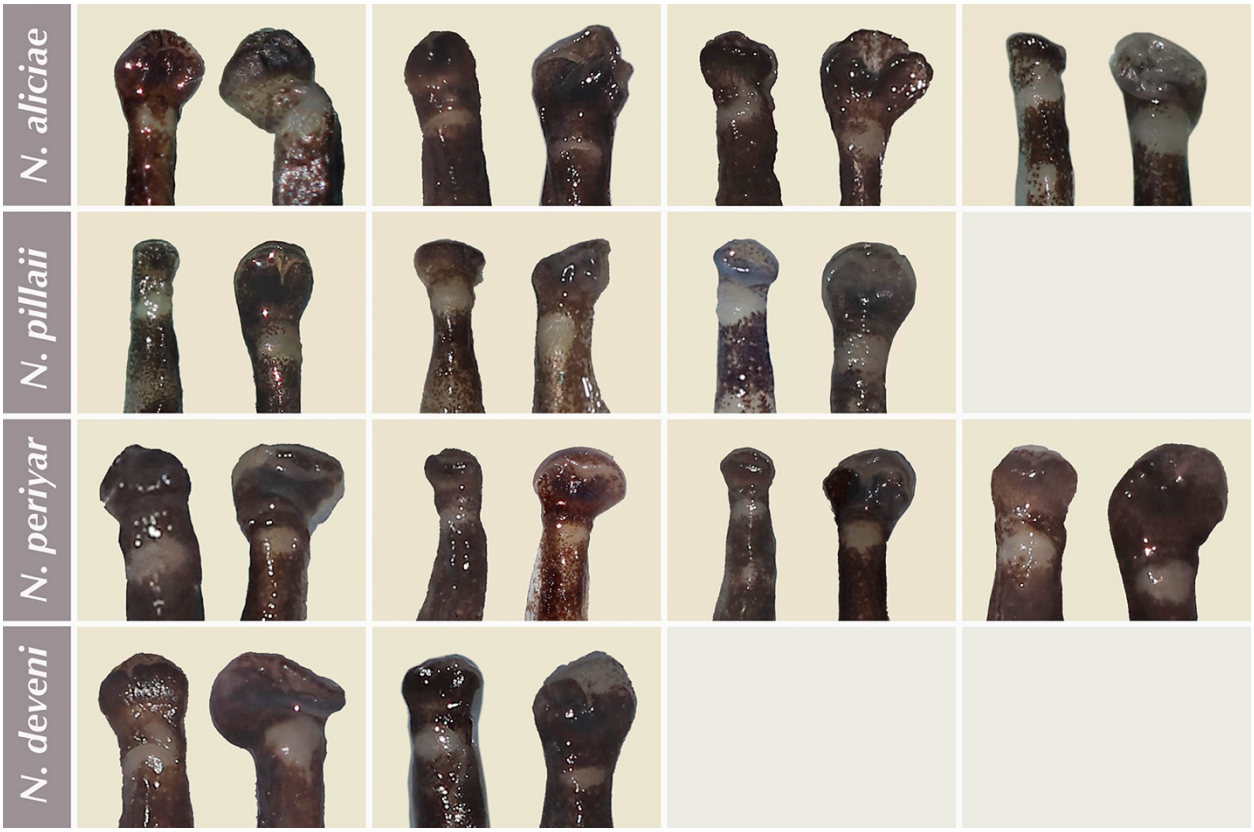

CHAPTER 2

Revisiting Linnaean and Wallacean Shortfalls in Mindanao Fanged Frogs: the *Limnonectes magnus* Complex Consists of Only Two Species

ROBIN KURIAN ABRAHAM[1], MARK WILLIAM HERR[1], VIKTORIA V. STERKHOVA[1], RAYANNA OTTERHOLT[1,2], CAMERON D. SILER[3], MARITES BONACHITA-SANGUILA[4], AND RAFE M. BROWN[1,5]

[1] Biodiversity Institute and Department of Ecology and Evolutionary Biology, 1345 Jayhawk Blvd., University of Kansas, Lawrence, KS 66045, USA

[2] Haskell Indian Nations University, 155 E Indian Avenue, Lawrence, KS 66046, USA

[3] Sam Noble Oklahoma Museum of Natural History and Department of Biology, University of Oklahoma, 2401 Chautauqua Avenue, Norman, OK 73072, USA

[4] Biodiversity Informatics and Research Center, Father Saturnino Urios University, San Francisco Street, Butuan City, 8600 Agusan del Norte, Philippines

[5] CORRESPONDENCE: email rafe@ku.edu

ABSTRACT: We revisit the question of species diversity among Mindanao Fanged Frogs of the *Limnonectes magnus* Complex, consisting of *L. magnus, L. diuatus, L. ferneri,* and a previously-hypothesized putative new species, inferred in the first molecular phylogenetic studies of the genus, almost two decades ago. Using a multilocus molecular DNA sequence dataset and comprehensive sampling of 161 individuals from throughout the Mindanao Pleistocene Aggregate Island Complex landmasses (a distinct faunal region of the southern Philippines) we characterize geographically-structured genetic diversity, focusing on the phylogenetic placement of individuals from each species' type locality. We also present new morphometric data from large samples of freshly-collected material from the type localities of each included species; together with examination of the name-bearing original type specimens, we conclude that an overestimation of species diversity has occurred and has been exacerbated by the indiscriminate acceptance of the hypothesis of the existence of widespread "cryptic" species in this group. We place *L. ferneri* in synonymy with *L. diuatus*, clarify the identification of the latter taxon with respect to *L. magnus*, and apply this name to the widespread, generalist, highly variable giant Fanged Frog distributed throughout the Mindanao faunal region of the southern Philippines.

Key words: Geographic radiation; Mindanao Pleistocene Aggregate Island Complex; Stream frogs

ISLAND archipelagos have provided numerous examples of the evolutionary processes and biogeographic patterns involved in generating biodiversity, especially the interplay of geological processes, colonization, and isolation (Paulay 1994; Brown et al. 2013; Brown 2016).

Home to numerous clades of co-distributed terrestrial vertebrates (Brown and Diesmos 2000), the Philippine Archipelago recently has been the focus of several integrative studies of amphibian radiations (Setiadi et al. 2011; Blackburn et al. 2013; Brown et al. 2013, 2015). A particularly interesting group are the fanged frogs of the genus *Limnonectes*, which consists of 73 named species distributed across Southeast Asia. This diverse clade includes 10 described, morphologically diagnosable, and noncontroversial (taxonomically unproblematic) endemic species in the Philippine archipelago (Evans et al. 2003; Setiadi et al. 2011).

In a recent review, Brown et al. (2013) distinguished between the archipelago's partially or fully characterized adaptive radiations (Brown et al. 2013, 2015) and the possibly non-adaptive, "geographic" radiations (Setiadi et al. 2011; Brown and Siler 2014; Brown et al. 2015, 2016). The latter, loosely defined category (Brown et al. 2013) includes clades with one or more representative species on each island bank, or Pleistocene Aggregate Island Complex (PAIC; Brown and Diesmos 2002; Brown and Guttman 2002). In these clades, or suites of taxa (in cases of non-monophyly (Brown and Guttman 2002; Evans et al. 2003), species have been characterized as ecologically similar, with little to no evidence of a phenotype–environment correlation or within-island, ecologically associated diversification (Brown et al. 2013; Brown and Siler 2014). Of particular interest are clades that show a mixture of diversification patterns, with single ecological generalists on some islands, and evidence of intra-island diversification, habitat and reproductive mode specialization, and multiple sympatric species on some islands (Inger et al. 1986; Alcala and Brown 1998; Brown and Iskandar 2000; Evans et al. 2003; Setiadi et al. 2011; Brown et al. 2013, 2015, 2016). One unclear case of potentially mixed, adaptively- versus non-adaptively radiated frogs are the Philippine Fanged Frogs, genus *Limnonectes,* which are comprised of no fewer than three invasions of the archipelago (Inger 1954; Evans et al. 2003;

Brown et al. 2013) and which have differentiated (or ecologically sorted) into composite communities with conspicuously distinct size classes (Setiadi et al. 2011).

We undertook this study to estimate the phylogeny of a Philippine endemic clade comprising *Limnonectes magnus* (Stejneger 1910) and related taxa (Inger 1954; Brown and Alcala 1977; Evans et al. 2003; Siler et al. 2009; Setiadi et al. 2011), with the goal of clarifying species boundaries (uncertainty around which has slowed the pace of taxonomic descriptions and recognition of biodiversity, constituting the so-called "Linnaean Shortfall;" Raven and Wilson 1992) and characterizing the geographical distributions of these units, which has been so poorly understood (the "Wallacean Shortfall;" Lomolino et al. 2010).

Limnonectes magnus, a large bodied Mindanao faunal region "fanged" frog (male holotype SVL: 113 mm; Stejneger 1910) was described from the mid-lower elevation slopes (≤ 1,200 m above sea level, m asl) of Mt. Apo, the country's highest mountain (2,954 m asl), located on southeast Mindanao Island (Fig. 1), at the southern extent of the archipelago. Brown and Alcala (1977) later named *Rana diuata* (= *Limnonectes diuatus*; male holotype SVL 58.4 mm) from higher elevations of Mt. Hilong-hilong, in the Diuata Mountain Range (northeastern Mindanao) and Siler et al. (2009) described *Limnonectes ferneri* (male holotype SVL 84.3 mm) from the Municipality of Monkayo, Davao del Norte Province, southeast Mindanao. Aside from Mindanao Island proper, large-bodied Fanged Frogs from other Mindanao Pleistocene Aggregate Island Complex (e.g., Samar, Leyte, Bohol, Camiguin Sur) have been reported for more than half a century (Inger 1954; Brown and Alcala 1970) and consistently identified as *L. magnus* (Siler et al. 2009).

Evans et al. (2003) subsequently demonstrated that populations historically identified as *L. magnus* may not be a monophyletic assemblage, suggesting that a second (assumed then to be

undescribed) species may occupy the Mindanao PAIC (Brown and Diesmos 2009), including the islands of Basilan, Bohol, Leyte, Mindanao, Samar and many smaller islands (e.g., Biliran, Camiguin Sur, Dinagat, Siargao) associated with these major landmasses (Fig. 1). Their analyses included what Evans et al. (2003) considered to be topotypic samples of *L. magnus* (genetic samples, collected at the type locality: high elevation, Mt. Apo; Stejneger 1910). Referring to this second, widespread taxon as "*Limnonectes* cf. *magnus*," Evans et al.'s (2003) model-based phylogenetic analyses of mitochondrial DNA sequence data revealed that populations from Mindanao were sister to those from Samar, which were, in turn, most closely related to the Bohol Island population. Specimens Evans et al. (2003) referred to as the widespread lineage ("*L.* cf. *magnus*") were genotyped from throughout the Mindanao PAIC (Fig. 1), including lower elevation foothills of Mt. Apo itself. Other than the description of a third Mindanao PAIC species (*L. ferneri* Siler, McVay, Diesmos, and Brown, 2009), no further progress on this group has been made and field workers have simply adopted the name *Limnonectes magnus* for the high elevation Mt. Apo population and *L.* cf. *magnus* for the widespread, low elevation populations on all the islands of the Mindanao PAIC faunal region (Plaza and Sanguila 2015; Sanguila et al. 2016).

Here we leveraged 30 years of genetic sampling (1990–2020) from throughout the Mindanao PAIC, including sequences and from specimens reported by Evans et al. (2003), and Siler et al. (2009) as well as material from the type localities of *L. magnus* (Stejneger 1910), *L. diuatus* (Brown and Alcala 1977) and *L. ferneri* (Siler et al. 2009). We reconsider species boundaries within the *L. magnus* Complex (Brown et al. 2000; Brown and Diesmos 2002) using a mitochondrial gene fragment (mtDNA: 16S) to screen genetic variation and guide reduced sampling of three nuclear gene loci for 19 population/species With our combined, multilocus

phylogenetic estimate, and consideration of morphometric variation, we find no support for the continued recognition of *L. ferneri* and conservatively conclude that only two species of large-bodied Fanged Frogs reside in the Mindanao faunal region: (1) a single widespread, low-elevation species corresponding to true *L. magnus* (Stejneger 1910) and (2) a single high elevation species referable to *L. diuatus* (Brown and Alcala 1977; with *L. ferneri* [Siler et al. 2009] now relegated to synonymy).

MATERIALS AND METHODS

Sampling, Molecular Data, Alignment, and Phylogenetic Analyses

We collected DNA sequences from 161 individuals, collected from 49 localities (Appendix I). We sequenced one mitochondrial gene region corresponding to the ribosomal RNA subunit (16S rRNA) and from a resulting preliminary mitochondrial "barcode" phylogeny, we selected 19 individuals for subsequent gene sequencing of three nuclear loci: Lactase (LCT), Carnitine palmitoyltransferase II (CPT-2) and Proopiomelanocortin (POMC). Primers, PCR methods, thermal profiles, and sequencing protocols follow (Brown et al. 2013, 2015). We selected closely-related outgroup species on the basis of uncontroversial higher-level phylogenetic relationships of the family Ranidae (Feng et al. 2017). All novel sequences were deposited in GenBank (Appendix 1).

The 16S dataset (706 bp), including our sequences and outgroups from GenBank, was aligned using the default parameters of the MAFFT algorithm (Katoh and Standley 2013). The combined nuclear dataset (LCT, CPT-2, POMC) for 19 individuals had a length of 2,156 bp. To assess gene congruence, we estimated gene trees with maximum likelihood using the program RAxML HPC v8.0.0 (Stamatakis 2014), and scrutinized trees inferred from these partitions for the presence of strongly supported topological conflict. Not finding strongly supported and

conflicting topologies, we felt justified in concatenating our data (16S + three nuclear genes; aligned in MAFFT) for subsequent analyses.

We conducted maximum likelihood analyses of our multilocus (16S + three nuclear genes) dataset, using the same partitions but with the GTR + Γ model for each of 200 independent best-tree searches and the rapid-bootstrapping algorithm. One hundred replicate tree search inferences were performed, each initiated with a random starting tree. Nodal support was assessed with 1,000 bootstrap pseudoreplicates (Stamatakis 2014). We considered nodes to be strongly supported when bootstrap values ≥ 70% (Hillis and Bull 1993). For our multilocus dataset we performed additional likelihood analyses, using IQ-TREE (Trifinopoulos et al. 2016), which employed 1,000 bootstrap pseudoreplicates via the ultrafast bootstrap approximation algorithm. Ultrafast bootstrap support values ≥ 0.95 indicate well-supported nodes in IQ-TREE analyses (Minh et al. 2013).

Partitioned Bayesian analyses for the concatenated (16S + three nuclear genes) dataset were conducted in BEAST 2 (Bouckaert et al. 2014) on the CIPRES gateway server (Miller et al. 2010). We partitioned the nuclear DNA by locus, with gene-specific protein-coding regions partitioned by codon position. The corrected Akaike Information Criterion (AICc) model to find selection parameters and the "greedy" search algorithm for finding the best models for Bayesian analysis (Darriba et al. 2012), were used to select the best model of nucleotide substitution for each partition. We ran four analyses, each with four Metropolis-coupled chains, an incremental heating of 0.02, and an exponential distribution with 25 as the rate parameter prior on branch lengths. All analyses were run for 10×10^6 generations (sampling every 1,000 generations). We set the burn-in to the default value of 25%, hence discarding the initial 5×10^6 generations. To assess stationarity, we used trace plots and effective sample size values (> 200) on TRACER

v1.7 (Rambaut et al. 2018). We constructed a 50% majority consensus tree with posterior probabilities estimates of nodal support, using the remaining sampled trees. We considered nodal support with Bayesian posterior probabilities values ≥ 0.95 as significant (Huelsenbeck and Rannala 2004).

Analysis of Adult Phenotype

We measured the following 15 standard, continuous morphological characters, following methods and definitions of Brown and Guttman (2002) and Emerson (1996): snout–vent length (SVL), head length, snout length, tympanum diameter, head width, forearm length, femur length, tibia length, tarsus length, foot length, hand length, eye–narial distance, inter-narial distance, fang length and fang height. To eliminate bias caused by ontogenetic variation, each character (except SVL) was scaled to the same size by adjusting their shape according to allometry (Thorpe, 1983; Lleonart et al., 2000). Measurements from 98 male and 62 female adult individuals of Fanged Frogs (from a set of 161, including sub-adults; Fig. 1) from throughout the Mindanao PAIC were adjusted for allometric growth using the following equation: $X_{adj} = \log (X) - \beta [\log (SVL) - \log (SVL_{mean})]$, where X_{adj} = adjusted value; X = measured value; β = unstandardised regression coefficient for each population found by regressing each mensural character on SVL; SVL = measured snout-vent length; SVL_{mean} = overall average SVL of all samples. All downstream analyses were performed on the adjusted values.

Prior to attempting statistical procedures, we performed an F-test to test for heteroskedasticity for each character across populations for each of the sexes, and for characters that violated homogeneity of variance, we performed Kruskal–Wallis Rank Sum tests to test whether samples originate from the same distribution.

We also transformed data to account for differences in body size by performing separate linear regressions between SVL and each of the remaining 14 variables. We then substituted residuals of these regressions for the raw data for those characters in all further univariate and multivariate analyses. We did not transform the SVL data themselves but did include this measure of body size in subsequent univariate analyses. After ensuring that data conformed to assumptions of normality by performing separate Shapiro-Wilk tests on each variable in the dataset (results not shown; *P*'s ≤0.05), we tested if the different populations display mean differences in single morphometric characters with two-way analyses of variance (ANOVAs) using sex (males, females) as factors. We followed this up with a Tukey HSD test to determine specifically, which population pair of character means differed after adjusting for multiple testing. All morphological analyses were performed and visualized in R (Team RDC 2019). Specimens and genetic material are deposited at the University of Kansas, the Field Museum of Natural History, the Texas Natural History Collection of the University of Texas at Austin, the Cincinnati Museum of Natural History, and the National Museum of the Philippines (institutional abbreviations follow Sabaj, 2019).

We used principal components analysis to find the best low-dimensional representation of variation in the data to determine whether morphological variation could form the basis of detectable group structure. Eigenvalues >1 were retained according to Kaiser's criterion (Kaiser 1960) and the R package "hypervolume" (Blonder et al. 2014) was used to construct hypervolumes using Gaussian kernel density estimation to estimate the probability density function of the retained principal components. To characterize clustering and distance in morphospace, and to determine whether either past taxonomy, and/or preliminary results from 16S mitochondrial gene phylogeography could be used to distinguish putative species, a

discriminant analysis of principal components was performed to find the linear combinations of morphological variables that have the largest between-group variance and the smallest within-group variance. This approach relies on data transformation using principal components analysis as a preliminary step before a subsequent discriminant analysis, ensuring that variables included in the latter step are uncorrelated and number fewer than the sample size (Jombart et al. 2010).

Analysis of Acoustic Data

Calls were recorded by using a Nagra VI digital recorder at a sampling rate of 44.1 kHz. We inspected vocalizations as oscillograms and spectrograms that were generated using the R package SEEWAVE (Sueur et al. 2008). We measured call parameters including mean dominant frequency (maximum frequency using the analytical programs selection spectrum function over the duration of the entire call), mean call duration (time between onset of first pulse and offset of last pulse in a call), and call rise (time between onset of first pulse and onset of pulse of maximum amplitude) and fall times (time between onset of pulse of maximum amplitude and offset of last pulse) using Raven© Pro 1.5 with the Hanning window type and a DFT (discrete Fourier transform) window size of 256 points and 50% overlap with 44.1 Hz sampling rate (Bioacoustics Research Group, Cornell Lab of Ornithology 2012). We present ranges followed by mean ± 1 SD in parentheses.

Allocation of Mindanao Giant Fanged Frog Names

Given past differences in assignment of species' taxonomic epithets to Giant Fanged Frogs of the Mindanao faunal region (Inger 1954; Brown and Alcala 1970, 1977; Evans et al. 2003; Siler et al. 2009), we endeavored to definitively assign existing names to genetically- and phenotypically characterized units, by incorporating both classes of data, deliberately collected

from specimens from the type locality of each species. We also examined and incorporated data from the type specimens of each species, as a final specifying measure, to independently confirm/refute our assignment of available names to groups demonstrably representing distinct evolutionary lineages (species).

RESULTS

Phylogenetic Analyses

Our RAxML maximum likelihood analysis of 16S mtDNA data generated a single point estimate topology of a log likelihood of –logL 12343.50 (Fig. 1). The preferred topology suggests that *Limnonectes magnus* (sensu lato) is non-monophyletic (Fig. 1); that is, the high elevation Mt. Apo population—considered by Evans et al. (2003) to likely represent true *L. magnus*—is in fact more closely related to *L. diuatus* than it is to the widespread *L.* cf. *magnus* from low elevation Mindanao and the remaining Mindanao faunal regions islands.

The 16S mtDNA maximum likelihood tree containing populations sampled from throughout the Mindanao PAIC infers the presence of two subclades with strong bootstrap support, with moderate levels of genetic divergence between these two clades, and low levels of divergence within each clade (Supplemental Figs. 1, 2). One strongly supported subclade corresponds to the Mindanao endemic, high elevation clade containing the type locality of the *L. diuatus* (Green clade: high elevations [≥ 1000 m] from Mt. Hilong-Hilong, northeast Mindanao; Fig. 1), along with closely-related haplotype clades from Mt. Lumot (*L. diuatus* 1: Orange clade, Municipality of Gingoog, Misamis Oriental, Northern Mindanao), and Mt. Apo (*L. diuatus* 2: Red clade, Municipality of Toril, Davao City Province, southeastern Mindanao), and *L. ferneri* (Green clade: Municipality of Monkayo, Davao del Norte Province, southcentral Mindanao).

The second, moderately supported subclade included three weakly supported groups from across low elevations of the Mindanao PAIC. One contained haplotype clade (*L. magnus* 1: Yellow clade) is limited to Bohol whereas another (*L. magnus* 2: Purple clade) is distributed among the islands of Samar, Leyte and Dinagat. A third haplotype clade (*L. magnus* 3: Blue clade) is widely-distributed throughout Mindanao, Samar, Dinagat, Siargao, and Camiguin Sur. Pairwise divergence for 16S within the lowland *L. magnus* clade was as high as 3.4% (Supplemental Fig. 1), whereas that within the high elevation *L. diuatus* clade was 4% at maximum. Divergence between these two clades ranged 5–7.5% (Supplemental Fig. 1).

Bayesian and Maximum Likelihood IQ-TREE analyses of our complete, multilocus, concatenated dataset (16S + three nuclear genes) both estimated two primary clades (Fig. 2). Populations sampled from high elevation sites (≥ 1,000 m) on Mindanao Island formed a clade, as did remaining samples from lower elevation sites throughout the Mindanao PAIC (Fig. 2). The high elevation clade (united by only moderate support) contains type locality *L. diuatus* 1 (Orange clade) and *L. diuatus* 2 (Red clade), and includes two moderately-supported clades of *L. diuatus* and *L. ferneri*. The Mindanao PAIC widespread clade of mostly low elevation *L. magnus* contains two poorly-supported subclades: Bohol, Samar, Dinagat, Siargao, Camiguin Sur, and Mindanao and another from Bohol, Samar, Leyte, and Dinagat.

Morphometric Characterization of Phenotype

Following transformation (except SVL which was not transformed), we rejected the null hypothesis of equal variances (homoscedasticity) for internarial distance ($F = 0.471$; $P = 0.043$), for which we implemented the Kruskal-Wallis test ($\chi^2 = 11.54$, $df = 4$, $P > 0.05$), which was found to be significantly different across populations. For all other variables we implemented an ANOVA. Our Shapiro-Wilk tests confirmed that our mensural characters satisfied the

assumption of normality ($P > 0.05$) (individual P-values not shown). Our ANOVAs showed that there were differences among populations for every character except femur length ($P = 0.928$) and inter-narial distance ($P = 0.07$) in males, and for fang length ($P = 0.98$) and fang height ($P = 0.71$) in females. Our non-parametric tests were consistent with the ANOVA results, except for inter-narial distance in males ($P = 0.48$), but this does not affect our conclusions. The Tukey test further revealed differences between males of true *L. diuatus* (Green) and *L. diuatus* 1 (Orange) for numerous characters (all characters except SVL, femur length, eye-narial distance and internarial distance), whereas comparisons between the *L. magnus* (Purple) and *L. magnus* (Yellow) populations yielded the few significant differences (only foot length differed significantly; Table 2).

Among males, the first four principal components had eigenvalues >1 and accounted for 75.2% of the total variation. And among females, the first five principal components had eigenvalues >1 and accounted for 81.2% of the total variation. These were retained for the discriminant analysis, the results of which are as follows. In males, the first principal component accounted for 36.2% of the variation and possessed heavy loadings for snout length, tibia length, tarsus length and foot length, indicating that these characters explained most of the variation along the first axis; this axis did not form the basis of group separation for any a posteriori recognized groups. The second component accounted for 20.5% of the variation with heavy loadings for head width and forearm length (Table 1). In females, the first principal component accounted for 36.7% of the variation with strong loadings for tibia length, tarsus length, and inter-narial distance, and second principal component accounted for 14.7% of the variation with highest loadings for tympanum diameter and foot length (Table 1). These formed the basis of discrete structure, separating the high elevation Mindanao Island Fanged Frog populations from

those widely-distributed throughout the Mindanao PAIC (Fig. 3).

When we applied Discriminant Analysis procedures to our a priori designated groups (DAPC), not surprisingly we found discrete clustering of the high elevation populations (*L. diuatus* (Green) + *L. ferneri* + *L. diuatus* 1 (Orange)) versus the widespread *L. magnus*; our minimum-spanning network, based on the squared distances between populations, demonstrated marked distance in morphospace between these two primary groups (Fig. 3).

In both our phylogenetic estimates (Figs. 1, 2), we found two primary clades; this dichotomy also formed the basis of group structure in our PCA analysis and these two groups were successfully, and discretely, discriminated in morphospace by our DAPC, particularly for adult males which are larger than females and possess the secondary sexual character of prominent fangs on the lower jaw (Fig 3). Within these groups, additional units could not be discretely identified (Fig. 3). Tendencies towards minimal group separation was observed within the high elevation clade (with the caveat that morphometric data from this lineage were not available from Mt. Apo) but extensive overlap among the groups (haplotype clades; Fig. 1) of low elevation *L. magnus* was evident (Fig. 3).

Allocation of Available Names

***Limnonectes magnus* (Stejneger 1910) versus *"L.* cf. *magnus*" sensu Evans et al. (2003).—**In their phylogenetic analysis of the genus *Limnonectes*, Evans et al.'s (2003) assignment of the name *Limnonectes magnus* to the high elevation Mt. Apo population was based on Stejneger's (1910:437) report that the holotype (USNM 35231) specimen originated "between Todaya and camp, 4,000 to 6,000 feet elevation" (1,219–1,828 m above sea level) and the assumption that "camp" referred to Lake Venado (an endorheic lake on Mt. Apo, situated at 7,200 feet (2,194 m) above sea level, which has been featured in numerous expedition accounts

(e.g., Hoogstral 1951; Inger 1954) and where E.A. Mearns was known to have made collections. Thus, the assumption that the holotype of *L. magnus* originated between 1,219 and 2,194 m on Mt. Apo, combined with the fact that the several immature specimens sequenced by Evans et al. (2003) were collected (by RMB in 1991, deposited at Cincinnati Museum of Natural History) between 1,200 and 1,550 m on Mt. Apo, lent support to what seemed at the time to be a reasonable assumption.

However, three newly-available lines of evidence argue against Evans et al.'s (2003) assignment. First, the high elevation genotype (then assumed to be *L. magnus*, but reassigned herein to *L. diuatus*, see below) was also collected and genetically confirmed at lower elevations, in the vicinity of Barangay Baracatan (Municipality of Toril; Davao City Province) at 900 m. Second, the larger-bodied, widespread, low-elevation form was also collected and genotyped by Evans et al. (2003) from as high as 1,275 m (Barangay Baracatan). The fact that both forms were collected sympatrically indicates a wider elevational range for the high elevation taxon than previously appreciated, and introduces the possibility that Evans et al.'s (2003) assumption could be questioned. Third, and more importantly, examination of the holotype (USNM 35231; male, 110 mm SVL; no paratypes were designated by Stejneger [1910]) makes it clear that the name *L. magnus* applies to the larger bodied, widespread, low-elevation species, which Inger (1954:287) characterized as "frequently in excess of 100 mm, and occasionally over 120 mm snout to vent." We note that this body size is far larger than the high-elevation form (*L. diuatus*, see below) in which adult male body size varies 58.4–84.3 (Brown and Alcala 1977; Siler et al. 2009). The holotype specimen (Fig. 4) is an adult male (sex confirmed by gonadal inspection) with evident secondary sexual characteristics typical of full-sized adult male *L. magnus* (hypertrophied jaw adductor musculature, greatly enlarged head, with jaw [in ventral aspect] laterally expanded).

The holotype's boldly contrasting transverse tibial bars, pale subarticular tubercles, pale ventral surfaces of finger discs, and smooth dorsal skin are all in agreement with the widespread, low-elevation species (Fig. 6) and stand in contrast to the diffuse tibial markings, dark gray/black subarticular tubercles, dark ventral surfaces of finger discs, bright white ventrum (Figs. 2, 8), and irregularly shagreened dorsal skin texture of the high-elevation species (Figs. 5, 8). Stejneger (1910:52) and Inger (1954:277) both commented on the widespread Mindanao population's uniquely distinctive color pattern, with posterior abdomen and ventral surfaces of rear limbs densely spotted with dark brown pigment. This conspicuous color pattern has been observed by the authors at numerous localities on Mindanao, Bohol, Samar, and Leyte; it is evident in the holotype as well (Fig. 4), although unpigmented ventral surfaces in *L. magnus* have been documented (Fig. 6).

In summary, with newly-acquired evidence from additional genetic data, plus definitive examination of the holotype of *L. magnus* (USNM 35231), all available data point to the same conclusion and we have no hesitation in reversing Evans et al.'s (2003) assignment of the name *Limnonectes magnus* (Stejneger 1910) to the low-elevation, widespread species of Mindanao PAIC Fanged Frog (Fig. 1; Table 3).

***Limnonectes diuatus* (Brown and Alcala 1977).—**In their description of *Rana diuata*, Brown and Alcala (1977) recognized the high-elevation population from Mt. Hilong-hilong (approximately "altitude 1,000+ m," of the Diuata Mountain Range, Municipality of Cabadbaran, Agusan del Norte Province) as a new species. They diagnosed it from *L. magnus* (numerous specimens of which was available at that time; represented by large sample sizes from various islands of the Mindanao PAIC; Brown and Alcala 1977) by its smaller body size (male SVL: 37.4–57.7 mm; $n = 3$; female: 62.5–63.1; $n = 2$ [*L. magnus*, in contrast, was reported 90.6–

108.5 mm SVL in males and 80.3–93.6 in females]), darker, more uniform overall dorsal and lateral coloration, dark brown throat and sternal region pigmentation (absent in *L. magnus*), its more "rugose" skin texture, shorter first finger (relative to second), its "somewhat more dilated" toe discs, and shorter relative tibia length. With the advantage provided by the current-day availability of extensive collections from the Mindanao PAIC (Brown et al. 2013; Sanguila et al. 2016), plus genetic data presented here, it is encouraging that the majority of these qualitative characterizations are generally confirmed (Figs. 2, 4, 5)—albeit possibly non-diagnostic in the sense that they do not represent non-overlapping ranges of discrete variation. Still, genetic data presented here indicate that all high-elevation Mindanao populations collected on Mt. Hilong-hilong, Mt. Magdiwata, Mt. Balatukan, Mt. Lumot, and Mt. Apo are closely-related (Figs. 1, 2), and correspond to the smaller-bodied, range-limited, high-elevation form which exhibits geographically-structured genetic variation (mountain-specific haplotype clades) in rapidly-coalescing mitochondrial DNA (Fig. 1), but shows no such strongly-supported geographically-based genetic substructure in our multilocus phylogenetic estimate (Fig. 2). Having incorporated examination of the *L. diuatus* type series, and a combined multivariate analysis of the greatly-expanded sampling for high-elevation Mindanao Fanged Frogs, we take the absence of group/sample-based structure in our continuous morphometric data (broad overlap in *L. diuatus* and other high elevation populations in PCA, despite some separation in PC1 of our DAPC analysis, which is somewhat limited by the absence of morphometric data from adults of the Mt. Apo population), shallow genetic divergences in mtDNA (Fig. 1), and the lack of mountain massif-based genetic structure in nDNA (Fig. 2) to conservatively refer all Mindanao Island "sky island" populations to a single species, *Limnonectes diuatus* (Brown and Alcala 1977).

***Limnonectes ferneri* Siler, McVay, Diesmos, and Brown 2009.—**In their description of *L. ferneri,* Siler et al. (2009) described the population of Mindanao Fanged Frogs from the Simulaw River Drainage, Mt. Pasian (Municipality of Monkayo, Davao del Norte Province), emphasizing that in contrast to the generally smaller *L. diuatus* with traditional amphibian female-larger sexual size dimorphism, *L. ferneri* possessed reversed sexual size dimorphism, typical of larger-bodied *Limnonectes* (Inger 1954; Brown and Alcala 1977; Setiadi et al. 2011). Characters apparently diagnostic for *L. ferneri,* and distinguishing the species from *L. diuatus*, included its larger (male SVL 79.6–84.3 mm vs. smaller [male SVL 37.4–58.4], especially males) body size, less rugose skin texture, Finger I longer than Finger II (vs. fingers subequal), densely (vs. sparsely) distributed dermal asperities, snout round (vs. acuminate), and absence of dorsolateral folds/ridges (vs. present). With the consideration of larger sample sizes, from multiple localities (Fig. 1), and which extend the known range of *L. diuatus* from Brown and Alcala's (1977) original diagnosis, we view most of Siler et al.'s (2009) character comparisons as no longer diagnostic. Aside from the problem of interpreting subjective/categorical characterizations ("dense" vs. "sparse;" "smooth" vs. "rugose"), we note—as have many others—that many purportedly "diagnostic" traditional taxonomic characters in anuran systematics can be demonstrably biased by circumstances of preservation, inter-populational variation, reproductive cycle at time of preservation, and inter-observer bias (Hayek et al. 2001). Together with the genetic data presented here, indicating a very close relationship between *L. diuatus* from the species' type locality and the *L. ferneri* type series, we have no hesitation in placing *L. ferneri* Siler, McVay, Diesmos, and Brown 2009 in synonymy with *L. diuatus* (Brown and Alcala 1977). It should be noted that although Brown and Alcala (1977) reported *L. diuatus* male body size to vary 37.4–58.4 mm, Siler et al. (2009) were unable to

confirm sexual maturity in the type series beyond a single male (SVL 58.4 mm) and a single female (62.3 mm). Excluding immature specimens and combining size variation from both species' type series, we emphasize that *L. diuatus* does in fact exhibit reversed sexual size dimorphism (males on average slightly larger; male SVL 58.4–84.3 mm; females 62.3–69.3).

TAXONOMIC SUMMARY

Limnonectes magnus (Stejneger)

(Figs. 4, 6)

Rana magna: Stejneger 1910:437. Holotype male (USNM 35231) from "Mount Apo, Mindanao, between Todaya and camp, 4,000 to 6,000 feet altitude" (=Philippines, Mindanao Island, Davao City del Sur Province, Municipality of Bansalan, Barangay Sibulan, Sitio Tudaya). [examined].

Rana macrodon blythi Boulenger 1882:24 (in part, misidentification).

Rana modesta Roux 1918:412 (in part, misidentification).

Rana modesta magna Smith 1927:211 (in part, misidentification).

Rana macrodon magna Stejneger: Inger 1954:287 (in part, misidentification).

Rana magna magna Stejneger: Inger 1958:254 (correction, reidentification).

Rana (Euphlyctis) magna Stejneger: Dubois 1981:239 (by implication).

Euphlyctis magna (Stejneger): Poynton and Broadley 1985:124 (transferred to genus *Euphlyctis* Fitzinger by implication).

Limnonectes (Limnonectes) magnus (Stejneger): Dubois 1987:63 "1986" (transferred to genus *Limnonectes* Fitzinger by implication).

Limnonectes cf. *magnus*: Evans, Brown, McGuire, Supriatna, Andayani, Diesmos, Iskandar, Melnick, and Cannatella 2003:794; Setiadi, McGuire, Brown, Zubairi, Iskandar, Andayani, Supriatna, and Evans 2011:221 (misidentification).

Identification.—*Limnonectes magnus* differs from all other Philippine congeners by a combination of the following characters: adult large-bodied (males: 59.4–164.4 mm SVL; females 47.6–130.8); skin on dorsum smooth, slightly rugose laterally with irregular dark markings (Fig. 2); white-tipped asperities limited to sacral region or absent; tympanum not partially concealed by supratympanic fold (Fig. 6C); interdigital webbing of foot complete; subarticular tubercles and ventral surfaces of toe discs pale cream to gray; finger discs non-expanded; discs of toes slightly expanded (Fig. 6D, E); snout rounded in dorsal and lateral aspect; supralabial region with two or three broad, diffuse, indistinct dark blotches; dorsal coloration variable from light brown or gray to olive brown or dark brown; inguinal region and ventral surfaces of hindlimbs with densely spotted dark pigmentation in ≥ 88% of specimens; ventral throat, sternal region, and other body surfaces otherwise cream to pale yellow. Male advertisement call amplitude-modulated ("keh-keh-keh-keh…"), with 10–16 rapid, loud, and invariant notes.

Distribution and natural history.—*Limnonectes magnus* is has been reported from numerous low-elevation habitat types, usually in the vicinity of water (ponds, lakes, seepages, streams, rivers; see also comments by Inger 1954). The species has been recorded most frequently below 1,200 m, but a few confirmed *L. magnus* specimens have been collected as high as 1,350 m. It exhibits a widespread distribution, and has been documented throughout the Mindanao PAIC, including on the islands of Mindanao, Siargao, Camiguin Sur, Dinagat, Samar,

Leyte, Bohol and, Basilan and presumably, Biliran (Taylor 1920; Inger 1954; Diesmos et al. 2015; Sanguila et al. 2016). The tadpole and larval development of this species has not been described.

Advertisement call.—We include the following brief description of the male advertisement call (Fig. 7) of *Limnonectes magnus,* based on the recordings of two males (specimens not collected) recorded by RMB at Barangay Pasonanca, Municipality of Zamboanga City, Western Mindanao Island (1,130 m elevation, west side of Pasonanca Natural Park, at an area known locally as "Nancy") in the evening ~1730–1900 h (ambient temperature of 21.5°C). To the best of our knowledge, this constitutes the first description of vocalizations of the species.

The call of *Limnonectes magnus* is a stereotyped, repetitive, rapidly-pulsed, amplitude-modulated pulse train, sounding to the human ear like "keh-keh-keh-keh-keh-keh-keh…" and lasting several seconds, followed by several minutes of silence. Call duration 1.64–2.95 s (2.24 ± 0.30, n = 47 calls from two specimens; Fig. 7); rise time 80.1–91.4 (86.46 ± 3.1) ms; fall time 1,100–1,681.9 (1391.79 ± 157.36) ms; notes (pulses) per call 10–16 (13 ± 1.22); note repetition rate 2.7–3.11 (2.8 ± 0.58). Spectral properties of *L. magnus* calls were invariant across recordings available and the majority of call energy was concentrated between 0.6 and 1.5 kHz. Our two recording segments exhibited an invariant dominant frequency of 1.4 kHz for one male, and 1.2 kHz in the other; rich harmonic structure was evident up to 3.5 kHz. Over a four night survey at this locality, the two focal individuals intermittently called for several hours, starting near sunset (1800 h), and extending for 2–3 hrs after dark; calling activity was initiated by one male, initially with short calls of 2–5 notes, then the second male responded, resulting in more intensely alternating call exchanges for 3–8 minutes, followed by periods of silence of 30–75 minutes, until another bout of calling began again (RMB, personal observation). During

vocalizations, males remained partially concealed beneath boulders (2–4 m diameter), in the immediate vicinity of waterfalls and loudly-cascading water.

Limnonectes diuatus (Brown and Alcala)

(Figs. 2, 5, 8)

Rana diuata: Brown and Alcala 1977:669. Holotype male (CAS 133500) from "Taguibo River, south side of Mt. Hilong-hilong, altitude 1000+ meters, Diuata Mountains, Cabadbaran Agusan del Norte Province, Mindanao Island, Philippines." [examined].

Limnonectes ferneri Siler, McVay, Diesmos, and Brown 2009:106. Holotype male (PNM 9506) from "Simulaw River Drainage, 2.3 km N, 1.0 km E of Peak 1409, Mt. Pasian (7° 58′16.26″ N, 126° 17′50.52″ E; WGS-84), Municipality of Monkayo, Davao Del Norte Province, Mindanao Island, Philippines." [examined; **new synonymy**].

Limnonectes (Limnonectes) diuatus (Brown and Alcala), Dubois 1987:63 "1986" (transferred to genus *Limnonectes* Fitzinger by implication).

Limnonectes magnus (Stejneger) Evans, Brown, McGuire, Supriatna, Andayani, Diesmos, Iskandar, Melnick, and Cannatella 2003:794; Setiadi, McGuire, Brown, Zubairi, Iskandar, Andayani, Supriatna, and Evans 2011:221 (misidentifications).

Identification.—*Limnonectes diuatus* differs from all known congeners by a combination of the following characters: medium-bodied (SVL males: 58.4–84.3 mm; females 62.3–69.3); skin of dorsum smooth to shagreened, laterally highly rugose, with 2–4 longitudinal rows of large dermal tubercles (or tubercular ridges), each associated with a black spots (Fig. 2),

with or without spiculate texture from aggregations of white-tipped asperities (Siler et al. 2009: Fig. 4); tympanum usually fully exposed, or partially concealed along dorsoposterior margin by less-prominent, obtusely-angled (posteroventrally) supratympanic fold (Fig. 8C); interdigital webbing of foot complete; subarticular tubercles, toe discs, and ventral surfaces of feet dark gray to black; finger discs slightly expanded; discs of toes moderately expanded (Fig. 7D,E); snout acuminate to round in dorsal view, angled posteroventrally in lateral aspect (Fig. 8C); supralabial region with 4–6 distinct, round, dark brown spots (Figs. 2, 5, 8); dorsal coloration dark brown to nearly black brown; ventral surfaces of body bright white to pale cream; when present, dark brown ventral pigmentation concentrated on throat, sternal region, and in some specimens, posterior distal surfaces of limbs (Fig. 2); loreal region vertically flat, not concave, pigmented as surrounding lateral head surfaces (medium brown); known from high-elevation riparian habitats (above 900 m, usually above 1,200 m) only on Mindanao Island. Male advertisement call unrecorded.

Distribution and natural history.—*Limnonectes diuatus* occurs in high-elevation riparian habitats (montane streams and small, rapidly-cascading, high-gradient rivers; Brown and Alcala 1977; Siler et al. 2009; Diesmos et al. 2015; Sanguila et al. 2016) on Mindanao Island, above 900 m (usually ≥ 1,200 m) including Mt. Apo, Mt. Pasian, Mt. Hilong-hilong, Mt. Magdiwata, Mt. Balatucan, Mt. Lumot, and most likely numerous additional montane sites of eastern and possibly central Mindanao. A single unvouchered record for Mt. Kitanglad (Bukidnon, Central Mindanao) exists (Diesmos et al. 2015). The absence of recordings of the vocalizations of this species should be taken as a challenge for future field work—both from sites where it occurs exclusively (high-elevations, ≥ 1,400 m) and at lower, mid-elevations (900–

1,200 m), where it may occur syntopically with *L. magnus*. The tadpole and larval development of this species has not been described.

DISCUSSION

Our re-evaluation of the phylogenetic relationships, clarification of the taxonomy, and consideration of island and elevational distributions of *Limnonectes magnus* and allied taxa leads to the conclusion that only two valid Giant Fanged Frog species can demonstrably be said to exist on the Mindanao PAIC (Stejneger 1910; Taylor 1920; Inger 1954; Brown and Alcala 1977). Rather than resulting in the previously anticipated increase in species numbers, this exercise argues for the placement of *L. ferneri* (Siler et al. 2009) in synonymy with *Rana diuata* Brown and Alcala 1977 (=*Limnonectes diuatus*) and reverses Evans et al.'s (2003) assignment of available names (Brown et al. 2013; Diesmos et al. 2015; Sanguila et al. 2016). Moreover, genetic identification of all insular populations, (including name-bearing type specimens, and expanded genetic data from relevant type localities) and robust statistical characterizations of phenotypic data, failed to identify unambiguous support for additional, unrecognized lineages and/or putative new species. Our conservative interpretation at this point, stems from the lack of agreement among available data streams (e.g., mtDNA phylogeny, multilocus phylogeny, morphometric analyses, traditional characters) and the absence of comparable data from all relevant populations (recordings of advertisement calls are unavailable for *L. diuatus* or from allopatric populations [Bohol vs. Mindanao] of *L. magnus*). Consideration of the Bohol Island population of *L. magnus* illustrates these points. With only a phylogeny estimated from single locus mitochondrial sequences (Fig. 1) and a morphometric analysis (Fig. 3), one might be tempted to suggest that the allopatric Bohol population could be an example of an unrecognized, morphologically cryptic, new species—embodying a popularly potentially widespread predicted

phenomenon in southeast Asian amphibian systematics and biodiversity science (Bickford et al. 2007; Inger et al. 2009; Matsui et al. 2010)—and which it may very well prove to be. However, analyses from individual and combined nuclear genes (not shown) did not result in strong support for Bohol populations as a distinctive, first-diverging lineage, as observed in the mtDNA gene tree (Fig. 1). Further, our multilocus Bayesian and likelihood estimates differed substantially in support at several nodes relevant to Bohol samples, which were not even inferred to be monophyletic (Fig. 2). Finally, additional lines of evidence germane to the question of the Bohol population, such as ecological information, bioacoustics, or data from larval phenotypes are unavailable. Although we acknowledge that a markedly divergent or structurally distinctive mate-recognition signal (the male anuran advertisement call; Wells 2007) would cause reconsideration of our interpretation (Herr et al. in press), at present we hold in abeyance any additional taxonomic changes until a time when changes to synonymy are unavoidable and bolstered with appropriate evidence. Until such gaps in our data and sampling are ameliorated, we would consider it speculative and even irresponsible to assert strong conclusions regarding possible existence of additional species. As such, we refrain from proposing new names or other liberal taxonomic changes, which might cascade into downstream error in synonymy (Frost 2020), create additional misunderstanding for biodiversity information products (AmphibiaWeb 2020) and national red list summaries (Gonzalez et al. 2018), and/or result in extraneous, wasteful expenditure of conservation resources (Diesmos and Brown 2011; Leviton et al. 2018). The emergence of conspicuous case studies, involving sequential reconsiderations of seemingly straightforward anuran taxonomic revisions, using increasingly sophisticated analytical approaches (e.g., multispecies coalescent-based methods and empirical characterizations of gene flow), and the power of statistical species delimitation procedures, coupled with technology

allowing locus sampling from across the genome (Hutter et al. 2019) have made clear the weaknesses, pitfalls, and potential for error associated with making strong conclusions based on single-locus studies, and even those based on a handful of loci (Brown and Guttman 2002; Brown and Siler 2014; Chan et al. 2020).

The emergent interpretation of a widespread low-elevation, larger-bodied generalist species (*L. magnus*) distributed on many Mindanao faunal region islands, versus a high-elevation montane species (*L. diuatus*) restricted to the higher reaches of isolated "sky island" massifs of Mindanao likely would have become apparent earlier, if high elevation herpetological survey work on Mindanao had not been so infrequent over the last three decades (Sanguila et al. 2016). This lack of modern, high quality biodiversity surveys has resulted in a general lack of genetic material and specimen-associated data (ecology, bioacoustics, larval biology, etc.), all of which have the potential to contribute to the pluralistic, integrative species delimitation standards of today (Fujita et al. 2012; Carstens et al. 2013). Another factor, which likely delayed the resolution of Mindanao Fanged Frog taxonomy, may have been the small number of sexually mature specimens in the original type series (Stejneger 2010; Brown and Alcala 1977; Siler et al. 2009). In the case of *L. diuatus*, inclusion of immature specimens in the original type series, also mistakenly gave the impression of females-larger sexual size dimorphism, and small male body size in this species (Brown and Alcala 1977; Siler et al. 2009).

The collection of the original holotype specimen of *L. magnus* at the very upper limit of its elevational distribution (Stejneger 1910) and collection of the type series of *L. diuatus* near the lower extent of its range (Brown and Alcala 1977; precisely at the point where we now conclude they are narrowly sympatric and syntopic) further contributed to biologists' confusion, as did the inadvertent switching of names for "*L. magnus*" and "*L.* cf. *magnus*" on the tips of the

first-available phylogenetic estimate (Evans et al. 2003). With our redefinition of each species, clarification of their status with respect to one another via diagnoses presented here, and characterization of their geographical ranges and elevational limits (confirmed with genetic data), we anticipate that field biologists will have the necessary tools to properly identify, further study, and assess the conservation status of these still poorly-known taxa.

In addition to full descriptions of the advertisement calls of both species, proper descriptions of tadpoles and larval development of both taxa are long overdue. With careful study of their microhabitats, and focus on whether they partition resources in areas of elevational sympatry, it should be possible to characterize their general natural history and true extent of occurrence. It is clear that this study would not have been possible without the existence of (and our access to) the relevant name-bearing type specimens, which provided the crucial clues and other bits of evidence needed to make sense of the historical uncertainty surrounding *Limnonectes magnus, L. diuatus, L. ferneri,* and other hypothesized species of Mindanao Fanged Frogs (Brown and Diesmos 2002; Evans et al. 2003), all of which underscores the importance of properly vouchered specimens and specimen-associated data in freely-available natural history museums and biodiversity repositories (McLean et al. 2016; Miralles et al. 2020). Given the half-century of confusion that has resulted from indiscriminate acceptance of assumptions from earlier taxonomy, and the practice of relying on "expert" opinions for policy-making (IUCN 2020), the case of *L. magnus* provides an important lesson regarding the pitfalls of misinterpretation that may develop when actual biodiversity surveys have not been conducted. In such cases, the data needed to inform conservation status assessments are unavailable (McLean et al. 2016; Miralles et al. 2020), and yet this lack of data is often itself incorrectly interpreted for

when implementing legal policy (Brown and Diesmos 2002; Hilton-Taylor 2000; Leviton et al. 2018; Gonzalez et al. 2018; Betts et al. 2020; Brown et al. 2020).

The case of Mindanao Fanged Frog classification is compelling for several reasons. *Limnonectes magnus* is one of the most widespread, common, and abundant, supposedly well studied species in the southern portions of the archipelago (Taylor 1920; Inger 1954; Alcala and Brown 1988; Sanguila et al. 2016). Its distribution is well characterized (Brown and Alcala 1970; Diesmos et al. 2015) and challenges to its conservation have been reasonably well discussed (Diesmos and Brown 2011; Brown et al. 2012; Gonzalez et al. 2018; IUCN 2020). Naturally, we might ask why has it taken so long for biologists to "connect the dots" from scientific names, to name-bearing type specimens (the Linnaen Shortfall; Lomolino et al 2010) and, eventually, to actual biological populations? Our experience suggests that current trends towards increasingly restrictive research permit systems and sociopolitical obstacles to biodiversity research is to blame, and represents a worrisome trend. Even if recent wholesale re-classification of Philippine amphibians to increasingly higher "threatened" conservation status categories justifies bureaucratic obstacles to research (Gonzalez et al. 2018), we argue that limiting biologists' access to species occurrence data (the Wallacean Shortfall) will always be counter-productive. Based on first principles of biodiversity science (taxonomy, species occurrence data), an understanding of species boundaries and their real-world geographical distributions are destined to remain the crucial gold standard for formulation and implementation of effective conservation efforts (Diesmos and Brown 2011; Brown et al. 2014; Diesmos et al. 2015; Leviton et al. 2018).

Acknowledgements.—Support for our work in the Philippines has been generously provided by the US National Science Foundation (NSF EF 0334928, DEB 0073199, 0344430,

0743491, and 0804115); most recent studies focusing on Philippine *Limnonectes* were funded by DEB 1654388 to RMB). We thank J. Vindum, A. Leviton, R. Drewes, and D. Blackburn, R. Sison and A.C. Diesmos (PNM), R. Inger, A. Resetar, H. Voris (FMNH), K. de Queiroz, R. Crombie (USNM), T. LaDuc, D. Cannatella (TNHC), J. Hanken, J. Losos, and J. Rosado (MCZ) for access to specimens and provision of workspace during visits to collections where Philippine *Limnonectes* specimens are housed. Special thanks are due to J. L. Welch (USNM) who photographed and provided digital images of the holotype of *L. magnus.* Phylogenetic analyses were conducted in part on Cornell's Computational Biology Services Unit *BioHPC* cluster and KU's Center for Research Computing. We especially appreciate the logistical support of the Philippine Biodiversity Monitoring Bureau, BMB (formerly Parks and Wildlife Bureau, PAWB) of the Department of Environment and Natural Resources and we thank authorities at DENR for their facilitation of research agreements, collecting permits and export permits necessary for this and related studies. Specimens were collected by RMB, KU students, and colleagues under the aegis of three formal Memoranda of Agreement between the University of Kansas and the Biodiversity Monitoring Bureau (BMB, formerly Parks and Wildlife Bureau, PAWB) of the Philippine central government (MOAs, 2004, 2009, 2015, endorsed by Chancellor of the University of Kansas [KU] and the Secretary of the Department of the Environment and Natural Resources [DENR], Quezon City, Manila) and a formal Specimen Repository Agreement at the KU Biodiversity Institute (KU-BI), stipulating ownership by the National Museum of the Philippines (PNM). With local municipal permissions obtained in the form of Prior Informed Consent certificates (PICs, obtained from all collection sites), specimens were subsequently collected under BMB Gratuitous Permits to Collect (PCs) Biological Specimens (185, 185-Renewal, 201, 201-Renewal, 212, 212-Renewal, 221, 221-Renewal, 228, 228-Renewal, 228-

Ammendment, 228-3rd Renewal, 228-4th Renewal, 246, 246-Renewal, 258, 258-Renewal, 258-Ammendment, 292, 292-Renewal and exported under the auspices of DENR Regional Office(s) Wildlife Certification Export permit(s), with coordinated institutional permits (APHIS, CITES, COSE F&W 3-177s) and Designated Port Exemptions archived by the KU-BI's administrative Office of the Director. Authorizations for the handling of live animals were provided to RMB by KU's Institutional Animal Care and Use Committee (IACUC AUS No. 185-05, 2004–2019).

We reserve special thanks for our collaborators in fieldwork: J. and B. Fernandez, A. C. Diesmos, N. Antoque, J. Cantil and V. Yngente; and we thank the Zamboanga City Water District and provincial, municipal, and local Pasonanca protected area officials who graciously provided access to Pasonanca Natural Park for this and related studies. Finally, thanks are due to P. De Mello for helping with formatting the base map used in Figure 1 and we thank Chan Kin Onn for constructive critique of an earlier draft of the manuscript.

LITERATURE CITED

Alcala, A.C., and W.C. Brown. 1998. Philippine Amphibians: An Illustrated Field Guide. Bookmark Press, Philippines.

AmphibiaWeb**.** 2020. Electronic database accessible at: https://amphibiaweb.org (accessed 20 October 2020). University of California, Berkeley, CA, USA.

Betts, J., R.P. Young, C. Hilton-Taylor, M. Hoffmann, J.P. Rodríguez, S.N. Stuart and E.J. Milner-Gulland. 2020. A framework for evaluating the impact of the IUCN Red List of threatened species. Conservation Biology 34:632–643.

Bickford, D., D.J. Lohman, N.S. Sodhi, … I. Das. 2007. Cryptic species as a window on diversity and conservation. Trends in Ecology and Evolution 22:148–155. doi: 10.1016/j.tree.2006.11.004

Blackburn, D.C., C.D. Siler, A.C. Diesmos, J.A. McGuire, D.C. Cannatella and R.M. Brown. 2013. An adaptive radiation of frogs in a Southeast Asian island archipelago. Evolution 67:2631–2646.

Blonder, B., C. Lamanna, C. Violle and B.J. Enquist. 2014. The n-dimensional hypervolume. Global Ecology and Biogeography 23:595–609.

Bouckaert, R., J. Heled, D. Kühnert, T. Vaughan, C.-H. Wu, D. Xie, M.A. Suchard, A. Rambaut and A.J. Drummond. 2014. BEAST 2: a software platform for Bayesian evolutionary analysis. PLOS Computational Biology 10:e1003537. DOI: http://dx.doi.org/10.1371/journal.pcbi.1003537

Brown, R.M. and A.C. Diesmos 2009. Philippines, Biology. Encyclopedia of Islands. University of California Press, USA.

Brown, R.M. 2016. Biogeography of vertebrates. Pp. 211–220 in The Encyclopedia of Evolutionary Biology. Vol. 1 (R.M. Kliman, ed.). Academic Press/Elsevier Inc., UK.

Brown, R.M., and A.C. Diesmos. 2002. Application of lineage-based species concept to oceanic island frog populations: the effects of differing taxonomic philosophies on the estimation of Philippine biodiversity. The Silliman Journal 42:133–162.

Brown, R.M., and S.I. Guttman. 2002. Phylogenetic systematics of the *Rana signata* complex of Philippine and Bornean stream frogs: reconsideration of Huxley's modification of Wallace's Line at the Oriental–Australian faunal zone interface. Biological Journal of the Linnean Society 76:393–461.

Brown, R.M., and D.T. Iskandar. 2000. Nest site selection, larval hatching, and advertisement calls, of *Rana arathooni* from southwestern Sulawesi (Celebes) Island, Indonesia. Journal of Herpetology 34:404–413.

Brown, R.M., and C.D. Siler. 2014. Spotted stream frog diversification at the Australasian faunal zone interface, mainland versus island comparisons, and a test of the Philippine 'dual-umbilicus' hypothesis. Journal of Biogeography 41:182–195.

Brown, R.M., J.A. McGuire and A.C. Diesmos. 2000. Status of some Philippine frogs referred to *Rana everetti* (Anura: Ranidae), description of a new species, and resurrection of *Rana igorota* Taylor 1922. Herpetologica 56:81–104.

Brown, R.M., A.C. Diesmos, M.B. Sanguila, C.D. Siler, M.L.D. Diesmos and A. C. Alcala. 2012. Amphibian conservation in the Philippines. FrogLog 104:40–43.

Brown, R.M., C.D. Siler, C.H. Oliveros, … A.C. Alcala. 2013. Evolutionary processes of diversification in a model island archipelago. Annual Review of Ecology, Evolution, and Systematics 44:411–435.

Brown, R.M., J.A. Weghorst, K.V. Olson, …C.D. Siler. 2014. Conservation genetics of the Philippine tarsier: cryptic genetic variation restructures conservation priorities for an island archipelago primate. PLoS ONE 9: e104340. doi:10.1371/journal.pone.0104340.

Brown, R.M., C.D. Siler, S.J. Richards, A.C. Diesmos and D.C. Cannatella. 2015. Multilocus phylogeny and a new classification for Southeast Asian and Melanesian forest frogs (family Ceratobatrachidae). Zoological Journal of the Linnean Society 174:130–168.

Brown, R.M., Y.-C. Su, B. Barger, C.D. Siler, M.B. Sanguila, A.C. Diesmos and D.C. Blackburn. 2016. Phylogeny of the island archipelago frog genus *Sanguirana*: Another endemic Philippine radiation that diversified 'Out-of-Palawan'. Molecular Phylogenetics and Evolution 94:531–536.

Brown, R.M., C.G. Meneses, P.S. Wood, Jr., J.B. Fernandez, M.A. Cuesta, M.A. Clores, C. Tracy, M. Buehler and C.D. Siler. 2020. Unexpected discovery of another new species of

Philippine False Gecko (Gekkonidae; *Pseudogekko*) from the Bicol Peninsula of Luzon Island. Herpetologica 76:315–329.

Brown, W.C., and A.C. Alcala. 1970. The zoogeography of the herpetofauna of the Philippine Islands, a fringing archipelago. Proceedings of the California Academy of Sciences 38:105–130.

Brown, W.C., and A.C. Alcala. 1977. A new frog of the genus *Rana* from the Philippines. Proceedings of the Biological Society of Washington 90:669–675.

Carstens, B.C, T.A. Pelletier, N.M. Reid and J.D. Saltler. 2013. How to fail at species delimitation. Molecular Ecology 22:4369–4383

Chan, K.O., C.R. Hutter, P.L. Wood, Jr., L.L. Grismer, I. Das, and R.M. Brown. 2020. Gene flow creates a mirage of cryptic species in a Southeast Asian spotted stream frog complex. Molecular Ecology 29: https://doi.org/10.1111/mec.15603

Darriba, D., G.L. Taboada, R. Doallo and D. Posada. 2012. jModelTest 2: more models, new heuristics and parallel computing. Nature Methods 9:772.

Diesmos, A.C., and R.M. Brown. 2011. Diversity, Biogeography, and Conservation of Philippine Amphibians. In Biology and Conservation of Tropical Asian Amphibians. Biology of the Amphibians in the Sunda Region, South-east Asia." Pp. 26–49 in Das, I., A. Haas and A. A. Tuen (eds.). Institute of Biodiversity and Environmental Conservation, Universiti Malaysia Sarawak, Kota Samarahan, Sarawak, Malaysia.

Diesmos, A.C., J.L. Watters, N.A. Huron, … C.D. Siler. 2015. Amphibians of the Philippines, part I: checklist of the species. Proceedings of the California Academy of Sciences 62:457–539.

Emerson, S.B. 1994. Testing patter predictions of sexual selection: a frog example. The American Naturalist 143:848–869.

Evans, B.J., R.M. Brown, J.A. McGuire, J. Supriatna, N. Andayani, A.C. Diesmos, D. Iskandar, D.J. Melnick and D.C. Cannatella. 2003. Phylogenetics of fanged frogs: testing biogeographical hypotheses at the interface of the Asian and Australian faunal zones. Systematic Biology 52:794–819.

Feng, Y.-J., D.C. Blackburn, D. Liang, D.M. Hillis, D.B. Wake, D.C. Cannatella and P. Zhang. 2017. Phylogenomics reveals rapid, simultaneous diversification of three major clades of Gondwanan frogs at the Cretaceous–Paleogene boundary. Proceedings of the National Academy of Sciences 114:E5864–E5870. DOI: https://doi.org/10/1073/pnas.1704632114

Frost, D.R. 2020. Amphibian Species of the World 6.0: An Online Reference (accessed 20 October 2020). Electronic Database accessible at http://research.amnh.org/herpetology/amphibia/index.html. American Museum of Natural History, New York, USA.

Fujita, M.K., A.D. Leaché, F.T. Burbrink, J.A. McGuire and C. Moritz. 2012. Coalescent-based species delimitation in an integrative taxonomy. Trends in Ecology and Evolution 27:480–488.

Gonzalez, J.C.T., C.A.A. Layusa, L.E. Afuang, … P.S. Ong. 2018. Review and update of the 2004 National List of Threatened Terrestrial Fauna of the Philippines. Sylvatrop. The Technical Journal of Philippine Ecosystems and Natural Resources 28:73–144.

Hayek, L.-A.C., W.R. Heyer and C. Gascon, 2001. Frog morphometrics: a cautionary tale. Alytes 18:153–177.

Herr, M.W., J. Goyes Vallejos, C.G. Meneses, R.K. Abraham, R. Otterholt, C.D. Siler, E.L.B. Rico, and R.M. Brown. In press. A new, morphologically cryptic species of fanged frog, genus *Limnonectes* (Amphibia: Anura: Dicroglossidae), from Mindoro Island, central Philippines. Copeia.

Hillis, D.M., and J.J. Bull. 1993. An empirical test of bootstrapping as a method for assessing confidence in phylogenetic analysis. Systematic Biology 42:182–192.

Hilton-Taylor, C. 2000. IUCN red list of threatened species. IUCN https://www.iucnredlist.org/.

Hoogstral, H. 1951. Philippine Zoological Expedition 1946–1947: narrative and itinerary. Fieldiana Zoology 33:1–86.

Huelsenbeck, J.P., and B. Rannala. 2004. Frequentist properties of Bayesian posterior probabilities of phylogenetic trees under simple and complex substitution models. Systematic Biology 53:904–913.

Hutter, C.R., K.A. Cobb, D.M. Portik, S.L. Travers, P.L. Wood, Jr., and R. M. Brown. 2019. FrogCap: a modular sequence capture probe set for phylogenomics and population genetics for all frogs, assessed across multiple phylogenetic scales. BioRxiv https://doi.org/10.1101/825307 (posted 1 November 2019).

Inger, R.F. 1954. Systematics and zoogeography of Philippine Amphibia. Fieldiana Zoology 33:181–531.

Inger, R.F., H.K. Voris and P. Walker. 1986. Larval transport in a Bornean ranid frog. Copeia 1986:523–525.

Inger, R.F., B. L. Stuart and D.T. Iskandar. 2009. Systematics of a widespread Southeast Asian frog, *Rana chalconota* (Amphibia: Anura: Ranidae). Zoological Journal of the Linnean Society 155:123–47.

International Union for the Conservation of Nature (IUCN). 2020. The IUCN Red List of Threatened Species. Version 2020-1. https://www.iucnredlist.org. Downloaded on 19 March 2020.

Jombart, T., S. Devillard and F. Balloux. 2010. Discriminant analysis of principal components: a new method for the analysis of genetically structured populations. BMC Genetics 11:94.

Kaiser, H.F. 1960. The application of electronic computers to factor analysis. Educational and Psychological Measurement 20:141–151.

Katoh, K., and D.M. Standley. 2013. MAFFT multiple sequence alignment software version 7: improvements in performance and usability. Molecular Biology and Evolution 30:772–780.

Leviton, A.E, C.D. Siler, J.L. Weinell and R. M. Brown. 2018. A synopsis of the snakes of the Philippines: a synthesis of data from biodiversity repositories, field studies, and the literature. Proceedings of the California Academy of Sciences 64:399–568.

Lleonart, J., J. Salat and G.J. Torres. 2000. Removing allometric effects of body size in morphological analysis. Journal of Theoretical Biology 205:85–93.

Lomolino, M.V., B.R. Riddle, R.J. Whittaker and J.H. Brown. 2010. Biogeography. Sinauer Associates, Inc. Publishers, USA.

Matsui, M., N. Kuraishi, J.-P. Jiang, H. Ota, A. Hamidy, N.L. Orlov and K. Nishikawa. 2010. Systematic reassessments of fanged frogs from China and adjacent regions (Anura: Dicroglossidae). Zootaxa 2345:33–42.

McLean, B.S., K.C. Bell, J.L. Dunnum, B. Abrahamson, J.P. Colella, E.R. Deardorff, J.A. Weber, A.K. Jones, F. Salazar-Miralles and J.A. Cook. 2016. Natural history collections-

based research: progress, promise, and best practices. Journal of Mammalogy 97:287–297.

Miller, M.A., W. Pfeiffer and T. Schwartz. 2010. Creating the CIPRES Science Gateway for inference of large phylogenetic trees. Pp. 1–8 in 2010 gateway computing environments workshop (GCE). DOI: 10.1109/GCE.2010.5676129

Miralles, A., T. Bruy, K. Wolcott, … F.O. Glöckner. 2020. Repositories for taxonomic data: Where we are and what is missing. Systematic Biology 53:1–23.

Minh, B.Q., M.A.T. Nguyen and A. von Haeseler. 2013. Ultrafast approximation for phylogenetic bootstrap. Molecular Biology and Evolution 30:1188–1195.

Paulay, G. 1994. Biodiversity on oceanic islands: its origin and extinction. American Zoologist 34:134–144.

Plaza, J.L., and M.B. Sanguila. 2015. Preliminary report of anurans of Mount Hilong-hilong, Agusan Del Norte, eastern Mindanao, Philippines. Asian Herpetological Research 6:18–33.

Rambaut, A., A.J. Drummond, D. Xie, G. Baele and M.A. Suchard. 2018. Posterior summarisation in Bayesian phylogenetics using Tracer 1.7. Systematic Biology 67:901–904.

Raven, P.H., and E.O. Wilson. 1992. A fifty-year plan for biodiversity surveys. Science 258:1099–1100.

Sabaj, M.H. 2019. Standard symbolic codes for institutional resource collections in herpetology and ichthyology: An online reference. American Society of Ichthyologists and Herpetologists, USA. Available at http://www.asih.org. Accessed on 1 June 2020.

Sanguila, M.B., K.A. Cobb, C.D. Siler, A.C. Diesmos, A.C. Alcala and R.M. Brown. 2016. The amphibians and reptiles of Mindanao Island, southern Philippines, II: the herpetofauna of northeast Mindanao and adjacent islands. ZooKeys 624:1–132. DOI: https://doi.org/10.3897/zookeys.624.9814

Setiadi, M.I., J.A. McGuire, R.M. Brown, M. Zubairi, D.T. Iskandar, N. Andayani, J. Supriatna and B.J. Evans. 2011. Adaptive radiation and ecological opportunity in Sulawesi and Philippine fanged frog (*Limnonectes*) communities. The American Naturalist 178:221–240.

Siler, C.D., J.D. McVay, A.C. Diesmos and R.M. Brown. 2009. A new species of fanged frog, genus *Limnonectes* (Amphibia: Anura: Dicroglossidae) from southeast Mindanao Island, Philippines. Herpetologica 65:105–114.

Stamatakis, A. 2014. RAxML version 8: a tool for phylogenetic analysis and post-analysis of large phylogenies. Bioinformatics 30:1312–1313.

Stejneger, L. 1910. Description of a new frog from the Philippine Islands. Smithsonian Miscellaneous Collections 52:437–439.

Sueur, J., T. Aubin and C. Simonis. 2008. Seewave, a free modular tool for sound analysis and synthesis. Bioacoustics 18:213–226.

Taylor, E.H. 1920. Philippine Amphibia. Philippine Journal of Science 16:213–359.

R Core Team. 2013. R: A language and environment for statistical computing. R Foundation for Statistical Computing, Vienna, Austria. URL: http://www.r-project.org/.

Thorpe, R.S. 1983. A review of the numerical methods for recognising and analysing racial differentiation. Pp. 404–423 in Numerical Taxonomy: Proceedings of a NATO Advanced Studies Institute NATO ASI series (J. Felsenstein, ed.). Springer Verlag, Germany.

Trifinopoulos, J., L.-T. Nguyen, A. von Haeseler and B.Q. Minh. 2016. W-IQ-TREE: a fast online phylogenetic tool for maximum likelihood analysis. Nucleic Acids Research 44:W232–W235. DOI: http://dx.doi.org/10.1093/nar/gkw256.

Wells. K. D. 2007. The Ecology and Behavior of Amphibians. University of Chicago Press, Chicago, USA.

Wiens, J.J., J.S. Sukumaran, R.A. Pyron and R.M. Brown. 2009. Evolutionary and biogeographic origins of high tropical diversity in old world frogs (Ranidae). Evolution 63:1217–1231.

APPENDIX I

Taxa, museum repository catalog numbers, localities, and GenBank numbers for all samples included in this study

Species	Field No.	Catalog No.	Island	Locality	Elev (m)	GenBank accession numbers			
						16S	LCT	CPT2	POMC
Limnonectes diautus (*L. ferneri* type)	JWF 94091	CMNH 5572	Mindanao	Mt. Pasian, Simulaw River Drainage, Municipality of Monkayo, Davao del Norte Province		MN759154			
Limnonectes diautus (*L. ferneri* type)	JWF 94093	PNM 9506 (Holotype)	Mindanao	Mt. Pasian, Simulaw River Drainage, Municipality of Monkayo, Davao del Norte Province		MN759153	X		MT631750
Limnonectes diautus (*L. ferneri* type)	JWF 94094	CMNH 5573	Mindanao	Mt. Pasian, Simulaw River Drainage, Municipality of Monkayo, Davao del Norte Province		MN759155			
Limnonectes diautus	RMB 16161	KU 333370	Mindanao	Mt. Hilong-hilong, May-Impit, Municipality of Remedios T. Romualdez, Agusan del Norte Province	1,150	MN759175	X	MT631729	MT631754
Limnonectes diautus	RMB 16164	KU 333373	Mindanao	Mt. Hilong-hilong, May-Impit, Municipality of Remedios T. Romualdez, Agusan del Norte Province	1,150	MN759145			

Species	Field No.	Catalog No.	Island	Locality	Elev (m)	GenBank accession numbers			
						16S	LCT	CPT2	POMC
Limnonectes diautus	RMB 16224	KU 333374	Mindanao	Mt. Hilong-hilong, May-Impit, Municipality of Remedios T. Romualdez, Agusan del Norte Province	1,150	MN759176			
Limnonectes diautus	RMB 16225	KU 333375	Mindanao	Mt. Hilong-hilong, May-Impit, Municipality of Remedios T. Romualdez, Agusan del Norte Province	1,150	MN759144			
Limnonectes diautus	RMB 16232	KU 333381	Mindanao	Mt. Hilong-hilong, May-Impit, Municipality of Remedios T. Romualdez, Agusan del Norte Province	1,150	MN759178	X	MT631728	
Limnonectes diautus	RMB 16235	KU 333384	Mindanao	Mt. Hilong-hilong, May-Impit, Municipality of Remedios T. Romualdez, Agusan del Norte Province	1,150	MN759179	X	MT631725	MT631752
Limnonectes diautus	RMB 16236	KU 333385	Mindanao	Mt. Hilong-hilong, May-Impit, Municipality of Remedios T. Romualdez, Agusan del Norte Province, Mindanao Island.	1,150	MN759180			
Limnonectes diautus	RMB 16237	KU 333386	Mindanao	Mt. Hilong-hilong, May-Impit,	1,150	MN759181			

Species	Field No.	Catalog No.	Island	Locality	Elev (m)	GenBank accession numbers			
						16S	LCT	CPT2	POMC
				Municipality of Remedios T. Romualdez, Agusan del Norte Province					
Limnonectes diautus	RMB 16238	KU 333387	Mindanao	Mt. Hilong-hilong, May-Impit, Municipality of Remedios T. Romualdez, Agusan del Norte Province	1,150	MN759182			
Limnonectes diautus	RMB 16239	KU 333388	Mindanao	Mt. Hilong-hilong, May-Impit, Municipality of Remedios T. Romualdez, Agusan del Norte Province	1,150	MN759183			
Limnonectes diautus	RMB 16250	KU 333389	Mindanao	Mt. Hilong-hilong, May-Impit, Municipality of Remedios T. Romualdez, Agusan del Norte Province	1,150	MN759184			
Limnonectes diautus	RMB 16278	KU 333393	Mindanao	Mt. Hilong-hilong, May-Impit, Municipality of Remedios T. Romualdez, Agusan del Norte Province	990	MN759186			
Limnonectes diautus	ACD 4274	KU 320079	Mindanao	Mt. Balatukan Natural Park, Sitio San Isidro, Boy Scout Camp, Barangay Lumotan,	1,450	MN759095	X	MT631732	MT631751

Species	Field No.	Catalog No.	Island	Locality	Elev (m)	GenBank accession numbers			
						16S	LCT	CPT2	POMC
				Municipality of Gingoog, Misamis Oriental Province					
Limnonectes diautus 1	ACD 4276	KU 320081	Mindanao	Mt. Balatukan Natural Park, Sitio San Isidro, Boy Scout Camp, Barangay Lumotan, Municipality of Gingoog, Misamis Oriental Province	1,450	MN759096			MT631753
Limnonectes diautus 1	ACD 4316	KU 320085	Mindanao	Mt. Balatukan Natural Park, Sitio San Isidro, Boy Scout Camp, Barangay Lumotan, Municipality of Gingoog, Misamis Oriental Province	1,450	MN759097	X	MT631739	MT631755
Limnonectes diautus 1	ACD 4324	KU 320090	Mindanao	Mt. Balatukan Natural Park, Sitio San Isidro, Boy Scout Camp, Municipality of Gingoog, Misamis Oriental Province	1,450	MN759098			
Limnonectes diautus 1	RMB 16582	KU 333428	Mindanao	Mt. Lumot, Barangay Civoleg, Municipality of Gingoog, Misamis Oriental Province	1,236	MN759192	X	MT631733	MT631749
Limnonectes diautus 1	RMB 16627	KU 333438	Mindanao	Mt. Lumot, Barangay Civoleg,	1,236	MN759194			

Species	Field No.	Catalog No.	Island	Locality	Elev (m)	GenBank accession numbers			
						16S	LCT	CPT2	POMC
				Municipality of Gingoog, Misamis Oriental Province					
Limnonectes diautus 2	PNM-CMNH H1197	NA	Mindanao	Mt. Talomo; Mt. Apo Natural Park, Sitio San Roque, Barangay Baracatan, Municipality of Toril, Davao Province	1,530–1,776	MN759156	X	MT631727	MT631757
Limnonectes diautus 2	PNM-CMNH H1198	NA	Mindanao	Mt. Talomo; Mt. Apo Natural Park, Sitio San Roque, Barangay Baracatan, Municipality of Toril, Davao Province	1,530–1,775	MN759157			
Limnonectes diautus 2	PNM-CMNH H1199	NA	Mindanao	Mt. Talomo; Mt. Apo Natural Park, Sitio San Roque, Barangay Baracatan, Municipality of Toril, Davao Province	1,530–1,770	MN759158			
Limnonectes diautus 2	PNM-CMNH H1200	NA	Mindanao	Mt. Talomo; Mt. Apo Natural Park, Sitio San Roque, Barangay Baracatan, Municipality of Toril, Davao Province	1,530–1,774	MN759159			
Limnonectes diautus 2	PNM-CMNH H1205	NA	Mindanao	Mt. Talomo; Mt. Apo Natural Park, Sitio San Roque, Barangay Baracatan, Municipality of Toril, Davao Province	1,530–1,771	MN759160			

Species	Field No.	Catalog No.	Island	Locality	Elev (m)	GenBank accession numbers			
						16S	LCT	CPT2	POMC
Limnonectes diautus 2	PNM-CMNH H1206	NA	Mindanao	Mt. Talomo; Mt. Apo Natural Park, Sitio San Roque, Barangay Baracatan, Municipality of Toril, Davao Province	1,530–1,778	MN759164	X	MT631737	MT631758
Limnonectes diautus 2	PNM-CMNH H1244	NA	Mindanao	Mt. Talomo; Mt. Apo Natural Park, Sitio San Roque, Barangay Baracatan, Municipality of Toril, Davao Province	1,530–1,772	MN759161	X	MT631741	MT631756
Limnonectes diautus 2	PNM-CMNH H1246	NA	Mindanao	Mt. Talomo; Mt. Apo Natural Park, Sitio San Roque, Barangay Baracatan, Municipality of Toril, Davao Province	1,530–1,773	MN759162			
Limnonectes diautus 2	PNM-CMNH H1247	NA	Mindanao	Mt. Talomo; Mt. Apo Natural Park, Sitio San Roque, Barangay Baracatan, Municipality of Toril, Davao Province	1,530–1,777	MN759163			
Limnonectes magnus 1	CDS 4668	KU 323586	Bohol	Raja Sikatuna Natural Park, Magsaysay Park, Barangay Riverside, Municipality of Bilar, Bohol Province	250	MN759130			
Limnonectes magnus 1	CDS 4675	KU 323589	Bohol	Raja Sikatuna Natural Park, Magsaysay Park,	250	MN759131			

Species	Field No.	Catalog No.	Island	Locality	Elev (m)	GenBank accession numbers			
						16S	LCT	CPT2	POMC
				Barangay Riverside, Municipality of Bilar, Bohol Province					
Limnonectes magnus 1	CDS 4678	KU 323591	Bohol	Raja Sikatuna Natural Park, Magsaysay Park, Barangay Riverside, Municipality of Bilar, Bohol Province	250	MN759132			
Limnonectes magnus 1	CDS 4468	KU 323612	Bohol	Raja Sikatuna Natural Park, Magsaysay Park, Barangay Riverside, Municipality of Bilar, Bohol Province	250	MN759129	X	MT631740	MT631745
Limnonectes magnus 1	CDS 4778	KU 323615	Bohol	Raja Sikatuna Natural Park, Barangay Danicop, Municipality of Sierra Bullones, Bohol Province	250	MN759133			
Limnonectes magnus 1	CDS 4821	KU 323619	Bohol	Raja Sikatuna Natural Park, Barangay Danicop, Municipality of Sierra Bullones, Bohol Province	250	MN759134	X	MT631734	MT631760
Limnonectes magnus 1	CDS 4856	KU 323622	Bohol	Raja Sikatuna Natural Park, Barangay Danicop, Municipality of Sierra Bullones, Bohol Province	250	MN759135			

Species	Field No.	Catalog No.	Island	Locality	Elev (m)	GenBank accession numbers			
						16S	LCT	CPT2	POMC
Limnonectes magnus 1	CDS 4867	KU 323627	Bohol	Raja Sikatuna Natural Park, Barangay Danicop, Municipality of Sierra Bullones, Bohol Province	250	MN759136			
Limnonectes magnus 1	CDS 4989	KU 323634	Bohol	Raja Sikatuna Natural Park, Barangay Danicop, Municipality of Sierra Bullones, Bohol Province	250	MN759137	X	MT631726	MT631744
Limnonectes magnus 1	RMB 2887	KU 327507	Bohol	Raja Sikatuna Natural Park, Barangay Danicop, Bohol Province	390	MN759219			
Limnonectes magnus 2	CDS 1804	KU 306022	Samar	Barangay Poblacion, Municipality of San Jose de Buan, Northern Samar Province		MN759107			
Limnonectes magnus 2	CDS 1826	KU 306024	Samar	Taft Forest, Barangay San Rafael, Municipality of Taft, Eastern Samar Province		MN759108			
Limnonectes magnus 2	CDS 1827	KU 306025	Samar	Taft Forest, Barangay San Rafael, Municipality of Taft, Eastern Samar Province		MN759109			
Limnonectes magnus 2	CDS 1828	KU 306026	Samar	Taft Forest, Barangay San Rafael,		MN759110			

Species	Field No.	Catalog No.	Island	Locality	Elev (m)	GenBank accession numbers			
						16S	LCT	CPT2	POMC
				Municipality of Taft, Eastern Samar Province					
Limnonectes magnus 2	CDS 1839	KU 306028	Samar	Taft Forest, Barangay San Rafael, Municipality of Taft, Eastern Samar Province		MN759111			
Limnonectes magnus 2	CDS 1840	KU 306029	Samar	Taft Forest, Barangay San Rafael, Municipality of Taft, Eastern Samar Province		MN759112			
Limnonectes magnus 2	CWL 149	KU 306039	Samar	Taft Forest, Barangay San Rafael, Municipality of Taft, Eastern Samar Province		MN759143			
Limnonectes magnus 2	CWL 161	KU 306041	Samar	Catbalogan City, Samar Province		MN759246			
Limnonectes magnus 2	CWL 162	KU 306042	Samar	Catbalogan City, Samar Province		MN759247			
Limnonectes magnus 2	CWL 163	KU 306043	Samar	Catbalogan City, Samar Province		MN759248			
Limnonectes magnus 2	CWL 164	KU 306044	Samar	Catbalogan City, Samar Province		MN759249			
Limnonectes magnus 2	CWL 165	KU 306045	Samar	Catbalogan City, Samar Province		MN759146			
Limnonectes magnus 2	CDS 1929	KU 306063	Dinagat	Barangay San Juan, Municipality of Loreto, Dinagat Province		MN759116			

Species	Field No.	Catalog No.	Island	Locality	Elev (m)	GenBank accession numbers			
						16S	LCT	CPT2	POMC
Limnonectes magnus 2	CDS 1934	KU 306068	Dinagat	Barangay San Juan, Municipality of Loreto, Dinagat Province		MN759118			
Limnonectes magnus 2	RMB 8548	KU 310190	Samar	Barangay San Rafael, Municipality of Taft, Eastern Samar Province		MN759233			
Limnonectes magnus 2	RMB 8640	KU 310212	Samar	Barangay San Rafael, Municipality of Taft, Eastern Samar Province		MN759234			
Limnonectes magnus 2	CDS 2805	KU 310587	Samar	Barangay San Rafael, Municipality of Taft, Eastern Samar Province		MN759121			
Limnonectes magnus 2	CDS 2833	KU 310591	Samar	Barangay San Rafael, Municipality of Taft, Eastern Samar Province		MN759122			
Limnonectes magnus 2	CDS 3078	KU 310604	Samar	Barangay San Rafael, Municipality of Taft, Eastern Samar Province		MN759123			
Limnonectes magnus 2	CDS 3106	KU 310615	Samar	Barangay San Rafael, Municipality of Taft, Eastern Samar Province		MN759124			
Limnonectes magnus 2	CDS 3216	KU 310969	Leyte	Pilim, San Vicente, Municipality of Baybay, Leyte Province		MN759125			

Species	Field No.	Catalog No.	Island	Locality	Elev (m)	GenBank accession numbers			
						16S	LCT	CPT2	POMC
Limnonectes magnus 2	CDS 3301	KU 310972	Leyte	Pilim, San Vicente, Municipality of Baybay, Leyte Province		MN759126			
Limnonectes magnus 2	CDS 3304	KU 310975	Leyte	Pilim, San Vicente, Municipality of Baybay, Leyte Province		MN759127			
Limnonectes magnus 2	CDS 3395	KU 310979	Leyte	Pilim, San Vicente, Municipality of Baybay, Leyte Province		MN759128			
Limnonectes magnus 2	RMB 8947	KU 326360	Leyte	Visayas State University Campus, Municipality of Baybay, Leyte Province		MN759236			
Limnonectes magnus 2	RMB 8953	KU 326361	Leyte	Visayas State University Campus, Municipality of Baybay, Leyte Province		MN759237			
Limnonectes magnus 2	CDS 6992	KU 337806	Samar	Mt. Huraw, Barangay Uno, Municipality of San Jose de Buan, Northern Samar Province		MN759139	X	MT631738	MT631743
Limnonectes magnus 2	CDS 7071	KU 337809	Samar	Mt. Huraw, Barangay Uno, Municipality of San Jose de Buan, Northern Samar Province		MN759140			

Species	Field No.	Catalog No.	Island	Locality	Elev (m)	GenBank accession numbers			
						16S	LCT	CPT2	POMC
Limnonectes magnus 2	CDS 7072	KU 337810	Samar	Mt. Huraw, Barangay Uno, Municipality of San Jose de Buan, Northern Samar Province		MN759141			
Limnonectes magnus 2	CDS 7174	KU 337811	Samar	Mt. Huraw, Barangay Uno, Municipality of San Jose de Buan, Northern Samar Province		MN759142			
Limnonectes magnus 2	RMB 18467	KU 337814	Samar	Kadakan River, Barangay San Rafael, Municipality of Taft, Eastern Samar Province		MN759204			
Limnonectes magnus 2	RMB 18471	KU 337818	Samar	Kadakan River, Barangay San Rafael, Municipality of Taft, Eastern Samar Province		MN759205			
Limnonectes magnus 2	RMB 18475	KU 337822	Samar	Kadakan River, Barangay San Rafael, Municipality of Taft, Eastern Samar Province		MN759206			
Limnonectes magnus 2	RMB 18478	KU 337825	Samar	Kadakan River, Barangay San Rafael, Municipality of Taft, Eastern Samar Province		MN759207			
Limnonectes magnus 2	RMB 18482	KU 337829	Samar	Kadakan River, Barangay San Rafael, Municipality of Taft,		MN759208			

Species	Field No.	Catalog No.	Island	Locality	Elev (m)	GenBank accession numbers			
						16S	LCT	CPT2	POMC
				Eastern Samar Province					
Limnonectes magnus 2	RMB 18696	KU 337833	Samar	Kadakan River, Barangay San Rafael, Municipality of Taft, Eastern Samar Province		MN759209			
Limnonectes magnus 2	RMB 18744	KU 337837	Samar	Kadakan River, Barangay San Rafael, Municipality of Taft, Eastern Samar Province		MN759210	X	MT631736	MT631759
Limnonectes magnus 2	RMB 19080	KU 337852	Samar	DENR House, Barangay San Rafael, Municipality of Taft, Eastern Samar Province		MN759212			
Limnonectes magnus 2	RMB 19101	KU 338896	Samar	Barangay San Rafael, Municipality of Taft, Eastern Samar Province		MN759213			
Limnonectes magnus 2	CDS 6439	KU 340593	Samar	Kadakan River, Barangay San Rafael, Municipality of Taft, Eastern Samar Province		MN759138	X		MT631748
Limnonectes magnus 3	ACD 7076	Deposited at PNM	Siargao	Barangay del Carmen, Surigao del Norte Province		MN759106			
Limnonectes magnus 3	CDS 2005	KU 306004	Dinagat	Barangay Esperanza, Municipality of Loreto, Dinagat Province		MN759120			

Species	Field No.	Catalog No.	Island	Locality	Elev (m)	GenBank accession numbers			
						16S	LCT	CPT2	POMC
Limnonectes magnus 3	CDS 1841	KU 306030	Samar	Taft Forest, Barangay San Rafael, Municipality of Taft, Eastern Samar Province		MN759113			
Limnonectes magnus 3	CDS 1844	KU 306033	Samar	Taft Forest, Barangay San Rafael, Municipality of Taft, Eastern Samar Province		MN759114			
Limnonectes magnus 3	CDS 1928	KU 306062	Dinagat	Barangay San Juan, Municipality of Loreto, Dinagat Province		MN759115			
Limnonectes magnus 3	CDS 1931	KU 306065	Dinagat	Barangay San Juan, Municipality of Loreto, Dinagat Province		MN759117			
Limnonectes magnus 3	CDS 1979	KU 306072	Dinagat	Barangay Esperanza, Municipality of Loreto		MN759119			
Limnonectes magnus 3	CWL 252	KU 306076	Dinagat	Barangay San Juan, Municipality of Loreto, Dinagat Province		MN759147			
Limnonectes magnus 3	CWL 253	KU 306077	Dinagat	Barangay San Juan, Municipality of Loreto, Dinagat Province		MN759148			
Limnonectes magnus 3	CWL 257	KU 306081	Dinagat	Barangay San Juan, Municipality of Loreto, Dinagat Province		MN759149			

Species	Field No.	Catalog No.	Island	Locality	Elev (m)	GenBank accession numbers			
						16S	LCT	CPT2	POMC
Limnonectes magnus 3	CWL 299	KU 306082	Dinagat	Barangay Esperanza, Municipality of Loreto, Dinagat Province		MN759150	X	MT631730	MT631747
Limnonectes magnus 3	CWL 300	KU 306083	Dinagat	Barangay Esperanza, Municipality of Loreto, Dinagat Province		MN759152			
Limnonectes magnus 3	CWL 324	KU 306084	Dinagat	Barangay Esperanza, Municipality of Loreto, Dinagat Province	340	MN759245			
Limnonectes magnus 3	RMB 8540	KU 309273	Samar	Barangay San Rafael, Municipality of Taft, Eastern Samar Province		MN759232			
Limnonectes magnus 3	RMB 8707	KU 309274	Samar	Barangay San Rafael, Municipality of Taft, Eastern Samar Province		MN759235			
Limnonectes magnus 3	RMB 7956	KU 309687	Camiguin Sur	Sitio Kampana, Barangay Pandan, Municipality of Mambajao, Camiguin Province		MN759220			
Limnonectes magnus 3	RMB 7971	KU 309691	Camiguin Sur	Sitio Kampana, Barangay Pandan, Municipality of Mambajao, Camiguin Province		MN759221			
Limnonectes magnus 3	RMB 7976	KU 309696	Camiguin Sur	Sitio Kampana, Barangay Pandan, Municipality of		MN759222			

Species	Field No.	Catalog No.	Island	Locality	Elev (m)	GenBank accession numbers			
						16S	LCT	CPT2	POMC
				Mambajao, Camiguin Province					
Limnonectes magnus 3	RMB 8065	KU 309702	Camiguin Sur	Sitio Kampana, Barangay Pandan, Municipality of Mambajao, Camiguin Province		MN759223			
Limnonectes magnus 3	RMB 8096	KU 309707	Camiguin Sur	Sitio Pamahawan, Barangay Pandan, Municipality of Mambajao, Camiguin Province		MN759224			
Limnonectes magnus 3	RMB 8292	KU 309975	Dinagat	Sitio Cambinlia (Sudlon), Barangay Santiago, Municipality of Loreto, Dinagat Islands Province		MN759225			
Limnonectes magnus 3	RMB 8295	KU 309978	Dinagat	Sitio Cambinlia (Sudlon), Barangay Santiago, Municipality of Loreto, Dinagat Islands Province		MN759226			
Limnonectes magnus 3	RMB 8365	KU 309981	Dinagat	Sitio Cambinlia (Sudlon), Barangay Santiago, Municipality of Loreto, Dinagat Islands Province		MN759227			
Limnonectes magnus 3	RMB 8389	KU 309985	Dinagat	Sitio Cambinlia (Sudlon), Barangay Santiago,		MN759228			

Species	Field No.	Catalog No.	Island	Locality	Elev (m)	GenBank accession numbers			
						16S	LCT	CPT2	POMC
				Municipality of Loreto, Dinagat Islands Province					
Limnonectes magnus 3	RMB 8482	KU 309989	Dinagat	Sitio Cambinlia (Sangay 2), Barangay Santiago, Municipality of Loreto, Dinagat Islands Province		MN759229			
Limnonectes magnus 3	RMB 8520	KU 310181	Samar	Barangay San Rafael, Municipality of Taft, Eastern Samar Province		MN759230			
Limnonectes magnus 3	RMB 8523	KU 314384	Mindanao	Pasonanca Natural Park, Sitio Canucutan, Barangay Pasonanca, Municipality of Zamboanga, Zamboanga del Sur Province		MN759089	X	MT631735	MT631746
Limnonectes magnus 3	ACD 3714	KU 314385	Mindanao	Pasonanca Natural Park, Sitio Canucutan, Barangay Pasonanca, Municipality of Zamboanga, Zamboanga del Sur Province		MN759151			
Limnonectes magnus 3	ACD 3728	KU 314387	Mindanao	Pasonanca Natural Park, Sitio Canucutan, Barangay Pasonanca,		MN759090			

Species	Field No.	Catalog No.	Island	Locality	Elev (m)	GenBank accession numbers			
						16S	LCT	CPT2	POMC
				Municipality of Zamboanga, Zamboanga del Sur Province					
Limnonectes magnus 3	ACD 3772	KU 314391	Mindanao	Pasonanca Natural Park, Sitio Canucutan, Barangay Pasonanca, Municipality of Zamboanga, Zamboanga del Sur Province		MN759238			
Limnonectes magnus 3	RMB 8982	KU 314394	Mindanao	Pasonanca Natural Park, Tumaga River, Municipality of Zamboanga, Zamboanga del Sur Province		MN759239			
Limnonectes magnus 3	RMB 9116	KU 314396	Mindanao	Pasonanca Natural Park, Tumaga River, Municipality of Zamboanga, Zamboanga del Sur Province		MN759240			
Limnonectes magnus 3	RMB 9118	KU 314399	Mindanao	Pasonanca Natural Park, Sitio Canucutan, Barangay Pasonanca, Municipality of Zamboanga, Zamboanga del Sur Province		MN759241			

Species	Field No.	Catalog No.	Island	Locality	Elev (m)	GenBank accession numbers			
						16S	LCT	CPT2	POMC
Limnonectes magnus 3	RMB 9258	KU 314402	Mindanao	Pasonanca Natural Park, Sitio Canucutan, Barangay Pasonanca, Municipality of Zamboanga, Zamboanga del Sur Province		MN759242			
Limnonectes magnus 3	RMB 9316	KU 314404	Mindanao	Pasonanca Natural Park, Sitio Canucutan, Barangay Pasonanca, Municipality of Zamboanga, Zamboanga del Sur Province		MN759243			
Limnonectes magnus 3	RMB 9330	KU 314406	Mindanao	Pasonanca Natural Park, Sitio Canucutan, Barangay Pasonanca, Municipality of Zamboanga, Zamboanga del Sur Province		MN759244			
Limnonectes magnus 3	RMB 9332	KU 314428	Mindanao	Pasonanca Natural Park, Sitio Kilometer 24, Barangay Baluno, Municipality of Zamboanga, Zamboanga del Sur Province		MN759165			

Species	Field No.	Catalog No.	Island	Locality	Elev (m)	GenBank accession numbers			
						16S	LCT	CPT2	POMC
Limnonectes magnus 3	RMB 10034	KU 314438 (Holotype)	Mindanao	Pasonanca Natural Park, Sitio Zambales, Barangay Baluno, Municipality of Zamboanga, Zamboanga del Sur Province		MN759166			
Limnonectes magnus 3	RMB 10374	KU 314446	Mindanao	Pasonanca Natural Park, Sitio Zambales, Barangay Baluno, Municipality of Zamboanga, Zamboanga del Sur Province		MN759167			
Limnonectes magnus 3	RMB 10484	KU 319384	Mindanao	Mt. Magdiwata, Barangay Bayugan II, Municipality of San Francisco, Agusan del Sur Province		MN759091			
Limnonectes magnus 3	ACD 3856	KU 319385	Mindanao	Mt. Magdiwata, Barangay Bayugan II, Municipality of San Francisco, Agusan del Sur Province		MN759092			
Limnonectes magnus 3	ACD 3908	KU 319395	Mindanao	Mt. Magdiwata, Barangay Bayugan II, Municipality of San Francisco, Agusan del Sur Province		MN759093			

Species	Field No.	Catalog No.	Island	Locality	Elev (m)	GenBank accession numbers			
						16S	LCT	CPT2	POMC
Limnonectes magnus 3	ACD 4108	KU 320078	Mindanao	Mt. Balatukan Natural Park, Sitio San Isidro, Boy Scout Camp, Municipality of Gingoog, Misamis Oriental Province		MN759094			
Limnonectes magnus 3	ACD 4237	KU 321148	Mindanao	Pasonanca Natural Park, Sitio Nancy, Barangay La Paz, Municipality of Zamboanga, Zamboanga del Sur Province		MN759168			
Limnonectes magnus 3	RMB 11148	KU 321160	Mindanao	Pasonanca Natural Park, Sitio Nancy, Barangay La Paz, Municipality of Zamboanga, Zamboanga del Sur Province		MN759169			
Limnonectes magnus 3	RMB 11178	KU 326655	Mindanao	Barangay Kimlawis, Municipality of Kiblawan, Davao del Sur Province		MN759100			
Limnonectes magnus 3	ACD5263	KU 326656	Mindanao	Sitio Dasal Mangisi, Barangay Tablu, Municipality of Zamboanga, Zamboanga del Sur Province		MN759105			
Limnonectes magnus 3	ACD 5427	KU 327476	Mindanao	Barangay Kimlawis, Municipality of		MN759099			

Species	Field No.	Catalog No.	Island	Locality	Elev (m)	GenBank accession numbers			
						16S	LCT	CPT2	POMC
				Kiblawan, Davao del Sur Province					
Limnonectes magnus 3	ACD 5252	KU 327479	Mindanao	Barangay Kimlawis, Municipality of Kiblawan, Davao del Sur Province		MN759101			
Limnonectes magnus 3	ACD 5265	KU 327482	Mindanao	Barangay Kimlawis, Municipality of Kiblawan, Davao del Sur Province		MN759102			
Limnonectes magnus 3	ACD 5268	KU 327485	Mindanao	Barangay Kimlawis, Municipality of Kiblawan, Davao del Sur Province		MN759103			
Limnonectes magnus 3	ACD 5271	KU 327499	Mindanao	Sitio Dasal Mangisi, Barangay Tablu, Municipality of Zamboanga, Zamboanga del Sur Province		MN759104			
Limnonectes magnus 3	ACD 5415	KU 333344	Mindanao	Mt. Hilong-hilong, Intersection of Dayhopan and Agay Rivers, Eye Falls, Municipality of Remedios T. Romualdez, Agusan del Norte Province		MN759170			
Limnonectes magnus 3	RMB 15737	KU 333350	Mindanao	Mt. Hilong-hilong, Intersection of Dayhopan and Agay Rivers, Eye Falls, Municipality of	470	MN759171			

Species	Field No.	Catalog No.	Island	Locality	Elev (m)	GenBank accession numbers			
						16S	LCT	CPT2	POMC
				Remedios T. Romualdez, Agusan del Norte Province					
Limnonectes magnus 3	RMB 15785	KU 333355	Mindanao	Mt. Hilong-hilong, Intersection of Dayhopan and Agay Rivers, Eye Falls, Municipality of Remedios T. Romualdez, Agusan del Norte Province	470	MN759172			
Limnonectes magnus 3	RMB 15790	KU 333360	Mindanao	Mt. Hilong-hilong, Intersection of Dayhopan and Agay Rivers, Eye Falls, Municipality of Remedios T. Romualdez, Agusan del Norte Province	470	MN759173			
Limnonectes magnus 3	RMB 15891	KU 333365	Mindanao	Mt. Hilong-hilong, Intersection of Dayhopan and Agay Rivers, Eye Falls, Municipality of Remedios T. Romualdez, Agusan del Norte Province	470	MN759174			
Limnonectes magnus 3	RMB 15896	KU 333380	Mindanao	Mt. Hilong-hilong, May-Impit, Municipality of Remedios T. Romualdez, Agusan del Norte Province	470	MN759177			

Species	Field No.	Catalog No.	Island	Locality	Elev (m)	GenBank accession numbers			
						16S	LCT	CPT2	POMC
Limnonectes magnus 3	RMB 16231	KU 333390	Mindanao	Mt. Hilong-hilong, May-Impit, Municipality of Remedios T. Romualdez, Agusan del Norte Province	1,150	MN759185			
Limnonectes magnus 3	RMB 16275	KU 333395	Mindanao	Mt. Hilong-hilong, May-Impit, Municipality of Remedios T. Romualdez, Agusan del Norte Province	990	MN759187			
Limnonectes magnus 3	RMB 16280	KU 333400	Mindanao	Mt. Hilong-hilong, Municipality of Remedios T. Romualdez, Agusan del Norte Province	990	MN759188			
Limnonectes magnus 3	RMB 16357	KU 333404	Mindanao	Mt. Hilong-hilong, Municipality of Remedios T. Romualdez, Agusan del Norte Province	170	MN759189			
Limnonectes magnus 3	RMB 16361	KU 333414	Mindanao	Mt. Hilong-hilong, Municipality of Remedios T. Romualdez, Agusan del Norte Province	170	MN759190			
Limnonectes magnus 3	RMB 16372	KU 333423	Mindanao	Mt. Lumot, Haribon Site, Municipality of Gingoog, Misamis Oriental Province	170	MN759191			
Limnonectes magnus 3	RMB 16419	KU 333433	Mindanao	Mt. Lumot, Camp 2, Municipality of		MN759193			

Species	Field No.	Catalog No.	Island	Locality	Elev (m)	GenBank accession numbers			
						16S	LCT	CPT2	POMC
				Gingoog, Misamis Oriental Province					
Limnonectes magnus 3	RMB 16587	KU 333480	Mindanao	Mt. Lumot, Camp 3, Sitio Kibuko-Boundary with Barangay Lawaan, Gingoog River, Municipality of Gingoog, Misamis Oriental Province	1,236	MN759195			
Limnonectes magnus 3	RMB 16958	KU 333481	Mindanao	Mt. Lumot, Camp 3, Sitio Kibuko-Boundary with Barangay Lawaan, Gingoog River, Municipality of Gingoog, Misamis Oriental Province	420	MN759196			
Limnonectes magnus 3	RMB 16982	KU 333482	Mindanao	Mt. Lumot, Camp 3, Sitio Kibuko-Boundary with Barangay Lawaan, Gingoog River, Municipality of Gingoog, Misamis Oriental Province	420	MN759197			
Limnonectes magnus 3	RMB 16983	KU 333483	Mindanao	Mt. Lumot, Camp 3, Sitio Kibuko-Boundary with Barangay Lawaan, Gingoog River, Municipality of	420	MN759198			

Species	Field No.	Catalog No.	Island	Locality	Elev (m)	GenBank accession numbers			
						16S	LCT	CPT2	POMC
				Gingoog, Misamis Oriental Province					
Limnonectes magnus 3	RMB 16984	KU 333485	Mindanao	Mt. Lumot, Camp 3, Sitio Kibuko-Boundary with Barangay Lawaan, Gingoog River, Municipality of Gingoog, Misamis Oriental Province	420	MN759214			
Limnonectes magnus 3	RMB 20765	KU 333487	Mindanao	Mt. Lumot, Camp 3, Sitio Kibuko-Boundary with Barangay Lawaan, Gingoog River, Municipality of Gingoog, Misamis Oriental Province		MN759215			
Limnonectes magnus 3	RMB 20767	KU 333488	Mindanao	Mt. Lumot, Camp 3, Sitio Kibuko-Boundary with Barangay Lawaan, Gingoog River, Municipality of Gingoog, Misamis Oriental Province	420	MN759216			
Limnonectes magnus 3	RMB 20862	KU 333490	Mindanao	Mt. Lumot, Camp 3, Sitio Kibuko-Boundary with Barangay Lawaan, Gingoog River, Municipality of	420	MN759217			

Species	Field No.	Catalog No.	Island	Locality	Elev (m)	GenBank accession numbers			
						16S	LCT	CPT2	POMC
				Gingoog, Misamis Oriental Province					
Limnonectes magnus 3	RMB 20883	KU 333491	Mindanao	Mt. Lumot, Camp 3, Sitio Kibuko-Boundary with Barangay Lawaan, Gingoog River, Municipality of Gingoog, Misamis Oriental Province	420	MN759218			
Limnonectes magnus 3	RMB 20884	KU 335041	Mindanao	Pasonanca Natural Park, Sitio Catala, Catala Creek, Municipality of Zamboanga City, Zamboanga del Sur Province	420	MN759199			
Limnonectes magnus 3	RMB 17312	KU 335043	Mindanao	Pasonanca Natural Park, Sitio Catala, Catala Creek, Municipality of Zamboanga City, Zamboanga del Sur Province		MN759200			
Limnonectes magnus 3	RMB 17314	KU 335045	Mindanao	Pasonanca Natural Park, Sitio Catala, Catala Creek, Municipality of Zamboanga City, Zamboanga del Sur Province		MN759201			
Limnonectes magnus 3	RMB 17316	KU 335049	Mindanao	Pasonanca Natural Park, Sitio Catala,		MN759202			

Species	Field No.	Catalog No.	Island	Locality	Elev (m)	GenBank accession numbers			
						16S	LCT	CPT2	POMC
				Catala Creek, Municipality of Zamboanga City, Zamboanga del Sur Province					
Limnonectes magnus 3	RMB 17320	KU 335052	Mindanao	Pasonanca Natural Park, Sitio Catala, Catala Creek, Municipality of Zamboanga City, Zamboanga del Sur Province		MN759203			
Limnonectes magnus 3	RMB 17376	KU 337842	Samar	Kadak-an River, Barangay San Rafael, Municipality of Taft, Eastern Samar Province		MN759211	X	MT631731	MT631742
Limnonectes magnus 2	RMB 18843	CMNH 5513	Mindanao	Mt. Apo, Barangay Ilomavis, Municipality of Kidapawan, Davao del Norte Province		AY313703			
Limnonectes magnus 1	NA	PNM 7829	Bohol	Municipality of Bilar, Bohol Province		AY313706			
Limnonectes magnus 1	NA	USNM 534311	Samar	Bagakay Mines, Municipality of Bagakay, Samar Province		AY313704			

APPENDIX II

Specimens Examined

Limnonectes acanthi: PHILIPPINES: Palawan Island: *Palawan Province*: Puerto Princesa City: Barangay Irawan, Irawan Watershed (KU 308975, 308979, 308989–92, 309049, 309051, 309056–57, 309065, 309083–85, 309139–45, PNM 7604); Municipality of Brooke's Point: Barangay Mainit (KU 309146–54, 309437–38, 326332–35, 326353, 327464, PNM 7605); Municipality of Quezon: Barangay Poblacion (KU 309155–63); Municipality of Nara, Barangay Estrella Falls (TNHC 59903, PNM 6694, 7607); Palawan Island, *Palawan Province* (FMNH 51185–89, 51190–95, 51196, 99, 51200–04; 51205–17, 51219–20, 51222–29, 51230–40); KU Palawan Island, *Palawan Province* (FMNH 51185–95); Municipality of Puerto Princesa, Mt. Bloomfield (PNM 6280, 6295, 6301); Barangay Lamod, sitios Kayasan & Tagabinet (PNM 6375–77, 6390–94, 6409–10, 6431–33, 6440–43); Municipality of Iwahig, WNW of Iwahig Town, Malatgaw River (CAS–SU 21432–34, 21437, 21439–41, 21444–49, 21465); Tugbuni Creek, ca 10 km S Iwahig (CAS–SU 21496–21501); ca. 8 km S. of Iwahig (CAS–SU 21525–26); Malatgaw River tributary, ca. 5 km W. of Iwahig (CAS–SU 21502–21508); 9 km SW of Iwahig (CAS–SU 21520–24); ca. 9 kn SSW of Iwahig (21509–17, 21519, 21527–41); Malatgaw River tributary, ca. 1.5 km SSW of Iwahig (CAS–SU 21432–24, 21453–60); Malabosog Creek, 95.5 km NE of Puerto Princesa (CAS 157215–16, 158100–04);Malabosog Creek, 95.5 km NE of Puerto Princesa (CAS 158131–33); W of coast road, 96.5 km NE of Puerto Princesa (158136–40); Pelotan Creek, 94 km NE of Puerto Princesa (CAS 158144–48); Langogan River tributary, 1.5 km upstream from mouth, 85 km NE Puerto Princesa (CAS 158151–53); Puerto Princesa District, Municipality of Iwahig, Iwahig Penal Colony, Sitio Balsahan (USNM 229492–93); Municipality of Narra, Taritien Barrio, Estrella Falls (USNM 287281–83, 287342–45);

Municipality of Quezon, National Museum compound (USNM 287370–73); Municipality of Brooke's Point, Barangay Macagua (USNM 158204, 158205–09); Boundary of Barangay Samarinana and Saulog: Mt. Mantalingahan Range, Area "Pitang" (KU 309155); Palawan Island (MCZ A-14268–69, 23171–73); Sugod Island, *Palawan Province*: Municipality of Puerto Princesa, Barangay Cabayugan (PNM 6306, 6319–21, 6345, 6356. 6365); Balabac Island, *Palawan Province* (FMNH 51196–204); Minagas Point, Dalawan Bay (USNM 158285–94); Busuanga Island, *Palawan Province* (FMNH 51205–17, 51219–20, 51222–40, KU 79043, 79045, 79059, 79060); CAS 62577, holotype); Siñgai (CAS-SU 5986–99, 6026–29, 6038–40, 14710–13; CAS-SU 6000–03, MCZ A–14067–69, paratypes); Coron Island *Palawan Province* (CAS-SU 5943–45, 5954, 13965–67 CAS 158154–77); Wayan Creek, 1–3 km N of San Nicolas (CAS 62133–35, 62562, paratypes); 6 km NE San Nicolas (KU 79041–60); Culion Island, *Palawan Province* (FMNH 51241–79, CAS–SU 3284); 6.5 km SW Culion Town (KU 79061–68).

Limnonectes cf. *acanthi* (Mindoro) (Philippines, Mindoro Island, Oriental Mindoro Province, Municipality of Bongabong, Barangay Carmundo, Sitio Paypay-Ama, Paypay-Ama River (PNM 9870, holotype; KU 302084–88 KU 302085–86, 302089; 303343, 303369–78, paratopotypes; KU 302090–91, 302093, 302095, 302097, 302100, 302109–11); Municipality of Victoria, Barangay Loyal (KU 302112–18); Barangay Loyal, Sitio Panguisan, Panguisan River (KU 303470–78); Municipality of Gloria, Barangay Malamig (KU 302108, 303344; KU 303346–54); Sitio Balogbog, Cueba Simbahan (KU 303379–80); Sitio Pastohan, Tanguisian Falls (KU 303381–402); Occidental Mindoro Province, Municipality of Calintaan, Barangay New Dagupan (KU 303266); Municipality of Magsaysay, Barangay Nicolas, Sitio Banban (KU 303404–30; KU 304131–32); Municipality of Sablayan, Barangay Batong Buhay, Sitio Batulai,

Mt. Siburan (KU 303430–52; KU 305450–51, 306637); Barangay Malisbong, Sitio Aruyan (KU 335863–83); Barangay Burgos, Sitio Posoy, Posoy River (KU 303453–69); Municipality of Paluan, Barangay Harrison, Sitio Ulasan, local name "Matingaram" (KU 308307, 308309, 308313–18, 308321–23, 308327, 308360, 308362–63, 308367–68, 308370–71, 308385, 308391, 308393, 308422, 308457, 308462, 308464–65, 308469, 308472); Municipality of Puerto Galera, Barangay San Isidro, Sitio Minolo, Ponderosa Golf Resort (TNHC 54920); Municipality of San Teodoro, Barangay Villaflor, Tamaraw Falls, approximately km 15 from Puerto Galera on Calapan-to-Puerto Galera road (TNHC 54921–29, 55023, 55025, 55029, 55033, USNM 556073–94); Municipality of Baco, Barangay Lantuyan, near Cabinuangang River (USNM 508558–63, USNM 508564–72); Municipality of Tarogin, ca. 30 km S of Calapan Town, Mt. Halcon SE slope (CAS-SU 22146, CAS-SU 22145, CAS-SU 22147–49, CAS–SU 22150, CAS-SU 22576, CAS-SU 22577, 23508, CAS-SU 23499, 23501, 23525, 23505, 23514–15, 23519–20, CAS-SU 23485, 23487, 23496–97, 23512–13, 23522, 23489, 23498, 23502); Municipality of Tarogin, Mt. Halcon (CAS-SU 22240, CAS–SU 22288–22295, 23500, 23510–11, 23517–18, 23521, CAS-SU 22151); Semirara Island, Oriental Mindoro Province, Municipality of Caluya, Barangay Tinogboc (KU 302105–07); Mindoro Island, Oriental Mindoro Province, Municipality of Baco, Mt. Baco, Alangsa River (USNM 508534–57); Occidental Mindoro Province, Municipality of Paluan, Barangay Harrison, Sitio Ulasan, Local Name "Matingaram"(KU 308308, 308310–12, 308319–20, 308324–26, 308361, 308364–66, 308369, 308372–76, 308386–90, 308392, 308394, 308416–21, 308423, 308430, 308451–52, 308456, 308461, 308463, 308467–68, 308470–87, 308500, 308528, 308538, 308561–69, 308586, 308589, 308590–92); Municipality of Paluan, Barangay 1, Sitio Ipol (KU 308593, 308597, 308599).

Limnonectes diuatus: PHILIPPINES: Mindanao Island, *Agusan del Norte Province*: Municipality of Cabadbaran, Tagibo River, south side of Mt. Hilong-hilong (FMNH 197934, CAS 133430–32, 133434, 139389–93, MCZ A-88036, paratypes; 133500, holotype); Municipality of Remedios T. Romualdez, Mt. Hilong-hilong, Barangay San Antonio, 1130 m, local area name "May Impit" (KU 333325, 333369–75, 333381–89, 333392–93); *Davao Del Norte Province*: Municipality of Monkayo, Simulaw River Drainage, Mt. Pasian (CMNH 5572, 5573, PNM 9506 paratypes and holotype of *Limnonectes ferneri*); Dinagat Island, *Dinagat Islands Province*: Municipality of Loreto, Barangay Santiago, Sitio Cambinlia (Sudlon) (KU 309992–310000).

Limnonectes leytensis: PHILIPPINES: Mindanao Island, "Mindanao" FMNH (14868, batch of 16 specimens); MCZ A-14137–14141, + 11 duplicates); "*Zamboanga Province*" (63200, 6900); "Zamboanga" (MCZ A-10480); *Zamboanga Del Norte Province*: Katipunan (CAS-SU 13960); 1 km S of Gumay, 7 km SE Buena Suerte, Dapitan River (CAS 147303; "*Cotobato Province*:" 50060–131; "Takayan, near Saub, Cotabato Coast (=S. Cotabato and/or Sulturan Kudarat Provinces) (MCZ A-23198–99, 14134–36); *Davao City Province*: Municipality of Kalinan, Barangay Malagos, Malagos Eagle Station (TNHC 61940–41); *Lanao del Norte Province*: Municipality of Kolambugan, Marata Bogan (CAS-SU 6060); *Lanao del Sur Province*: Municipality of Marawi, "Viscar Landing, Lake Lanao:" MCZ A-25755); *Misamis Occidental Province*: Municipality of Misamis (CAS-SU 13956); *Misamis Oriental Province*: Municipality of Cartegena Bo, Plaridel (CAS-SU 16910–12); Leyte Island, *Leyte Province* (FMNH 60789–91, 42855–84, 54121–22); Leyte City (CAS-SU 15483); Calabian (MCZ A-14099); Camiguin SUR Island, *Camiguin Province*: Mambajao (CAS-SU 23088–23091); Negros Island, *Negros Oriental Province*: Dumaguete City (KU 306006, 306008–09, 306011–12,

306014, 306016–18); “Philippines” (FMNH 99212–24); “Negros Island” (FMNH 61524–29); Municipality of Dumaguete City, Barangay Valinad (MCZ A-45654, 45660–61); Samar Island (FMNH 61453–64; 96180, 96206, 96208, 96228–32, 96241, 96248, 172611–21); *Northern Samar Province*: Municipality of San Isidro, Matuquinao (CAS-SU 18161); Basilan Island (FMNH 174049–51, 174034); *Basilan Province* (MCZ A-14125-14133); *Basilan Province,* Port Holland (CAS 60377–78, MCZ A-14103–14110); Mt. Abung-abung, “NE of Maluso” (MCZ A-22741–42); Jolo Island (FMNH 40538–39); Jolo Isl., Sulu Archipelago (MCZ A-10481); Bohol Island, *Bohol Province*: Municipality of Sierra Bullones, ca. 13 km SE Sierra Bullones Town, Cantaub (CAS-SU 23243, 23246–47, 23252, 23258, 23274, 23280, 23283, 23293, 23330–01); Municipality of Sierra Bullones, 10 km SE of Sierra Bullones Town, Dusita (CAS-SU 23140–42, 23144, 23251, 23272, 23284, 23287, 23291, 23299, 23307, 23317, 23326–30, 23331–35, 23241, 23265, CAS 131950–51); Dinagat Island, *Dinagat Province* (MCZ A-14100–02, 14270); Tawi-Tawi Island, Sulu Archipelago (MCZ A-10479, 14111–19, 14271–72).

Limnonectes macrocephalus: PHILIPPINES: Luzon Island, “Northern Luzon” (FMNH 161676–78, 161680, 161694–96, 161698); *Kalinga Province*: Municipality of Lubuanga (KU 306049, 306053, 306056, 306058, 306059); *Ifugao Province* (FMNH 174591–93, 175262, 175264–66, 175267, 175269, 175278); *Mountain Province*: Mt. Data (MCZ A-28294, paratype); *Benguet Subprovince*: Baguio City: (CAS 62546, MCZ A-14491, paratype, MCZ A-14155–75,+ 4 duplicates); *Laguna Province* (CAS-SU 14706, 14748–49); Municipality of Siniloan (CAS-SU 14733–35); Municipality of Los Baños, University of the Philippines Campus, Mt. Makiling (TNHC 54952); *Camarines Sur Province*: Municipality of Naga City, Barangay Panicuason, Mt. Isarog National Park, Mt. Isarog (TNHC 61913, 62744–45); *Albay Province*: Municipality of Tiwi, Barangay Banhaw, Sitio Purok 7, Mt. Malinao (TNHC 61914, 62746); Municipality of

Malinao, Barangay Tagoytoy, Sitio Kumangingking, Mt. Malinao (TNHC 61917, 62747); Barangay Labnig, Sitio Palali (CAS-SU 140046); *Quezon Province*: Municipality of Tayabas, Sampaloc (CAS-SU 14731–32; Cavite Province (CAS 15714–15); Polillo Island, *Quezon Province*: Municipality of Polillo (KU 303480, 303481, 307505); Catanduanes Island, *Catanduanes Province* (FMNH 248015, 259811–12).

Limnonectes magnus: PHILIPPINES: Camiguin Sur Island: *Camiguin Province*: Municipality of Mambajao (KU 302139–40); 5.5 km NE Catarman Town, Mt. Mambajao, Sangsangan (CAS-SU, 24119–20, 24122–24, CAS-SU 24056–57, 24059, 24078); Nasawa Crater, Mt. Hibok-hibok (CAS-SU 22862); 4.5 km S of Mambajao Town, Catibawasan Falls (CAS-SU 22856); Barrio Naasag, Sitio Vulcan (CAS-SU 23095–96); Dinagat Island: *Suriago del Norte Province*: Municipality of Loreto (KU 306003, 306062–63, 306068–70); Samar Island: *Eastern Samar Province*: Municipality of Taft (KU 306036, 306041–42, 306077, 306082–84, 306028–30, 306033, 309272–74); *Western Samar Province*: Municipality of Paranat, Barangay San Isidro, Sitio Nasarang (TNHC 54947–50; Municipality of Tarabucan, Matuquinao (CAS-SU 18174–79 18182–83, 18188–90, 18192, 18194–95, 18198; Sequinan (CAS 11235; Mindanao Island: *Bukidnon Province*: Mt. Kitanglad (FMNH 258974; Municipality of Malaybalay, Kalasungay (CAS-SU 16800, CAS-SU 16799); *Davao City Province*: Mt. Apo (MCZ A-2597, paratype); Municipality of Gumay, W side of Dapitan Peak, 6 km SE of Buena Suerte (CAS 19981); Municipality of Calinan, Barangay Malagos, Baguio District, Eagle Foundation Malagos Eagle camp (TNHC 59904–05, 59941); *Davao del Sur Province*: Municipality of Toril, Barangay Baracatan ("Upper Baracatan"), Sitio San Roque (TNHC 59906, 59942); *Misamis Occidental Province*: Mt. Malindang (CAS-SU 13968); *Zamboanga City Province*: Municipality of Zamboanga City, Barangay Pasonanca (CAS 61870–71); *Agusan Del Norte Province*: W side

of Mt. Hilong-hilong (CAS 133792, 133554, CAS–SU 133673–74); Municipality of Cabadbaran, S side of Mt. Hilong-hilong Peak, crossing of Taguibo and Dalaydayan rivers (CAS-SU 186128); *Zamboanga del Norte Province*: Municipality of Katipunan, Labao (CAS-SU 16804); Bohol Island: *Bohol Province*: Municipality of Carmen, Chocolate Hills Complex, Barangay Buena Vista (TNHC 56397–402); Municipality of Sierra Bullones, 11 mi SE Sierra Bullones Town (CAS 23415, 23417, 23420); Sandayong Barrio (CAS 17170–17211; Cantub Barrio (CAS 17135–37); Cantub, 15 km SE Sierra Bullones Town (CAS-SU 23429–30); 11 mi SE Sierra Bullones, Dusita (MCZ A-23167–70), "Bohol Island" (CAS 23416, 23418–19, 23424); Leyte Island, *Leyte Province*: Municipality of Calabian (MCZ A-14152, paratype of *Rana magna visayanus* Inger 1954); Basilan Island, *Basilan Province*: Basilan Isl. (MCZ A-14152–54, 14267).

Limnonectes micrixalus: Basilan Island, *Basilan Province*: Mt. Abung-abung (CAS 20144, 60143, holotype and paratype of *Rana micrixalus* Taylor, 1923; MCZ A-14187); Mindanao Island, *Zamboanga City Province*: Municipality of Zamboanga City (CAS 61874, paratype of *Rana micrixalus* Taylor, 1923).

Limnonectes palavanensis: PHILIPPINES: Palawan Island: *Palawan Province*: Municipality of Brooke's Point: Barangay Mainit (KU 309133–35, 309136, 309138); S slope of Thumb Peak, 330–660 m, WNW of Iwahig (CAS 14744, CAS-SU 20421–26, CAS 20432–34, CAS 20438, CAS 20445–47, CAS 20449, CAS 20451, CAS-SU 20448); 7–8 km SW of Santiago (CAS 20466–71); Municipality of Iwahig, Thumb Peak, Iwahig Penal Colony (MCZ A-14214–16).

Limnonectes parvus: PHILIPPINES: Mindanao Island: *Zamboanga del Norte Province*: Mt. Malindang: Dapitan River (CAS 139445–46); *Misamis Occidental Province*: Dapitan Peak

(CAS 145767–68); between Sitio Masawan and Sitio Gandawan (CAS 17511); *Misamis Occidental Province*: W side of Dapitang Peak, 1 km E of Masawan (CAS 20399); Municipality of Gumay, New Piñan, 5–6 km S Buena Suerte, headwaters of the Dapitan River, 7–8 km SE of Masawan (CAS 145760–61); W. side Dapitan Peak, 1500 m, 5 km E of Masawan (CAS–SU 20396); New Piñan, Municipality of Gumay, W. side Dapitan Peak, 6 km SE of Buena Suerte (CAS-SU 20403); Dapitan River, 833 m, New Piñan, ca. 2 km SE Municipality of Gumay, 8 kn SE Buena Suerte (CAS–SU 20411).

Limnonectes visayanus: PHILIPPINES: Masbate Island: *Masbate Province*: Municipality of Mobo (KU 302171, CAS-SU 144253–59); Mt. Mobo, Tugbo watershed (CAS-SU 1442609–61, CAS-SU 144327, CAS-SU 14482–84; CAS 144345); Panay Island: *Antique Province*: Municipality of Culasi (KU 302157–59, 302161, 302165); Municipality of Pandan (KU 302176, 302180–84); Municipality of San Remigio (KU 306816); Municipality of Valderrama, Barangay Lublub, base of Mt. Baloy (TNHC 56337); *Aklan Province*: Municipality of Makato, Castillo Barrio (CAS 139164–139166); Municipality of Makato, Castillo Barrio (CAS-SU 137590); Calagna-an Island, *Iloilo Province*: Barangkalan (CAS 124121, 124293–97); Siquijor Island, *Siquijor Province* (FMNH 61439–43, CAS-SU 23126; Municipality of Lazi, Po-o (CAS-SU 16796–97); 1.5 km N of Maria Town (CAS-SU 23908); Municipality of San Jua, Tag-ibo Barrio, 2 km from coast (CAS-SU 16777, 16779, 16780, 16783–85, 16787–88, 16790, 16792, 16794); Sicogon Island, *Iloilo Province*: Buaya area (CAS 124950–58, CAS 12442–44); Poro Island, *Cebu Province*: 0.4 km N of Poro Town (CAS 124515); Negros Island: *Negros Occidental Province*: Municipality of Cauayan (KU 302145); *Negros Oriental Province*: Municipality of Sibulan, Barangay Janya-janay, Sitio Balinsasayo, Cuenos, Lake Balinsasyo (TNHC 61911, 61921, 62879); Municipality of Valencia, Barangay Bongbong, Camp Lookout, Mt. Talinis, in

Cuernos de Negros range (TNHC 62880–82, KU 302189–90, 302192, 302196, 302203–04); Tahiro River, 120 m above sea level (MCZ A-110944–48; Municipality of Bayanan, Malyong (CAS 17078–81); "Negros Island" (FMNH 61504–23, 57204–33, 57234–41, 57244, 57246–47, 61403–09, 61444–48, 77721–22); Municipality of Sibulan Lake Balinsasaayo, 1000 m above sea level, Cuernos de Negros Range (MCZ A-110949); Municipality of Luzuriaga, Barangay Palinpino (MCZ A-28295, paratype); Municipality of Dumaguete, Dumaguete City (MCZ A-26809); 15 km from Dumaguete City, Camp Lookout (CAS 14723); ca. 35 km W of Bais Town, along Mamagyan River, Sitio Panyabunan (CAS 17091); Municipality of Siaton (CAS 156051–56; Hacienda Louisiana (CAS-SU 14725–30); ca. 23 km W of Bais Town, 0.5 km W of Mayaposi Hill, upper Mabaja Creek (CAS 16671, 16776, CAS-SU 16672–83; W. of Mariposi Hill, 20 km W of Bais Town, Mabaja River (CAS 17074–76); ca. 20 km W of Bais, Pagyabunan (CAS 16749–51; ca. 3 km W of Palimpinon, Ocoy River (CAS 16685–16736); Pulopaantao, SE slope of Makawili Peak, Mt. Canlaon (CAS 16650–70); Cebu Island, *Cebu Province*: 3 km NW of Cebu City (CAS-SU 23857, 23861, 23913); Minglanilla area (CAS-SU 131911–13); Municipality of Carmen, Matinao-an (CAS 131903); Guimaras Island, Guimaras Subprovince: near Buenavista (CAS 125305–07); Jordan area (CAS 125308–09).

Limnonectes woodworthi: PHILIPPINES: Catanduanes Island: *Catanduanes Province*: Municipality of San Miguel (KU 302231, 302234); Polillo Island: *Quezon Province*: Municipality of Polillo (KU 302224, 302227, 302228, 303483–85, 307528, 307531–34; CAS 61001, paratype): Luzon Island; *Laguna Province*: Municipality of Los Baños, Mt. Makiling (CAS 61184–89, 61191–93; 61824–29; 62565–73, paratypes;, MCZ A-10555, paratype); "Los Baños creek, between College and Camp Eldridge (MCZ A-14239–40); Municipality of Los Baños, University of the Philippines Campus, Mt. Makiling (54953–55); *Quezon* Province:

Municipality of Atimonan, Barangay Malinao Ilaya (TNHC 61942); *Zambales Province*: Municipality of Olongapo, SBMA Naval Base, "Nav-mag" area, Ilanin Forest (Triboa Bay) (TNHC 62947–55); Camarines *Sur Province*: Municipality of Naga City, Barangay Panicuason, Mt. Isarog (TNHC 61912, 62956); *Albay Province*: Municipality of Tiwi, Barangay Banhaw, Sitio Purok 7, Mt. Malinao (TNHC 61915, 62957); Municipality of Tobaco, Barangay Bongabong (TNHC 61916, 62959–60); Municipality of Malinao, Barangay Tagoytoy, Sitio Kumangingking, Mt. Malinao (TNHC 61918, 62958); *Sorsogon Province*: Municipality of Irosin, Barangay San Rogue, Mt. Bulusan, Bulusan Lake (TNHC 61919–20, 62961–64); Polillo Island, *Quezon Province* (MCZ A-14241–49, paratypes + 24 untagged duplicates); Municipality of Polillo, Barangay Sibucan, Sitio Tambangin (TNHC 54989).

TABLE 1.— Summary statistics and factor loadings for the first five components extracted in a principal components analysis of Mindanao PAIC Fanged Frog populations, analysed separately by sex. See text for discussion of heavily-loading individual characters (bolded for emphasis).

	Males					Females				
Characters	1	2	3	4	5	1	2	3	4	5
Snout–Vent l	0.1121	0.2913	0.0954	-0.489	-0.2669	0.1498	0.166	-0.123	-0.417	-0.0266
Head Length	0.263	-0.3611	0.1472	-0.3103	-0.0728	0.3234	0.2779	-0.0886	0.2877	0.199
Snout Length	**0.3828**	-0.0012	0.1083	0.0213	0.2602	0.3002	0.2078	-0.0434	0.0296	-0.2654
Tympanum I	0.1818	-0.3285	0.1634	0.1682	0.2948	0.122	**0.3505**	-0.0152	-0.3774	-0.3612
Head Width	0.1681	**-0.3848**	0.0746	-0.119	-0.4067	0.2586	0.2146	-0.0231	0.3487	0.2386
Forearm Len	0.1028	**0.3893**	0.1447	-0.2911	-0.2478	0.3273	-0.1601	-0.0091	-0.257	0.2027
Femur Lengt	0.2715	0.1965	-0.0835	0.3061	-0.3325	0.2663	-0.3952	0.1159	0.2283	-0.0475
Tibia Length	**0.3609**	0.186	0.131	0.0371	0.1584	**0.3573**	-0.2471	0.0786	-0.1256	-0.1436
Tarsus Lengt	**0.3554**	0.2086	-0.0751	0.1073	0.0177	**0.3464**	-0.2408	0.0399	-0.1674	-0.1445
Foot Length	**0.3297**	0.1963	-0.0018	0.2538	-0.2449	0.2642	**-0.4184**	0.1445	0.1095	-0.0955
Hand Length	0.263	-0.3611	0.1472	-0.3103	-0.0728	0.3234	0.2779	-0.0886	0.2877	0.199
Eye–Narial D	0.2834	0.1651	0.2381	-0.0352	0.4691	0.3154	0.2417	-0.0586	-0.206	-0.0418
Internarial Di	0.1357	-0.2249	0.1202	0.493	-0.3343	**-0.0328**	0.1302	0.1083	0.4146	-0.7279
Fang Length	0.1949	-0.1014	-0.6397	-0.136	0.0556	0.0195	0.1686	0.6784	-0.0564	0.0104
Fang Height	0.2344	-0.0584	-0.6104	-0.0828	0.0768	-0.0038	0.1619	0.67	-0.0648	0.1911
Standard dev	2.3307	1.7555	1.2847	1.0594	0.9235	2.3459	1.4838	1.384	1.2338	1.0188
Eigenvalues	5.4324	3.0819	1.6504	1.1223	0.8528	5.5034	2.2016	1.9156	1.5222	1.038
Proportion o	0.3622	0.2055	0.11	0.0748	0.0569	0.3669	0.1468	0.1277	0.1015	0.0692
Cumulative F	0.3622	0.5676	0.6776	0.7525	0.8093	0.3669	0.5137	0.6414	0.7428	0.8121

TABLE 2.— ANOVA and Tukey HSD tests on 15 morphometric characters of male and female adult individuals. Asterisks (*) denote characters that were found to be different based on α = 0.05. Characters include (1) snout–vent length, (2) head length, (3) snout length, (4) tympanum diameter, (5) head width, (6) forearm length, (7) femur length, (8) tibia length, (9) tarsus length (10), foot length, (11) hand length, (12) eye–narial distance, (13) internarial distance [Kruskal-Wallis *P*-value in brackets], (14) odontoid length, (15) odontoid height.

	1	2	3	4	5
Males					
ANOVA	0.000*	0.000*	0.000*	0.000*	0.000*
Tukey HSD					
L. diuatus (Green) - *L. diuatus* 1 (Orange)	0.995	0.000*	0.000*	0.003*	0.000*
L. magnus 3 (Blue) - *L. diuatus* (Green)	0.000*	0.111	0.000*	0.409	0.994
L. magnus 3 (Blue) - *L. diuatus* 1 (Orange)	0.019*	0.000*	0.315	0.016*	0.000*
L. magnus 2 (Purple) - *L. diuatus* (Green)	0.849	0.051*	0.000*	0.000*	0.905
L. magnus 2 (Purple) - *L. diuatus* 1 (Orange)	0.871	0.001*	0.399	0.682	0.001*
L. magnus 1 (Yellow) - *L. diuatus* (Green)	0.984	0.999	0.021*	0.542	0.93
L. magnus 1 (Yellow) - *L. diuatus* 1 (Orange)	1	0.001*	0.441	0.379	0.001*
L. magnus 3 (Blue) - *L. magnus* 2 (Purple)	0.000*	0.934	0.999	0.000*	0.953
L. magnus 3 (Blue) - *L. magnus* 1 (Yellow)	0.012*	0.859	0.994	0.943	0.822
L. magnus 2 (Purple) - *L. magnus* 1 (Yellow)	0.798	0.709	0.987	0.805	0.68
Females					
ANOVA	0.000*	0.000*	0.000*	0.000*	0.014*
Tukey HSD					
L. diuatus (Green) - *L. diuatus* 1 (Orange)	0.845	0.000*	0.46	0.608	0.231
L. magnus 3 (Blue) - *L. diuatus* (Green)	0.004*	0.000*	0.000*	0.007*	0.014*
L. magnus 3 (Blue) - *L. diuatus* 1 (Orange)	0.000*	0.998	0.122	0.000*	0.998
L. magnus 2 (Purple) - *L. diuatus* (Green)	0.474	0.008*	0.005*	0.000*	0.808
L. magnus 2 (Purple) - *L. diuatus* 1 (Orange)	0.104	0.794	0.429	0.000*	0.84
L. magnus 1 (Yellow) - *L. diuatus* (Green)	0.22	0.000*	0.001*	0.001*	0.46
L. magnus 1 (Yellow) - *L. diuatus* 1 (Orange)	0.027*	0.997	0.486	0.000*	0.875
L. magnus 3 (Blue) - *L. magnus* 2 (Purple)	0.584	0.35	0.998	0.008*	0.426
L. magnus 3 (Blue) - *L. magnus* 1 (Yellow)	0.263	0.828	0.788	0.708	0.242
L. magnus 2 (Purple) - *L. magnus* 1 (Yellow)	1	0.818	0.991	0.115	0.998

6	7	8	9	10	11	12	13	14	15
0.000*	0.928	0.000*	0.000*	0.000*	0.000*	0.000*	0.070 [0.481]	0.001*	0.054*
0.000*	0.915	0.000*	0.000*	0.000*	0.000*	0.991	0.558	0.014*	0.046*
0.000*	0.503	0.000*	0.000*	0.000*	0.111	0.000*	0.998	0.972	0.695
0.000*	1	0.999	0.417	0.691	0.000*	0.002*	0.395	0.018*	0.13
0.979	0.949	0.000*	0.000*	0.000*	0.051*	0.000*	0.665	0.824	0.999
0.000*	0.989	0.719	0.032*	0.368	0.001*	0.002*	0.916	0.002*	0.046*
0.998	1	0.000*	0.007*	1	0.999	0.000*	0.835	0.59	0.998
0.002*	0.925	0.977	0.591	0.006*	0.001*	0.009*	0.28	0.617	0.28
0.000*	0.85	0.105	0.014*	0.619	0.934	0.998	0.177	0.17	0.69
0.047*	0.84	0.984	0.999	0.005*	0.859	0.95	0.868	0.719	0.997
1	0.974	0.99	0.837	0.035*	0.709	0.978	0.366	0.226	1
0.000*	0.000*	0.000*	0.000*	0.000*	0.000*	0.000*	0.005*	0.982	0.71
0.013*	0.000*	0.000*	0.000*	0.000*	0.000*	0.254	0.168	1	0.92
0.000*	0.016*	0.000*	0.000*	0.000*	0.000*	0.000*	0.997	1	0.918
0.018	0.005*	0.95	0.999	0.019*	0.998	0.000*	0.116	1	0.999
0.040*	0.67	0.000*	0.000*	0.288	0.008*	0.000*	0.685	0.987	0.841
0.981	0.002*	1	0.905	0.002*	0.794	0.008*	0.858	0.984	1
0.000*	0.113	0.000*	0.000*	0.012*	0.000*	0.000*	0.792	1	1
0.23	0.002*	0.988	0.839	0.003*	0.997	0.000*	0.005*	0.999	0.926
0.001	0.64	0.942	0.6	0.375	0.35	0.994	0.689	0.982	0.988
0.528	0.915	0.998	0.666	0.669	0.828	0.958	0.215	1	0.891
0.034*	0.94	0.987	0.186	0.913	0.818	0.921	0.083	0.995	0.832

TABLE 3.—Four data streams, assessed for the presence/absence of support for each haplotype clade (color-coded to match Fig. 1) summarized among Mindanao PAIC Fanged Frog populations of the *Limnonectes magnus* Complex (=*L. magnus*, *L. diuatus*, and *L. ferneri*). "Y" = yes; "N" = no (see Diagnosis sections for character states).

	Clade in mitochondrial tree	Clade in nuclear tree	Supported by Morphometrics	Diagnosed with traditional character states
Highland Clade: *L. diuatus*				
L. diuatus 1 (Orange)	Y	N	N	N
L. diuatus 2 (Red)	Y	Y	Y	Y
L. diuatus (Green)	Y	Y	Y	Y
L. ferneri (Green)	N	N	N	Y
Lowland Clade: *L. magnus*				
L. magnus 1 (Yellow)	Y	N	N	N
L. magnus 2 (Purple)	Y	Y	N	N
L. magnus 3 (Blue)	Y	Y	N	N

FIGURE CAPTIONS

FIG. 1.—Maximum likelihood point estimate, illustrating relationships of Mindanao PAIC Fanged Frogs, inferred from analysis of 16S mitochondrial gene). Nodal support: black dots = strong support (≥ 70 maximum likelihood bootstrap percentages). Sequences from Evans et al. (2003) correspond to bold branches with colored arrows. For full museum catalog voucher information, see Appendix 1 and Supplemental Figure 2.

FIG. 2.— Bayesian maximum clade credibility tree, illustrating relationships among Mindanao PAIC fanged frogs, inferred from analysis of four concatenated loci (16S rRNA, CPT-2, LCT, POMC). Nodal support: Bayesian posterior probabilities, and bootstrap percentages from a separate maximum likelihood analysis, which inferred the same topology (see text for details) Clades color-coded as in Fig. 1.

FIG. 3.—Discriminant and principal components analyses for (A) males and (B) females; dots = individuals; ellipses = groups identified by discriminant analysis of principal components. Three-dimensional plots in (C) males and (D) females depict first three principal components (larger circles = specimens; minute kernels = gaps and/or clusters identified by the hypervolume multivariate kernel density estimation). Color-coding as in Figure 1.

FIG. 4.—Adult male holotype (USNM 35231) of *Limnonectes magnus* from Mt. Apo (collected between Todaya and Camp), Mindanao Island.

FIG. 5.— Adult male holotype (PNM 9506) of *Limnonectes ferneri* from Mt. Pasian, Municipality of Monkayo, Davao Del Norte Province, Mindanao Island, Philippines (Brown and Alcala 1977).

FIG. 6.—Adult male specimen of *Limnonectes magnus* (KU 314438) in (A) dorsal, (B) ventral, and (C) right lateral head views; (D) plantar surface (ventral aspect of left foot); (E) palmar surface (ventral aspect of left hand).

FIG. 7.—Comparative spectrogram (frequency in kHz versus time in s) and corresponding oscillogram (relative amplitude in dB versus time in s) of the advertisement vocalization of *Limnonectes magnus*. The calls of *L. diuatus* (and its junior synonym, *L. ferneri*) have never been recorded.

FIG. 8.—Adult male specimen of *Limnonectes diuatus* (KU 320090) in (A) dorsal, (B) ventral; and (C) right lateral head views; (D) plantar surface (ventral aspect of left foot); (E) palmar surface (ventral aspect of left hand).

Supplemental Material Fig. 1.—Heatmap of uncorrected pairwise p-distances calculated from 16S rRNA gene sequences of the *Limnonectes magnus* Group (*L. magnus, L. diuatus,* and *L. ferneri*). The colors red to green indicate low to high divergences.

Supplemental Material Fig. 2.—Maximum likelihood tree inferred from 16S mitochondrial gene sequences, with tips labelled corresponding to museum voucher specimen catalog numbers.

Figures:

Fig. 1

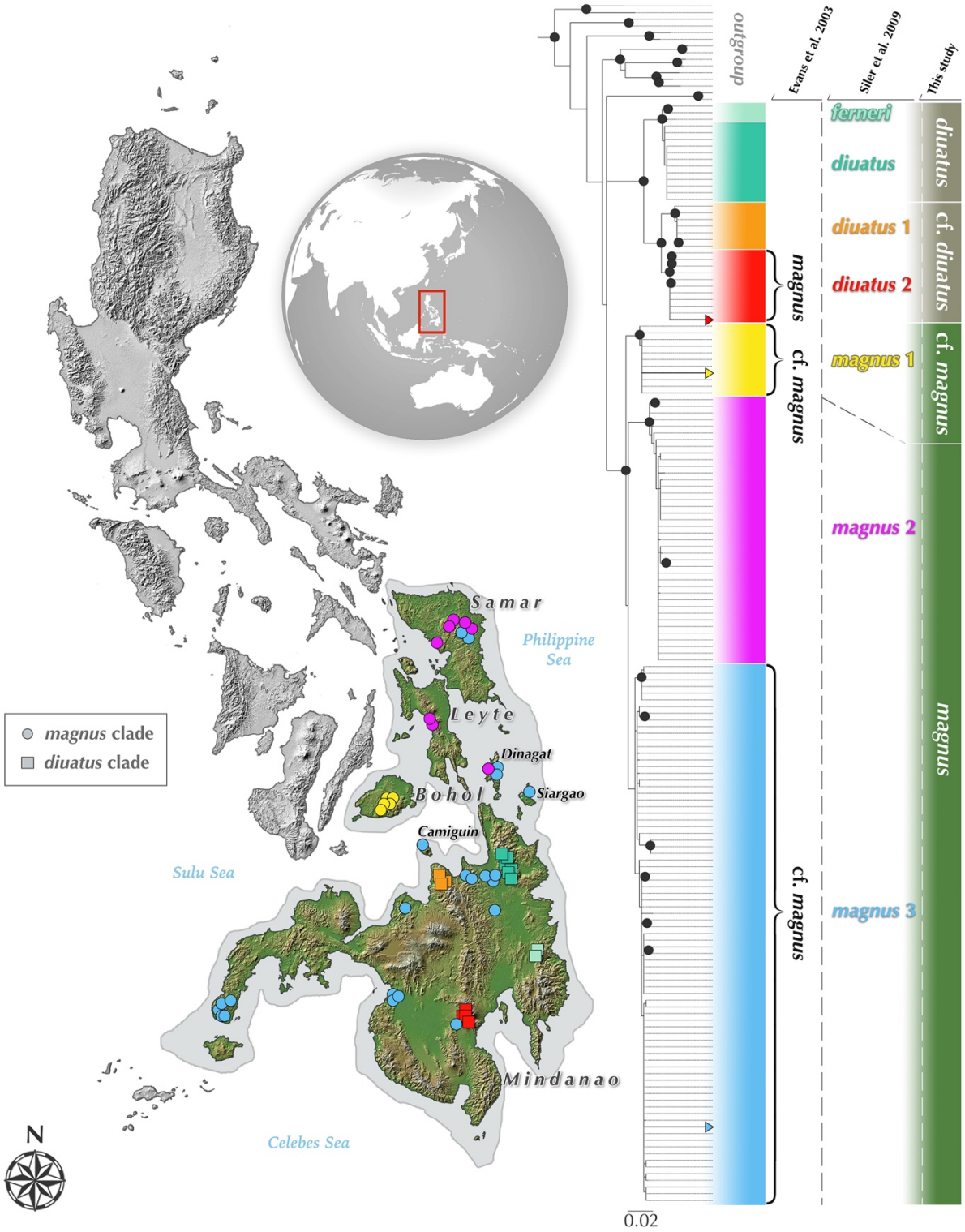

Fig. 2

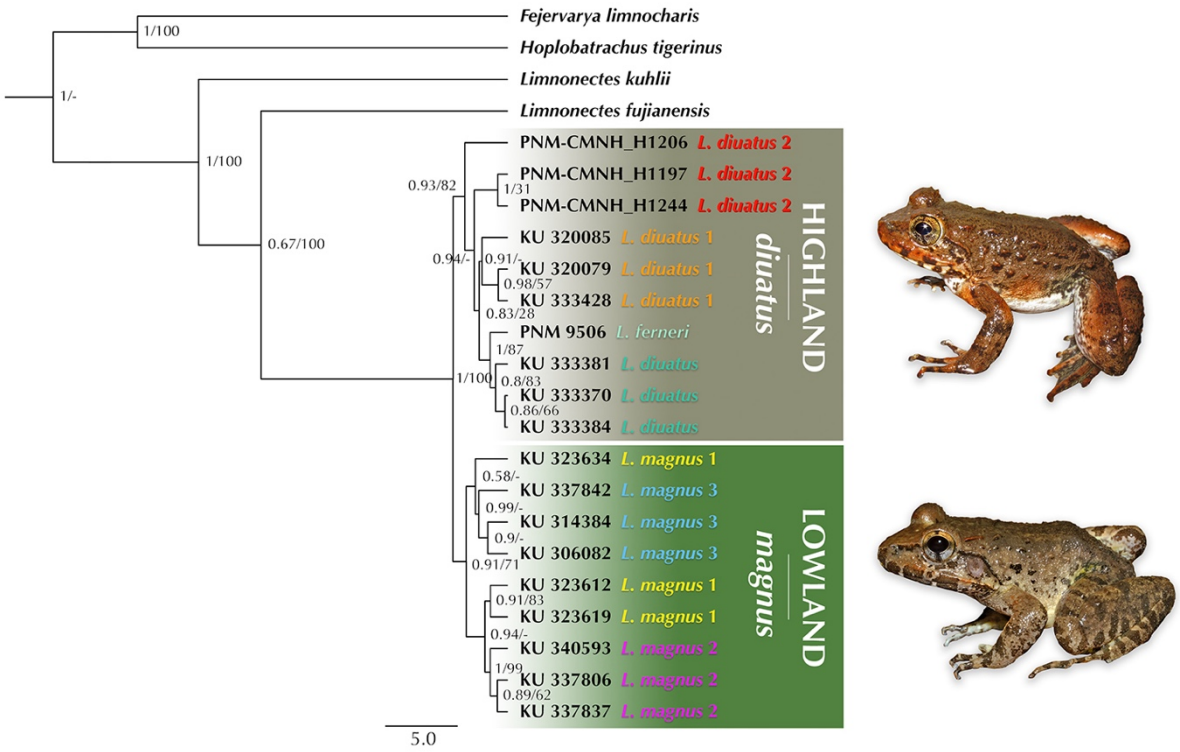
Fejervarya limnocharis
Hoplobatrachus tigerinus
Limnonectes kuhlii
Limnonectes fujianensis
PNM-CMNH_H1206 L. diuatus 2
PNM-CMNH_H1197 L. diuatus 2
PNM-CMNH_H1244 L. diuatus 2
KU 320085 L. diuatus 1
KU 320079 L. diuatus 1
KU 333428 L. diuatus 1
PNM 9506 L. ferneri
KU 333381 L. diuatus
KU 333370 L. diuatus
KU 333384 L. diuatus
KU 323634 L. magnus 1
KU 337842 L. magnus 3
KU 314384 L. magnus 3
KU 306082 L. magnus 3
KU 323612 L. magnus 1
KU 323619 L. magnus 1
KU 340593 L. magnus 2
KU 337806 L. magnus 2
KU 337837 L. magnus 2
HIGHLAND diuatus
LOWLAND magnus
1/100
1/-
1/100
0.67/100
0.93/82
1/31
0.94/-
0.91/-
0.98/57
0.83/28
1/87
1/100
0.8/83
0.86/66
0.58/-
0.99/-
0.9/-
0.91/71
0.91/83
0.94/-
1/99
0.89/62
5.0

Fig. 3

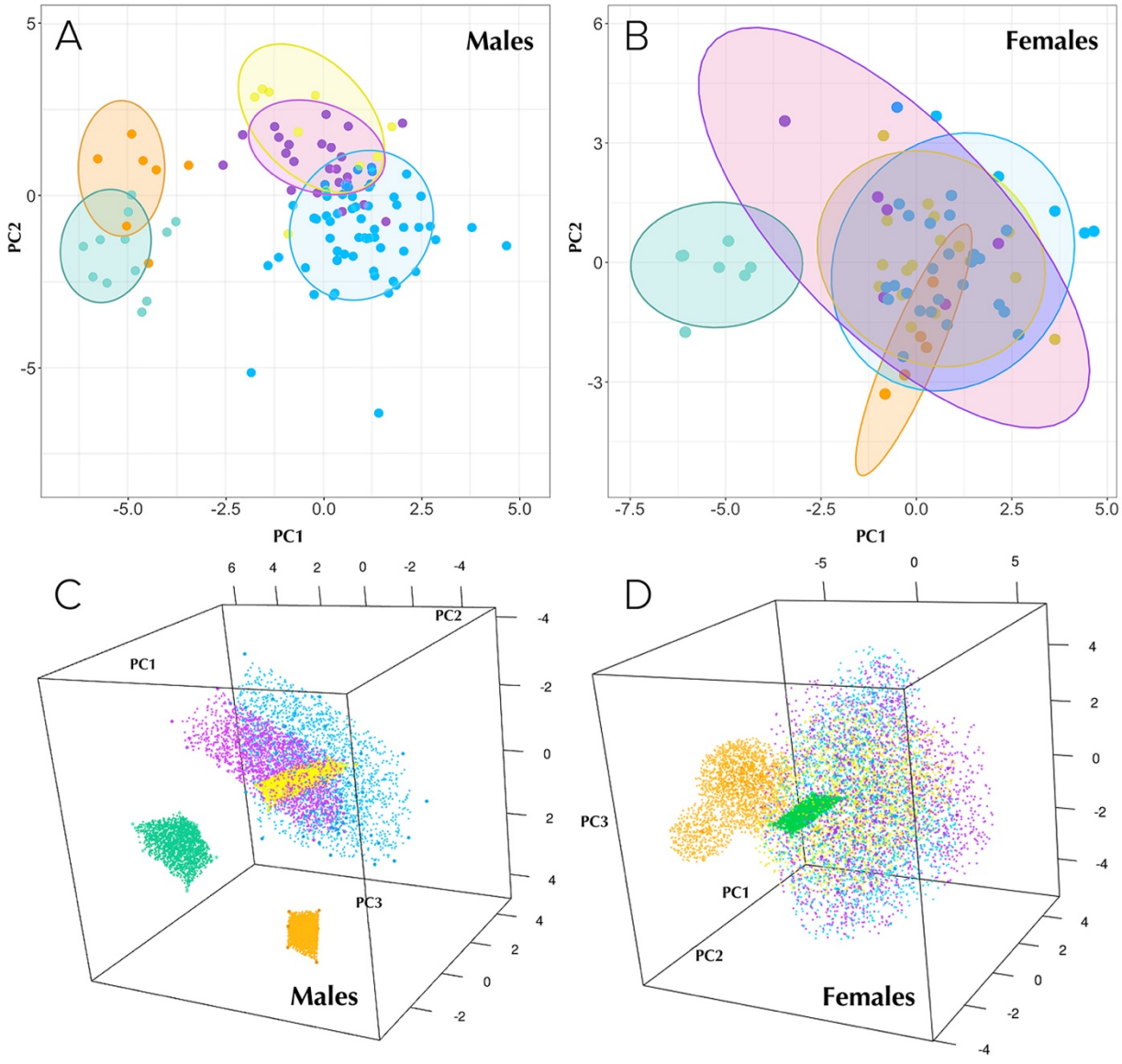
A
Males
PC2
PC1
B
Females
PC2
PC1
C
PC1
PC2
PC3
Males
D
PC3
PC1
PC2
Females

Fig. 4

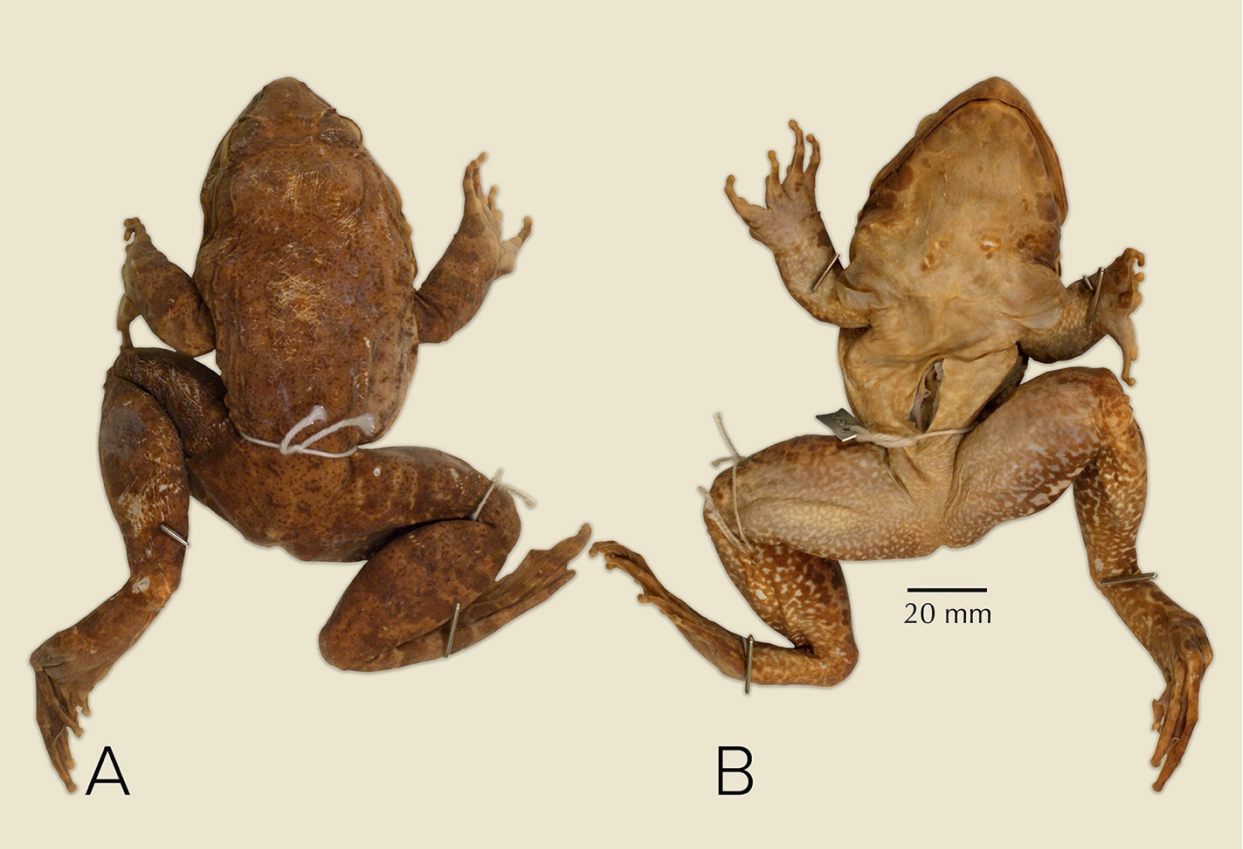

Fig. 5

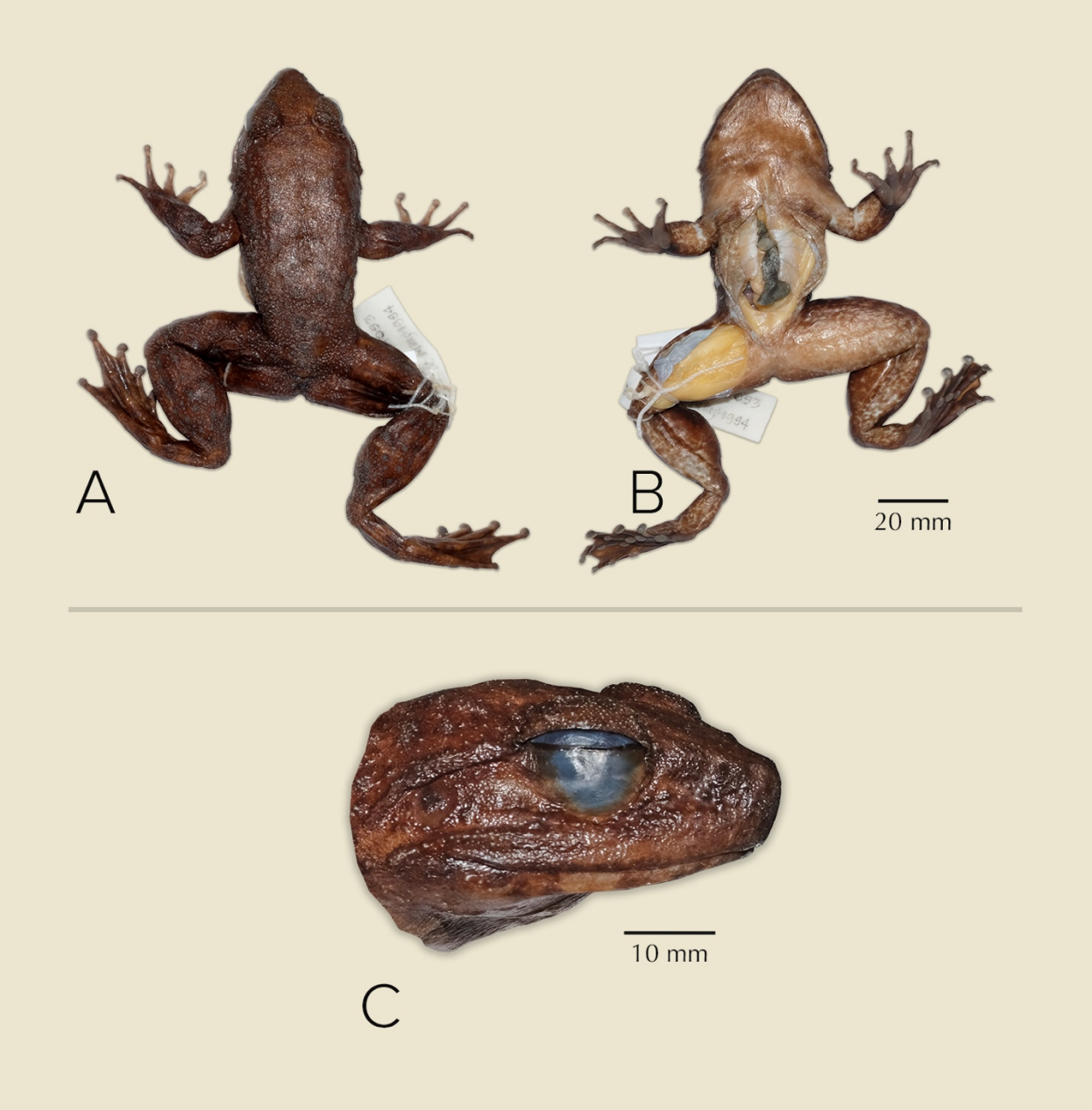

Fig. 6

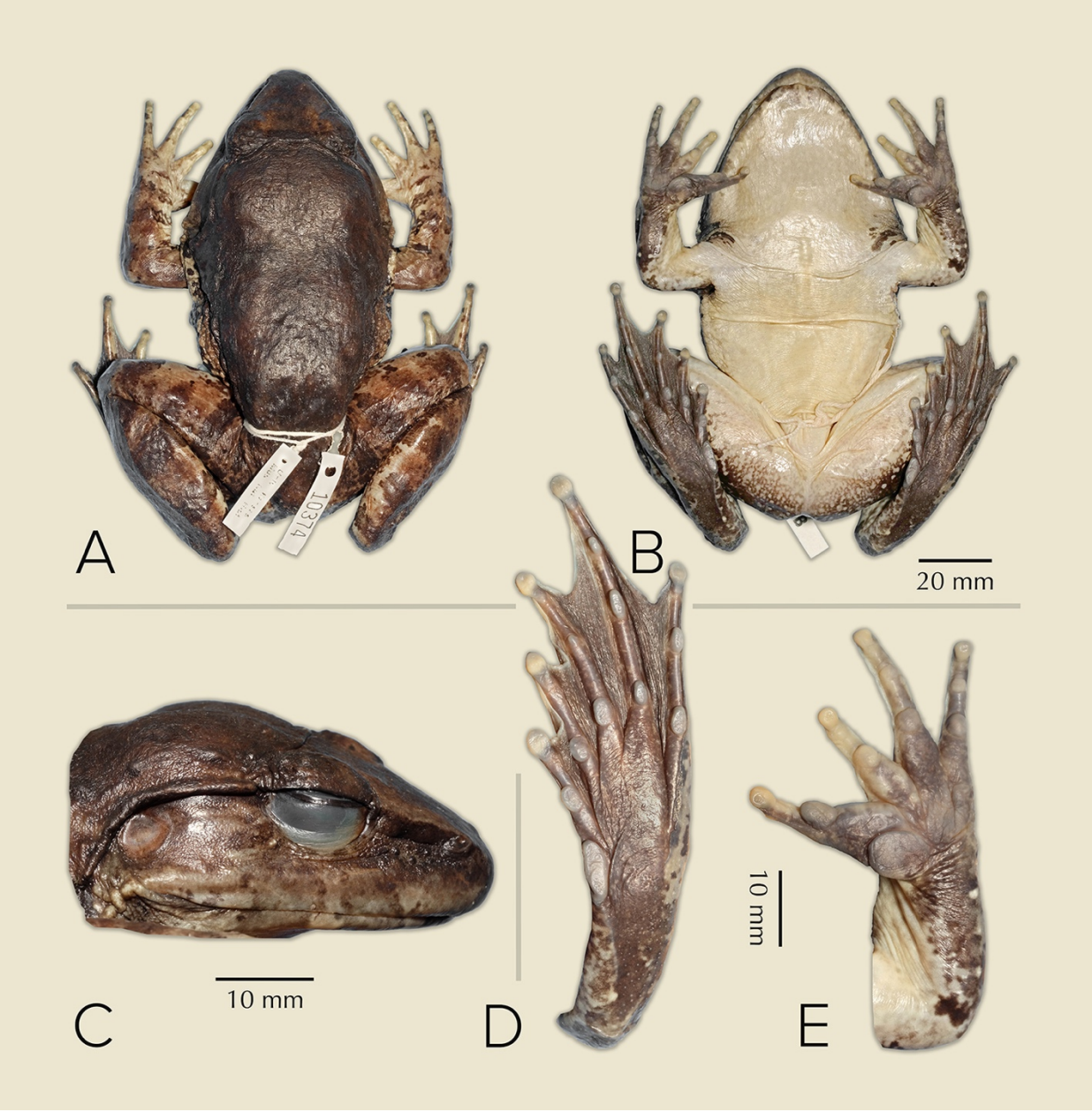

Fig. 7

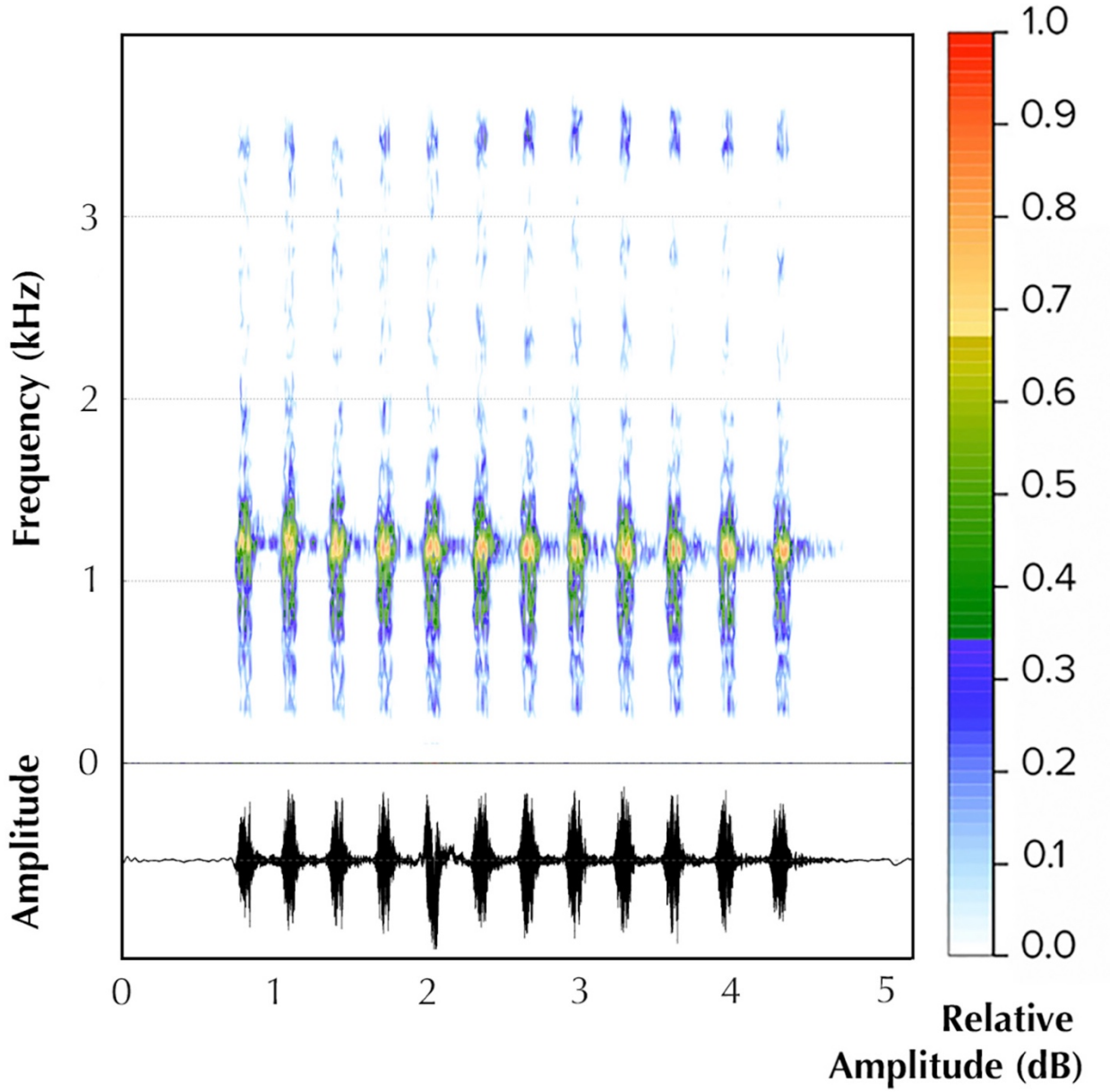
Frequency (kHz)
3
2
1
0
Amplitude
0
1
2
3
4
5
1.0
0.9
0.8
0.7
0.6
0.5
0.4
0.3
0.2
0.1
0.0
Relative
Amplitude (dB)

Fig. 8

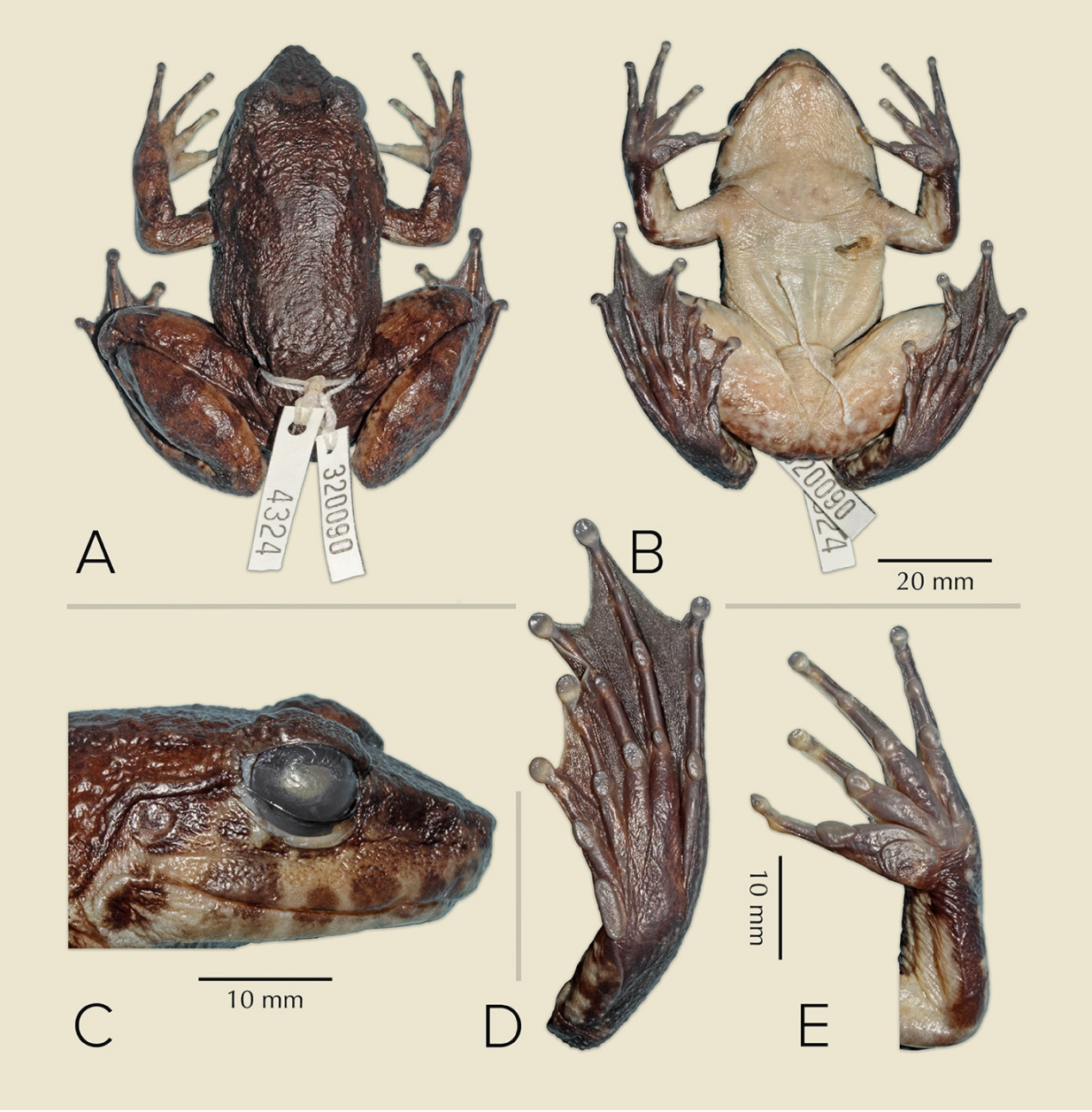

Supplemental Material Fig. 1

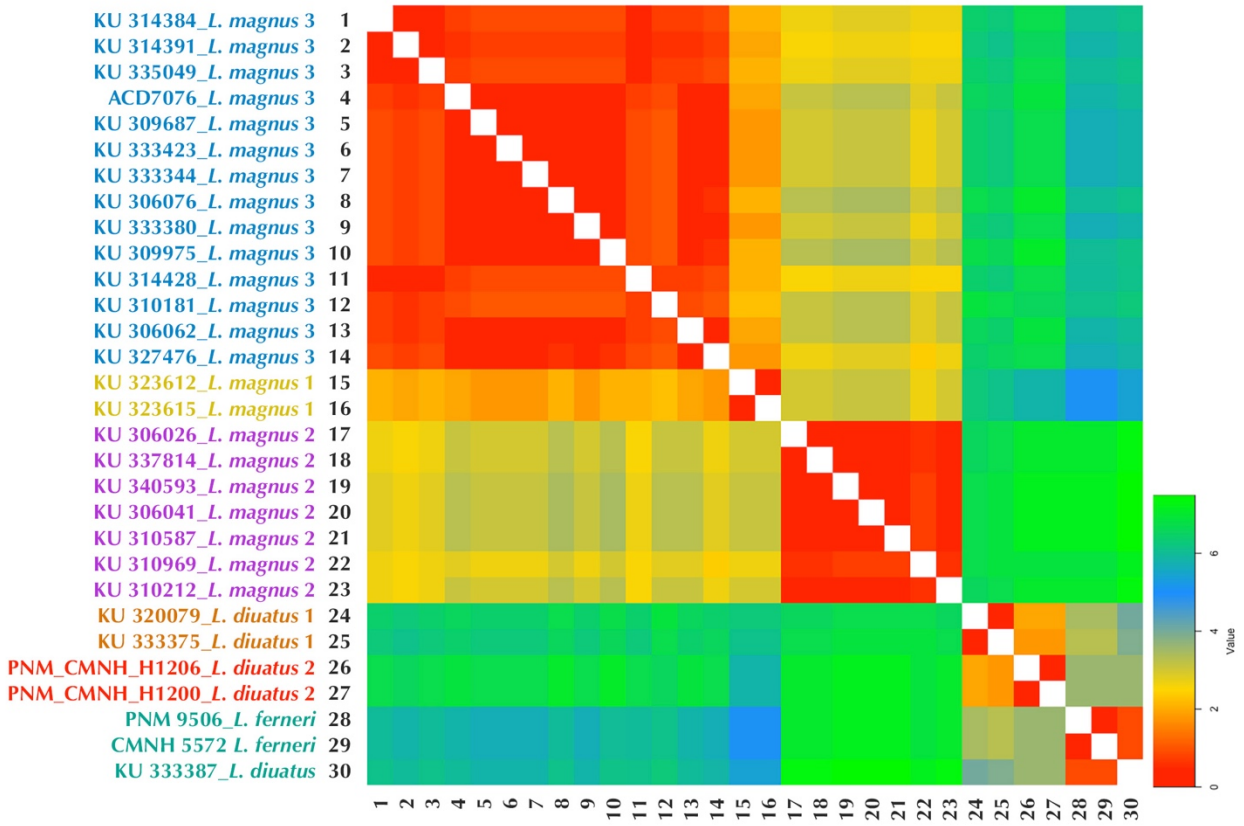

Supplemental Material Fig. 2

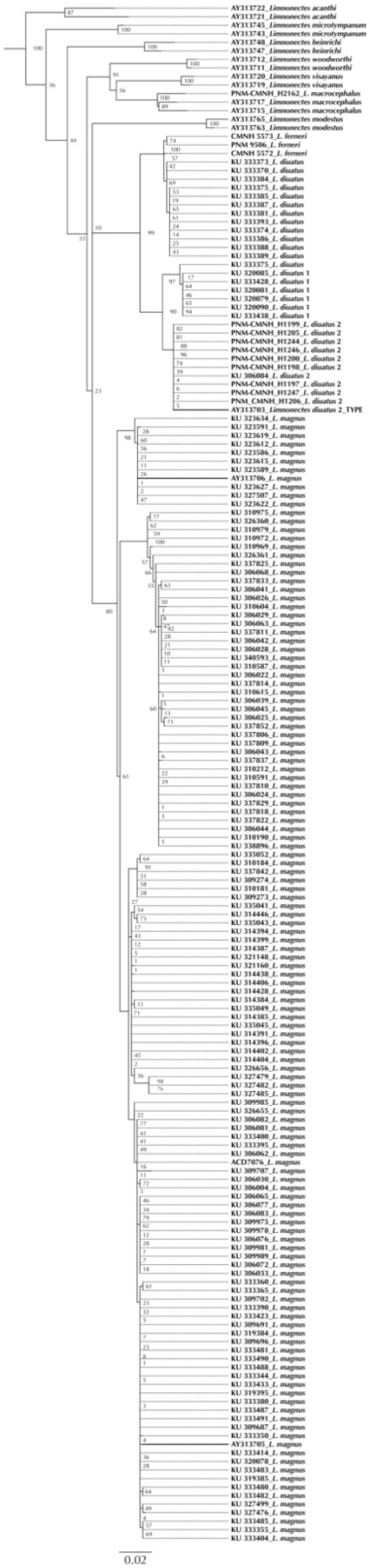

CHAPTER 3

A genomic assessment of the Mindanao Giant Fanged frogs of the *Limnonectes magnus* and *L. diuatus* complexes

Robin Kurian Abraham & Rafe M. Brown

Abstract

The Mindanao giant Fanged Frogs of the *Limnonectes magnus* and *L. diuatus* species complexes have been recently identified as two broad haplotypes corresponding to the lowlands of the Mindanao Pleistocene Aggregate Island Complexes and the highlands of Mindanao Island respectively, as part of a discovery step based on morphological and traditional Sanger genetic data. Using unprecedented numbers of sequence capture loci of over 6000 loci, this study revisits these two species complexes with a validation species delimitation approach. The findings here confirm the presence of a unique, isolated population of *L. magnus* on the western island of Bohol and a second mildly admixed population widespread across the Mindanao PAIC excluding Bohol. The results also reveal the presence of two to four distinct populations of montane restricted *L. diuatus* that are isolated from each other on their respective north-south-tending mountain ranges on the island of Mindanao.

Introduction

The topic of what constitutes a species—and the nature of boundaries among species—has been debated and contested for decades and is still under scrutiny, especially considering conservation implications in the ongoing biodiversity crisis (Harrison & Larson, 2014; Sites & Crandall, 1997). Traditional definitions on what constitutes a species varies from them being defined as

organismal entities that are diagnosably distinct, reproductively isolated, monophyletic groups of organisms to entities that lie across a continuum between varieties and species (Coyne & Orr, 1989; De Queiros, 1998; De Queiros, 1999; Darwin 1859; Mayr, 1942; Simpson, 1961; Wiley, 1978). Even with the advent of molecular approaches such as Sanger sequencing, species delimitation has been a challenging task (Barley et al., 2013; Jörger & Schrödl, 2013; Leavitt, Moreau & Lumbsch, 2015). Most molecular phylogenies have been and are still being estimated using mitochondrial and/or a handful of nuclear genes, and cryptic species diversity is inferred based on phylogenetic placement, subjective genetic distance thresholds, or divergence-based species delimitation analyses (Korshunova et al., 2019; Struck et al., 2018; Trontelj and Fier, 2009). However, recent advances in genomic sequencing has improved our capacity to better explore species boundaries within an evolutionary framework (Coates, Byrne & Moritz 2018). Many of the same clades identified by Sanger based phylogenies have later been revealed, with genomic data, to have been inflated (Brown & Siler, 2014; Chan et al., 2020).

Cross-species hybridization or introgression is known to play an important role in speciation processes and is thus an important parameter to consider for species identification (Abbott et al., 2013; Jiao et al., 2020; Mallet et al., 2016). The latest genome-scale analyses are prompting the reconsideration of the nature of species, which are increasingly being demonstrated to maintain phenotypic distinctiveness despite extensive gene flow along with the recognition of introgression as a vital source for adaptive traits (Lanier & Knowles, 2012; Chafin et al., 2020). Network models of diversification and the resulting copious reticulations across large scale phylogenies have been presenting challenges to many phylogeographic and speciation concepts and methods that were not as evident during the locus-poor Sanger era (Butlin, 2005; Feder, Egan & Nosil, 2012; Nosil & Feder, 2012). Such reticulations are becoming increasingly

conspicuous at the level of diverging species and adaptive radiations, and is revealing the recognition of ephemeral species between lineages with any geographic co-occurrence (Edwards et al., 2016; Rheindt & Edwards, 2011). The opposite can also be true where gene flow among species can mislead species tree estimation methods that accommodate the coalescent process but not gene flow (Folk et al., 2018; Leaché & Rannala, 2011). In a recent study, Chan et al. (2020) demonstrated how geneflow creates the illusion of cryptic species in frogs and how this may have resulted in the inflated perception of numbers of species in a Southeast Asian widespread species "complex" suspected of being a morass of undiagnosed "cryptic" species (Brown & Guttman 2002; Brown & Diesmos 2002; Brown & Siler 2014; Chan et al., 2020).

Island systems add layers of complexity that impact geneflow and thus species boundaries in various ways (Brown, 2009; Brown &Diesmos, 2009; Garg et al., 2018; Jaros, Tribsch, & Comes, 2018). Islands in Southeast Asia are renowned for their biogeographical significance, with some groups of islands and straits being conduits for species dispersal, while others prove to be barriers (Bird, Taylor & Hunt, 2005; Brown et al., 2013; Brown 2016; Cros et al., 2020). The Philippines archipelago comprises of several island banks, or Pleistocene Aggregate Island Complexes (PAICs) that demonstrate the species dispersal/barrier pattern at a smaller scale (Brown and Diesmos 2002; Brown and Guttman 2002). And some of the larger PAICs consist of large islands with disparate mountain ranges that serve as biogeographically significant geological features nested within the islands (Brown et al., 2013; Heaney, 1985).

The Fanged Frogs (genus *Limnonectes*) are a diverse group found throughout insular Southeast Asia (Alcala 1986; Alcala and Brown 1989; Brown 2007; Diesmos et al. 2015; AmphibiaWeb 2020; Frost, 2020). A distinct community of around 11 species of *Limnonectes* has been recognized in the Philippines, and is known for their varied colonization histories into

the archipelago from surrounding island systems (Evans et al, 2003; Setiadi et al. 2011; Herr et al., in press). Our recent assessment of the Philippine endemic taxa *Limnonectes magnus*, *L. diuatus* and *L. ferneri* revealed geographically structured genetic diversity and taxonomic corrections to correspond (Abraham et al., accepted pending revision; revision returned, November 2020). The results of this study revealed the presence of two strongly-supported subclades, one of *Limnonectes magnus* and the other of *L. diuatus* (with *L. ferneri* found to be a junior synonym of *L. diuatus*), with moderate levels of genetic divergence between the two clades, and low levels of divergence within each clade. In that study, we demonstrated that the *L. magnus* population on Bohol was shown to form a distinct, but weakly supported haplotype clade, in a single-locus, 16S mitochondrial gene tree analysis. Similarly, another second haploype clade was found to be distributed among the islands of Samar, Leyte and Dinagat, and a third, widely-distributed haplotype clade was documented from throughout the Mindanao PAIC landmasses except Bohol (Samar, Dinagat, Siargao, Mindanao, and Camiguin Sur). The same phylogeny showed the *L. diuatus* clade to comprise of two distinct Mindanao endemic, high elevation haploypes; one from the Mt. Hilong-hilong range along with a closely-related haplotype clade of the former *L. ferneri* occurring to the south in the mountain range in the Municipality of Monkaya. The second *L. diuatus* haplotype clade comprised of a population from Mt. Lumot in north-central Mindanao, along with another one on Mt. Apo to the south (Fig. 1). However, these population level haplotype clades were not corroborated by a three-locus nuclear phylogeny in the same study, emphasizing the uncertainty inherent in phylogenetic estimates (even when critical nodes are seemingly well-supported) if these are based on only a handful of loci—or, worse yet, a single mitochondrial locus.

In this study, we revisit the problem of species diversity in Mindanao giant Fanged Frogs (sensu Stejneger, 1910; Taylor, 1920; Inger, 1954; Brown & Alcala, 1977), using the full 6,000-locus power of the Dicroglossidae frog family modular subset of the greater FrogCap (>14,000 loci) probset of Hutter et al. (2019; see also Chan et al., 2020). Using unprecedented numbers of sequence capture loci (genomic inference from across the genome) and sparse non-negative matrix factorization, hybrid-index and phylogenetic network approaches to species-delimitation statistical procedures. We focussed, in particular on the dissimilar geographic template for diversification in these two distinct clades (Brown & Alcala, 1977; Evans et al., 2003; Siler et al., 2009). Investigating putative species boundaries in the industry standard, two-stage ("Discovery" vs. "Validation") species delimitation approach, we empirically distinguished between the two currently-recognized clades corresponding to *Limnonectes magnus* and *L. diuatus* clades (Diesmos et al., 2015; Abraham et al., in review 2020). Finally, we applied particular focus on the among-island, haplotype sub-clade differentiation identified in the *L. magnus* group, and compared the outcomes of those validation procedures to the results of within-island, the sky island haplotype sub-clade differentiation characterized in the *L. diuatus* group. Our approach identifies a possible novel case of concurrent, hierarchically-arranged, habitat-vicariance species-pump mechanism of diversification, nested within a PAIC-level, among island, landmass fission-fusion (sea level vicariance) species pump—all of which highlights the impact of the complex geographic template of the dynamic Philippine island archipelago, for processes of evolutionary diversification (Brown and Diesmos 2009; Brown et al. 2013; Brown 2016).

Methods

We sequenced 32 ingroup samples comprising of representatives of *Limnonectes magnus*, *L. diuatus*, *L. ferneri* (these three represented by samples from throughout each's respective distribution—including each species' type locality) and a previously hypothesized new species from across the Mindanao PAIC (Table 1). Tissue samples for molecular work were obtained from the University of Kansas Biodiversity Institute. We extracted genomic DNA using the automated Promega Maxwell® RSC Instrument (Tissue DNA kit) and subsequently quantified it using the Promega Quantus® Fluorometer.

Probe design, library preparation, and sequencing:

Probe design follows Hutter et al. (2019) and is summarized as follows. Probes were synthesized as biotinylated RNA oligos in a myBaits kit (Arbor Biosciences™, formerly MYcroarray® Ann Arbor, MI) by individually matching 25 publicly available transcriptomes to the *Nanorana parkeri* and *Xenopus tropicalis* genomes using the program BLAT 3.50 (Kent, 2002). We clustered matching sequences by their genomic coordinates to detect presence/absence across species and to achieve full locus coverage. To narrow the locus selection to coding regions, we matched each cluster to available coding region annotations from the *N. parkeri* genome using the program EXONERATE (Slater and Birney, 2005). We then aligned loci from all matching species using MAFFT 7.313 (Katoh and Standley, 2013), and kept those that had at least three taxa and were at least 100 bp long. We selected markers based on phylogenetic representation, informativeness, and other filters explained in Hutter et al. (2019). For each marker, we used the *N. parkeri* genome sequence as the chosen design marker. To create a .fasta file of bait sequences as individual entries, we separated the selected markers into 120 bp-long sequences with 2x tiling (50% overlap among baits) using an R script. These markers have an additional bait at each end, extending into the intronic region to increase the coverage and capture success

of these areas. We then filtered the baits, retaining those without sequence repeats; a GC content of 30%–50%; and also baits that did not match to their reverse complement or multiple genomic regions. Additionally, we included 646 UCEs that contain at least 10% informative sites (Alexander et al., 2017). Finally, we used the myBaits-2 kit (40,040 baits) with 120mer sized baits with our chosen filtered bait sequences.

Library preparation was performed by Arbor Biosciences following the myBaits V3.1 manual and briefly follows: (1) genomic DNA was sheared to 300–500 bp; (2) adaptors were ligated to DNA fragments; (3) each library was amplified for 6 cycles using unique combinations of i7 and i5 indexing primers attached to the adapters to later identify individual samples; (4) biotinylated 120mer RNA library baits were hybridized to the sequences; (5) target sequences were selected by adhering to magnetic streptavidin beads; (6) enrichment incubation times ranged 18–21 hours; (7) target regions were amplified via PCR for 10 cycles; and (8) samples were pooled and sequenced on an Illumina HiSeq PE-3000 with 150 bp paired-end reads. Sequencing was performed at the Oklahoma Medical Research Foundation DNA Sequencing Facility.

Bioinformatics:

The bioinformatics pipeline for filtering adapter contamination, assembling markers, trimming, and exporting alignments are available on GITHUB, using version 2 of the pipeline (https://github.com/chutter/FrogCap-Sequence-Capture). We filtered adapter contamination and other sequencing artefacts from raw reads using the program FASTP (default settings; Chen et al., 2018). Paired-end reads were merged using the program BBMerge (Bushnell et al., 2017), which avoids inflating coverage for these regions due to uneven lengths from cleaning (Zhang et al., 2014). The cleaned reads were then assembled de novo using the program Merged singletons

and paired-end reads were assembled de novo using the program SPADES v.3.12 (Bankevich et al. 2012), which runs BAYESHAMMER (Nikolenko et al. 2013) error correction on the reads internally. Data were assembled using several different k-mer values (21, 33, 55, 77, 99, 127), in which orthologous contigs resulting from the different k-mer assemblies were merged. We then used the DIPSPADES (Safanova et al. 2015) function to assemble contigs that were polymorphic by generating a consensus sequence from both haplotypes from orthologous regions such that polymorphic sites were resolved randomly. We then matched consensus haplotype contigs against reference marker sequences used to design the probes separately for our three probe sets with BLAST (dc-megablast). Contigs were discarded if they failed to match ≥ 30% of the reference marker, and contig matches fewer than 50 bp were removed. The contigs were then matched against the reference probe sequences with BLAT 3.50 (Kent, 2002), keeping only those contigs that uniquely matched to the probe sequences. The final set of matching loci was then aligned on a locus-by-locus basis using MAFFT 7.313 using the algorithm L-INS-i (auto and default parameters; Katoh & Standley 2013).

We externally trimmed alignments using a custom R script, where at least 50 percent of the samples must have sequence data present externally, with at least three taxa per alignment. The alignments were saved separately into usable datasets for phylogenetic analyses and data type comparisons: (1) Introns: the exon previously delimited was trimmed out of the original contig and the two remaining intronic regions were concatenated; (2) Exons: each alignment was adjusted to be in an open-reading frame and trimmed to the largest reading frame that accommodated >90% of the sequences, alignments with no clear reading frame were discarded; (3) Exons-combined: exons from the same gene, which may be linked (Lanier and Knowles, 2012; Scornavacca and Galtier, 2017), were concatenated and treated as a single locus; and (4)

UCEs were also saved as a separate dataset. We applied internal trimming only to the intron and UCE alignments using the program trimAl (automatic1 function; Capellagutiérrez et al., 2009). All alignments were externally trimmed to ensure that at least 50 percent of the samples had sequence data present.

Phylogeny:

We supplemented previous Sanger datasets with additional 16S mitochondrial gene sequences from 20 individuals, accumulated over the last two decades of fieldwork, and included new samples collected at or near all species' type localities (Brown & Alcala, 1977; Brown et al., 2013; Diesmos et al., 2015; Evans et al., 2003; Inger, 1954; Setiadi et al., 2011; Siler et al., 2009; Taylor, 1920). From preliminary analyses of these data (not shown), we selected a 100-tip subset, maximizing geographical and taxonomic coverage and subjected these to genomic data collection using the FrogCap probeset, sequence capture protocol, and data analysis pipeline (Chan et al., 2020; Hutter et al., 2019). We assembled two phylogenomic datasets, consisting of (A) mitogenomic (14,504 bp, 30 gene regions; hereafter mtDNA); and (B) nuclear (78,939 bp, 75 genes; hereafter nuDNA). We estimated phylogenetic relationships with Maximum Likelihood (ML), Bayesian (BA), and Species Tree Summary (STS) procedures. The ML analysis was conducted with IQ-TREE v1. (Nguyen et al., 2015). We performed a partitioned analysis (partitioned by gene) and selected the best-fit substitution model using ModelFinder (Kalyaanamoorthy et al., 2017). We then assessed branch support using 1,000 ultrafast bootstrap replicates and performed BA analysis using BEAST 2.6 (Bouckaert et al., 2019; Hoang et al., 2017). We similarly partitioned data by gene and estimated the best-fit substitution model for each partition via model averaging using bModelTest (Bouckaert & Drummond, 2017). We selected relaxed log-normal and Yule models for the molecular clock and tree priors with all

other priors set to default values. We executed two separate MCMC runs at 50,000,000 (mtDNA) and 100,000,000 (nuDNA and combined) generations each and checked for convergence using the program Tracer v1.7 (Rambaut et al., 2014). For the STS analysis, we first estimated gene trees for each marker using IQ-TREE (same settings as above). We then used ASTRAL-III (Zhang et al., 2018) to estimate a species tree using default settings. ML and BA analyses were performed on all datasets, whereas performed the STS analysis only on nuDNA (numerous mitochondrial markers were too short).

We used three species delimitation procedures that were designed for various datatypes: mPTP v0.2.4 (Kapli et al., 2017), bGMYC (Reid & Carstens, 2019), and BPP v4.1.4 (Yang & Rannala, 2010; Yang, 2015). The mPTP analysis is a single-locus method and hence, was performed on the mtDNA dataset (concatenated fragments were treated as a single locus). We used the ML phylogeny as input and confidence of delimitation schemes was assessed using two independent MCMC chains at 5,000,000 generations each. The bGMYC analysis accounts for uncertainties in phylogenetic estimation and model parameters and was performed on 100 randomly selected trees from the posterior distribution of the BEAST analysis (combined dataset). For each tree, we ran the MCMC sampler for 50,000 generations with a burn-in of 40,000 and a thinning interval of 100. The BPP analysis was performed on a subset of 54 most informative loci from the nuDNA dataset. We used a diffuse prior of $\alpha = 3$, $\beta = 0.004$ for θ and $\alpha = 3$, $\beta = 0.002$ τ. The MCMC was set to 100,000 samples with burn-inn = 8,000 and sample frequency = 2. Convergence was assessed by comparing the consistency of posterior distributions (Rambaut et al., 2014). We consider the intersection (agreement) of all three methods and datatypes as appropriately conservative, yet strong statistical support for validation of proposed, or unconfirmed candidate species.

SNP detection:

We conducted variant calling for SNPs (single nucleotide polymorphisms), with a custom pipeline in R, available at (https://github.com/chutter/FrogCap-Sequence-Capture; variant-pipeline_stable-v1). We used GATK v4.1 following developer-best-practices recommendations for discovering and calling variants (McKenna et al. 2010; Van der Auwera et al. 2013). To discover potential variant data (e.g. SNPs, indels), we used a consensus sequence from each alignment from the target group as a reference and mapped cleaned reads back to consensus reference markers for each sample. We used BWA ("bwa mem" function; Li 2013) to map cleaned reads (cleaned-reads dataset explained above) to our reference markers, adding the read group information (e.g. Flowcell, Lane, Library) obtained from the fastq header files. We then used SAMTOOLS to convert the mapped reads SAM file to a cleaned BAM file, and merged BAM files with our unmapped reads, as required for downstream analyses (Li et al. 2009). We used the program PICARD to mark exact duplicate reads and reformatted each dataset for variant calling. We used GATK to locate variant and invariant sites in order to generate a preliminary variant dataset using the GATK program HaplotypeCaller, to call haplotypes, in GVCF format, for each sample individually. We then used the GATK GenomicsDBImport program after processing each sample, to aggregate samples from separate datasets into their own combined database. Using these databases, we used the GenotypeGVCF function to genotype the combined sample datasets and output separate ".vcf" files for each marker, containing variant data, from all samples, for final filtration. The preliminary variant set was filtered into a final dataset refining as follows: (1) All variants were kept after moderate filtering to remove probable errors filtered at a quality score > 5; (2) High quality variants were kept including SNPs, MNPs (multi-nucleotide polymorphisms), and indels filtered at a quality > 20; (3) SNPs specifically were

chosen after high-quality filtering (quality > 20); and (4) our final dataset consisted of one high-quality SNP from each exon that was most variable across samples. Finally, we used a custom script to convert these SNPs to a structure-formatted file.

Population structure determining exercises:

We examined population ancestry using a program based on sparse non-negative matrix factorization (sNMF). We estimated ancestry coefficients for 1–10 ancestral populations (K) using 100 replicates for each K. The cross-entropy criterion (Frichot and François, 2015) was then used to determine the best K based on the prediction of masked genotypes. The sNMF analysis was implemented through the R package *LEA* (Frichot and François, 2015). We also inferred clustering using an unsupervised network clustering method NetView (Neuditschko et al. 2012), that uses genetic distances to assign individuals to populations without prior knowledge of individual ancestry. Euclidean genetic distances were used as input and the NetView analysis was implemented using the R package netview (Neuditschko et al. 2012; Steinig et al. 2016). In order to substantiate admixture among populations, we also implemented a hybrid-index analysis (Buerkle, 2005) using the R package gghybrid (Bailey 2018) after removing loci with a minor allele frequency >0.1 in both parental reference sets. We performed a total of 10,000 MCMC iterations with the first 50% discarded as burn-in.

Results

Phylogenetic relationships of the Limnonectes magnus and L. diuatus clades:

Results from our combined Philippines *Limnonectes* phylogeny (Fig. 2; from Brown et al., in review) showed that the *L. magnus* and *L. diuatus* clades are not sister taxa as implied in our

Sanger phylogenies (Abraham et al., in review). Thus, downstream analyses in this study were performed separately on the *L. magnus* and *L. diuatus* datasets.

The ML, BA, and STS phylogenomic analyses within the data types of mtDNA vs. nuDNA converged on similar well-supported topologies, except for low support for the position of *L. diuatus* in BA and analyses of mtDNA (Fig. 2). The BEAST analysis results of the combined data included strong support for all nodes, and combined similarities from our nuDNA topology (Fig 2, right: *L. diuatus* first-diverging relative to *L. magnus*). Between the mtDNA and nuDNA data types, we observed flipping (exchanges of position) of successively-branching lineages, involving *L. magnus* and *L. diuatus* which changed position between topologies (Fig. 2).

The species delimitation procedures all strongly supported the recognition of named species *L. palavanensis*, *L. micrixalus, L. acanthi*, and *L. macrocephalus*; likewise, all methods converged on support for four new species, *L. palavanensis* sp. 2, *L. palavanensis* sp. 3, *L. acanthi* sp. 2, and *L. macrocephalus* sp. 2 (results not shown; Brown et al., in review). The bGMYC analysis of combined data conservatively grouped as single *L. diuatus* (and nearly *L. magnus*, which bGMYC proposed division of a single individual from remaining intraspecific sampling), whereas BPP analysis of 54 nuDNA loci and mPTP analysis of 30 mtDNA gene regions proposed the recognition of *L. diuatus* as a distinct group (results not shown; Brown et al., in review).

Population structure:

For the *Limnonectes magnus* clade, the sNMF analysis determined an optimal number of 2 ancestral populations, comprising of (1) a non-admixed population in Bohol, and (2) another non-admixed population in Dinagat + Siurgao. The population in the central islands of Samar and Leyte and the southern island of Mindanao exhibited a cline with low levels of admixture

from the Bohol population (Fig. 3). In contrast, in the *L. diuatus* clade, there was very little to no admixture detected in the inferred ancestral populations (Fig. 3). The cross-entropy criterion of the sNMF analysis inferred K=3 or 4 as the best predicted numbers of ancestral populations, with K=3 being only slightly better (Fig. 3). We included plots for both values of K because the four populations were distinct in other analyses (Figs. 3 & 4). The NetView results (Fig. 5) for the *L. magnus* clade showed two clusters comprising of both admixed (blue + (blue + yellow): Samar, Leyte, Mindanao) and non-admixed (yellow: Bohol) groups, whereas the Mindanao island endemic *L diuatus* clade showed two distinct clusters; one comprising of ancestral populations on the western (central) mountain range (orange + red) of the island, and another on the island's eastern range (light green + dark green). Our hybrid index analysis confirmed two non-admixed populations (Bohol and Dinagat + Siurgao), and others, with varying degrees of the admixture in the populations on Samar, Leyte and Mindanao for the *L. magnus* group (Fig. 6). The results for the *L. diuatus* group revealed all four populations in Monkayo (light green), Mt. Hilong-hilong (dark green), Mt. Lumot (orange) and Mt. Talomo (red) as having distinct and different allele frequencies from one another barring very miniscule introgression of the Monkayo population in the Mt. Hilong-hilong one (Fig. 7).

Discussion

Our novel genomic data, orders of magnitude more data than have ever been applied to these populations previously (Emerson et al. 2000; Evans et al. 2003; Setiadi et al. 2011; Brown et al., in review) provide unprecedented insight into species boundaries in Mindanao giant Fanged Frogs (Brown and Diesmos 2002; Brown, 2007; Ron and Brown 2008; Brown and Stuart 2012; Diesmos and Brown 2014).

Using several different approaches, "Validation-stage," ancestral population membership analyses, have now responded to "Discovery-stage" earlier characterizations using a few Sanger loci (Abraham et al. in review) and sequence-capture + mitogenomic analyses of 75 Tree-of-Life "legacy loci" (Feng et al. 2017; Brown et al. in review). This has rendered *Limnonectes magnus* and *L. diuatus* population (and putative species) boundaries more explicit than previous studies employing purely single locus or multilocus Sanger data, or even mitogenomic + phylogenomic nuclear datasets (Abraham et al. in review; Brown et al. in review). Our findings confirm the presence of a unique, isolated population of *L. magnus* on the western island of Bohol, which we recovered in single locus mitochondrial DNA studies, but were unable to reproduce using these data plus a few Sanger nuclear loci (Abraham et al. in review). Despite including three samples from lowland Mindanao, we were able to successfully amplify only one from the Zamboanga peninsula, which shows the same low level of admixture as that in Samar in the extreme north of the species' range, and thus we would expect the intervening areas in lowland Mindanao to have the same low levels of Bohol-into-Mindanao ancestral population admixture as observed in the single Mindanao sample of Zamboanga. Our genomic results and two-stage Discovery–Validation delimitation procedures likely confirm the presence of a new cryptic species of fanged frog, endemic to Bohol Island (see Herr et al. in press, for a discussion of one such cryptic species, recently validated and formally described from the Philippine island of Mindoro). Although for a long time Bohol was not recognized for vertebrate endemism, recent phylogeographic studies have revealed geographic structure and the presence of unique haplogroups from the island (Hosner, Nyári & Moyle, 2013; Hosner et al., 2018).

We also show the presence of two to four distinct populations (see below) of montane restricted *L. diuatus* that are isolated from each other on their respective north-south-tending

mountain ranges on the island of Mindanao (one central, another eastern; Fig 2). We take a conservative approach by recognizing two haplotypes, rather than four, for the purposes of further taxonomic investigations—although our Hybrid-index and PCA results show four separate clusters. Our Netview results in this study allude to two pairs of clusters, and the morphometric assessment of a larger sample size of these populations (Abraham et al., in review) do not support four phenotypically distinct morphologies, but rather two. These two populations now warrant further investigation for additional morphological, bioacoustics, and/or larval characters, which could shed light on biologically-relevant traits (i.e., mate-recognition factors, ontogenetic trajectories; Duellman and Trueb 1994; Wells, 2010) reflecting unique, genomic, and species-level putative identities as biologically relevant, independent evolutionary lineages (Simpson 1961; Wiley, 1978; Frost and Hillis 1990; de Queiroz, 1998, 1999). At present, though recent surveys have helped update species inventories for the sky islands, there is still as yet insufficient data to warrant the recognition of more than two species of high elevation frogs in the *L. diuatus* clade (Sanguila et al., 2016). A "species pump" model of biodiversity generation and maintenance that has been proposed, based on action of oscillating sea levels that resulted in the repeated formation and fragmentation of PAICs (the PAIC Diversification Model) has been used to address the remarkable levels of biodiversity in the Philippines archipelago (Heaney 1985; Esselstyn & Brown, 2009; Esselstyn et al., 2009; Lomolino et al. 2010; Brown et al. 2013; Oaks et al., 2013, 2019). Similar mechanisms of "species pumping" invoked for within-island biodiversity, including patterns of recolonization of disparate montane habitats from shared lowland rainforest refugia to generate elevation restricted contemporaneous montane taxa, can help explain these frogs' distribution patterns in isolated mountain chains on Mindanao, with little opportunity for continued geneflow since divergence from the intermediate

lowlands/valleys (Hewitt, 2011; Kooyman et al., 2019; Lowe & Walker, 2014; Oliver et al., 2020; Schmitt, 2009; Brown et al. 2013:fig. 5).

In the near future, with the increasing transition from Sanger based to large genomic datasets, species boundaries are being reconsidered and redrawn. But even without expensive datasets (and until these methods become cheaper and accessible for those in biodiversity rich tropical nations), robust, integrative approaches utilizing behavioral, ecological, life-history, developmental, larval and bioacoustics data, though challenging to come by, have been instrumental in resolving cryptic species complexes, as recently demonstrated for a Philippine cryptic species complex (Herr et al. in press). But caution needs to be considered for the premise that there is vast undescribed cryptic biodiversity yet to be recognized based on the former limited-loci PCR based assessments, which can now be contested with the results from genomic datasets for species complexes (Chan et al., 2020). Not only is the need for restraint in the widespread belief in cryptic species complexes (Bickford et al., 2007) imminent, but exploring newly discovered diversity alongside revisiting described groups with an integrative taxonomic approach (Harris & Froufe, 2005; Padial et al., 2010), incorporating genomic data of organisms, will go a long way in estimating accurate levels of biodiversity.

References

Abbott, R., Albach, D., Ansell, S., Arntzen, J. W., Baird, S. J., Bierne, N., Boughman, J., Brelsford, A., Buerkle, C.A., Buggs, R., & Butlin, R. K. (2013). Hybridization and speciation. Journal of Evolutionary Biology, 26(2), 229-246.

Abraham, R. K., Herr, M. W., Sterkhova, V. V., Otterholt, R., Siler, C. D., Sanguila, M. B., Brown, R. M. (in review). Revisiting Linnaean and Wallacean shortfalls in Mindanao Fanged

Frogs: the *Limnonectes magnus* Complex consists of only two species, Herpetological Monographs.

Alcala, A. C. (1986). Guide to Philippine flora and fauna. Vol. X. Amphibians and reptiles. Natural Resource Management Center, Ministry of Natural Resources and the University of the Philippines, Manila, Philippines.

Alcala, A. C., & Brown, W. C. (1998). Philippine amphibians: an illustrated field guide. Bookmark Inc., Makati City, Philippines.

Alexander, A. M., Su, Y. C., Oliveros, C. H., Olson, K. V., Travers, S. L., & Brown, R. M. (2017). Genomic data reveals potential for hybridization, introgression, and incomplete lineage sorting to confound phylogenetic relationships in an adaptive radiation of narrow-mouth frogs. Evolution, 71(2), 475-488.

AmphibiaWeb (2020). Electronic database accessible at: https://amphibiaweb.org (accessed 02 November 2020). University of California, Berkeley, CA, USA.

Bailey, R. I. (2018). *gghybrid*: Evolutionary analysis of hybrids and hybrid zones. R package version 0.0. 0.9000.

Bankevich, A., Nurk, S., Antipov, D., Gurevich, A. A., Dvorkin, M., Kulikov, A. S., Lesin, V.M., Nikolenko, S.I., Pham, S., Prjibelski, A.D., & Pyshkin, A. V. (2012). SPAdes: a new genome assembly algorithm and its applications to single-cell sequencing. Journal of Computational Biology, 19(5), 455-477.

Barley, A. J., White, J., Diesmos, A. C., & Brown, R. M. (2013). The challenge of species delimitation at the extremes: diversification without morphological change in Philippine sun skinks. Evolution, 67(12), 3556-3572.

Bickford, D., Lohman, D. J., Sodhi, N. S., Ng, P. K., Meier, R., Winker, K., Ingram, K.K., & Das, I. (2007). Cryptic species as a window on diversity and conservation. Trends in Ecology & Evolution, 22(3), 148-155.

Bird, M. I., Taylor, D., & Hunt, C. (2005). Palaeoenvironments of insular Southeast Asia during the Last Glacial Period: a savanna corridor in Sundaland?. Quaternary Science Reviews, 24(20-21), 2228-2242.

Blischak, P. D., Chifman, J., Wolfe, A. D., & Kubatko, L. S. (2018). HyDe: a Python package for genome-scale hybridization detection. Systematic Biology, 67(5), 821-829.

Brown, R. M., & Diesmos, A. C. (2002). Application of lineage-based species concepts to oceanic island frog populations: the effects of differing taxonomic philosophies on the estimation of Philippine biodiversity. Silliman Journal, 42(1), 133-162.

Brown, R. M. (2007). Introduction to Robert F. Inger's Systematics and Zoogeography of Philippine Amphibia. Invited forward to the reprint of Inger's 1954 monograph, pp. 1–17. In: Systematics and Zoogeography of Philippine Amphibia. Natural History Publications, Kota Kinabalu.

Brown, R. M. (2009). Frogs in Island Archipelagos. Pp. 347–351 In: Gillespie, R., and D. Clague (Eds.). Encyclopedia of Islands. University of California Press, Berkeley.

Brown, R. M., & Guttman, S. I. (2002). Phylogenetic systematics of the *Rana signata* complex of Philippine and Bornean stream frogs: reconsideration of Huxley's modification of Wallace's Line at the Oriental-Australian faunal zone interface. Biological Journal of the Linnean Society 76, 393–461.

Brown, R. M. & A. C. Diesmos. (2009). Philippines, Biology. Pp. 723–732 In: Gillespie, R., and D. Clague (Eds.). Encyclopedia of Islands. University of California Press, Berkeley.

Brown, R. M., Siler, C. D., Oliveros, C. H., Esselstyn, J. A., Diesmos, A. C., Hosner, P. A., Linkem, C.W., Barley, A.J., Oaks, J.R., Sanguila, M.B., & Welton, L. J. (2013). Evolutionary processes of diversification in a model island archipelago. Annual Review of Ecology, Evolution, and Systematics, 44, 411-435.

Brown, R. M., & B. L. Stuart. (2012). Patterns of biodiversity discovery through time: an historical analysis of amphibian species discoveries in the Southeast Asian mainland and island archipelagos. Pp 348–389 In: Gower, D. J., K. G. Johnson, J. E. Richardson, B. R. Rosen, L. Rüber, and S. T. Williams (Eds.) Biotic Evolution and Environmental Change in Southeast Asia. Cambridge University Press.

Brown, R. M., & Siler, C. D. (2014). Spotted stream frog diversification at the Australasian faunal zone interface, mainland versus island comparisons, and a test of the Philippine 'dual-umbilicus' hypothesis. Journal of Biogeography, 41(1), 182-195.

Brown, R. M. (2016). Biogeography of Land Vertebrates. In: Kliman, R.M. (ed.), The Encyclopedia of Evolutionary Biology. Vol. 1, pp. 211–220. Oxford: Academic Press/Elsevier Inc.

Brown, R. M., Hutter, C. R., Wood Jr, P. L., Abraham, R. K., Vallejos, J. G., Herr, M. W., & Chan K. O. (In Prep) Sequence-capture phylogenomics enable archipelago-wide assessment of Philippine Fanged Frog biodiversity, Biology Letters.

Brown, W.C., & Alcala, A.C. (1977). A new frog of the genus *Rana* from the Philippines. Proceedings of the Biological Society of Washington 90, 669–675.

Buerkle, C. A. (2005). Maximum-likelihood estimation of a hybrid index based on molecular markers. Molecular Ecology Notes, 5(3), 684-687.

Bushnell, B., Rood, J., & Singer, E. (2017). BBMerge–accurate paired shotgun read merging via overlap. PloS One, 12(10), e0185056.

Butlin, R. K. (2005). Recombination and speciation. Molecular Ecology, 14(9), 2621-2635.

Capella-Gutiérrez, S., Silla-Martínez, J. M., & Gabaldón, T. (2009). trimAl: a tool for automated alignment trimming in large-scale phylogenetic analyses. Bioinformatics, 25(15), 1972-1973.

Chafin, T. K., Douglas, M. R., & Douglas, M. E. (2020). Genome-wide local ancestries discriminate homoploid hybrid speciation from secondary introgression in the red wolf (Canidae: Canis rufus). bioRxiv.

Chan, K. O., Hutter, C. R., Wood Jr, P. L., Grismer, L. L., Das, I., & Brown, R. M. (2020). Gene flow creates a mirage of cryptic species in a Southeast Asian spotted stream frog complex. Molecular Ecology, 29(20), 3970-3987.

Chen, S., Huang, T., Zhou, Y., Han, Y., Xu, M., & Gu, J. (2017). AfterQC: automatic filtering, trimming, error removing and quality control for fastq data. BMC Bioinformatics, 18(3), 91-100.

Coates, D. J., Byrne, M., & Moritz, C. (2018). Genetic diversity and conservation units: dealing with the species-population continuum in the age of genomics. Frontiers in Ecology and Evolution, 6, 165.

Coyne, J. A., & Orr, H. A. (1989). Two rules of speciation. In Otte, D., Endler, J. (Eds.), Speciation and its Consequences (pp. 180–207). Sunderland, MA: Sinauer Associates.

Cros, E., Chattopadhyay, B., Garg, K. M., Ng, N. S., Tomassi, S., Benedick, S., Edwards, D.P., & Rheindt, F. E. (2020). Quaternary land bridges have not been universal conduits of gene flow. Molecular Ecology, 29(14), 2692-2706.

Darwin, C. (1859). The Origin of Species; And, the Descent of Man. Modern library.

De Queiroz, K. (1998). The general lineage concept of species, species criteria, and the process of speciation. Endless forms: species and speciation. Pp. 57–75. In D. J. Howard and S. H. Berlocher (Eds.), Endless Forms: Species and Speciation. Oxford University Press, New York, New York, U.S.A.

De Queiroz K. 1999. The general lineage concept of species and the defining properties of the species category. Pp. 49–89. In , R. A. Wilson (Ed.), Species: New Interdisciplinary Essays. Massachusetts Institute of Technology Press, Cambridge, Massachusetts, U.S.A.

Diesmos, A. C., A. C. Alcala, C. D. Siler, & R. M. Brown. (2014). Status and Conservation of Philippine Amphibians. Pp. 310–336 In: Heatwole, H., and I. Das (Eds.). Conservation Biology of Amphibians of Asia. Status of Conservation and Decline of Amphibians: Eastern Hemisphere. Natural History Publications (Borneo), Kota Kinabalu, Malaysia.

Diesmos, A. C., Watters, J. L., Huron, N. A., Davis, D. R., Alcala, A. C., Crombie, R. I., Afuang, L.E., Gee-Das, G., Sison, R.V., Sanguila, M.B. & Penrod, M. L. (2015). Amphibians of the Philippines, part I: checklist of the species. Proceedings of the California Academy of Sciences, 62(20), 457-539.

Duellman, W. E., & Trueb, L. (1994). Biology of Amphibians, John Hopkins Univ. Press, Baltimore, Maryland, U.S.A.

Edwards, S. V., Potter, S., Schmitt, C. J., Bragg, J. G., & Moritz, C. (2016). Reticulation, divergence, and the phylogeography–phylogenetics continuum. Proceedings of the National Academy of Sciences, 113(29), 8025-8032.

Emerson, S. B., Inger, R. F., & Iskandar, D. (2000). Molecular systematics and biogeography of the fanged frogs of Southeast Asia. Molecular Phylogenetics and Evolution, 16(1), 131-142.

Esselstyn, J. A., & Brown, R. M. (2009). The role of repeated sea-level fluctuations in the generation of shrew (Soricidae: Crocidura) diversity in the Philippine Archipelago. Molecular Phylogenetics and Evolution, 53(1), 171-181.

Esselstyn, J. A., Timm, R. M., & Brown, R. M. (2009). Do geological or climatic processes drive speciation in dynamic archipelagos? The tempo and mode of diversification in Southeast Asian shrews. Evolution: International Journal of Organic Evolution, 63(10), 2595-2610.

Evans, B. J., Brown, R. M., McGuire, J. A., Supriatna, J., Andayani, N., Diesmos, A., Iskandar, D., Melnick, D.J., & Cannatella, D. C. (2003). Phylogenetics of fanged frogs: testing biogeographical hypotheses at the interface of the Asian and Australian faunal zones. Systematic Biology, 52(6), 794-819.

Feder, J. L., Egan, S. P., & Nosil, P. (2012). The genomics of speciation-with-gene-flow. Trends in Genetics, 28(7), 342-350.

Feng, Y. J., Blackburn, D. C., Liang, D., Hillis, D. M., Wake, D. B., Cannatella, D. C., & Zhang, P. (2017). Phylogenomics reveals rapid, simultaneous diversification of three major clades of Gondwanan frogs at the Cretaceous–Paleogene boundary. Proceedings of the National Academy of Sciences, 114(29), E5864-E5870.

Folk, R. A., Soltis, P. S., Soltis, D. E., & Guralnick, R. (2018). New prospects in the detection and comparative analysis of hybridization in the tree of life. American Journal of Botany, 105(3), 364-375.

Frichot, E., & François, O. (2015). LEA: An R package for landscape and ecological association studies. Methods in Ecology and Evolution, 6(8), 925-929.

Frost, D. R., & Hillis, D. M. (1990). Species in concept and practice: herpetological applications. Herpetologica, 86-104.

Frost, D. R. 2020. Amphibian Species of the World: an Online Reference. Version 6.0. American Museum of Natural History, New York, USA., Electronic Database accessible at http://research.amnh.org/herpetology/amphibia/index.html

Garg, K. M., Chattopadhyay, B., Wilton, P. R., Prawiradilaga, D. M., & Rheindt, F. E. (2018). Pleistocene land bridges act as semipermeable agents of avian gene flow in Wallacea. Molecular Phylogenetics and Evolution, 125, 196-203.

Harris, D. J., & Froufe, E. (2005). Taxonomic inflation: species concept or historical geopolitical bias?. Trends in Ecology & Evolution, 20(1), 6-7.

Harrison, R. G., & Larson, E. L. (2014). Hybridization, introgression, and the nature of species boundaries. Journal of Heredity, 105(S1), 795-809.

Heaney, L. R. (1985). Zoogeographic evidence for middle and late Pleistocene land bridges to the Philippine Islands. Modern Quaternary Research in Southeast Asia, 9, 127-144.

Herr, M. W., Vallejos, J. G., Meneses, C. G., Abraham, R. K., Otterholt, R., Siler, C. D., Rico, E. L. B., & Brown, R. M. (in press). A New, Morphologically Cryptic Species of Fanged Frog, Genus *Limnonectes* (Amphibia: Anura: Dicroglossidae), from Mindoro Island, Central Philippines, Copeia.

Hewitt, G. M. (2011). Quaternary phylogeography: the roots of hybrid zones. Genetica, 139(5), 617-638.

Hosner, P. A., Nyári, Á. S., & Moyle, R. G. (2013). Water barriers and intra-island isolation contribute to diversification in the insular A ethopyga sunbirds (A ves: N ectariniidae). Journal of Biogeography, 40(6), 1094-1106.

Hosner, P. A., Campillo, L. C., Andersen, M. J., Sánchez-González, L. A., Oliveros, C. H., Urriza, R. C., & Moyle, R. G. (2018). An integrative species delimitation approach reveals

fine-scale endemism and substantial unrecognized avian diversity in the Philippine Archipelago. Conservation Genetics, 19(5), 1153-1168.

Hutter, C. R., Cobb, K. A., Portik, D., Travers, S. L., Wood, P. L., & Brown, R. M. (2019). FrogCap: A modular sequence capture probe set for phylogenomics and population genetics for all frogs, assessed across multiple phylogenetic scales. bioRxiv, 825307.

Inger, R. F. (1954). Systematics and zoogeography of Philippine Amphibia. Fieldiana Zoology, 33, 181-531.

Jaros, U., Tribsch, A., & Comes, H. P. (2018). Diversification in continental island archipelagos: new evidence on the roles of fragmentation, colonization and gene flow on the genetic divergence of Aegean Nigella (Ranunculaceae). Annals of Botany, 121(2), 241-254.

Jiao, X., Flouri, T., Rannala, B., & Yang, Z. (2020). The impact of cross-species gene flow on species tree estimation. Systematic Biology, 69(5), 830-847.

Jörger, K. M., & Schrödl, M. (2013). How to describe a cryptic species? Practical challenges of molecular taxonomy. Frontiers in Zoology, 10(1), 59.

Katoh, K., & Standley, D. M. (2013). MAFFT multiple sequence alignment software version 7: improvements in performance and usability. Molecular Biology and Evolution, 30(4), 772-780.

Kent, W. J. (2002). BLAT—the BLAST-like alignment tool. Genome Research, 12(4), 656-664.

Kooyman, R. M., Morley, R. J., Crayn, D. M., Joyce, E. M., Rossetto, M., Slik, J. F., Strijk, J.S., Su, T., Yap, J.Y.S., & Wilf, P. (2019). Origins and assembly of Malesian rainforests. Annual Review of Ecology, Evolution, and Systematics, 50, 119–143.

Korshunova, T., Picton, B., Furfaro, G., Mariottini, P., Pontes, M., Prkić, J., Fletcher, K., Malmberg, K., Lundin, K., & Martynov, A. (2019). Multilevel fine-scale diversity challenges the 'cryptic species' concept. Scientific Reports, 9(1), 1-23.

Lanier, H. C., & Knowles, L. L. (2012). Is recombination a problem for species-tree analyses?. Systematic Biology, 61(4), 691-701.

Leavitt, S. D., Moreau, C. S., & Lumbsch, H. T. (2015). The dynamic discipline of species delimitation: progress toward effectively recognizing species boundaries in natural populations. In Recent Advances in Lichenology (pp. 11-44). Springer, New Delhi.

Lanier, H. C., & Knowles, L. L. (2012). Is recombination a problem for species-tree analyses?. Systematic Biology, 61(4), 691-701.

Leaché, A. D., & Rannala, B. (2011). The accuracy of species tree estimation under simulation: a comparison of methods. Systematic Biology, 60(2), 126-137.

Li, H., Handsaker, B., Wysoker, A., Fennell, T., Ruan, J., Homer, N., Marth, G., Abecasis, G., & Durbin, R. (2009). The sequence alignment/map format and SAMtools. Bioinformatics, 25(16), 2078-2079.

Li, H. (2013). Aligning sequence reads, clone sequences and assembly contigs with BWA-MEM. arXiv preprint arXiv:1303.3997.

Lomolino, M. V., Brown, J. H., & Sax, D. F. (2010). Island biogeography theory. The theory of island biogeography revisited, Princeton: Princeton University Press

Lowe, J. J., & Walker, M. J. (2014). Reconstructing quaternary environments. Routledge.

Mallet, J., Besansky, N., & Hahn, M. W. (2016). How reticulated are species?. BioEssays, 38(2), 140-149.

Mayr, E. (1978). Origin and history of some terms in systematic and evolutionary biology. Systematic Zoology, 27(1), 83-88.

McKenna, A., Hanna, M., Banks, E., Sivachenko, A., Cibulskis, K., Kernytsky, A., Garimella, K., Altshuler, D., Gabriel, S., Daly, M., & DePristo, M. A. (2010). The Genome Analysis Toolkit: a MapReduce framework for analyzing next-generation DNA sequencing data. Genome Research, 20(9), 1297-1303.

Neuditschko, M., Khatkar, M. S., & Raadsma, H. W. (2012). NetView: a high-definition network-visualization approach to detect fine-scale population structures from genome-wide patterns of variation. PloS One, 7(10), e48375.

Nosil, P., & Feder, J. L. (2012). Genomic divergence during speciation: causes and consequences. Philosophical Transactions of the Royal Society B: Biological Sciences, 367(1587), 332–342.

Oaks, J. R., Sukumaran, J., Esselstyn, J. A., Linkem, C. W., Siler, C. D., Holder, M. T., & Brown, R. M. (2013). Evidence for climate-driven diversification? A caution for interpreting ABC inferences of simultaneous historical events. Evolution: International Journal of Organic Evolution, 67(4), 991-1010.

Oaks, J. R., Siler, C. D., & Brown, R. M. (2019). The comparative biogeography of Philippine geckos challenges predictions from a paradigm of climate-driven vicariant diversification across an island archipelago. Evolution, 73(6), 1151-1167.

Oliver, P. M., Brown, R. M., Karin, B. R., & Grismer, L. L. (2020). Mountain endemism in Malesian geckos: can biotic interactions push lizards up hills?. Israel Journal of Ecology and Evolution, 1(aop), 1-12.

Padial, J. M., Miralles, A., De la Riva, I., & Vences, M. (2010). The integrative future of taxonomy. Frontiers in Zoology, 7(1), 1-14.

Rambaut, A., Drummond, A. J., & Suchard, M. (2014). Tracer v1. 6, Available from http://beast.bio.ed.ac.uk/Tracer.

Rheindt, F. E., & Edwards, S. V. (2011). Genetic introgression: an integral but neglected component of speciation in birds. The Auk, 128(4), 620-632.

Ron, S., & R. M. Brown. (2008). Filling the black hole: challenges in taxonomy to protect amphibians. Pp. 133 In: Stuart, S.N., Hoffmann, M., Chanson, J.S., Cox, N.A., Berridge, R, Ramani, P. and Young B.E. (Eds.) Threatened Amphibians of the World. Lynx Ediciones, Barcelona, Spain; IUCN - The World Conservation Union, Gland, Switzerland; and Conservation International, Arlington Virginia, USA

Sanguila, M. B., Cobb, K. A., Siler, C. D., Diesmos, A. C., Alcala, A. C., & Brown, R. M. (2016). The amphibians and reptiles of Mindanao Island, southern Philippines, II: the herpetofauna of northeast Mindanao and adjacent islands. ZooKeys, (624), 1.

Schmitt, T. (2009). Biogeographical and evolutionary importance of the European high mountain systems. Frontiers in Zoology, 6(1), 9.

Scornavacca, C., & Galtier, N. (2017). Incomplete lineage sorting in mammalian phylogenomics. Systematic Biology, 66(1), 112-120.

Setiadi, M. I., McGuire, J. A., Brown, R. M., Zubairi, M., Iskandar, D. T., Andayani, N., Supriatna, J., & Evans, B. J. (2011). Adaptive radiation and ecological opportunity in Sulawesi and Philippine fanged frog (*Limnonectes*) communities. The American Naturalist, 178(2), 221-240.

Simpson, G. G. (1961). Principles of Animal Taxonomy. New York, NY: Columbia University Press, 347.

Sites, J. W., & Crandall, K. A. (1997). Testing species boundaries in biodiversity studies. Conservation Biology, 11(6), 1289-1297.

Slater, G. S. C., & Birney, E. (2005). Automated generation of heuristics for biological sequence comparison. BMC Bioinformatics, 6(1), 31.

Steinig, E. J., Neuditschko, M., Khatkar, M. S., Raadsma, H. W., & Zenger, K. R. (2016). netview p: a network visualization tool to unravel complex population structure using genome-wide SNP s. Molecular Ecology Resources, 16(1), 216-227.

Stejneger, L. (1910). Description of a new frog from the Philippine Islands. Smithsonian Miscellaneous Collections. 52:437–439.

Struck, T. H., Feder, J. L., Bendiksby, M., Birkeland, S., Cerca, J., Gusarov, V. I., Kistenich, S., Larsson, K.H., Liow, L.H., Nowak, M.D., & Stedje, B. (2018). Finding evolutionary processes hidden in cryptic species. Trends in Ecology & Evolution, 33(3), 153-163.

Taylor, E.H. (1920). Philippine Amphibia. Philippine Journal of Science 16, 213–359.

Trontelj, P., & Fišer, C. (2009). Perspectives: Cryptic species diversity should not be trivialised. Systematics and Biodiversity, 7(1), 1-3.

Van der Auwera, G. A., Carneiro, M. O., Hartl, C., Poplin, R., Del Angel, G., Levy-Moonshine, A., Jordan, T., Shakir, K., Roazen, D., Thibault, J., & Banks, E. (2013). From FastQ data to high-confidence variant calls: the genome analysis toolkit best practices pipeline. Current protocols in bioinformatics, 43(1), 11-10.

Wells, K. D. (2010). The ecology and behavior of amphibians. University of Chicago Press.

Wen, D., Yu, Y., Zhu, J., & Nakhleh, L. (2018). Inferring phylogenetic networks using PhyloNet. Systematic Biology, 67(4), 735-740.

Wiley, E. O. 1978. The evolutionary species concept reconsidered. Systematic Zoology 21:17–26.

Zhang, J., Kobert, K., Flouri, T., & Stamatakis, A. (2014). PEAR: a fast and accurate Illumina Paired-End reAd mergeR. Bioinformatics, 30(5), 614-620.

Figures

Fig. 1. Single locus (16S) phylogeny of the *Limnonectes magnus* + *L. diuatus* species complex.

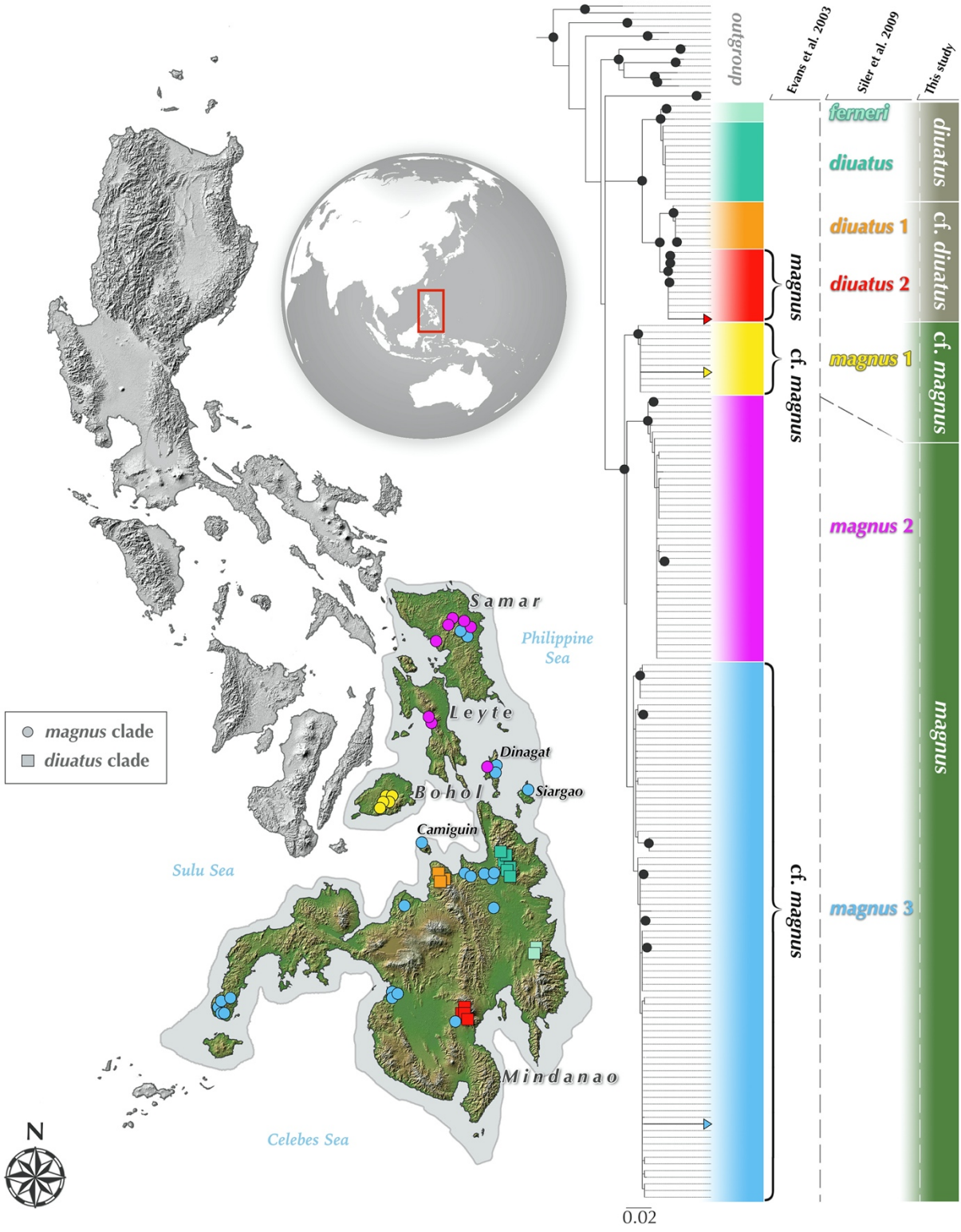

Fig. 2. mtGenome and nuDNA phylogenies showing non-sister group relationship between *Limnonectes magnus* and *L. diuatus* clades. (from Brown et al., in review).

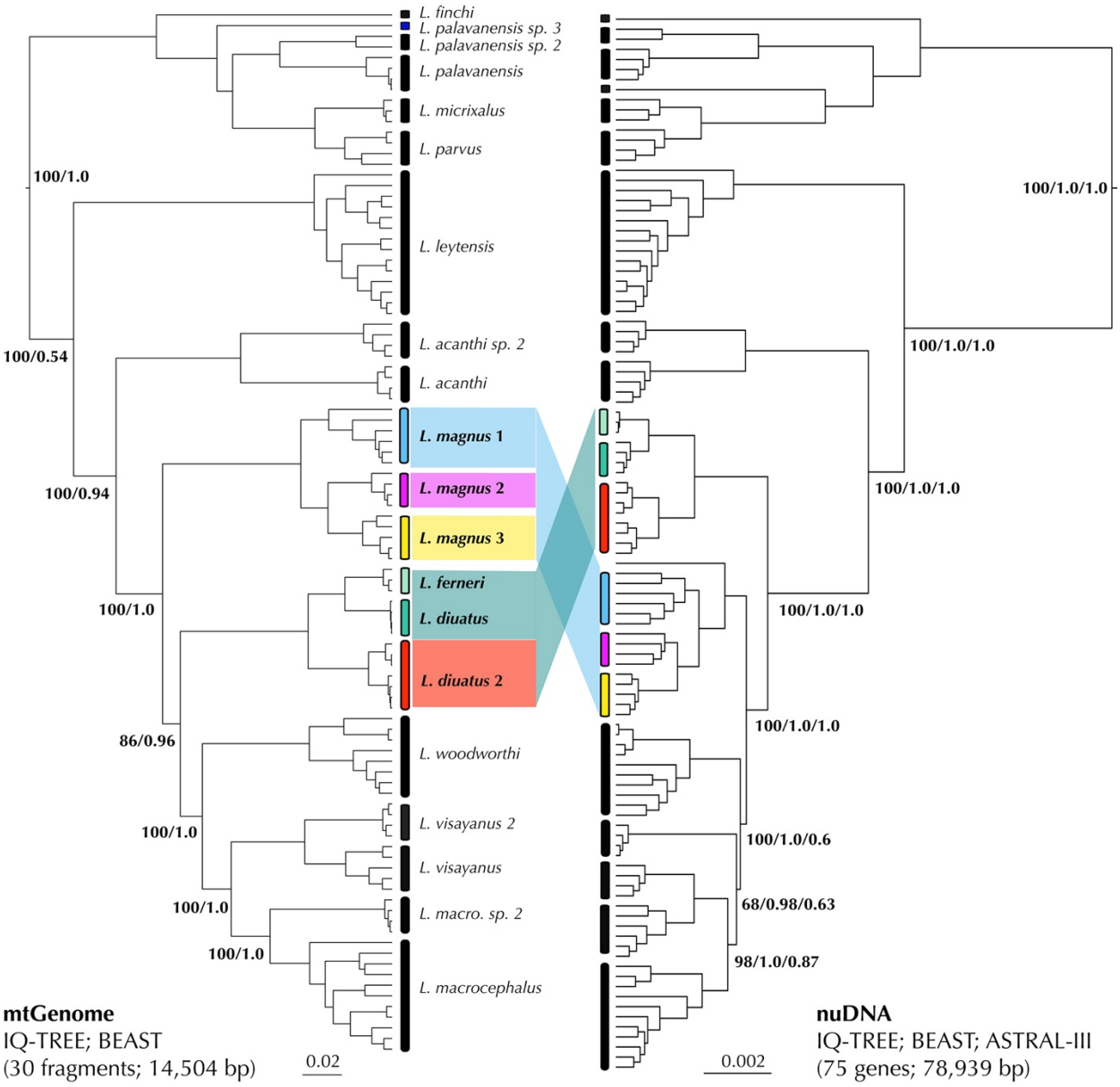

Fig. 3. Ancestry coefficient barplots from the sNMF analysis for the *Limnonectes magnus* (K =2) and *L. diuatus* (K = 3 & 4) clades respectively. Color coded piecharts of ancestry coefficient proportions are spatially visualized on the distribution map and labelled according to all clades and singleton taxa in the dataset (*L. magnus*: 1–15; *L. diuatus*: 16–30).

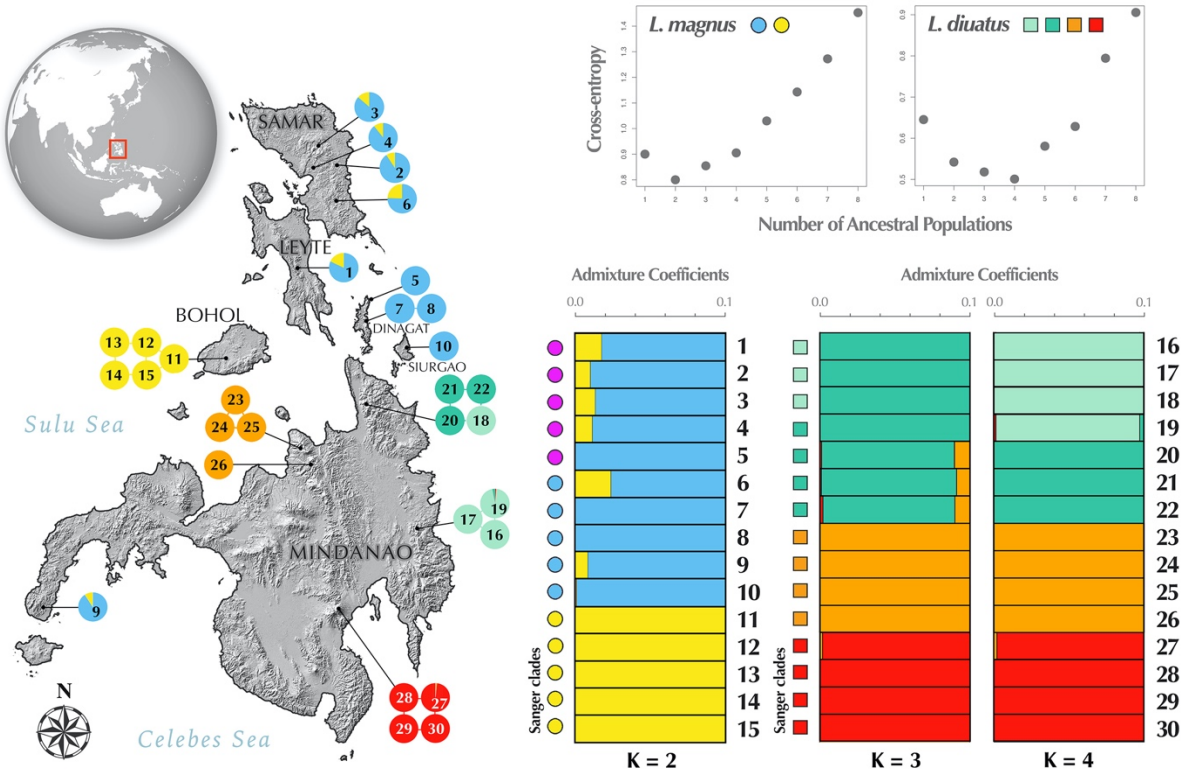

Fig. 4. Network clusters derived from NetView at k = 6 shows closely related individuals of the *Limnonectes magnus* and *L. diuatus* clades co-located within a cluster, and distantly related individuals are separated. Datapoints have been substituted with piecharts of ancestry coefficients from the sNMF analysis.

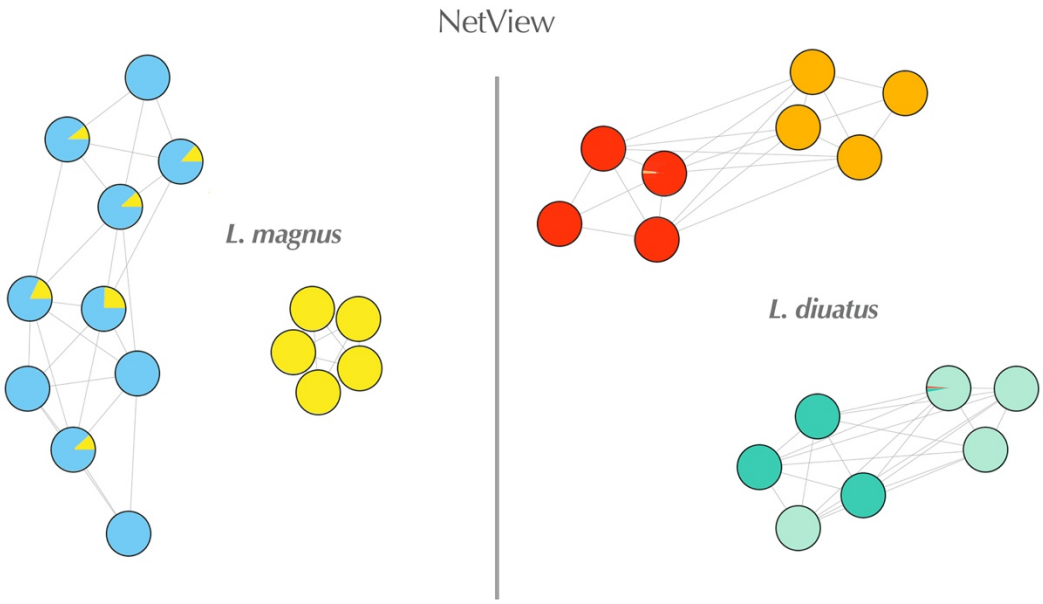

Fig. 5. PCA analysis plot on SNP data with datapoints substituted with piecharts of ancestry coefficients from the sNMF analysis at K = 2 for *L. magnus* (blue + yellow) and at K = 4 for *L. diautus* (dark green + light green + red + orange). PCAs were plotted separately for *L. magnus* and *L. diuatus*, but presented here together on a common plot.

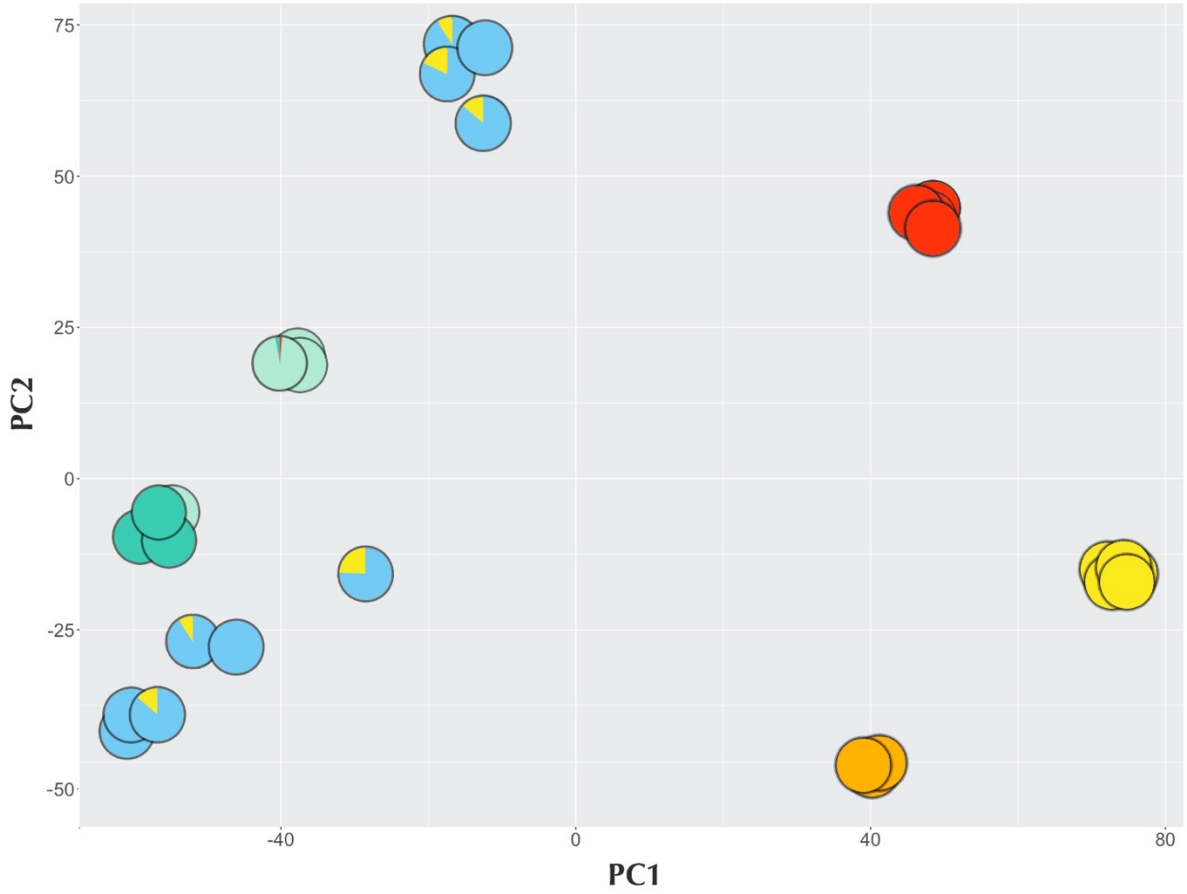

Fig. 6. Hybrid Index plots of the three clades of the *Limnonectes magnus* clade. Parental reference populations from Bohol (yellow) and Dinagat + Siurgao (blue) were selected based on consistently inferred non-admixed populations across the sNMF, NetView and PCA analyses.

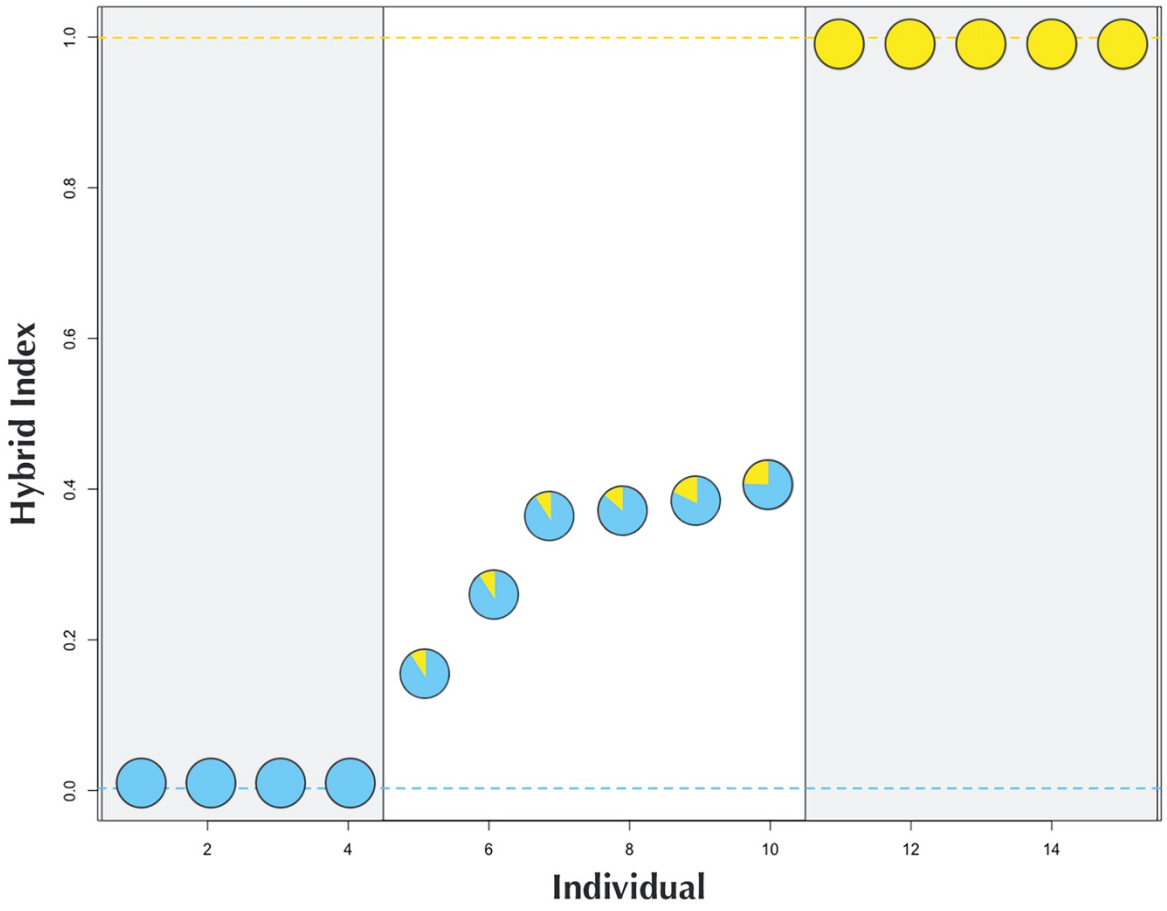

Fig. 7. Hybrid Index plots of the three clades of the *Limnonectes diuatus* clade.

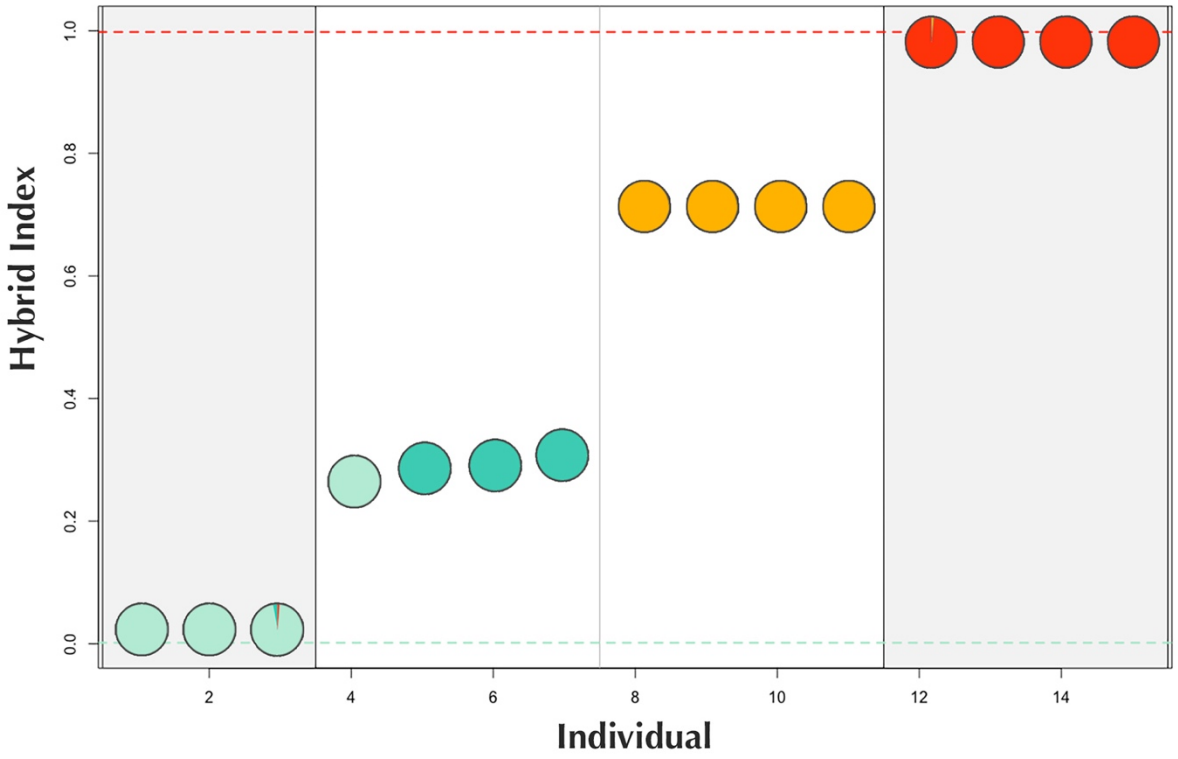

Table 1. List of taxa, samples, and populations included in this study.

Sl. No.	Sample	Field No.	Catalog No.	Location	Color
1	*Limnonectes magnus*	RMB 8947	KU 326360	Leyte	Hybrid
2	*Limnonectes magnus*	RMB 18478	KU 337825	Samar	Hybrid
3	*Limnonectes magnus*	CWL 165	KU 306045	Samar	Hybrid
4	*Limnonectes magnus*	CDS 6992	KU 337806	Samar	Hybrid
5	*Limnonectes magnus*	RMB 8523	KU 314384	Samar	Hybrid
6	*Limnonectes magnus*	RMB 10484	KU 319384	Mindanao	Hybrid
7	*Limnonectes magnus*	CWL 324	KU 306084	Dinagat	Blue
8	*Limnonectes magnus*	RMB 8389	KU 309985	Dinagat	Blue
9	*Limnonectes magnus*	CDS 1929	KU 306063	Dinagat	Blue
10	*Limnonectes magnus*	ACD 7076	Deposited at PNM	Siargao	Blue
11	*Limnonectes magnus*	RMB 2887	KU 327507	Bohol	Yellow
12	*Limnonectes magnus*	CDS 4989	KU 323634	Bohol	Yellow
13	*Limnonectes magnus*	CDS 4867	KU 323627	Bohol	Yellow
14	*Limnonectes magnus*	CDS 4678	KU 323591	Bohol	Yellow
15	*Limnonectes magnus*	CDS 4668	KU 323586	Bohol	Yellow
16	*Limnonectes diautus*	PNM-CMNH H 1244	PNM*	Mt. Talomo	Red
17	*Limnonectes diautus*	PNM-CMNH H 1205	PNM*	Mt. Talomo	Red
18	*Limnonectes diautus*	PNM-CMNH H 1199	PNM*	Mt. Talomo	Red
19	*Limnonectes diautus*	PNM-CMNH H 1197	PNM*	Mt. Talomo	Red
20	*Limnonectes diautus*	JWF 94094	CMNH 5573	Mt. Pasian	Light Green
21	*Limnonectes diautus*	JWF 94093	PNM 9506	Mt. Pasian	Light Green

22	*Limnonectes diautus*	JWF 94091	CMNH 5572	Mt. Pasian	Light Green
23	*Limnonectes diautus*	RMB 16235	KU 333384	Mt. Hilong-hilong	Dark Green
24	*Limnonectes diautus*	RMB 16225	KU 333375	Mt. Hilong-hilong	Dark Green
25	*Limnonectes diautus*	RMB 16224	KU 333374	Mt. Hilong-hilong	Dark Green
26	*Limnonectes diautus*	RMB 16164	KU 333373	Mt. Hilong-hilong	Dark Green
27	*Limnonectes diautus*	RMB 16582	KU 333428	Mt. Lumot	Orange
28	*Limnonectes diautus*	ACD 4324	KU 320090	Mt. Balatukan	Orange
29	*Limnonectes diautus*	ACD 4316	KU 320085	Mt. Balatukan	Orange
30	*Limnonectes diautus*	ACD 4274	KU 320079	Mt. Balatukan	Orange

* Deposited in National Museum of the Philippines and/or Cincinnati Museum of Natural History.

Table 2. Summaries for datasets analyzed in this study (PIS = parsimony informative sites; MBP = Missing Basepairs).

Dataset	Total markers	Basepairs	Prop. of Samples	Total PIS	Prop. of PIS	MBP	Prop. of MBP
Legacy	76	79872	0.9449	1114	0.01353	682.4868	0.018
Loci-combined	1109	728352	0.9614	728352	0.01604	1288.8476	0.0725
All markers	6812	4539040	0.8739	221749	0.0508	907.57	0.0499
Exon	6411	1915347	0.8804	38014	0.0187	105.0407	0.0037
Intron	6404	3372453	0.8815	233543	0.0692	884.5729	0.0578

CHAPTER 4

Phylogenomics of Spotted Philippine Stream Frogs: 12,000 loci provide insight into the status of isolated, admixed, island-endemic species and the possible consequences of gene flow during evolutionary radiation.

Robin Kurian Abraham & Rafe M. Brown

Abstract

The frog species *Pulchrana grandocula* and *P. similis* of the Philippine archipelago have been shown to be paraphyletic to each other by past Sanger phylogeny based-studies, and the question of whether the *Pulchrana grandocula – P. similis* species complex constitutes a single species or two is still at large. In this study, we endeavour to revisit this species complex with robust genomic data (constituting ~14,000 loci), and evaluate putative species boundaries with data from representative populations across the known range of these two species, along with testing for cross-species hybridization. We also investigate *P. guttmani* and *P. melanomenta* within this framework, and re-evaluate their phylogenetic placement. Our results reveal that the central islands of the eastern Philippines form a hybrid zone of the *P. similis* and *P. grandocula* genotypes and form a single cluster, exclusive of all remaining taxa. Our results also reveal that the singleton individuals representing *P. guttmani* and *P. melanomenta* were found to be highly admixed, with introgression from almost all genotypes included in our dataset. Overall, our phylogenetic network analysis results showed a remarkably high degree of introgression among all clades.

Introduction

A prominent debate in biology is that of species and species boundaries, which has significant conservation implications in the ongoing biodiversity crisis (Bickford et al. 2007; Sites & Crandall, 1997; Harrison & Larson, 2014; Chan et al. 2020); Traditional definitions on what constitutes a species varies from them being defined as organismal entities that are distinct, diagnosable, reproductively isolated, monophyletic groups of organisms to entities that lie across a continuum between varieties and species (Darwin 1859; Mayr, 1942). In spite of the introduction of molecular approaches such as Sanger sequencing, species delimitation has been a challenging task (Barley et al., 2013; Jörger & Schrödl, 2013; Leavitt, Moreau & Lumbsch, 2015). The majority of molecular phylogenies have been—and still are—estimated using mitochondrial and/or a handful of nuclear genes (e.g., Weinell et al., 2020; Abraham et al. in review; Ramesh et al., 2020; Vijayakumar et al., 2019). In many of these studies, cryptic species diversity is inferred based on phylogenetic placement, subjective genetic distance thresholds, or divergence-based species delimitation analyses (Barley et al. 2020; Korshunova et al., 2019; Struck et al., 2018; Trontelj and Fier, 2009). Recent advances in genomic sequencing, however, has improved our capacity to better explore species boundaries within an evolutionary framework (Coates, Byrne & Moritz 2018; Hutter et al. 2019). The very same clades identified by traditional, Sanger-based phylogenies have now been recovered with genomic-scale data and, by some measures, remain unchanged (e.g., Rösler et al. 2011; versus Wood et al. 2020), but others have been identified as possible cases of taxonomic "inflation" (Hillis, 2019; Issac et al., 2004). In such instances, species groups, or clades of closely-related species are said to have been over-described, or excessively split into named taxonomic units, among which divergences are shallower and/or phenotypic distinctiveness less pronounced than conventional species-level

taxonomic units (Chambers & Hillis, 2020; Koch et al., 2007, 2010; Welton et al., 2013; Ziegler & Vences, 2020).

Speciation processes are now known to be affected by cross-species hybridization and/or introgression and is thus an important parameter to be considered for species identification (Jiao et al., 2020; Mallet et al., 2016). Species tree estimation methods that accommodate the coalescent process but not take into account gene flow can be misled (Folk et al., 2018) by introgression and deep coalescence/incomplete lineage sorting (ILS), or a combination of these phenomena—all of which can create challenges for species tree reconstruction (Jiao et al., 2020; Wang et al., 2020). Species-level phylogenies exemplifying these challenges have been demonstrated in diverse organismal groups, from Oak trees, *Heliconius* butterflies, *Anopheles* mosquitoes, East African Cichlid fish, among others (Edelman et al., 2018; Hipp et al., 2020; Svardal et al., 2020; Thawornwattana et al., 2018). In a recent study on frogs, Chan et al. (2020) demonstrated how geneflow among Bornean Spotted Stream Frogs created an illusion of putatively cryptic species, which serves as a sober warning against uncritical acceptance of the expectation of widespread cryptic, undescribed species diversity in Southeast Asia (Stuart et al. 2006; Bickford et al., 2007; McLeod 2010; Nishikawa et al, 2012).

An interesting group of frogs found throughout Southeast Asia and Indochina are those of the spotted stream frogs of the genus *Pulchrana* (Frost, 2020; AmphibiaWeb, 2020). The Philippines is home to a unique assemblage of *Pulchrana* species, distributed non-randomly throughout the archipelago (Inger, 1954; Brown & Guttman, 2002). Contrary to earlier expectations of higher diversity in the Philippines, studies indicated that there are more species on the Asian mainland the land bridge islands than in the Philippines (Brown & Siler, 2014; Chan et al. 2014; Chan 2020; in press; Leong and Lim 2003). A relatively widely distributed species group in the

Philippines is the *P. grandocula – P. similis* complex, which straddles the eastern islands of the archipelago, from Luzon in the north to Mindanao in the south (Brown & Siler, 2014). This specie complex was found to have a pectinate phylogeny, with *P. similis* nested within *P. grandocula* (rather than two, reciprocally-monophyletic clades), calling into question the validity of *P. similis* as separate operational taxonomic unit. Thus, based on their findings, Brown and Siler (2014) suggested that the two species could represent either a single widespread Philippine endemic, or that the putative lineages involved possibly have not experience sufficient time to coalesce (Sukumaran & Knowles, 2017). Two additional species *P. guttmani* (from southern Mindano; Brown 2015) and *P. melanomenta* (from Tawi-tawi island in the Sulu Archipelago; Taylor 1920) were also included for the first time in the phylogeny and shown to be most closely related to *P. grandocula* and *P. similis*.

Although the paraphyly of *P. grandocula* with respect to *P. similis* was apparent in Brown and Siler (2014), this relationship was not strongly supported in either maximum likelihood or Bayesian analyses, and so question of whether this complex constitutes a single species or two is still at large. We endeavoured to address this unresolved question in the present study, using a novel genomic resource: FrogCap (Hutter et al. 2019).

With 14,000 loci in a complex group of *Pulchrana* species, we studied admixture and possible gene flow from 31 alignments for six species from the Philippines and two outgroup species from Borneo (see Table 1). In this study, we reinvestigate this species complex with robust genomic data, and evaluate putative species boundaries with data from representative populations across the known range of *P. grandocula* and *P. similis*. Further, we test whether cross-species hybridization has occurred in the processes of speciation, leading to current species

diversity this complex. Finally, we investigate two rarely-sampled species, *P. guttmani* and *P. melanomenta*, within this framework, and re-evaluate their phylogenetic placement.

Methods

Taxon sampling and DNA extraction:

We sequenced 25 ingroup samples of Philippine *Pulchrana* species, with 18 samples of our priority taxa *P. grandocula* and *P. similis* (Table 1).

Probe design, library preparation, and sequencing:

Probe design follows Hutter et al. (2019) and is summarized here. Probes were synthesized as biotinylated RNA oligos in a myBaits kit (by Arbor Biosciences™, formerly MYcroarray® Ann Arbor, MI) by using the program BLAT 3.50 to individually match 25 publicly available transcriptomes to the *Nanorana parkeri* and *Xenopus tropicalis* genomes (Kent, 2002). Matching sequences were clustered by their genomic coordinates to detect presence/absence across species and to achieve full locus coverage. Each cluster was matched to available coding region annotations from the *Nanorana parkeri* genome using the program EXONERATE in order to narrow the locus selection to coding regions (Slater and Birney, 2005). Loci from all matching species were then aligned using MAFFT 7.313 (Katoh and Standley, 2013), and kept if they had at least three taxa and were at least 100 bp long. Markers were selected based on phylogenetic representation, informativeness, and other filters explained in Hutter et al. (2019). For each marker, we used the *N. parkeri* genome sequence as the chosen design marker. To create a .fasta file of bait sequences as individual entries, we separated the selected markers into 120 bp-long sequences with 2x tiling (50% overlap among baits) using an R script. These markers have an additional bait at each end extending into the intronic region to increase the coverage and capture

success of these areas. Baits were then filtered, retaining those: without sequence repeats; a GC content of 30%–50%; and baits that did not match to their reverse complement or multiple genomic regions. Additionally, 646 UCEs that contain at least 10% informative sites were included (Alexander et al., 2017). Finally, we used the myBaits-2 kit (40,040 baits) with 120mer sized baits with our chosen filtered bait sequences.

Library preparation was performed by Arbor Biosciences following the myBaits V3.1 manual and briefly follows: (1) genomic DNA was sheared to 300–500 bp; (2) adaptors were ligated to DNA fragments; (3) each library was amplified for 6 cycles using unique combinations of i7 and i5 indexing primers attached to the adapters to later identify individual samples; (4) biotinylated 120mer RNA library baits were hybridized to the sequences; (5) target sequences were selected by adhering to magnetic streptavidin beads; (6) Enrichment incubation times ranged 18–21 hours; (7) target regions were amplified via PCR for 10 cycles; and (8) samples were pooled and sequenced on an Illumina HiSeq PE-3000 with 150 bp paired-end reads. Sequencing was performed at the Oklahoma Medical Research Foundation DNA Sequencing Facility.

Bioinformatics:

The bioinformatics pipeline for filtering adapter contamination, assembling markers, trimming, and exporting alignments are available on GITHUB, using the FrogCap bioinformatics pipeline (bioinformatics-pipeline_stable-v1; https://github.com/chutter/FrogCap-Sequence-Capture). Adapter contamination and other sequencing artefacts were filtered from raw reads using the program FASTP (default settings; Chen et al., 2018). In order to avoid inflating coverage for these regions due to uneven lengths from cleaning (Zhang et al., 2014), paired-end reads were merged using the program BBMerge (Bushnell et al., 2017). The cleaned reads were then

assembled de novo using the program Merged singletons and paired-end reads were assembled de novo using the program SPADES v.3.12 (Bankevich et al. 2012), which runs BAYESHAMMER (Nikolenko et al. 2013) error correction on the reads internally. Data were assembled using several different k-mer values (21, 33, 55, 77, 99, 127), in which orthologous contigs resulting from the different k-mer assemblies were merged. We used the DIPSPADES (Safanova et al. 2015) function to assemble contigs that were polymorphic by generating a consensus sequence from both haplotypes from orthologous regions such that polymorphic sites were resolved randomly. We then matched consensus haplotype contigs against reference marker sequences used to design the probes separately for our three probe sets with BLAST (dc-megablast). We discarded contigs if they failed to match ≥ 30% of the reference marker, and removed contig matches fewer than 50 bp. The contigs were then matched against the reference probe sequences with BLAT 3.50 (Kent, 2002), keeping only those contigs that uniquely matched to the probe sequences. The final set of matching loci was then aligned on a locus-by-locus basis using MAFFT 7.313 using the algorithm L-INS-i (auto and default parameters; Katoh & Standley 2013).

Alignments were externally trimmed using a custom R script, where at least 50 percent of the samples must have sequence data present externally, with at least three taxa per alignment. The alignments were saved separately into usable datasets for phylogenetic analyses and data type comparisons: (1) Introns: the exon previously delimited was trimmed out of the original contig and the two remaining intronic regions were concatenated; (2) Exons: each alignment was adjusted to be in an open-reading frame and trimmed to the largest reading frame that accommodated >90% of the sequences, alignments with no clear reading frame were discarded; (3) Loci-combined: exons from the same gene, which may be linked (Lanier and Knowles, 2012;

Scornavacca and Galtier, 2017), were concatenated and treated as a single locus; and (4) UCEs were also saved as a separate dataset. Internal trimming was applied only to the intron and UCE alignments using the program trimAl (automatic1 function; Capellagutiérrez et al., 2009). We trimmed all alignments externally to ensure that at least 50 percent of the samples had sequence data present.

Phylogeny:

The loci-combined and all-markers (introns+exons) (datasets for *Pulchrana* were analysed separately to assess variability in phylogenetic signal that could potentially stem from different classes of genomic data. Maximum likelihood and summary coalescent methods were performed separately on these datasets. Sequences were concatenated and IQ-TREE was used to estimate a ML phylogeny with the GTR+I+GAMMA substitution model applied to each partition. Branch support was assessed using 1,000 ultrafast bootstrap replicates (Hoang et al. 2017). IQ-TREE was also used to estimate individual gene trees within each dataset, using the best-fit substitution model (Kalyaanamoorthy et al. 2017). We also used the program PhyloNet v3.8 (Wen et al. 2018) to infer a species network that incorporates ILS and introgression. The complete set of gene trees from the intron dataset (7,416 gene trees; outgroups removed) were used to infer a species network using Maximum Pseudo-likelihood Inference (Yu & Nakhleh 2015). We performed six separate analyses (10 runs per analysis) with the number of allowable reticulations ranging from 2–7. Likelihood scores for the best run in each analysis were compared to determine the optimal number of reticulations.

SNP detection:

Variant calling for SNPs (single nucleotide polymorphisms) was conducted through a custom pipeline in R and is available at (https://github.com/chutter/FrogCap-Sequence-Capture; variant-

pipeline_stable-v1). We used GATK v4.1 (McKenna et al. 2010), following developer best practices recommendations for discovering and calling variants (Van der Auwera et al. 2013). To discover potential variant data (e.g. SNPs, indels), we used a consensus sequence from each alignment from the target group as a reference and mapped cleaned reads back to consensus reference markers for each sample. We used BWA ("bwa mem" function; Li 2013) to map cleaned reads (cleaned-reads dataset explained above) to our reference markers, adding the read group information (e.g. Flowcell, Lane, Library) obtained from the fastq header files. Next we used SAMTOOLS (Li et al. 2009) to convert the mapped reads SAM file to a cleaned BAM file, and merged BAM files with our unmapped reads, as required for downstream analyses. We used the program PICARD to mark exact duplicate reads that might have resulted from optical and PCR artifacts and reformatted each dataset for variant calling. To locate variant and invariant sites, we used GATK to generate a preliminary variant dataset using the GATK program HaplotypeCaller, to call haplotypes, in GVCF format, for each sample individually. After processing each sample, we used the GATK GenomicsDBImport program to aggregate samples from separate datasets into their own combined database. Using these databases, we used the GenotypeGVCF function to genotype the combined sample datasets and output separate ".vcf" files for each marker, containing variant data, from all samples, for final filtration. The preliminary variant set was filtered into a final dataset refining as follows: (1) All variants were kept after moderate filtering to remove probable errors filtered at a quality score > 5; (2) High quality variants were kept including SNPs, MNPs (multi-nucleotide polymorphisms), and indels filtered at a quality > 20; (3) SNPs specifically were chosen after high-quality filtering (quality > 20); and (4) our final dataset consisted of one high-quality SNP from each exon that was most

variable across samples. Finally, we used a custom script to convert these SNPs to a structure formatted file.

Population structure determining exercises:

We examined population ancestry using a program based on sparse non-negative matrix factorization (sNMF). We estimated ancestry coefficients for 1–10 ancestral populations (K) using 100 replicates for each K. We then used the cross-entropy criterion to determine the best K based on the prediction of masked genotypes. The sNMF analysis was implemented through the R package *LEA* (Frichot and François 2015). We also inferred clustering using an unsupervised network clustering method NetView (Neuditschko et al. 2012), that uses genetic distances to assign individuals to populations without prior knowledge of individual ancestry. Euclidean genetic distances were used as input and the NetView analysis was implemented using the R package netview (Neuditschko et al. 2012; Steinig et al. 2016).

Admixture among populations were confirmed using Bayesian hybrid-index analysis and the python program HyDe. A hybrid-index analysis calculates the proportion of allele copies originating from parental reference populations (Buerkle, 2005), whereas a HyDe analysis detects hybridization using phylogenetic invariants based on the coalescent model with hybridization (Blischak, Chifman, Wolfe, & Kubatko, 2018). Different combinations of plausible parental populations were tested, based on results from our population structure analysis. We performed the HyDe analysis on sequence data from the intron dataset. For this, we first assessed admixture at the population level using the *run_hyde* script that analyses all possible four-taxon configurations consisting of an outgroup (*Pulchrana picturata*) and a triplet of ingroup populations comprising two parental populations (P1 and P2) and a putative hybrid population (Hyb). We then performed analysis at the individual level using the *individual_hyde* script to

detect hybridization in individuals within populations that had significant levels of genomic material from the parental species. Lastly, we performed bootstrap resampling (500 replicates) of individuals within hybrid populations to obtain a distribution of gamma values to assess heterogeneity in levels of gene flow.

Results

Phylogenetic relationships:

Phylogenetic relationships inferred from the loci-combined (2188 loci) and all-markers (12,626 loci) datasets were identical in their topologies (Table 2). Maximum likelihood bootstrap branch support was strong throughout the topology estimated from the all-markers dataset (Fig. 1). However, the combined dataset produced the same topology, but with weaker support along the backbone (Supp. file); nevertheless, bootstrapping indicated strong support towards the tips of this topological estimate. The relationships suggest a pectinate relationship, with *Pulchrana grandocula* paraphyletic with respect to *P. similis*. Both of these OTUs were nested within a clade, also containing (singleton sampling) taxa *P. melanomenta* and *P. guttmani*, and this relationship was strongly-supported. Sister to this clade is a strongly-supported clade of western Philippine sister species, *P. mangyanam* and *P. moellendorffi* (Fig. 1).

Population structure:

For the *Pulchrana grandocula* + *similis* clade, the cross-entropy criterion of the sNMF analysis inferred K=3–6 ancestral populations, comprising of non-admixed *P. similis*, and two genotypes of *P. grandocula* (Fig. 1). The singleton individuals representing the two species of *P. guttmani* from southern Mindanao and *P. melanomenta* from the Sulu island of Tawi-tawi were found to be highly admixed, consisting of putative parental proportions identified as all the genotypes

included in our dataset. This was also true, albeit to a lesser degree, with *P. moellendorffi* of Palawan island. *P. mangyanam* of Mindoro Island (Fig. 1), in contrast, and the two outgroup taxa from Borneo, *P. picturata* and *P. signata* were identified as pure, largely non-admixed ancestral populations (species). The Netview results show the presence of two primary centres of genomic variation, or clusters (Fig. 2). One of these comprises the eastern Philippine island arc (Mindanao, Samar, Leyte, Luzon) species *P. grandocula* and *P. similis*; the other consists of all remaining Philippine taxa (Fig. 2). The Hybrid Index results demonstrate that populations on Samar, Leyte, Bohol and Dinagat exhibit variable degrees of admixture, ostensibly identified as having originated from the genomes of pure parentals, the non-admixed populations of *P. similis* from Luzon and *P. grandocula* from Mindanao (Fig. 3).

Species network, Gene flow and Introgression:

A phylogenetic species network comprising four reticulation events was found to be optimal (Fig. 4). The relationships among taxa followed our IQTree phylogeny. The inferred reticulation events were congruent with admixture patterns inferred from the sNMF results. The HyDe analysis at the individual level showed a spectrum of levels of hybridization from moderate (Gamma=0.54) to high (Gamma=0.01) among *P. grandocula* individuals (Table 3). Two individuals from Bohol (Gamma=0.01) and Dinagat (Gamma=0.05) were identified as the highest degrees of hybridization observed in this study, whereas the Samar and Leyte populations showed little admixture.

Discussion

In this study, we find the presence of geneflow across species boundaries, forming geographic hybrid zones, which may have misled taxonomic interpretations. This is particularly evident if

we consider past interpretations that these highly introgressed individuals, or populations, represented non-admixed species in phylogenetic analyses (Brown and Guttman 2002; Brown and Siler 2014).

Our phylogenetic results with genomic data constituting 14,000 loci reinforce the pectinate, nested relationship between the two proposed species (Inger, 1954; Brown & Guttman, 2002) in the *Pulchrana grandocula – P. similis* complex, and show *P. melanomenta* and *P. guttmani* as unique branches agreeing with Brown & Siler (2014)'s multilocus Sanger phylogeny (Fig. 1). Although the *P. guttmani* sample is from southern Mindanao, it falls outside of the *Pulchrana grandocula – P. similis* complex + *P. melanomenta* (Taylor 1920; an endemic species to the southern Sulu Archipelago island of Tawi-tawi) clade. Although not our focal group, we also find that *P. moellendorffi*'s (of Palawan island) placement agrees with that of Brown & Siler (2014), as sister to *P. mangyanum* of Mindoro island (Fig. 1).

Our sNMF, HyDe and Hybrid Index results reveal that the central islands of Bohol and Dinagat form a hybrid zone with variable admixture of *P. similis* genomic material identified in the *P. grandocula* genotype. This is curious because as far as we can determine at this point, *P. similis* genomic material is absent in more northern Samar and Leyte populations, which are closer to Luzon, which is home to the pure parental *P. similis* population (Fig. 1). Our Netview results revealed *P. similis* and *P. grandocula* to be a single cluster, exclusive of all remaining taxa. A single specimen of *P. grandocula* from Mindanao, with a small proportion of admixed *P. mangyanum* genetic material, grouped with this second cluster. The sNMF results also revealed that the singleton individuals representing *P. guttmani* and *P. melanomenta* were found to be highly admixed, with introgression from almost all genotypes included in our dataset. Despite being on the more remote island of Tawi-tawi, *P. melanomenta* has a higher percentage of *P.*

grandocula admixture than of *P. guttmani*, which is consistent with the branching pattern in our phylogeny (Fig. 1). As demonstrated for the closely-related Bornean species *P. picturata* (Chan et al. 2020), highly introgressed individuals can often mislead interpretation of phylogeny, and may potentially result in incorrect inferences of their taxonomic status. Lastly, our phylogenetic network analysis results showed a remarkably high degree of introgression among all clades, with significant introgression also occurring between *P. signata* and *P. picturata* of Borneo.

Now, if we were to consider that all the OTUs included in this study, each representing a well characterized species with non-controversial phenotypic characters differences including morphology, bioacoustics, larval, ontological, and biogeographic, where each is endemic to a specific island or PAIC or mountain range (Brown & Guttman, 2002), then the degree of hybridization and/or admixture elucidated in this study would, according to a strict interpretation, warrant the likely synonymization of numerous endemic, distinct species from the Philippines. However, as yet fully unrecognized selective forces have allowed these admixed 'species' to persist at high elevations in one case (*P. guttmani*) and as a small isolated island endemic in another (*P. melanomenta*). The recognition of these populations calls into question the conceptual identification of species identified as having originated by hybrid speciation (Chafin et al., 2020; Harrison & Larson, 2014; Schumer et al., 2014). It would now be interesting to further investigate if these admixed populations have the most ideal 'fitness' of their genotypes, giving them an advantage over others, to persist in their particular environments, or if they are maintained by their isolation as cohesive evolutionary lineages (Wiley, 1979; Frost & Hillis, 1990; de Queiroz, 2007). If either of these are indeed the case, then recognition of these admixed populations would merit being identified as distinct evolutionary lineages, i.e. species. Hence, a study focused on genotyping the statistical sample from both 'species' would be the

recommended follow-up, going forward, in order to determine if other individuals in these populations are admixed at a similarly fixed proportion of all individuals from the non-admixed populations, to test if examples of hybrid speciation contribute to the evolutionary radiations of island archipelagos.

References

Alexander, A. M., Su, Y. C., Oliveros, C. H., Olson, K. V., Travers, S. L., & Brown, R. M. (2017). Genomic data reveals potential for hybridization, introgression, and incomplete lineage sorting to confound phylogenetic relationships in an adaptive radiation of narrow-mouth frogs. Evolution, 71(2), 475-488.

AmphibiaWeb (2020). Electronic database accessible at: https://amphibiaweb.org (accessed 02 November 2020). University of California, Berkeley, CA, USA.

Bankevich, A., Nurk, S., Antipov, D., Gurevich, A. A., Dvorkin, M., Kulikov, A. S., Lesin, V.M., Nikolenko, S.I., Pham, S., Prjibelski, A.D., & Pyshkin, A. V. (2012). SPAdes: a new genome assembly algorithm and its applications to single-cell sequencing. Journal of Computational Biology, 19(5), 455-477.

Barley, A. J., White, J., Diesmos, A. C., & Brown, R. M. (2013). The challenge of species delimitation at the extremes: diversification without morphological change in Philippine sun skinks. Evolution, 67(12), 3556-3572.

Barley, A. J., Diesmos, A. C., Siler, C. D., Martinez, C. M., & Brown, R. M. (2020). Taxonomic revision of Philippine Sun Skinks (Reptilia: Squamata: Scincidae: *Eutropis*), and descriptions of eight new species. Herpetological Monographs, 34(1), 39-70.

Bickford, D., Lohman, D. J., Sodhi, N. S., Ng, P. K., Meier, R., Winker, K., Ingram, K.K., & Das, I. (2007). Cryptic species as a window on diversity and conservation. Trends in Ecology & Evolution, 22(3), 148-155.

Blischak, P. D., Chifman, J., Wolfe, A. D., & Kubatko, L. S. (2018). HyDe: a Python package for genome-scale hybridization detection. Systematic Biology, 67(5), 821-829.

Brown, R. M., & Diesmos, A. C. (2002). Application of lineage-based species concepts to oceanic island frog populations: the effects of differing taxonomic philosophies on the estimation of Philippine biodiversity. Silliman Journal, 42(1), 133-162.

Brown, R. M., & Guttman, S. I. (2002). Phylogenetic systematics of the *Rana signata* complex of Philippine and Bornean stream frogs: reconsideration of Huxley's modification of Wallace's Line at the Oriental–Australian faunal zone interface. Biological Journal of the Linnean Society, 76(3), 393-461.

Brown, R. M., & Siler, C. D. (2014). Spotted stream frog diversification at the Australasian faunal zone interface, mainland versus island comparisons, and a test of the Philippine 'dual-umbilicus' hypothesis. Journal of Biogeography, 41(1), 182-195.

Brown, R. M. (2015). A new species of stream frog of the genus *Hylarana* from the mountains of southern Mindanao Island, Philippines. Herpetologica, 71(3), 223-233.

Buerkle, C. A. (2005). Maximum-likelihood estimation of a hybrid index based on molecular markers. Molecular Ecology Notes, 5(3), 684-687.

Bushnell, B., Rood, J., & Singer, E. (2017). BBMerge–accurate paired shotgun read merging via overlap. PloS One, 12(10), e0185056.

Capella-Gutiérrez, S., Silla-Martínez, J. M., & Gabaldón, T. (2009). trimAl: a tool for automated alignment trimming in large-scale phylogenetic analyses. Bioinformatics, 25(15), 1972-1973.

Chambers, E. A., & Hillis, D. M. (2020). The multispecies coalescent over-splits species in the case of geographically widespread taxa. Systematic Biology, 69(1), 184-193.

Chafin, T. K., Douglas, M. R., & Douglas, M. E. (2020). Genome-wide local ancestries discriminate homoploid hybrid speciation from secondary introgression in the red wolf (Canidae: Canis rufus). bioRxiv.

Chan, K. O., Brown, R. M., Lim, K. K., Ahmad, N., & Grismer, L. (2014). A new species of frog (Amphibia: Anura: Ranidae) of the *Hylarana signata* complex from peninsular Malaysia. Herpetologica, 70(2), 228-240.

Chan, K. O., Hutter, C. R., Wood Jr, P. L., Grismer, L. L., Das, I., & Brown, R. M. (2020). Gene flow creates a mirage of cryptic species in a Southeast Asian spotted stream frog complex. Molecular Ecology, 29(20), 3970-3987.

Chan, Kin Onn, R. K. Abraham, L. L. Grismer and R. M. Brown. Accepted pending revision (revisions returned). A systematic review of the *Pulchrana picturata* complex with the description of a new species from Peninsular Malaysia, Sumatra, and southern Thailand. Raffles Bulletin of Zoology. https://doi.org/10.11646/zootaxa.0000.0.0

Chen, S., Zhou, Y., Chen, Y., & Gu, J. (2018). fastp: an ultra-fast all-in-one FASTQ preprocessor. Bioinformatics, 34(17), i884-i890.

Darwin, C. (1859). The Origin of Species; And, the Descent of Man. Modern library.

De Queiroz, K. (2007). Species concepts and species delimitation. Systematic Biology, 56(6), 879-886.

Edelman, N. B., Frandsen, P. B., Miyagi, M., Clavijo, B., Davey, J., Dikow, R. B., García-Accinelli, G., Van Belleghem, S.M., Patterson, N., Neafsey, D.E., & Challis, R. (2019).

Genomic architecture and introgression shape a butterfly radiation. Science, 366(6465), 594-599.

Folk, R. A., Soltis, P. S., Soltis, D. E., & Guralnick, R. (2018). New prospects in the detection and comparative analysis of hybridization in the tree of life. American Journal of Botany, 105(3), 364-375.

Frichot, E., & François, O. (2015). LEA: An R package for landscape and ecological association studies. Methods in Ecology and Evolution, 6(8), 925-929.

Frost, D. R., & Hillis, D. M. (1990). Species in concept and practice: herpetological applications. Herpetologica, 86-104.

Harrison, R. G., & Larson, E. L. (2014). Hybridization, introgression, and the nature of species boundaries. Journal of Heredity, 105(S1), 795-809.

Herr, M. W., Vallejos, J. G., Meneses, C. G., Abraham, R. K., Otterholt, R., Siler, C. D., Rico, E. L. B., & Brown, R. M. (in press). A New, Morphologically Cryptic Species of Fanged Frog, Genus *Limnonectes* (Amphibia: Anura: Dicroglossidae), from Mindoro Island, Central Philippines, Copeia.

Hillis, D. M. (2019). Species delimitation in herpetology. Journal of Herpetology, 53(1), 3-12.

Hipp, A. L., Manos, P. S., Hahn, M., Avishai, M., Bodénès, C., Cavender-Bares, J., J., Crowl, A.A., Deng, M., Denk, T., Fitz-Gibbon, S., & Gailing, O. (2020). Genomic landscape of the global oak phylogeny. New Phytologist, 226(4), 1198-1212.

Hutter, C. R., Cobb, K. A., Portik, D., Travers, S. L., Wood, P. L., & Brown, R. M. (2019). FrogCap: A modular sequence capture probe set for phylogenomics and population genetics for all frogs, assessed across multiple phylogenetic scales. bioRxiv, 825307.

Inger, R. F. (1954). Systematics and zoogeography of Philippine Amphibia. Fieldiana Zoology, 33, 181-531.

Isaac, N. J., Mallet, J., & Mace, G. M. (2004). Taxonomic inflation: its influence on macroecology and conservation. Trends in Ecology & Evolution, 19(9), 464-469.

Jiao, X., Flouri, T., Rannala, B., & Yang, Z. (2020). The impact of cross-species gene flow on species tree estimation. Systematic Biology, 69(5), 830-847.

Jörger, K. M., & Schrödl, M. (2013). How to describe a cryptic species? Practical challenges of molecular taxonomy. Frontiers in Zoology, 10(1), 59.

Katoh, K., & Standley, D. M. (2013). MAFFT multiple sequence alignment software version 7: improvements in performance and usability. Molecular Biology and Evolution, 30(4), 772-780.

Kent, W. J. (2002). BLAT—the BLAST-like alignment tool. Genome Research, 12(4), 656-664.

Koch, A., Auliya, M., Schmitz, A., Kuch, U., & Böhme, W. (2007). Morphological studies on the systematics of South East Asian water monitors (*Varanus salvator* Complex): nominotypic populations and taxonomic overview. Mertensiella, 16(109), e80.

Koch, A., Gaulke, M., & Boehme, W. (2010). Unravelling the underestimated diversity of Philippine water monitor lizards (Squamata: *Varanus salvator* complex), with the description of two new species and a new subspecies. Zootaxa, 2446(1), 1-54.

Leavitt, S. D., Moreau, C. S., & Lumbsch, H. T. (2015). The dynamic discipline of species delimitation: progress toward effectively recognizing species boundaries in natural populations. In Recent Advances in Lichenology (pp. 11-44). Springer, New Delhi.

Lanier, H. C., & Knowles, L. L. (2012). Is recombination a problem for species-tree analyses?. Systematic Biology, 61(4), 691-701.

Leong, T. M., & Lim, B. L. (2003). A new species of *Rana* (Amphibia: Anura: Ranidae) from the highlands of the Malay Peninsula, with diagnostic larval descriptions. Raffles Bulletin of Zoology, 51(1), 115-122.

Li, H., Handsaker, B., Wysoker, A., Fennell, T., Ruan, J., Homer, N., Marth, G., Abecasis, G., & Durbin, R. (2009). The sequence alignment/map format and SAMtools. Bioinformatics, 25(16), 2078-2079.

Li, H. (2013). Aligning sequence reads, clone sequences and assembly contigs with BWA-MEM. arXiv preprint arXiv:1303.3997.

Mallet, J., Besansky, N., & Hahn, M. W. (2016). How reticulated are species?. BioEssays, 38(2), 140-149.

Mayr, E. (1978). Origin and history of some terms in systematic and evolutionary biology. Systematic Zoology, 27(1), 83-88.

McKenna, A., Hanna, M., Banks, E., Sivachenko, A., Cibulskis, K., Kernytsky, A., Garimella, K., Altshuler, D., Gabriel, S., Daly, M., & DePristo, M. A. (2010). The Genome Analysis Toolkit: a MapReduce framework for analyzing next-generation DNA sequencing data. Genome Research, 20(9), 1297-1303.

McLeod, D. S. (2010). Elucidating the relationships within the *Limnonectes kuhlii* species complex (Amphibia: Anura: Dicroglossidae) (Doctoral dissertation, University of Kansas).

Neuditschko, M., Khatkar, M. S., & Raadsma, H. W. (2012). NetView: a high-definition network-visualization approach to detect fine-scale population structures from genome-wide patterns of variation. PloS One, 7(10), e48375.

Nishikawa, K., Matsui, M., Yong, H. S., Ahmad, N., Yambun, P., Belabut, D. M., Sudin, A., Hamidy, A., Orlov, N.L., Ota, H., & Yoshikawa, N. (2012). Molecular phylogeny and

biogeography of caecilians from Southeast Asia (Amphibia, Gymnophiona, Ichthyophiidae), with special reference to high cryptic species diversity in Sundaland. Molecular Phylogenetics and Evolution, 63(3), 714-723.

Ramesh, V., Vijayakumar, S. P., Gopalakrishna, T., Jayarajan, A., & Shanker, K. (2020). Determining levels of cryptic diversity within the endemic frog genera, *Indirana* and *Walkerana*, of the Western Ghats, India. Plos One, 15(9), e0237431.

Roesler, H., Bauer, A. M., Heinicke, M. P., Greenbaum, E., Jackman, T., Nguyen, T. Q., & Ziegler, T. (2011). Phylogeny, taxonomy, and zoogeography of the genus *Gekko* Laurenti, 1768 with the revalidation of *G. reevesii* Gray, 1831 (Sauria: Gekkonidae). Zootaxa, 2989(1), 1-50.

Safonova, Y., Bankevich, A., & Pevzner, P. A. (2015). dipSPAdes: assembler for highly polymorphic diploid genomes. Journal of Computational Biology, 22(6), 528-545.

Schumer, M., Rosenthal, G. G., & Andolfatto, P. (2014). How common is homoploid hybrid speciation?. Evolution, 68(6), 1553-1560.

Scornavacca, C., & Galtier, N. (2017). Incomplete lineage sorting in mammalian phylogenomics. Systematic Biology, 66(1), 112-120.

Sites, J. W., & Crandall, K. A. (1997). Testing species boundaries in biodiversity studies. Conservation Biology, 11(6), 1289-1297.

Slater, G. S. C., & Birney, E. (2005). Automated generation of heuristics for biological sequence comparison. BMC Bioinformatics, 6(1), 31.

Steinig, E. J., Neuditschko, M., Khatkar, M. S., Raadsma, H. W., & Zenger, K. R. (2016). netview p: a network visualization tool to unravel complex population structure using genome-wide SNP s. Molecular Ecology Resources, 16(1), 216-227.

Stuart, B. L., Inger, R. F., & Voris, H. K. (2006). High level of cryptic species diversity revealed by sympatric lineages of Southeast Asian forest frogs. Biology Letters, 2(3), 470-474.

Sukumaran, J., & Knowles, L. L. (2017). Multispecies coalescent delimits structure, not species. Proceedings of the National Academy of Sciences, 114(7), 1607-1612.

Svardal, H., Quah, F. X., Malinsky, M., Ngatunga, B. P., Miska, E. A., Salzburger, W., Genner, M.J., Turner, G.F., & Durbin, R. (2020). Ancestral hybridization facilitated species diversification in the Lake Malawi cichlid fish adaptive radiation. Molecular Biology and Evolution, 37(4), 1100-1113.

Taylor, E. H. (1920). Philippine amphibia. Philippine Journal of Science, 16(3), 213-359.

Than, C., Ruths, D., & Nakhleh, L. (2008). PhyloNet: a software package for analyzing and reconstructing reticulate evolutionary relationships. BMC Bioinformatics, 9(1), 322.

Thawornwattana, Y., Dalquen, D., & Yang, Z. (2018). Coalescent analysis of phylogenomic data confidently resolves the species relationships in the Anopheles gambiae species complex. Molecular Biology and Evolution, 35(10), 2512-2527.

Van der Auwera, G. A., Carneiro, M. O., Hartl, C., Poplin, R., Del Angel, G., Levy-Moonshine, A., Jordan, T., Shakir, K., Roazen, D., Thibault, J., & Banks, E. (2013). From FastQ data to high-confidence variant calls: the genome analysis toolkit best practices pipeline. Current protocols in bioinformatics, 43(1), 11-10.

Vijayakumar, S. P., Pyron, R. A., Dinesh, K. P., Torsekar, V. R., Srikanthan, A. N., Swamy, P., Stanley, E.L., Blackburn, D.C., & Shanker, K. (2019). A new ancient lineage of frog (Anura: Nyctibatrachidae: Astrobatrachinae subfam. nov.) endemic to the Western Ghats of Peninsular India. PeerJ, 7, e6457.

Wang, X., He, Z., Shi, S., & Wu, C. I. (2020). Genes and speciation: is it time to abandon the biological species concept?. National Science Review, 7(8), 1387-1397.

Weinell, J. L., Barley, A. J., Siler, C. D., Orlov, N. L., Ananjeva, N. B., Oaks, J. R., Burbrink, F.T., & Brown, R. M. (2020). Phylogenetic relationships and biogeographic range evolution in cat-eyed snakes, Boiga (Serpentes: Colubridae). Zoological Journal of the Linnean Society, 2020, 1–16.

Welton, L. J., Siler, C. D., Oaks, J. R., Diesmos, A. C., & Brown, R. M. (2013). Multilocus phylogeny and B ayesian estimates of species boundaries reveal hidden evolutionary relationships and cryptic diversity in Southeast Asian monitor lizards. Molecular Ecology, 22(13), 3495-3510.

Wen, D., Yu, Y., Zhu, J., & Nakhleh, L. (2018). Inferring phylogenetic networks using PhyloNet. Systematic Biology, 67(4), 735-740.

Wiley, E. O. 1978. The evolutionary species concept reconsidered. Systematic Zoology 21:17–26.

Wood, P. L., Guo, X., Travers, S. L., Su, Y. C., Olson, K. V., Bauer, A. M., Grismer, L.L., Siler, C.D., Moyle, R.G., Andersen, M.J., & Brown, R. M. (2020). Parachute geckos free fall into synonymy: Gekko phylogeny, and a new subgeneric classification, inferred from thousands of ultraconserved elements. Molecular Phylogenetics and Evolution, 106731.

Ziegler, T. & Vences, M. (2020). Molecular identification of water monitors (*Varanus salvator* complex) from confiscations and the pet trade, including phylogenetic placement of *V. s. ziegleri* – a molecular reference for species conservation enforcement and conservation breeding. – Der Zoologische Garten, 88, 31-50.

Zhang, J., Kobert, K., Flouri, T., & Stamatakis, A. (2014). PEAR: a fast and accurate Illumina Paired-End reAd mergeR. Bioinformatics, 30(5), 614-620.

Figures

Fig. 1. Ancestry coefficient barplots from the sNMF analysis for *Pulchrana grandocula-similis* species complex and allied taxa of the Philippines archipelago (only K=6 presented here). An IQTree phylogeny (all markers dataset; 12626 loci) is placed to correspond with the barplot. Color coded piecharts of ancestry coefficient proportions are spatially visualized on the distribution map and labelled according to all clades and singleton taxa in the dataset (1–31).

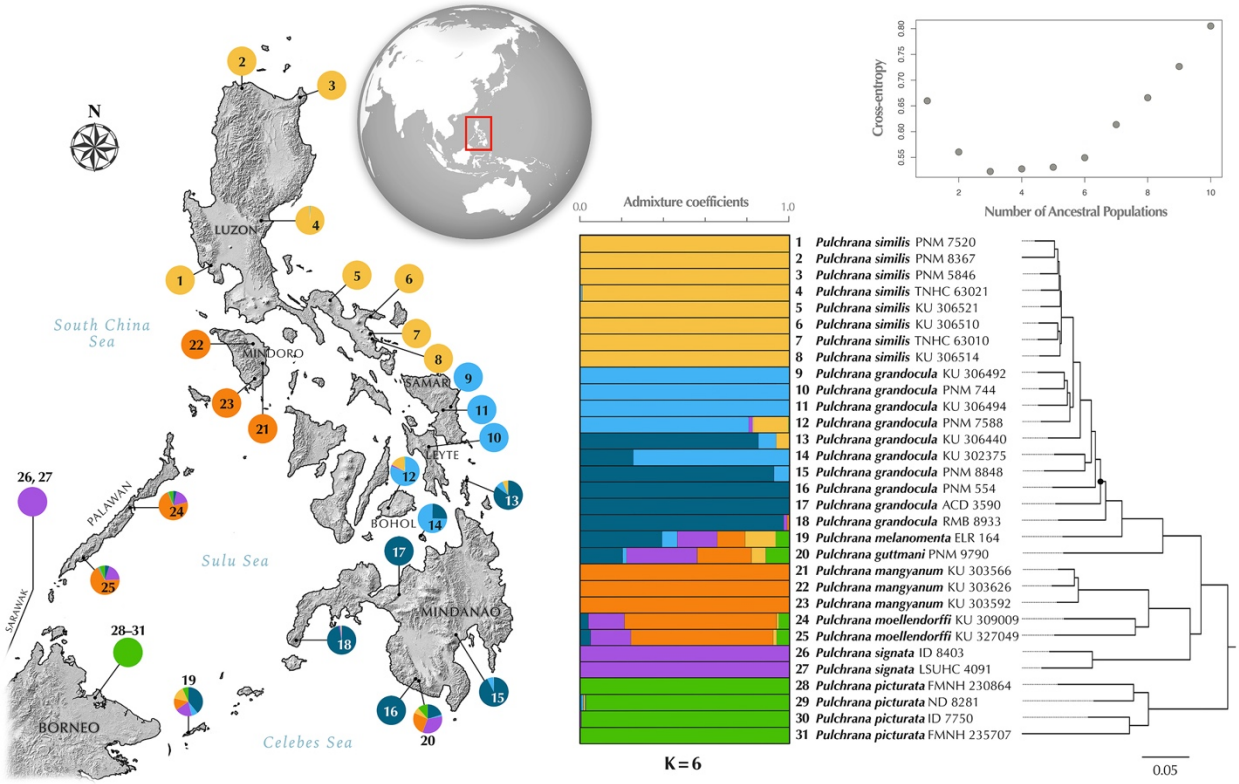

Fig. 2. Network clusters derived from NetView at k = 8 shows closely related individuals of the *Pulchrana grandocula* + *P. similis* and the *Pulchrana* clades that form the remaining species in the Philippines co-located within a cluster, and distantly related individuals are separated. Datapoints have been substituted with piecharts of ancestry coefficients from the sNMF analysis.

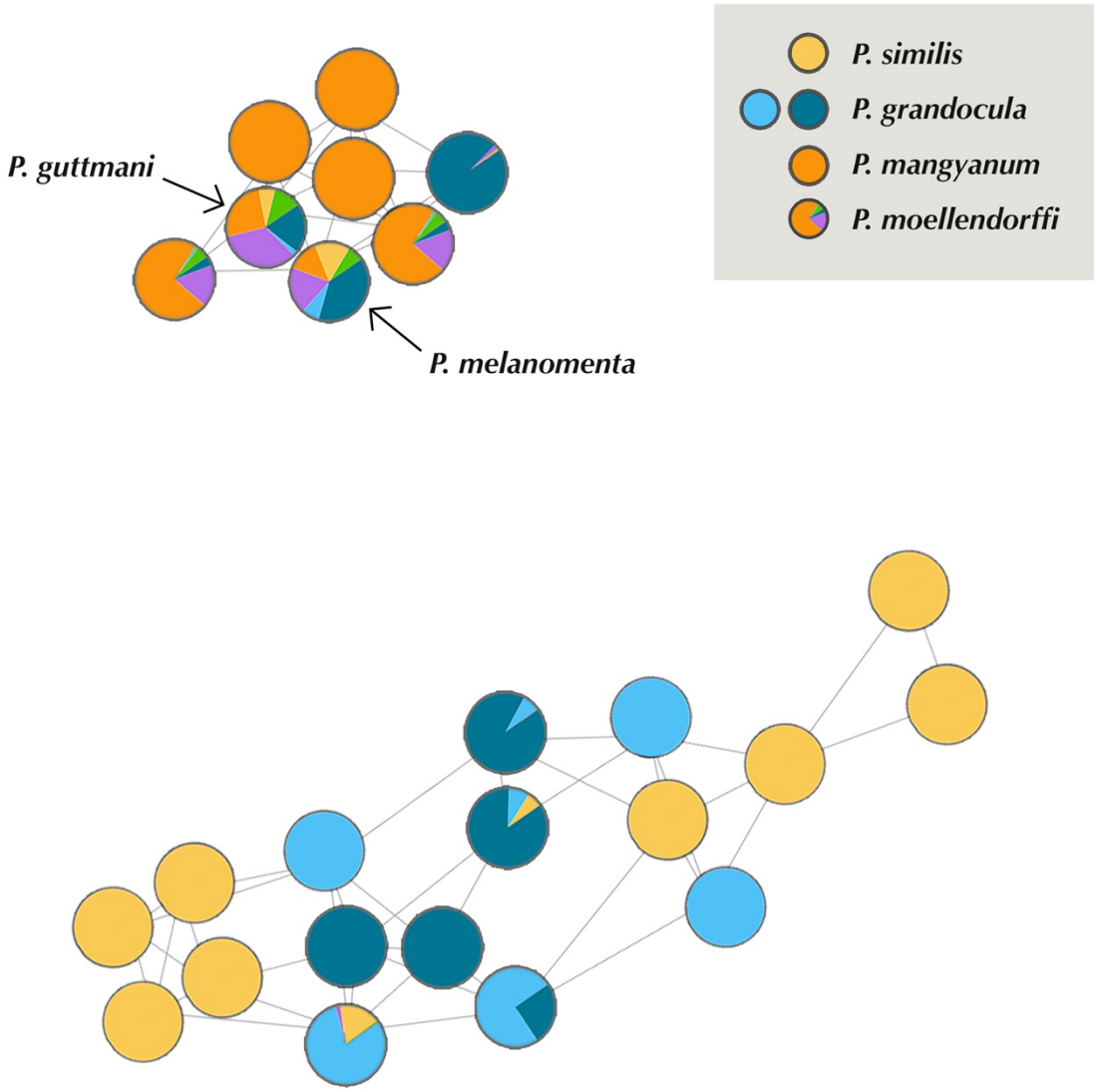

Fig. 3. Hybrid Index plots of the *Pulchrana grandocula–P. similis* species complex. The *Pulchrana grandocula* population of Mindanao (light & dark blue) and *P. similis* of Luzon (yellow) were selected as putative parentals based on inferred relatively slight- to non-admixed populations, across the sNMF and NetView analyses.

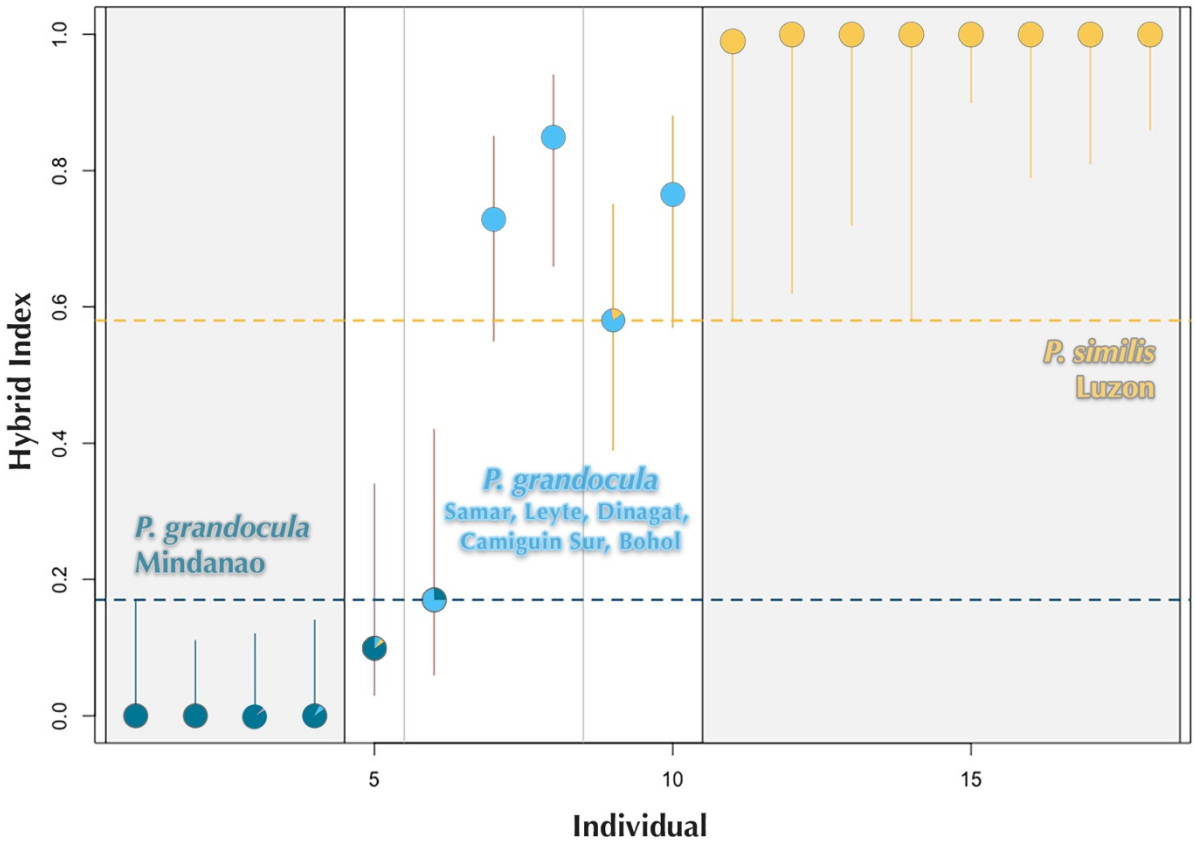

Fig. 4. Optimal species network for the *Pulchrana* group with four reticulation events inferred using Maximum Pseudo-likelihood Inference from 7,416 exon-derived gene trees.

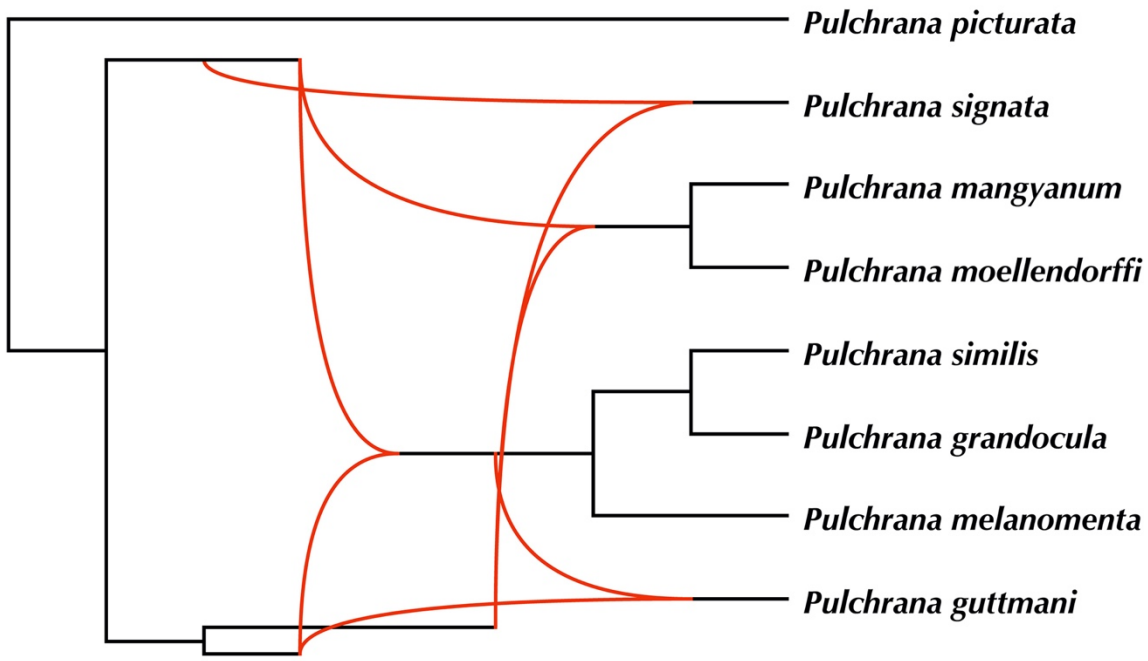

Table 1. List of taxa, samples, and populations included in this study.

Sample ID	Field No.	Catalog No.	Locality
Ingroup			
Pulchrana grandocula	Genetic sample only	ACD 3590	Mindanao, Lanao del Sur
Pulchrana grandocula	CDS 075	KU 302375	Camiguin Sur Island
Pulchrana grandocula	CDS 1833	KU 306494	Eastern Samar Province
Pulchrana grandocula	CDS 1918	KU 306440	Dinagat Island Province
Pulchrana grandocula	CDS 1806	KU 306492	Samar Province
Pulchrana grandocula	PNM/CMNH H 1630	PNM 554	Mindanao, Sarangani
Pulchrana grandocula	NA	PNM 744	Leyte
Pulchrana grandocula	RMB 2842	PNM 7588	Bohol Province
Pulchrana grandocula	RMB 3787	PNM 8848	Mindanao, Davao City
Pulchrana grandocula	NA	RMB 8933	Mindanao
Pulchrana similis	CDS 2078	KU 306510	Camarines Sur
Pulchrana similis	CDS 2112	KU 306514	Camarines Sur
Pulchrana similis	CDS 2162	KU 306521	Camarines del Norte
Pulchrana similis	RMB 812	PNM 5846	Aurora Province
Pulchrana similis	RMB 4254	PNM 7520	Cagayan Province
Pulchrana similis	GVAG 361	PNM 8367	Cagayan Province
Pulchrana similis	RMB 3532	TNHC 63010	Albay Province
Pulchrana similis	RMB 4501	TNHC 63021	Zambalaes Province
Pulchrana guttmani	PNM/CMNH H 1736	PNM 9790	Mindanao, Sarangani
Pulchrana melanomenta	Deposited at PNM	ELR 164	Tawi-tawi Province
Pulchrana mangyanum	RMB 4964	KU 303566	Mindoro
Pulchrana mangyanum	RMB 4860	KU 303592	Mindoro
Pulchrana mangyanum	NA	KU 303626	Mindoro
Pulchrana moellendorffi	RMB 7419	KU 309009	Palawan
Pulchrana moellendorffi	ACD 1277	KU 327049	Palawan
Outgroup			
Pulchrana signata	NA	ID 8403	Matang, Sarawak, Borneo
Pulchrana signata	NA	LSUHC 4091	Lambir Hills, Sarawak, Borneo
Pulchrana picturata	NA	ID 7750	Mount Kinabalu, Sabah, Borneo
Pulchrana picturata	NA	ND 8281	Sungai Tawau, Sabah, Borneo
Pulchrana picturata	NA	FMNH 230864	Lahad Datu, Sabah, Borneo
Pulchrana picturata	NA	FMNH 235707	Kota Marudu, Sabah, Borneo

Table 2. Summaries for datasets analyzed in this study (PIS = parsimony informative sites; MBP = Missing Basepairs; Loci-combined = exons from the same gene concatenated together).

Dataset	Total markers	Basepairs	Prop. of Samples	Total PIS	Prop. of PIS	MBP	Prop. of MBP
Legacy	28	680	0.9644	36921	0.0169	1678	0.0385
Loci-combined	2188	1370469	0.9735	30767	0.0220	1661	0.1088
All markers	12626	7861192	0.8646	449916	0.0577	926	00.0577
Exon	11974	5222748	0.8637	63229	0.0225	44	0.0028
Intron	11950	6635118	0.8619	523523	0.0790	1032	0.0704

Table 3. Results of HyDe analysis at the individual level. P-values <0.05 indicate significant levels of hybridization.

P1	Hybrid	P2	Zscore	Pvalue	Gamma
grand2	Pulchrana_grandocula_PNM_7588	grand1	1.4387	0.0751	**0.0134**
grand2	Pulchrana_grandocula_KU_306494	similis	3.7461	0.0001	**0.0404**
grand2	Pulchrana_grandocula_KU306440	grand1	3.5914	0.0002	**0.0514**
grand2	Pulchrana_grandocula_PNM_744	similis	5.7695	0.0000	**0.0596**
grand2	Pulchrana_grandocula_PNM_7588	similis	6.2964	0.0000	**0.0653**
grand2	Pulchrana_grandocula_KU306492	similis	6.8010	0.0000	**0.0705**
grand2	Pulchrana_grandocula_KU306440	similis	8.3205	0.0000	0.1335
Hyb1	Pulchrana_grandocula_KU_306494	similis	9.6164	0.0000	0.2216
Hyb1	Pulchrana_grandocula_PNM_744	similis	12.5430	0.0000	0.2662
Hyb1	Pulchrana_grandocula_KU306492	similis	12.7931	0.0000	0.2797
melano	Pulchrana_mangyanum_KU_303592	signata	14.8447	0.0000	0.4253
grand2	Pulchrana_grandocula_KU_302375	grand1	11.1244	0.0000	0.4375
melano	Pulchrana_mangyanum_KU_303566	signata	15.8971	0.0000	0.4387
melano	Pulchrana_mangyanum_KU_303626	signata	15.6771	0.0000	0.4500
grand1	Pulchrana_mangyanum_KU_303592	signata	15.6390	0.0000	0.4522
grand2	Pulchrana_mangyanum_KU_303592	signata	15.2989	0.0000	0.4571
Hyb1	Pulchrana_mangyanum_KU_303592	signata	15.9632	0.0000	0.4618
grand1	Pulchrana_mangyanum_KU_303566	signata	16.5269	0.0000	0.4657
grand1	Pulchrana_mangyanum_KU_303626	signata	15.9490	0.0000	0.4662
grand2	Pulchrana_mangyanum_KU_303566	signata	16.1135	0.0000	0.4668

guttman	Pulchrana_mangyanum_KU_303566	signata	14.7209	0.0000	0.4676
melano	Pulchrana_moellendorffi_KU_309009	signata	15.0230	0.0000	0.4690
grand2	Pulchrana_mangyanum_KU_303626	signata	15.7197	0.0000	0.4699
guttman	Pulchrana_mangyanum_KU_303592	signata	14.9436	0.0000	0.4706
Hyb1	Pulchrana_mangyanum_KU_303566	signata	16.8171	0.0000	0.4720
Hyb1	Pulchrana_mangyanum_KU_303626	signata	16.5017	0.0000	0.4730
guttman	Pulchrana_moellendorffi_KU_327049	signata	13.9738	0.0000	0.4745
guttman	Pulchrana_mangyanum_KU_303626	signata	14.3547	0.0000	0.4748
melano	Pulchrana_moellendorffi_KU_327049	signata	15.5874	0.0000	0.4818
grand1	Pulchrana_moellendorffi_KU_309009	signata	15.5685	0.0000	0.4834
guttman	Pulchrana_moellendorffi_KU_309009	signata	13.9123	0.0000	0.4849
grand1	Pulchrana_moellendorffi_KU_327049	signata	15.5190	0.0000	0.4872
grand2	Pulchrana_moellendorffi_KU_327049	signata	15.4794	0.0000	0.4915
Hyb1	Pulchrana_moellendorffi_KU_327049	signata	15.9554	0.0000	0.4928
grand2	Pulchrana_moellendorffi_KU_309009	signata	15.4633	0.0000	0.4937
Hyb1	Pulchrana_moellendorffi_KU_309009	signata	15.5069	0.0000	0.4981
signata	Pulchrana_moellendorffi_KU_309009	similis	15.0393	0.0000	0.5063
signata	Pulchrana_moellendorffi_KU_327049	similis	15.2898	0.0000	0.5075
signata	Pulchrana_mangyanum_KU_303626	similis	15.7254	0.0000	0.5278
signata	Pulchrana_mangyanum_KU_303566	similis	16.1560	0.0000	0.5300
signata	Pulchrana_mangyanum_KU_303592	similis	15.2487	0.0000	0.5411
grand2	Pulchrana_grandocula_KU_302375	similis	11.8859	0.0000	0.5497

Table 4. Results of HyDe analysis at the group level. P-values <0.05 indicate significant levels of hybridization.

P1	Hybrid	P2	Zscore	Pvalue	Gamma
Hyb1	similis	grand1	-99999.9000	1.0000	-1.1147
mangy	signata	melano	-3.4102	0.9997	-0.3936
grand2	similis	Hyb1	-99999.9000	1.0000	-0.3752
mangy	signata	similis	-1.9368	0.9736	-0.1636
grand2	grand1	Hyb1	-99999.9000	1.0000	-0.1362
grand2	similis	grand1	-99999.9000	1.0000	-0.0687
moell	signata	similis	-0.4135	0.6604	-0.0288
guttman	moell	mangy	-99999.9000	1.0000	-0.0072
moell	melano	similis	-99999.9000	1.0000	-0.0035
signata	melano	similis	-99999.9000	1.0000	-0.0022
mangy	melano	similis	-99999.9000	1.0000	-0.0022
moell	guttman	similis	-99999.9000	1.0000	-0.0021
guttman	grand1	melano	-99999.9000	1.0000	-0.0018
signata	grand2	similis	-99999.9000	1.0000	-0.0016
melano	mangy	moell	-99999.9000	1.0000	-0.0015
guttman	melano	similis	-99999.9000	1.0000	-0.0014
guttman	grand2	similis	-99999.9000	1.0000	-0.0012
signata	grand1	similis	-99999.9000	1.0000	-0.0011
Hyb1	mangy	moell	-99999.9000	1.0000	-0.0009
moell	grand1	similis	-99999.9000	1.0000	-0.0008

moell	grand2	similis	-99999.9000	1.0000	-0.0008
signata	Hyb1	similis	-99999.9000	1.0000	-0.0006
grand1	moell	mangy	-99999.9000	1.0000	-0.0006
mangy	grand2	similis	-99999.9000	1.0000	-0.0006
guttman	grand2	melano	-99999.9000	1.0000	-0.0004
melano	grand1	similis	-99999.9000	1.0000	-0.0002
grand2	mangy	moell	-99999.9000	1.0000	-0.0001
guttman	grand1	similis	-99999.9000	1.0000	-0.0001
mangy	grand1	similis	-99999.9000	1.0000	0.0000
grand2	moell	mangy	0.0287	0.4886	0.0001
grand1	mangy	moell	0.1470	0.4416	0.0006
Hyb1	moell	mangy	0.2085	0.4174	0.0009
guttman	Hyb1	similis	0.6785	0.2487	0.0013
guttman	similis	melano	0.3346	0.3690	0.0014
mangy	Hyb1	similis	1.4285	0.0766	0.0016
guttman	Hyb1	melano	0.4610	0.3224	0.0019
mangy	similis	melano	1.1006	0.1355	0.0022
mangy	grand2	melano	1.1121	0.1331	0.0022
moell	Hyb1	similis	2.0511	0.0201	0.0023
mangy	grand1	melano	1.3345	0.0910	0.0026
mangy	Hyb1	melano	1.7276	0.0420	0.0034
guttman	mangy	moell	1.6744	0.0470	0.0071
signata	guttman	similis	1.8642	0.0311	0.0092

mangy	guttman	similis	1.9607	0.0250	0.0106
melano	Hyb1	similis	1.8964	0.0290	0.0132
mangy	guttman	melano	2.7758	0.0028	0.0153
melano	grand2	similis	1.2481	0.1060	0.0163
moell	Hyb1	signata	-0.2937	0.6155	0.0180
moell	similis	signata	-0.4251	0.6646	0.0265
moell	grand2	signata	-0.4649	0.6790	0.0283
moell	grand1	signata	-0.9381	0.8259	0.0539
grand2	grand1	similis	5.4311	0.0000	0.0570
moell	guttman	signata	-1.1826	0.8815	0.0725
moell	melano	signata	-1.5721	0.9420	0.0852
grand2	Hyb1	grand1	6.0890	0.0000	0.0967
mangy	guttman	signata	-1.8092	0.9648	0.0989
mangy	Hyb1	signata	-2.1714	0.9851	0.1045
mangy	similis	signata	-2.2090	0.9864	0.1097
mangy	grand2	signata	-2.3902	0.9916	0.1166
mangy	grand1	signata	-2.6807	0.9963	0.1252
grand2	Hyb1	similis	10.4212	0.0000	0.1765
mangy	melano	signata	-4.3733	1.0000	0.1805
Hyb1	grand1	similis	11.6665	0.0000	0.2566
grand1	Hyb1	similis	-22.1328	1.0000	0.3957
melano	mangy	signata	15.4854	0.0000	0.4381
Hyb1	grand2	similis	-38.1963	1.0000	0.4400

grand1	mangy	signata	16.0448	0.0000	0.4615
grand2	mangy	signata	15.7154	0.0000	0.4647
Hyb1	mangy	signata	16.4317	0.0000	0.4690
guttman	mangy	signata	14.6749	0.0000	0.4710
Hyb1	grand2	grand1	-50.8084	1.0000	0.4717
melano	moell	signata	15.3121	0.0000	0.4756
guttman	moell	signata	13.9460	0.0000	0.4797
grand1	grand2	similis	-84.4852	1.0000	0.4844
grand1	moell	signata	15.5435	0.0000	0.4854
grand2	moell	signata	15.4712	0.0000	0.4926
Hyb1	moell	signata	15.7332	0.0000	0.4954
grand2	melano	grand1	-82.3936	1.0000	0.4956
grand2	melano	similis	-74.1235	1.0000	0.4958
guttman	mangy	melano	-176.0184	1.0000	0.4961
Hyb1	melano	grand1	-161.4755	1.0000	0.4961
Hyb1	melano	similis	-139.9821	1.0000	0.4966
mangy	signata	moell	-218.2706	1.0000	0.4973
guttman	mangy	similis	-180.8997	1.0000	0.4973
guttman	signata	melano	-193.8909	1.0000	0.4975
guttman	signata	similis	-199.2651	1.0000	0.4977
mangy	guttman	moell	-233.1639	1.0000	0.4982
Hyb1	moell	melano	-516.9903	1.0000	0.4985
Hyb1	moell	guttman	-183.6930	1.0000	0.4985

Hyb1	moell	grand1	-933.3084	1.0000	0.4991
Hyb1	mangy	melano	-508.7568	1.0000	0.4992
grand1	mangy	melano	-511.5291	1.0000	0.4993
grand1	moell	melano	-517.0483	1.0000	0.4994
Hyb1	moell	similis	-875.3935	1.0000	0.4994
grand2	mangy	melano	-507.5981	1.0000	0.4995
Hyb1	guttman	melano	-236.9147	1.0000	0.4995
grand2	moell	guttman	-182.4089	1.0000	0.4996
guttman	moell	melano	-179.3629	1.0000	0.4996
grand2	moell	melano	-509.9760	1.0000	0.4996
Hyb1	mangy	similis	-864.7555	1.0000	0.4996
Hyb1	mangy	grand1	-919.8553	1.0000	0.4996
Hyb1	guttman	similis	-502.7819	1.0000	0.4997
grand1	signata	melano	-531.1736	1.0000	0.4997
Hyb1	guttman	grand1	-544.5183	1.0000	0.4997
mangy	grand1	moell	-234.9070	1.0000	0.4998
Hyb1	signata	melano	-525.0919	1.0000	0.4999
Hyb1	signata	grand1	-935.9126	1.0000	0.4999
grand2	guttman	grand1	-394.8737	1.0000	0.4999
grand2	moell	grand1	-727.4599	1.0000	0.4999
grand2	signata	melano	-522.3870	1.0000	0.5000
grand1	mangy	similis	-994.8770	1.0000	0.5000
grand1	guttman	similis	-606.8734	1.0000	0.5000

mangy	grand2	moell	-230.9242	1.0000	0.5000
grand1	melano	similis	-204.2988	1.0000	0.5000
grand2	guttman	melano	-236.8957	1.0000	0.5001
grand2	signata	grand1	-734.3863	1.0000	0.5001
grand2	mangy	similis	-695.8518	1.0000	0.5002
Hyb1	signata	similis	-874.5363	1.0000	0.5002
grand2	mangy	grand1	-722.6213	1.0000	0.5002
grand2	moell	similis	-700.1455	1.0000	0.5002
grand1	moell	similis	-1010.4364	1.0000	0.5002
mangy	similis	moell	-232.1122	1.0000	0.5002
mangy	Hyb1	moell	-233.3518	1.0000	0.5002
grand1	signata	similis	-1002.5000	1.0000	0.5003
grand2	signata	Hyb1	-739.1476	1.0000	0.5003
grand2	guttman	similis	-375.0666	1.0000	0.5003
grand1	moell	guttman	-184.4483	1.0000	0.5003
melano	guttman	similis	-235.3670	1.0000	0.5004
mangy	melano	moell	-231.6595	1.0000	0.5004
grand2	signata	similis	-703.1532	1.0000	0.5004
grand1	guttman	melano	-240.2549	1.0000	0.5004
guttman	moell	similis	-183.3639	1.0000	0.5005
grand2	mangy	Hyb1	-727.9133	1.0000	0.5005
melano	mangy	similis	-507.2929	1.0000	0.5005
melano	signata	similis	-522.8817	1.0000	0.5005

grand2	guttman	Hyb1	-400.7028	1.0000	0.5006
melano	moell	similis	-510.8671	1.0000	0.5009
grand2	moell	Hyb1	-736.1305	1.0000	0.5009
grand2	melano	Hyb1	-85.5574	1.0000	0.5013
Hyb1	mangy	guttman	-181.2696	1.0000	0.5024
grand2	mangy	guttman	-181.2987	1.0000	0.5024
grand1	mangy	guttman	-181.9091	1.0000	0.5029
Hyb1	signata	guttman	-199.0710	1.0000	0.5029
grand1	signata	guttman	-199.5865	1.0000	0.5031
grand2	signata	guttman	-197.4601	1.0000	0.5036
signata	moell	similis	15.1651	0.0000	0.5069
signata	mangy	similis	15.7154	0.0000	0.5328
grand1	grand2	melano	1.4610	0.0720	0.9829
grand1	Hyb1	melano	2.5110	0.0060	0.9849
grand2	guttman	signata	2.8857	0.0020	0.9858
grand1	guttman	signata	2.5231	0.0058	0.9877
Hyb1	guttman	signata	2.3549	0.0093	0.9884
grand1	guttman	mangy	2.0982	0.0179	0.9887
moell	mangy	signata	2.3895	0.0084	0.9893
melano	guttman	signata	1.9404	0.0262	0.9902
grand2	guttman	mangy	1.7838	0.0372	0.9904
Hyb1	guttman	mangy	1.7201	0.0427	0.9907
melano	Hyb1	moell	3.2102	0.0007	0.9939

guttman	Hyb1	moell	1.0874	0.1384	0.9941
grand2	Hyb1	melano	0.4538	0.3250	0.9948
grand2	Hyb1	moell	2.5952	0.0047	0.9965
melano	similis	moell	1.7871	0.0370	0.9965
grand1	Hyb1	moell	3.2364	0.0006	0.9966
melano	grand1	moell	1.3108	0.0950	0.9975
grand2	Hyb1	guttman	0.9428	0.1729	0.9977
melano	similis	signata	1.1475	0.1256	0.9978
grand2	Hyb1	mangy	1.5604	0.0593	0.9979
guttman	similis	moell	0.3918	0.3476	0.9979
grand1	melano	guttman	0.4283	0.3342	0.9982
guttman	grand2	moell	0.3156	0.3761	0.9983
melano	guttman	moell	0.2977	0.3830	0.9983
melano	grand2	moell	0.8461	0.1987	0.9983
grand2	similis	signata	1.1502	0.1250	0.9984
grand1	Hyb1	mangy	1.4226	0.0774	0.9985
mangy	moell	melano	0.3526	0.3622	0.9985
melano	grand1	signata	0.7107	0.2386	0.9987
grand1	guttman	moell	0.2346	0.4072	0.9987
grand1	Hyb1	guttman	0.6669	0.2524	0.9988
grand2	similis	guttman	0.4550	0.3245	0.9988
grand2	Hyb1	signata	0.8791	0.1897	0.9988
grand1	similis	signata	1.1459	0.1259	0.9989

mangy	moell	similis	0.1862	0.4261	0.9992
grand1	similis	moell	0.8035	0.2108	0.9992
grand2	similis	moell	0.5542	0.2897	0.9992
grand2	grand1	mangy	0.5267	0.2992	0.9993
Hyb1	similis	signata	0.5653	0.2859	0.9994
grand2	similis	mangy	0.4235	0.3360	0.9994
grand2	grand1	signata	0.3905	0.3481	0.9995
melano	Hyb1	signata	0.2413	0.4047	0.9995
grand2	melano	guttman	0.0913	0.4636	0.9996
grand1	Hyb1	signata	0.3396	0.3671	0.9996
grand1	grand2	guttman	0.1307	0.4480	0.9997
grand1	grand2	moell	0.1521	0.4396	0.9998
melano	grand2	signata	0.0935	0.4627	0.9998
grand1	similis	melano	0.0343	0.4863	0.9998
grand1	similis	guttman	0.0426	0.4830	0.9999
grand1	similis	mangy	0.0362	0.4856	1.0000
grand2	melano	signata	-0.0935	0.5373	1.0002
grand2	grand1	moell	-0.1520	0.5604	1.0002
grand2	grand1	guttman	-0.1307	0.5520	1.0003
Hyb1	grand1	signata	-0.3395	0.6329	1.0004
Hyb1	melano	signata	-0.2411	0.5953	1.0005
grand1	grand2	signata	-0.3903	0.6519	1.0005
grand1	grand2	mangy	-0.5263	0.7007	1.0007

moell	mangy	similis	-0.1861	0.5738	1.0008
Hyb1	grand2	signata	-0.8780	0.8100	1.0012
Hyb1	grand1	guttman	-0.6661	0.7473	1.0012
guttman	grand1	moell	-0.2343	0.5926	1.0013
grand1	melano	signata	-0.7098	0.7611	1.0013
Hyb1	similis	guttman	-0.6776	0.7510	1.0014
Hyb1	grand1	mangy	-1.4204	0.9223	1.0015
Hyb1	similis	mangy	-1.4261	0.9231	1.0017
grand2	melano	moell	-0.8447	0.8009	1.0017
guttman	melano	moell	-0.2972	0.6168	1.0017
grand2	guttman	moell	-0.3151	0.6236	1.0017
Hyb1	melano	guttman	-0.4601	0.6773	1.0019
Hyb1	grand2	mangy	-1.5571	0.9403	1.0021
grand2	melano	mangy	-1.1096	0.8664	1.0022
Hyb1	similis	moell	-2.0463	0.9796	1.0023
Hyb1	grand2	guttman	-0.9405	0.8265	1.0024
grand1	melano	moell	-1.3075	0.9045	1.0025
grand1	melano	mangy	-1.3310	0.9084	1.0026
Hyb1	melano	mangy	-1.7218	0.9574	1.0034
Hyb1	grand1	moell	-3.2252	0.9994	1.0035
Hyb1	grand2	moell	-2.5860	0.9951	1.0035
Hyb1	grand2	melano	-0.4514	0.6741	1.0053
Hyb1	guttman	moell	-1.0810	0.8601	1.0060

Hyb1	melano	moell	-3.1904	0.9993	1.0062
guttman	similis	signata	-1.8469	0.9676	1.0094
guttman	Hyb1	mangy	-1.7039	0.9558	1.0096
guttman	grand2	mangy	-1.7664	0.9613	1.0099
guttman	melano	signata	-1.9212	0.9726	1.0101
guttman	similis	mangy	-1.9397	0.9738	1.0110
mangy	moell	signata	-2.3636	0.9910	1.0111
guttman	grand1	mangy	-2.0742	0.9810	1.0117
guttman	Hyb1	signata	-2.3273	0.9900	1.0120
guttman	grand1	signata	-2.4916	0.9936	1.0128
Hyb1	similis	melano	-1.8710	0.9693	1.0137
guttman	grand2	signata	-2.8441	0.9978	1.0148
Hyb1	grand1	melano	-2.4726	0.9933	1.0158
guttman	melano	mangy	-2.7327	0.9969	1.0160
grand2	similis	melano	-1.2274	0.8902	1.0171
grand2	grand1	melano	-1.4356	0.9244	1.0181
Hyb1	signata	moell	-99999.9000	1.0000	1.0190
grand2	signata	moell	-99999.9000	1.0000	1.0310
grand1	signata	moell	-99999.9000	1.0000	1.0642
guttman	signata	moell	-99999.9000	1.0000	1.0927
melano	signata	moell	-99999.9000	1.0000	1.1144
guttman	signata	mangy	-99999.9000	1.0000	1.1406
Hyb1	signata	mangy	-99999.9000	1.0000	1.1523

grand2	signata	mangy	-99999.9000	1.0000	1.1794
grand1	signata	mangy	-99999.9000	1.0000	1.2006

CHAPTER 5

Revisiting the Non-African Ranoidea frog phylogeny (Amphibia: Anura: Neobatrachia) with the genomic inclusion of all Paleoendemic Indian ranoid taxa

Robin Kurian Abraham & Rafe M. Brown

Abstract

With the advent of genetic and genomic methods in biology, hypotheses pertaining to amphibian relationships and biogeography gained great strides. Of particular interest is the group Ranoidea, which accounts for almost 30% of global frog diversity, whose center of diversity is the African-Eurasian region. The Indian paleoendemic ranoid families of Nyctibatrachidae, Ranixalidae and Micrixalidae have always had a contentious status in most global phylogenies, with little agreement between studies regarding their relationships to one another and with the remaining 15 ranoid families. In this study, we reinvestigate the relationships of these three Indian paleoendemic ranoid families with the help of unprecedented genomic data, along with testing biogeographical hypothesis pertaining to their evolutionary history. Our results recover for the first time, with robust support, a monophyletic, Indian subcontinent-wide ancient in-situ radiation comprising these three families. Our preliminary biogeography results based on this dataset support of a "ferry India" model that has been postulated in the past to suggest and insular interval for the migrating Indian plate from Gondwana to Eurasia.

Introduction

Since the time of land colonization (Brown, 2016), amphibians have been among the most successful and diverse groups of land vertebrates—culminating now in over 8000 described

species (AmphibiaWeb, 2020; Frost, 2020). Having survived multiple mass extinction events, amphibians have coexisted with the more aridity-tolerant, physiologically adaptable amniotes, despite their close affinity with the aquatic realm (Duellman & Trueb, 1994; Wells, 2010). With their biology requiring essentially moist and cool ambient conditions, amphibians (anurans [frogs, toads], salamanders, and caecilians) lead largely secretive lives, with anurans being predominantly nocturnal, terrestrial surface dwellers, and limbless caecilians largely fossorial (Duellman & Trueb, 1994; Wells, 2010). The Anura are the largest and most successful of the three orders of amphibians forming 88% of contemporary amphibian diversity (AmphibiaWeb, 2020). That is, until recently (Blaustein & Wake, 1990), when rapidly changing anthropogenic climate change (Stuart et al., 2004; Pounds et al., 2007), ecological disturbance, habitat destruction (Rowley et al 2010), invading pathogens and invasive species, and emerging infectious disease (Kriger & Hero, 2007; O'Hanlon et al., 2018) accelerated declines in frog populations the world over (Berridge et al., 2008; Byrne et al., 2019; Jetz & Pyron, 2018; Roelants et al., 2007; Zamudio et al., 2020). A refined understanding of the evolutionary history of these organisms is thus a vital step for illuminating the capacity, and limits, of these lineages, which historically persisted through catastrophic environmental changes throughout much of their evolutionary history—but now are facing mass extinction on an unprecedented scale (Gonzales et al., 2019).

Over the last 20 years, global amphibian phylogenies have aimed to address various questions, from intergroup relationships, to diversification rates, to identifying incomplete lineage sorting in deep lineages (Frost et al., 2006; Hime et al., 2020; Roelants et al., 2007; Scott, 2005). The first large-scale phylogenies over this period of the last two decades sought to estimate anuran relationships based on affinities from molecular phylogenetic analyses; these

radically destabilized taxonomy (Frost et al., 2006; Wiens, 2007); in hindsight, the analytical, methodological, and interpretation (classification) errors committed in these works were likely exacerbated by being their based on few loci, at a time when unsophisticated phylogenetic methods were still in use. Although some of subsequent reanalyzes arrived at relatively accurate (now widely accepted) topological relationships towards the tips of the tree (recent, shallow relationships), by today's standard they were nevertheless inadequate for resolving with confidence (and strong nodal support) the higher-level relationships (ancient, deep divergences and basal branching order), especially at familial levels. Amphibian family-level relationships have since varied from study to study, with interpretations focusing on causes relating to difference in number of genes included, and statistical phylogenetic inference procedures used (Feng et al., 2017; Frost et al., 2006; Hedges et al., 2015; Marjanović & Laurin, 2007; Moen et al., 2016; Pyron, 2011; Pyron & Wiens, 2011; Roelants et al., 2007; Streicher & Wiens, 2017). The most recent results of studies including more than just a handful of Sanger loci, however, have been begun to arrive at a phylogenetic consensus (review: AmphibiaWeb, 2020). And with the arrival of genomic resources and powerful phylogenomic methods of model-based phylogenetic inference, resolved phylogenetic estimates are now supported with traditional node-based measure of branch support (Yuan et al., 2018; Feng et al 2017) and novel insight into levels of gene tree incongruence at key nodes of interest (Hime et al., 2020; Hutter et al 2019).

Of the two or three traditionally-hypothesized clades of Anura, (a most 'primitive' Archaeobatrachia; a more 'advanced' group of frogs, the Neobatrachia), the latter has consistently been recognized as more phylogenetically diverse and species rich; today, estimates recognize that neobatrachians make up 95% of global anuran diversity (AmphibiaWeb, 2020; Hime et al., 2020). Within Neobatrachia, two superfamilies, Ranoidea and Hylodiea dominate in

terms of sheer numbers of representative taxa (Frost, 2020). Ranoidea predominantly is an old-world clade, in terms of the distribution of contained taxa; sub-Saharan Africa, Eurasia, Southeast Asia, and Oceania are noteworthy geographic centers of diversity (Bossyut et al., 2006; Wiens et al., 2007; Portik &Blackburn, 2016; AmphibiaWeb, 2020; Frost, 2020; Wiens et al., 2009). The constituent ranoid families recognized today include: Arthroleptidae, Brevicepitidae, Ceratobatrachidae, Conrauidae, Dicroglossidae, Hemisotidae, Hyperoliidae, Mantellidae, Micrixalidae, Nyctibatrachidae, Odontobatrachidae, Petropedetidae, Phrynobatrachidae, Ptychadenidae, Pyxicephalidae, Ranidae, Ranixalidae and Rhacophoridae (AmphibiaWeb, 2020; Frost, 2020; Hime et al., 2020).

Three ranoid families Micrixalidae, Nyctibatrachidae, and Ranixalidae true "paleoendemic" lineages (Stebbins & Major, 1965), presumed anciently-derived, and entirely restricted to the Indian subcontinent. These enigmatic, understudied, and misunderstood, exclusively Indian clades have been frought with instability, with variable, contradictory relationships depicted molecular phylogenies (Bossuyt & Milinkovitch, 2000, 2001; Bossuyt et al., 2006; Feng et al., 2017; Pyron & Wiens, 2011; Roelants, Jiang & Bossuyt, 2004; Roelants et al., 2007). The earliest phylogenies featuring these Indian paleoendemic families, with the exception of African ranoids depicted a polyphyletic arrangement of India's three paleoendemic clades of frogs (Bossuyt & Milinkovitch, 2000, 2001; Roelants, Jiang & Bossuyt, 2004). A subsequent phylogeny (using two mitochondrial sequence fragments and three nuclear genes) estimated by Bossuyt et al. (2006) included African and Asian ranoids and found Micrixalidae + Ranixalidae to be monophyletic sister clades and formed the outermost branch of the non-African ranoids, but Nyctibatrachidae was nested in a pectinate relationship between Ceratobatrachidae and Ranidae + Dicroglossidae + Mantellidae + Rhacophoridae (Supp. Fig. 1). Roelants et al (2007),

using a single mitochondrial gene region and four nuclear genes, depicted Micrixalidae and Nyctibatrachidae to be monophyletic sister clades, but Ranixalidae fell outside the remaining ranoid taxa (Supp. Fig. 2). Pyron & Wiens (2011)'s 12-marker (9 nuclear genes + 3 mitochondrial fragments) phylogeny recovered all three Indian paleoendemic taxa as polyphyletic (Nyctibatrachidae sister to Ceratobatrachidae; Ranixalidae sister to Dicroglossidae; and Micrixalidae sister to a large unresolved clade of these taxa and numerous others (Supp. Fig. 3). The shortcoming plaguing all these analyses was a lack of strong support for the placement of Indian's three paleoendemic frog families.

Feng et al. (2017), using a novel set of ~100 genes, performed a phylogenomic analysis, that found strong support for Ranixalidae and Micrixalidae as sister clades; Nyctibatrachidae was recovered sister to Ranidae (Fig. 4). Jetz & Pyron (2018), using a 11-locus Sanger dataset, found Ranixalidae sister to Dicroglossidae, Nyctibatrachidae sister to Ceratobatrachidae, and Micrixalidae sister to Petropedetidae (Supp. Fig. 5). Yuan et al. (2018), recently performed a phylogenomic analysis of several hundred loci for ranoids, in which they inferred Ranixalidae and Nyctibatrachidae to be sister (Micrixalidae was not included; Supp. Fig. 6). Finally, the most recent phylogeny by Hime et al. (2020) included only Nyctibatrachidae, but found strong support for a sister relationship with Ceratobatrachidae (Supp. Fig. 7).

The power of genomic data, inferred from across the amphibian tree of life, is unambiguously evident and widely-recognized today (AmphibiaWeb2020). Phylogenies estimated from datasets with robust gene- and taxon sampling are necessary for resolving relationships, inferring divergence times, and providing strongly-supported, credible tree topologies (with legitimate branch lengths) are crucial for all down-stream phylogenetic comparative methods, ancestral reconstructions, and quantitative biogeographical inference

(citations). Given the challenges in acquiring densely sampled genomic datasets for amphibian families with multi-continental distributions, recent phylogenomic undertakings have begun 'closing the gap' with respect to previous, sparsely-sampled (gene, and taxon sampling) analyses of the past 20 years (Hime et al., 2020; Hutter et al. 2019; Yuan et al., 2020). Achieving sampling for all recognized families of Ranoidea has been, until now, largely impossible for advances phylogenomic studies. This is because genetic resources (tissue samples) representing Indian paleoendemics families were not widely available in biodiversity repositories (tissues controlled by few individual researchers), combined with proprietary control over the first generation of genomic sequence resources (probesets and analysis pipelines not placed in the public domain). Finally, until this study, exemplar tissue samples for the family Micrixalidae been unavailable. In this project we include for the first time, all the three paleoendemic Indian ranoid families (Ranixalidae, Micrixalidae and Nyctibatrachidae, all sampled by us, from known localities and vouchered specimens). Additionally, we use our novel phylogenomic probeset (FrogCap; > 14,000 loci, with all resources and analysis pipelines freely available in the public domain; Hutter et al. 2019) to reconstruct the phylogeny of the Ranoidea and reevaluate the relationships of the Indian paleoendemic families in relation to all other families in Ranoidae—with the goal of stabilizing relationships towards future downstream analyses, plus increasing transparency in the process.

Methods

Probe design:

Probe design follows Hutter et al. (2019) and is summarized as follows. Probes were synthesized as biotinylated RNA oligos in a myBaits kit (Arbor Biosciences™, formerly MYcroarray® Ann

Arbor, MI) by individually matching 25 publicly available transcriptomes to the *Nanorana parkeri* and *Xenopus tropicalis* genomes using the program BLAT 3.50 (Kent, 2002). Matching sequences were clustered by their genomic coordinates to detect presence/absence across species and to achieve full locus coverage. To narrow the locus selection to coding regions, each cluster was matched to available coding region annotations from the *Nanorana parkeri* genome using the program EXONERATE (Slater and Birney, 2005). Loci from all matching species were then aligned using MAFFT 7.313 (Katoh and Standley, 2013), and kept if they had at least three taxa and were at least 100 bp long. Markers were selected based on phylogenetic representation, informativeness, and other filters explained in Hutter et al. (2019). For each marker, we used the *N. parkeri* genome sequence as the chosen design marker. To create a .fasta file of bait sequences as individual entries, we separated the selected markers into 120 bp-long sequences with 2x tiling (50% overlap among baits) using an R script. These markers have an additional bait at each end extending into the intronic region to increase the coverage and capture success of these areas. Baits were then filtered, retaining those: without sequence repeats; a GC content of 30%–50%; and baits that did not match to their reverse complement or multiple genomic regions. Finally, we used the myBaits-2 kit (40,040 baits) with 120mer sized baits with our chosen filtered bait sequences.

Taxon sampling:

We extracted genomic DNA from a set of 62 individual frog species (17 from the Indian subcontinent of which 15 have never been included in a genomic dataset before) from 14 representative families of the Ranoidea with one outgroup taxon from Microhylidae. In order to finalize our choice of taxa, we consulted previously published phylogenies and included similar taxonomic coverage of the different amphibian families. We did not include the African families

of Hemisotidae, Conrauidae, Hyperoliidae and Odontobatrachidae, and no Indian paleoendemic family has been closely related to these families in any phylogeny so far (Table 1).

Library preparation and sequencing:

Library preparation was performed by Arbor Biosciences following the myBaits V3.1 manual and briefly follows: (1) genomic DNA was sheared to 300–500 bp; (2) adaptors were ligated to DNA fragments; (3) each library was amplified for 6 cycles using unique combinations of i7 and i5 indexing primers attached to the adapters to later identify individual samples; (4) biotinylated 120mer RNA library baits were hybridized to the sequences; (5) target sequences were selected by adhering to magnetic streptavidin beads; (6) Enrichment incubation times ranged 18–21 hours; (7) target regions were amplified via PCR for 10 cycles; and (8) samples were pooled and sequenced on an Illumina HiSeq PE-3000 with 150 bp paired-end reads. Sequencing was performed at the Oklahoma Medical Research Foundation DNA Sequencing Facility.

Bioinformatics:

The bioinformatics pipeline for filtering adapter contamination, assembling markers, trimming, and exporting alignments are available on GITHUB, using version 2 of the pipeline (https://github.com/chutter/FrogCap-Sequence-Capture). Adapter contamination and other sequencing artefacts were filtered from raw reads using the program AFTERQC (Chen et al., 2017). Paired-end reads were merged using the program BBMerge (Bushnell et al., 2017), which avoids inflating coverage for these regions due to uneven lengths from cleaning (Zhang et al., 2014). The cleaned reads were then assembled de novo using the program SPADES v.3.12 (Bankevich et al., 2012) under a variety of k-mer schemes. SPADES also has built-in error correction, so error correction was not performed prior to assembly. The contigs were then

matched against the reference probe sequences with BLAT 3.50, keeping only those contigs that uniquely matched to the probe sequences. The final set of matching loci was then aligned on a locus-by-locus basis using MAFFT 7.313 using the algorithm L-INS-i.

We externally trimmed alignments using a custom R script, where at least 50 percent of the samples must have sequence data present externally, with at least three taxa per alignment. The alignments were saved separately into usable datasets for phylogenetic analyses and data type comparisons: (1) Introns: the exon previously delimited was trimmed out of the original contig and the two remaining intronic regions were concatenated; (2) Exons: each alignment was adjusted to be in an open-reading frame and trimmed to the largest reading frame that accommodated >90% of the sequences, alignments with no clear reading frame were discarded.

Phylogeny:

We concatenated our all-markers dataset (exons+introns), which had 12,824 loci, 5,767,383 nucleotide characters, and 3,119,940 parsimony-informative sites. We estimated phylogenetic relationships with Maximum Likelihood (ML) and Species Tree Summary (STS) procedures. The ML analysis was conducted with IQ-TREE v1. (Nguyen et al., 2015), and data were partitioned by gene, and the best-fit substitution model for the entire dataset was determined using ModelFinder (Kalyaanamoorthy et al., 2017). To assess nodal support, we performed 1000 ultrafast bootstrap support (Minh et al., 2013), and we adopted 95% as the percentage of bootstrap proportions considered to be strong support. We rooted the tree with the distantly-related Indian microhylid frog (AmphibiaWeb, 2020) *Uperodon triangularis*. For the STS analysis, we first estimated gene trees for each marker using IQ-TREE (same settings as above). We then used ASTRAL-III (Zhang et al., 2018) to estimate a species tree using default settings.

Biogeography:

We used BioGeoBEARS (Matzke, 2014), which implements user-specified Ancestral Range Estimation models from which the probability that each node and internal branch in a phylogeny occupies a given state (geographic range) can be estimated. Biogeographic stochastic mapping (Dupin et al. 2016) uses stochastic simulations based on the phylogeny and the specified ARE model and parameters to assign states to internal branches. We performed the ancestral range reconstruction analysis under six possible biogeographic range evolution models: the (1) Dispersal-Extinction-Cladogenesis (DEC), (2) DEC + *j*, (3) DIVALIKE, (4) DIVALIKE + *j*, (5) BAYAREALIKE and (6) BAYAREALIKE + *j* models, which differ in the types of range evolution processes that can occur during cladogenesis (Matzke 2013, 2014). The DEC model allows either vicariance or subset (partial sympatry) speciation if one of the daughter lineages has a narrow (i.e., a single area) range. The DIVALIKE model allows vicariant speciation even if both daughter lineages have widespread ranges, but sympatric speciation is prevented unless the ancestor occupies a single area. The BAYAREALIKE model does not allow range evolution to occur during cladogenesis. The models DEC + *j*, DIVALIKE + *j* and BAYAREALIKE + *j* allow founder speciation, whereby one daughter lineage acquires a narrow range not occupied by the ancestor, and range evolution processes allowed by DEC, DIVALIKE and BAYAREALIKE models, respectively (Matzke, 2013, 2014). All biogeographic models were conducted on an ultrametric version of our ML phylogeny, created using the *force.ultrametric* function of the Phytools R package (Revell et al., 2012). Geographic regions used for biogeographic analyses included Africa, Madagascar, the Indian subcontinent, Indochina, Sundaland, the Philippines, and Oceania (Fig. 2; inset).

Results

Phylogeny:

Even with the omission of four African families, we recovered a monophyletic Ranoidea, with Bootstrap Support/BS=100 (Fig. 1). The non-African Ranoid families formed a pectinate topology. The Mantellidae of Madagascar, was found to be reciprocally monophyletic with (sister to) the Asian Rhacophoridae. Together, the clade comprising these two families, is sister to the large family Ranidae. These three families, together, are sister to Dicroglossidae, albeit with weak support (BS=76). The three Indian paleoendemic families of Micrixalidae, Nyctibatrachidae and Ranixalidae formed a monophyletic, strongly-supported clade (BS=100); this Indian paleoendemic clade is sister to the Mantellidae + Rhacophoridae + Ranidae + Dicroglossidae clade and, together, all of these are the strongly-supported (BS=97) sister group to Ceratobatrachidae (Fig. 1).

The placement of the 17 species from the Indian subcontinent were as follows: *Fejervarya keralensis* and *Sphaerotheca dobsoni* were recovered within the Dicroglossidae; *Clinotarsus curtipes*, *Hydrophylax malabarica*, and *Indosylvirana flavescens* in Ranidae; *Ghatixalus variabilis, Rhacophorus malabaricus, Beddomixalus bijui, Pseudophilautus amboli*, and *Raorchestes theurkaufi* in Rhacophoridae. The *Nyctibatrachus, Micrixalus*, and *Indirana* species were recovered in their respective families of Nyctibatrachidae, Micrixalidae and Ranixalidae respectively, with strong support (BS=100; Fig. 1).

Our combined species tree (from 2339 gene trees) revealed the same topology with the monophyletic Indian paleoendemic clade, albeit with discordance along the backbone of the tree (Fig. 2).

Biogeography:

The ancestral-range reconstruction analyses, based on model selection with six models under consideration (Matzke, 2014), varied little when comparing reconstructions based on these six alternatives. The one exception was the results of ancestral range estimates under the BAYAREALIKE model (not shown; inferred to be sub-optimal to DEC). Our results from the other five models, including the ones accounting for long-distance ("jump") dispersal events, suggest that ancestral origins of all non-African ranoids was the Indian subcontinent. Model selection for an optimal ancestral range reconstruction indicated that our data are best explained by either a DEC + *j* model (LnL = -130.2 and AIC = 266.4; Table 2) or a DIVALIKE + *j* (LnL = -130.2 and AIC = 266.3). These two models, both including the *j* parameter received essentially same likelihood values, and lowest AIC scores but together, these two models were substantially preferred over their equivalents without the long-distance dispersal parameter (Table 2). If interpreted literally, our selection of the DEC + *j* model would suggest that founder-event speciation (i.e., inclusion of the jump-dispersal parameter *j*), should be considered when interpreting biogeographical patterns of range evolution among non-African Ranoidea, in addition to other processes (e.g., vicariance, dispersification; Lomolino et al., 2011; de Queiroz, 2015; Chan & Brown, 2017) traditionally-considered on the temporal/geographic scale of ancient continental radiations (Matzke 2013b). Nevertheless, we unambiguously identify a single common ancestor for all Indian paleoendemic frog families and they are tentatively consistent with, an increased support for, a possible interpretation that many, possibly all, non-African ranoid frog lineages could have originated on the rafting Indian subcontinent before or just as, it collided with Eurasia (Fig. 3).

Discussion

Recent phylogenomic estimates including frogs of the the superfamily Ranoidea have recovered non-African, Asian groups as monophyletic (Hime et al., 2020; Yuan et al., 2018) which is not surprising given earlier, Sanger-based phylogenetic studies with broad, comprehensive sampling (Bossyut et al., 2006; Wiens et al., 2009; Pyron & Wiens 2011; Chan & Brown, 2017). However, these studies did not include all the three paleoendemic Indian families (most previous studies included either one or two). Our topological results were most similar to Hime et al. (2020), albeit the exclusion of Micrixalidae and Ranixalidae in that study; in the absence of these two families, Hime et al. (2020) recovered Nyctibatrachidae as sister to Ceratobtrachidae. Similarly, Yuan et al. (2018) recovered Nyctibatrachidae and Ranixalidae as sister taxa and, together, nested in a clade containing all other Asian families. Thus, our novel finding of a single, strongly-supported clade, containing all three paleoendemic families, to the exclusion of all Asian ranoids, would appear to be unique in the sense both (1) the only study to date with comprehensive taxon-sampling for Indian-endemic frog families and (2) a first application of phylogenomics to the study of the evolutionary relationships of Indian paleoendemic frogs using known locality genetic resources, properly vouchered specimens, and legally sampled material.

In some aspects, our ancestral-range reconstruction is consistent with a previously-popularized "Out-of-India" interpretation (Bossuyt & Milinkovitch, 2001; Bossyut et al. 2006; Weins et al., 2009; Yuan et al., 2018). This so-called "ferry India" model (Bossuyt & Milinkovitch, 2001; Yuan et al., 2018), would suggest that a single common ancestral lineage may have originated on the Indian subcontinent, after this continental fragment broke free from Africa and Madagascar (a possible continental vicariant event, associated with the separation of Asian versus African ranoids; i.e., contrary to an alternative involving a series of multiple stepping-stone bouts of dispersal from Africa to India to Asia). Certainly, our novel, strongly-

supported monophyletic lineage of Indian paleoendemic frog families is likely to have originated on the rafting Indian subcontinent—given its age, and apparent restriction to India, this seems uncontroversial. Whether all non-African ranoid frog lineages exclusively originated on the Indian raft—and to what extent did they diversify on India during this period of isolation—are additional questions, each of which must be addressed carefully, and with full consideration of the uncertainty associated with constituent assumption (temporal framework, topological uncertainty, divergence date estimation, paleogeographic reconstruction, etc.), Nevertheless, the monophyly of the three paleoendemic Indian taxa, contrary to previous phylogenies (Bossuyt & Milinkovitch, 2001; Roelants et al., 2007; Yuan et al., 2018), which suggested polyphyletic relationships with various African and Asian groups, is a finding that likely will impact a more nuanced, and complete, eventual understanding of the biogeographical history of Indian paleoendemic frog lineages. However, caution must be taken with regard to interpretation of biogeographical analyses, given phylogenetic (topological and temporal) uncertainty (Ho & Phillips, 2009), paleo-reconstructions (Briggs, 2003; Chatterjee et al., 2013) widely-acknowledged, and currently unresolved analytical problems with the implementation of the long-distance dispersal parameter ("*j*" parameter) in model-selection-based biogeographical inference (Ree & Sanmartín, 2018), and our own lack of strong support at key nodes of interest (e.g., uncertain placement of Ceratobatrachidae and Dicroglossidae [for which the biogeography results could also probably have been biased by the inclusion of largely Indian taxa and much less of contemporary Asian/Southeast Asian taxa]; Fig. 1).

With complete phylogenomic data, for all Indian paleoendemic frog families, now available and soon to be in the public domain, we have taken one step closer to a complete realization of the characterization of a remarkable period in Earth's history, tied to our understanding the

evolutionary of early frog diversification, and a controversial, but nevertheless classic, biogeographic hypothesis.

References

AmphibiaWeb (2020). Electronic database accessible at: https://amphibiaweb.org (accessed 02 November 2020). University of California, Berkeley, CA, USA.

Bankevich, A., Nurk, S., Antipov, D., Gurevich, A. A., Dvorkin, M., Kulikov, A. S., Lesin, V.M., Nikolenko, S.I., Pham, S., Prjibelski, A.D., & Pyshkin, A. V. (2012). SPAdes: a new genome assembly algorithm and its applications to single-cell sequencing. Journal of Computational Biology, 19(5), 455-477.

Bossuyt, F., & Milinkovitch, M. C. (2000). Convergent adaptive radiations in Madagascan and Asian ranid frogs reveal covariation between larval and adult traits. Proceedings of the National Academy of Sciences, 97(12), 6585-6590.

Bossuyt, F., & Milinkovitch, M. C. (2001). Amphibians as indicators of early tertiary" out-of-India" dispersal of vertebrates. Science, 292(5514), 93-95.

Bossuyt, F., Brown, R. M., Hillis, D. M., Cannatella, D. C., & Milinkovitch, M. C. (2006). Phylogeny and biogeography of a cosmopolitan frog radiation: Late Cretaceous diversification resulted in continent-scale endemism in the family Ranidae. Systematic Biology, 55(4), 579-594.

Briggs, J. C. (2003). The biogeographic and tectonic history of India. Journal of Biogeography, 30(3), 381-388.

Bushnell, B., Rood, J., & Singer, E. (2017). BBMerge–accurate paired shotgun read merging via overlap. PloS One, 12(10), e0185056.

Chan, K. O., & R. M. Brown. (2017). Did True Frogs 'dispersify'? Biology Letters 13:20179299:1–6. doi.org/10.1098/rsbl.2017.0299.

Chatterjee, S., Goswami, A., & Scotese, C. R. (2013). The longest voyage: tectonic, magmatic, and paleoclimatic evolution of the Indian plate during its northward flight from Gondwana to Asia. Gondwana Research, 23(1), 238-267.

Chen, S., Zhou, Y., Chen, Y., & Gu, J. (2018). fastp: an ultra-fast all-in-one FASTQ preprocessor. Bioinformatics, 34(17), i884-i890.

de Queiroz, A. (2014). The monkey's voyage: how improbable journeys shaped the history of life. Basic Books, New York, USA.

Duellman, W. E., & Trueb, L. (1994). Biology of Amphibians, John Hopkins Univ. Press, Baltimore, Maryland, U.S.A.

Dupin, J., Matzke, N. J., Särkinen, T., Knapp, S., Olmstead, R. G., Bohs, L., & Smith, S. D. (2017). Bayesian estimation of the global biogeographical history of the Solanaceae. Journal of Biogeography, 44(4), 887-899.

Feng, Y. J., Blackburn, D. C., Liang, D., Hillis, D. M., Wake, D. B., Cannatella, D. C., & Zhang, P. (2017). Phylogenomics reveals rapid, simultaneous diversification of three major clades of Gondwanan frogs at the Cretaceous–Paleogene boundary. Proceedings of the National Academy of Sciences, 114(29), E5864-E5870.

Frost, D. R., Grant, T., Faivovich, J., Bain, R. H., Haas, A., Haddad, C. F., De Sa, R.O., Channing, A., Wilkinson, M., Donnellan, S.C., & Raxworthy, C. J. (2006). The amphibian tree of life. Bulletin of the American Museum of natural History, 2006(297), 1-291.

Frost, D.R. 2020. Amphibian Species of the World 6.0: An Online Reference (accessed 20 October 2020). Electronic Database accessible at

http://research.amnh.org/herpetology/amphibia/index.html. American Museum of Natural History, New York, USA.

Ho, S. Y., & Phillips, M. J. (2009). Accounting for calibration uncertainty in phylogenetic estimation of evolutionary divergence times. Systematic Biology, 58(3), 367-380.

Hutter, C. R., Cobb, K. A., Portik, D., Travers, S. L., Wood, P. L., & Brown, R. M. (2019). FrogCap: A modular sequence capture probe set for phylogenomics and population genetics for all frogs, assessed across multiple phylogenetic scales. bioRxiv, 825307.

Kalyaanamoorthy, S., Minh, B. Q., Wong, T. K., von Haeseler, A., & Jermiin, L. S. (2017). ModelFinder: fast model selection for accurate phylogenetic estimates. Nature Methods, 14(6), 587-589.

Katoh, K., & Standley, D. M. (2013). MAFFT multiple sequence alignment software version 7: improvements in performance and usability. Molecular Biology and Evolution, 30(4), 772-780.

Kent, W. J. (2002). BLAT—the BLAST-like alignment tool. Genome Research, 12(4), 656-664.

Lomolino, M.V., Riddle, B.R., Whittaker, R.J. & Brown, J.H. (2010). Biogeography , Vol. , 4th Edn. Sinauer Associates, Sunderland, MA.

Marjanović, D., & Laurin, M. (2007). Fossils, molecules, divergence times, and the origin of lissamphibians. Systematic Biology, 56(3), 369-388.

Matzke, N. J. (2013a). BioGeoBEARS: BioGeography with Bayesian (and likelihood) evolutionary analysis in R Scripts. R package, version 0.2, 1, 2013.

Matzke, N. J. (2013b). Probabilistic historical biogeography: new models for founder-event speciation, imperfect detection, and fossils allow improved accuracy and model-testing. Frontiers of Biogeography, 5(4).

Matzke, N. J. (2014). Model selection in historical biogeography reveals that founder-event speciation is a crucial process in island clades. Systematic Biology, 63(6), 951-970.

Minh, B. Q., Nguyen, M. A. T., & von Haeseler, A. (2013). Ultrafast approximation for phylogenetic bootstrap. Molecular Biology and Evolution, 30(5), 1188-1195.

Nguyen, L. T., Schmidt, H. A., Von Haeseler, A., & Minh, B. Q. (2015). IQ-TREE: a fast and effective stochastic algorithm for estimating maximum-likelihood phylogenies. Molecular Biology and Evolution, 32(1), 268-274.

Pyron, R. A., & Wiens, J. J. (2011). A large-scale phylogeny of Amphibia including over 2800 species, and a revised classification of extant frogs, salamanders, and caecilians. Molecular Phylogenetics and Evolution, 61(2), 543-583.

Ree, R. H., & Sanmartín, I. (2018). Conceptual and statistical problems with the DEC+ J model of founder-event speciation and its comparison with DEC via model selection. Journal of Biogeography, 45(4), 741-749.

Revell, L. J. (2012). phytools: an R package for phylogenetic comparative biology (and other things). Methods in Ecology and Evolution, 3(2), 217-223.

Roelants, K., Jiang, J., & Bossuyt, F. (2004). Endemic ranid (Amphibia: Anura) genera in southern mountain ranges of the Indian subcontinent represent ancient frog lineages: evidence from molecular data. Molecular Phylogenetics and Evolution, 31(2), 730-740.

Roelants, K., Gower, D. J., Wilkinson, M., Loader, S. P., Biju, S. D., Guillaume, K., Moriau, L., & Bossuyt, F. (2007). Global patterns of diversification in the history of modern amphibians. Proceedings of the National Academy of Sciences, 104(3), 887-892.

Scott, E. (2005). A phylogeny of ranid frogs (Anura: Ranoidea: Ranidae), based on a simultaneous analysis of morphological and molecular data. Cladistics, 21(6), 507-574.

Slater, G. S. C., & Birney, E. (2005). Automated generation of heuristics for biological sequence comparison. BMC Bioinformatics, 6(1), 31.

Wells, K. D. (2010). The ecology and behavior of amphibians. University of Chicago Press.

Wiens, J. J. (2007). Global patterns of diversification and species richness in amphibians. The American Naturalist, 170(S2), S86-S106.

Zhang, J., Kobert, K., Flouri, T., & Stamatakis, A. (2014). PEAR: a fast and accurate Illumina Paired-End reAd mergeR. Bioinformatics, 30(5), 614-620.

Figures

Fig. 1. Phylogenomic topology of Ranoidea frog families inferred from IQTree analysis for 12,824 loci. The Paleoendemic families from the Indian subcontinent as the branches highlighted in red.

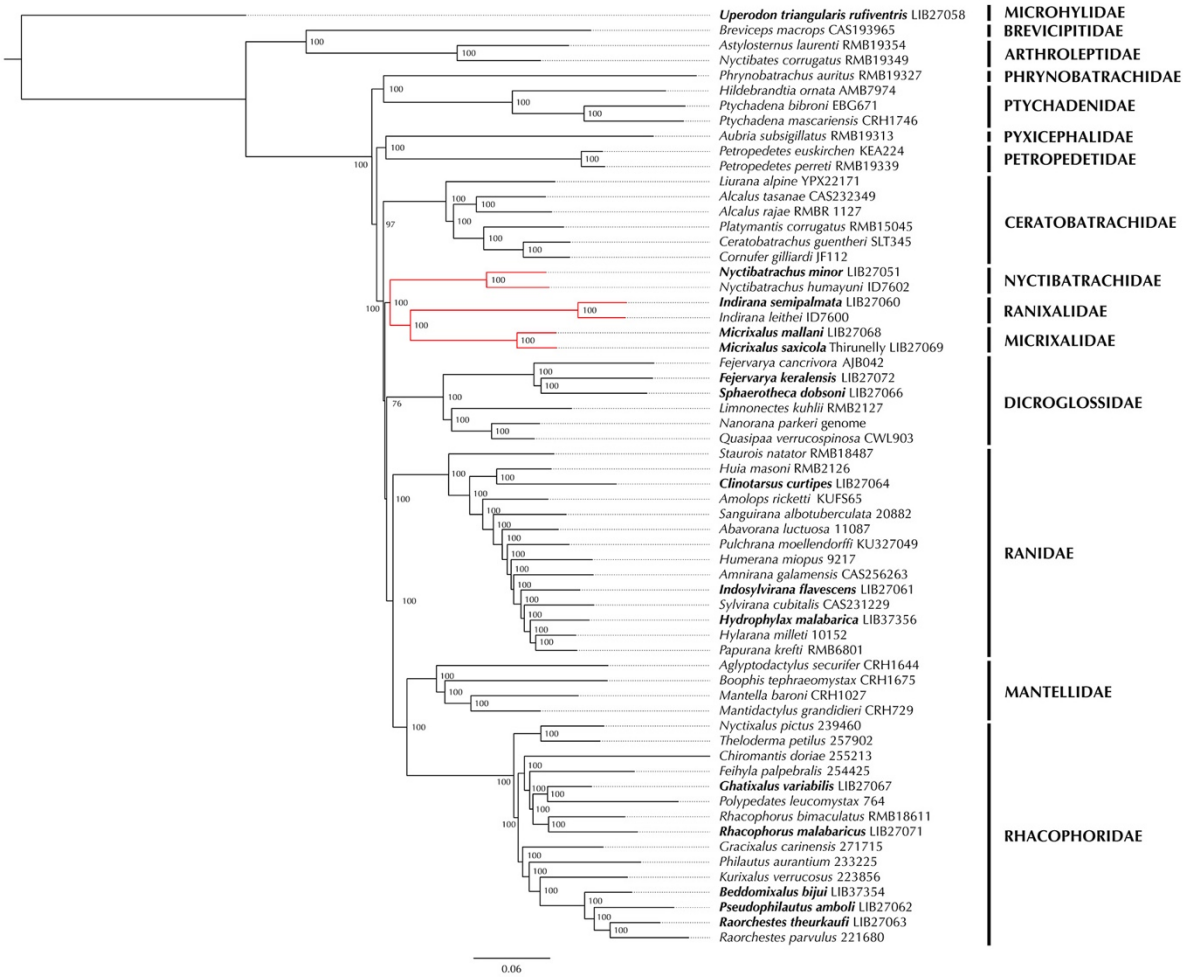

Fig. 2. Combined ML species tree topology for Afro-Asian Ranoidea with summary of conflicting and concordant homologs. The pie charts at each node present the fraction of homologs that supports that bipartition (orange), the fraction that supports the main alternative bipartition (blue), the fraction that supports other alternative bipartitions (green).

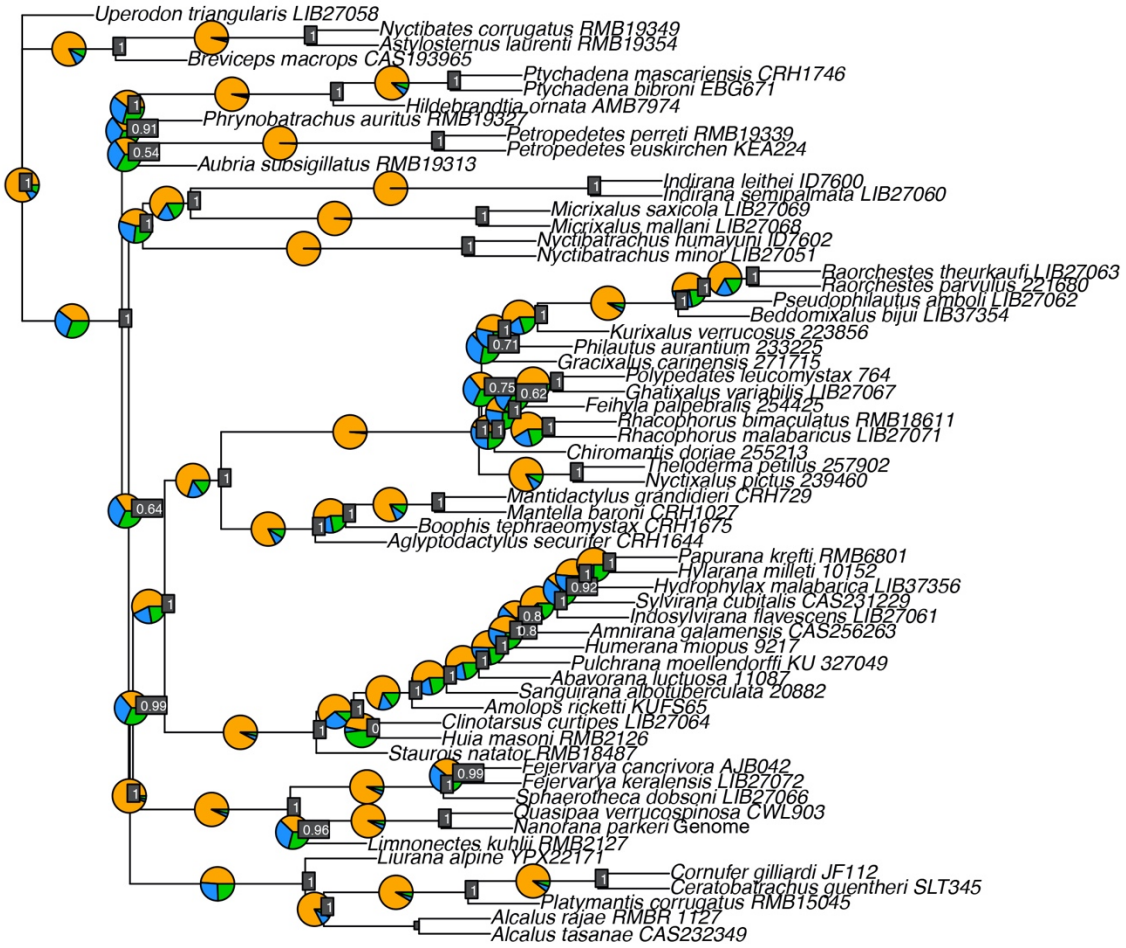

Fig. 3. Ancestral range reconstruction of Afro-Asian Ranoidea under the best-fitted DEC + *j* model. Colors correspond to the coded geographic states listed in the legend and inset map.

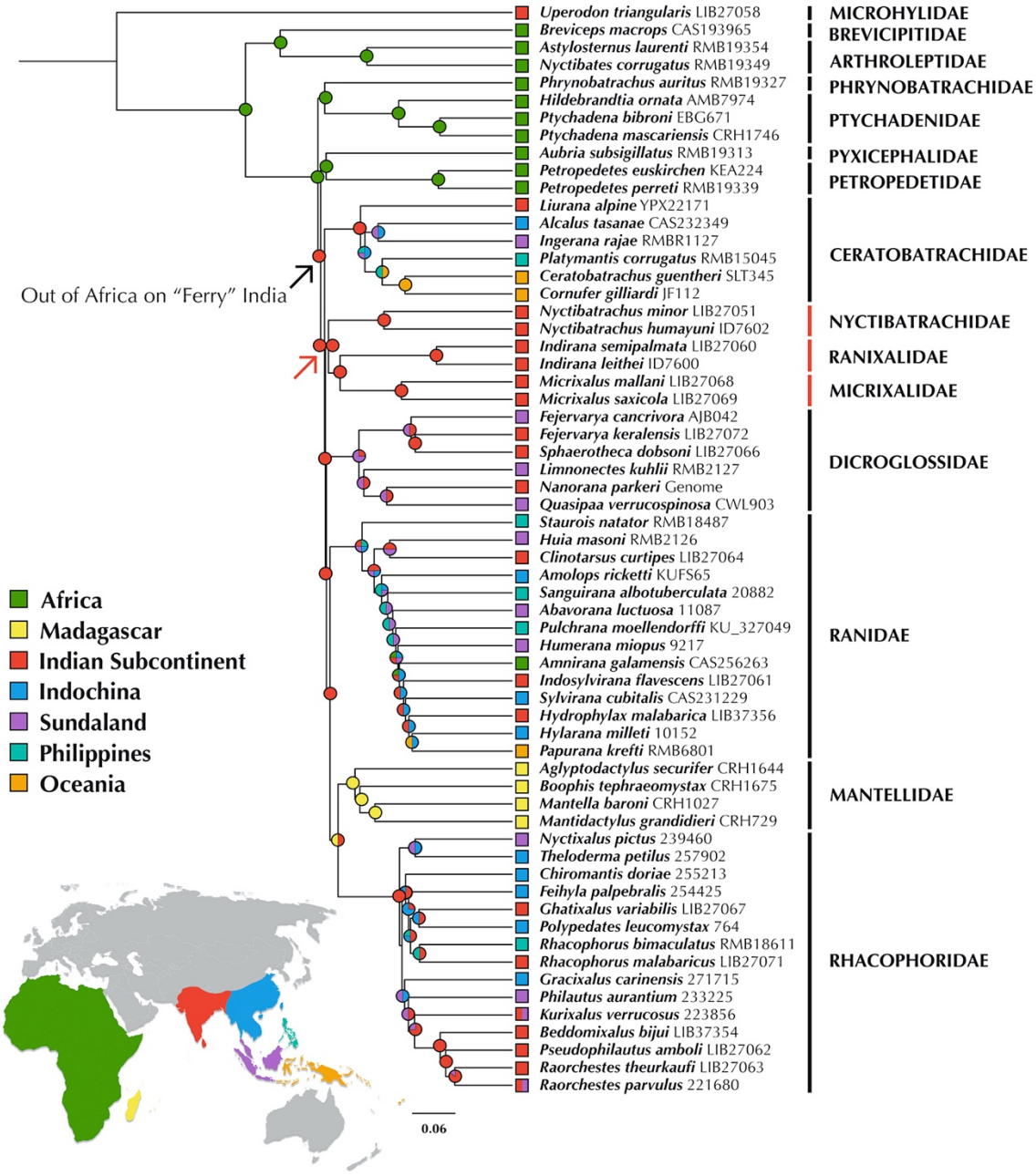

Table 1. List of species included in this study, and the biogeo regions they belong to.

Family	Species	Location	Biogeo Regions
Arthroleptidae	*Nyctibates_corrugatus*_RMB19349	West Africa	Africa
Brevicipitidae	*Breviceps_macrops*_CAS193965	Namibia, S. Africa	Africa
Petropedetidae	*Petropedetes_euskirchen*_KEA224	Cameroon, Eq. Guinea	Africa
Petropedetidae	*Petropedetes_perreti*_RMB19339	Cameroon	Africa
Phrynobatrachidae	*Phrynobatrachus_auritus*_RMB19327	West and Western South Africa	Africa
Ptychadenidae	*Ptychadena_bibroni*_EBG671	Northern & Central Africa	Africa
Ptychadenidae	*Hildebrandtia_ornata*_AMB7974	Africa	Africa
Pyxicephalidae	*Aubria_subsigillatus*_RMB19313	West Africa	Africa
Ranidae	Amnirana_galamensis_CAS256263	Africa	Africa
Ceratobatrachidae	*Liurana_alpina*_YPX22171	Southern Tibet	India
Dicroglossidae	*Nanorana_parkeri*_genome	Southern Tibet, Himalayas	India
Dicroglossidae	*Fejervarya_keralensis*_LIB27072	Southern Western Ghats	India
Dicroglossidae	*Sphaerotheca_dobsoni*_LIB27066	Western India	India
Micrixalidae	*Micrixalus_mallani*_LIB27068	Southern Western Ghats	India
Micrixalidae	*Micrixalus_saxicola*_LIB27069	Central Western Ghats	India
Microhylidae	*Uperodon_triangularis*_LIB27058	Central Western Ghats	India
Nyctibatrachidae	*Nyctibatrachus_humayuni*_ID7602	Northern Western Ghats	India
Nyctibatrachidae	*Nyctibatrachus_minor*_LIB27051	Southern Western Ghats	India
Ranidae	*Clinotarsus_curtipes*_LIB27064	Central & Southern Western Ghats	India
Ranidae	*Hydrophylax_malabarica*_LIB37356	Western India	India
Ranidae	*Indosylvirana_flavescens*_LIB27061	Central Western Ghats	India
Ranixalidae	*Indirana_leithei*_ID7600	Northern Western Ghats	India
Ranixalidae	*Indirana_semipalmata*_LIB27060	Southern Western Ghats	India
Rhacophoridae	*Beddomixalus_bijui*_LIB37354	Southern Western Ghats	India
Rhacophoridae	*Ghatixalus_variabilis*_LIB27067	Central Western Ghats	India
Rhacophoridae	*Pseudophilautus_amboli*_LIB27062	Northern & Central Western Ghats	India
Rhacophoridae	*Raorchestes_theurkaufi*_LIB27063	Southern Western Ghats	India
Rhacophoridae	*Rhacophorus_malabaricus*_LIB27071	Western Ghats	India
Ceratobatrachidae	*Alcalus_tasanae*_CAS232349	Myanmar, Thailand	Indochina
Ranidae	*Amolops_ricketti*_KUFS65	China, Indochina	Indochina
Ranidae	*Hylarana_milleti*_10152	Indochina	Indochina
Ranidae	*Sylvirana_cubitalis*_CAS231229	Myanmar, Indochina	Indochina
Rhacophoridae	*Gracixalus_carinensis*_271715	Myanmar, Thailand	Indochina
Rhacophoridae	*Kurixalus_verrucosus*_223856	China, Myanmar	Indochina
Rhacophoridae	*Raorchestes_parvulus*_221680	Eastern India to Pen. Malaysia	Indochina
Rhacophoridae	*Feihyla_palpebralis*_254425	China, Indochina	Indochina

Rhacophoridae	*Theloderma_petilus*_257902	Southern China and Vietnam	Indochina
Rhacophoridae	*Chiromantis_doriae*_255213	NE India, Myanmar	Indochina, India
Rhacophoridae	*Polypedates_leucomystax*_764	Eastern India to S. E. Asia	Indochina, India
Dicroglossidae	*Quasipaa_verrucospinosa*_CWL903	Southern China and Vietnam	Indochina, India, Sundaland
Ranidae	*Humerana_miopus*_9217	Thailand, Malaysia	Indochina, Sundaland
Mantellidae	*Aglyptodactylus_securifer*_CRH1644	Madagascar	Madagascar
Mantellidae	*Boophis_tephraeomystax*_CRH1675	Madagascar	Madagascar
Mantellidae	*Mantella_baroni*_CRH1027	Madagascar	Madagascar
Mantellidae	*Mantidactylus_grandidieri*_CRH729	Madagascar	Madagascar
Ptychadenidae	*Ptychadena_mascariensis*_CRH1746	Madagascar, Mascarene Islands	Madagascar
Ceratobatrachidae	*Ceratobatrachus_guentheri*_SLT345	Solomon Islands	Oceania
Ceratobatrachidae	*Cornufer_gilliardi*_JF112	New Britain	Oceania
Ranidae	*Papurana_krefti*_RMB6801	Solomon Islands, New Ireland	Oceania
Ceratobatrachidae	*Platymantis_corrugatus*_RMB15045	Philippines	Philippines
Ranidae	*Pulchrana_moellendorffi*_KU_327049	Philippines	Philippines
Ranidae	*Sanguirana_albotuberculata*_20882	Philippines	Philippines
Ranidae	*Staurois_natator*_RMB18487	Philippines	Philippines
Rhacophoridae	*Rhacophorus_bimaculatus*_RMB18611	Philippines	Philippines
Ceratobatrachidae	*Cornufer_gilliardi*_JF112	Borneo	Sundaland
Dicroglossidae	*Limnonectes_kuhlii*_RMB2127	Java, Indonesia	Sundaland
Ranidae	*Huia_masoni*_RMB2126	Java, Indonesia	Sundaland
Ranidae	*Abavorana_luctuosa*_11087	Pen. Malaysia, Borneo	Sundaland
Rhacophoridae	*Philautus_aurantium*_233225	Borneo	Sundaland
Rhacophoridae	*Nyctixalus_pictus*_239460	Western S. E. Asia	Sundaland
Dicroglossidae	*Fejervarya_cancrivora*_AJB042	Western S. E. Asia	Sundaland, Oceania

Table 2. Model schemes considered for BioGeoBEARS analyses with AIC scores.

Biogeographic Model	**i**	**likelihood**	**df**	**AIC**
DEC	0	-182.1	2	368.1
DEC + *j*	0	-130.2	3	266.4
DIVALIKE	0	-188.1	2	380.2
DIVALIKE + *j*	0	-130.2	3	266.3
BAYAREALIKE	0	-182.7	2	369.3
BAYAREALIKE + *j*	0	-132.3	3	270.7

Supplementary Files:

Supp. Fig. 1.

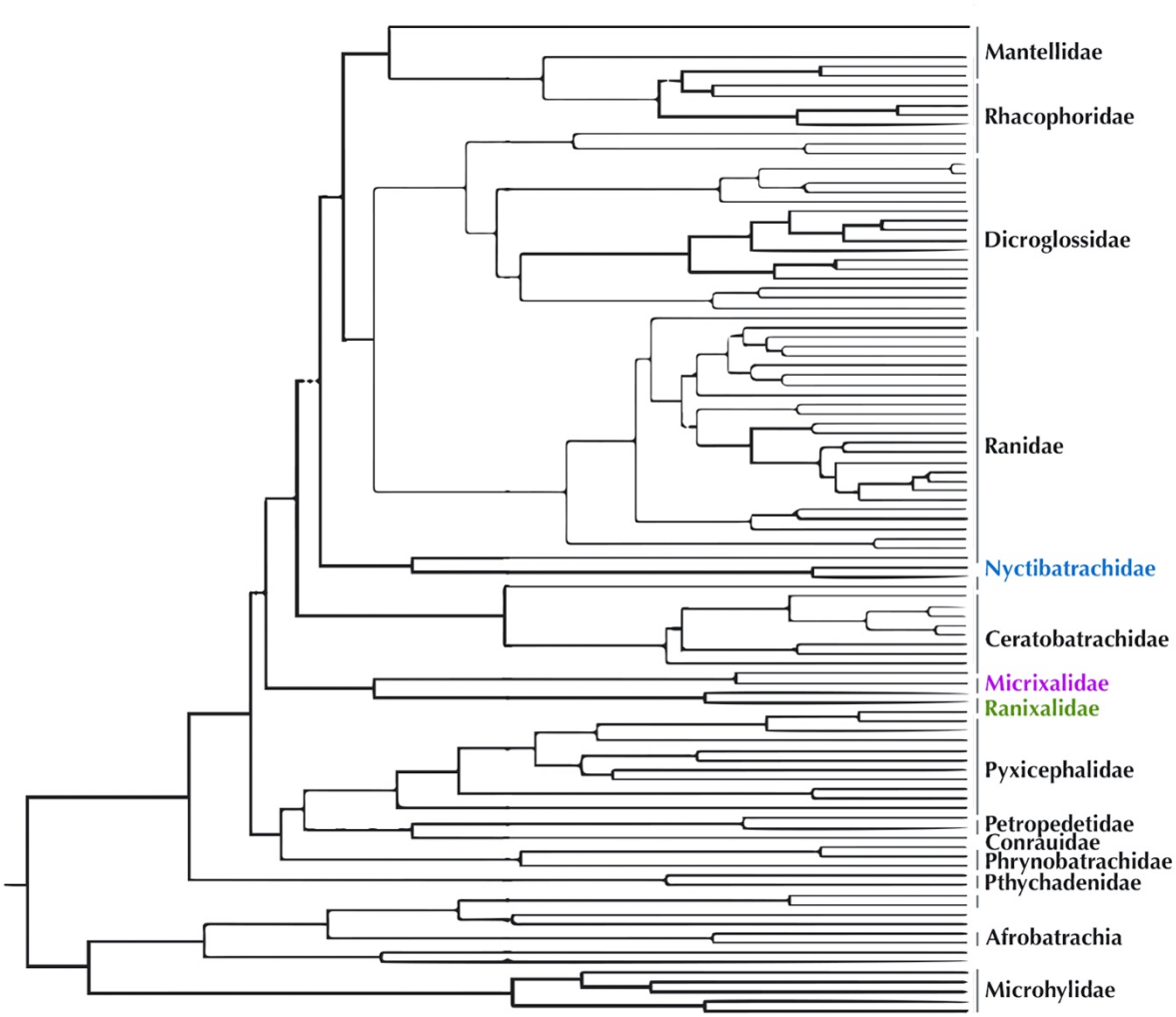

Supp. Fig. 2. ML tree (1 mitochondrial gene region + 4 nuclear loci) by Roelants et al. (2007)

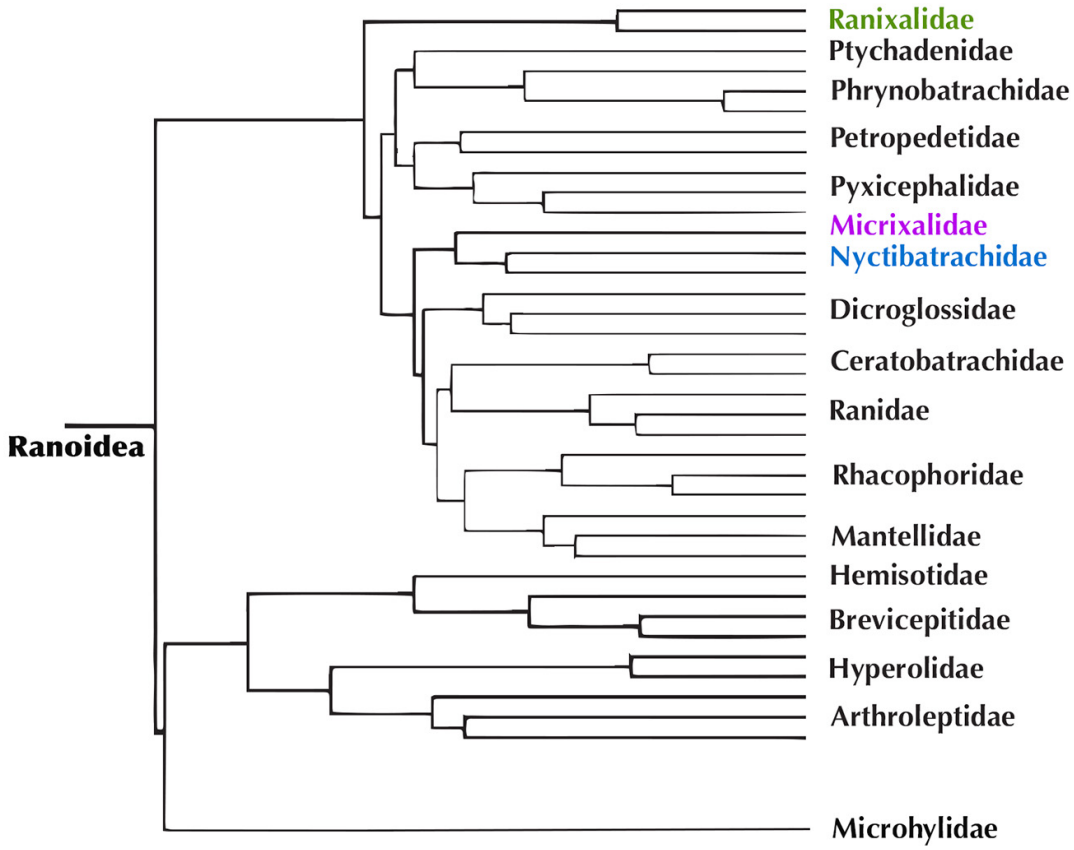

Supp. Fig. 3. ML tree (3 mitochondrial + 9 nuclear loci) by Pyron & Wiens (2011)

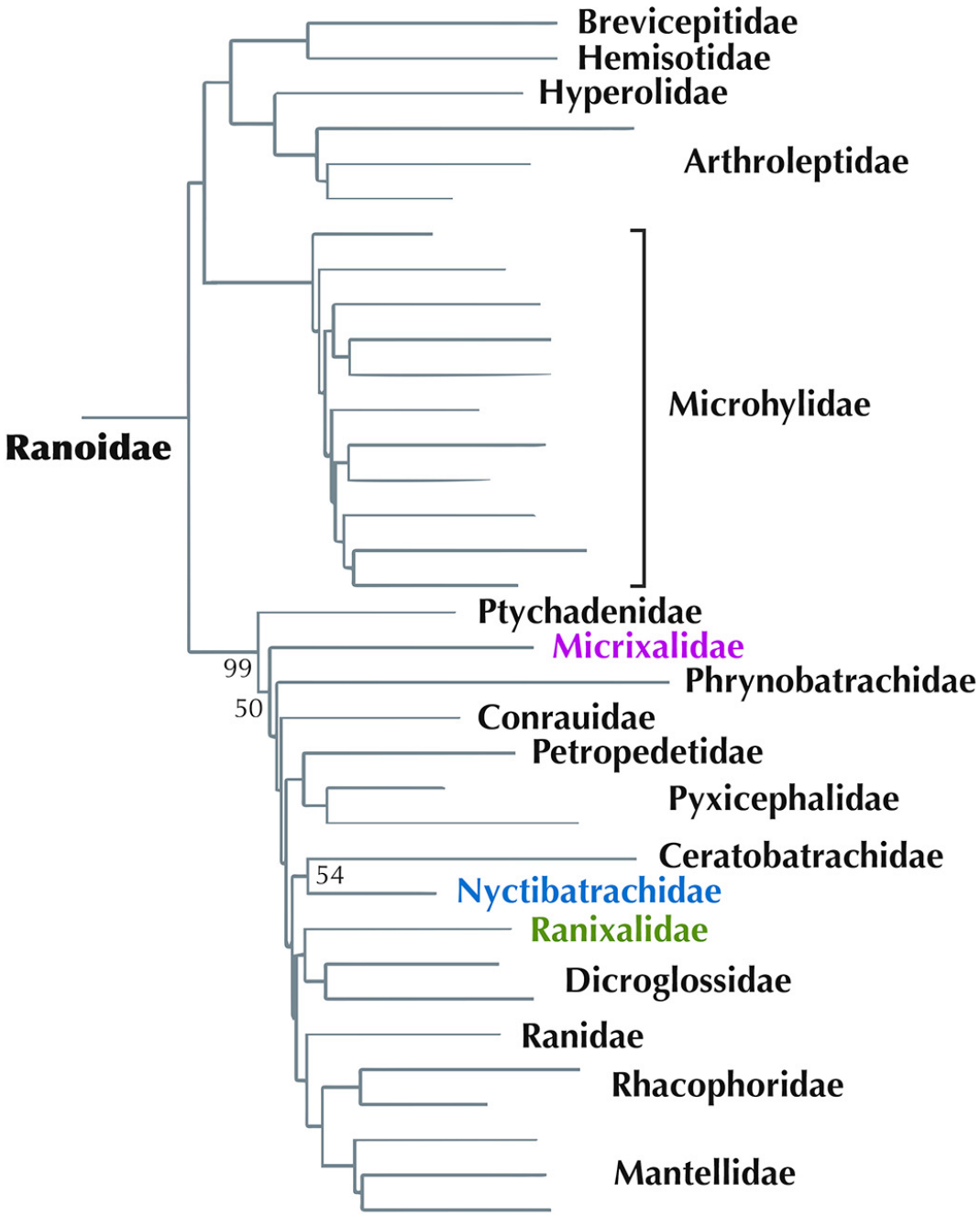

Supp. Fig. 4. Bayesian tree (97 nuclear loci) by Feng et al. (2017)

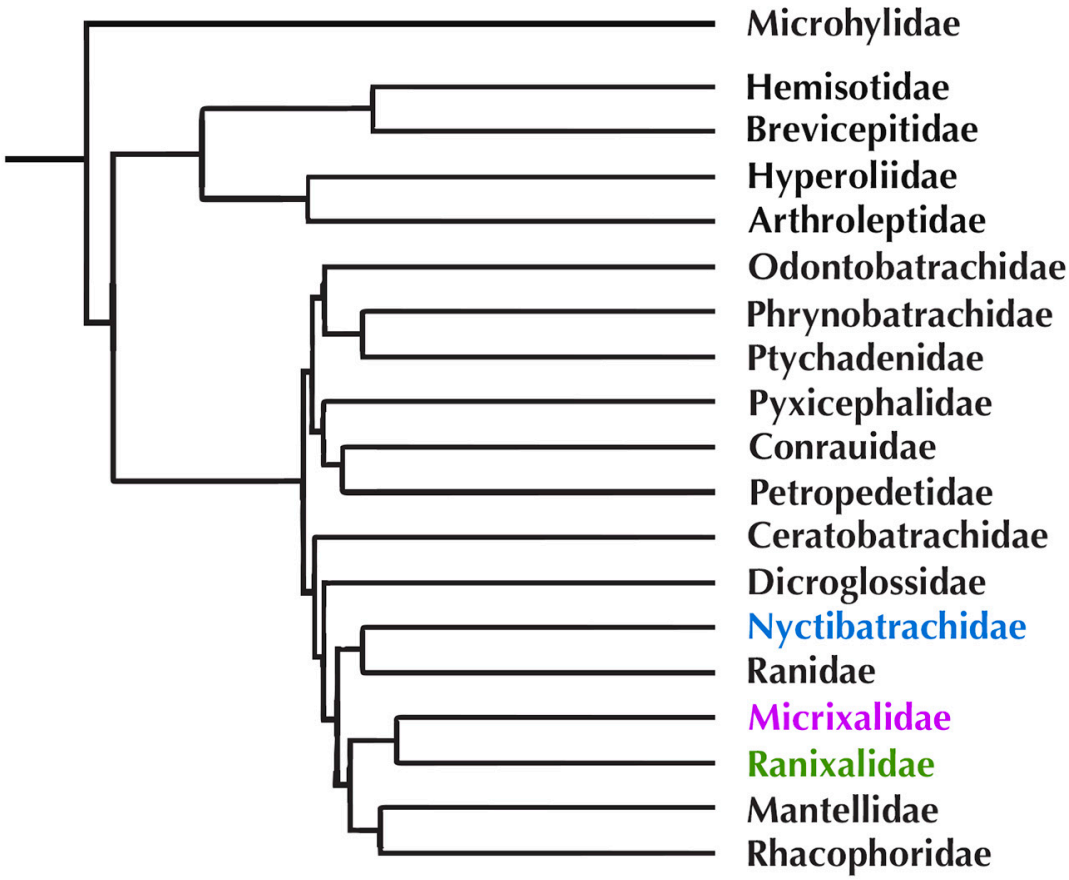

Supp. Fig. 5. Bayesian tree (5 mitochondrial gene regions + 10 nuclear loci) by Jetz & Pyron (2018)

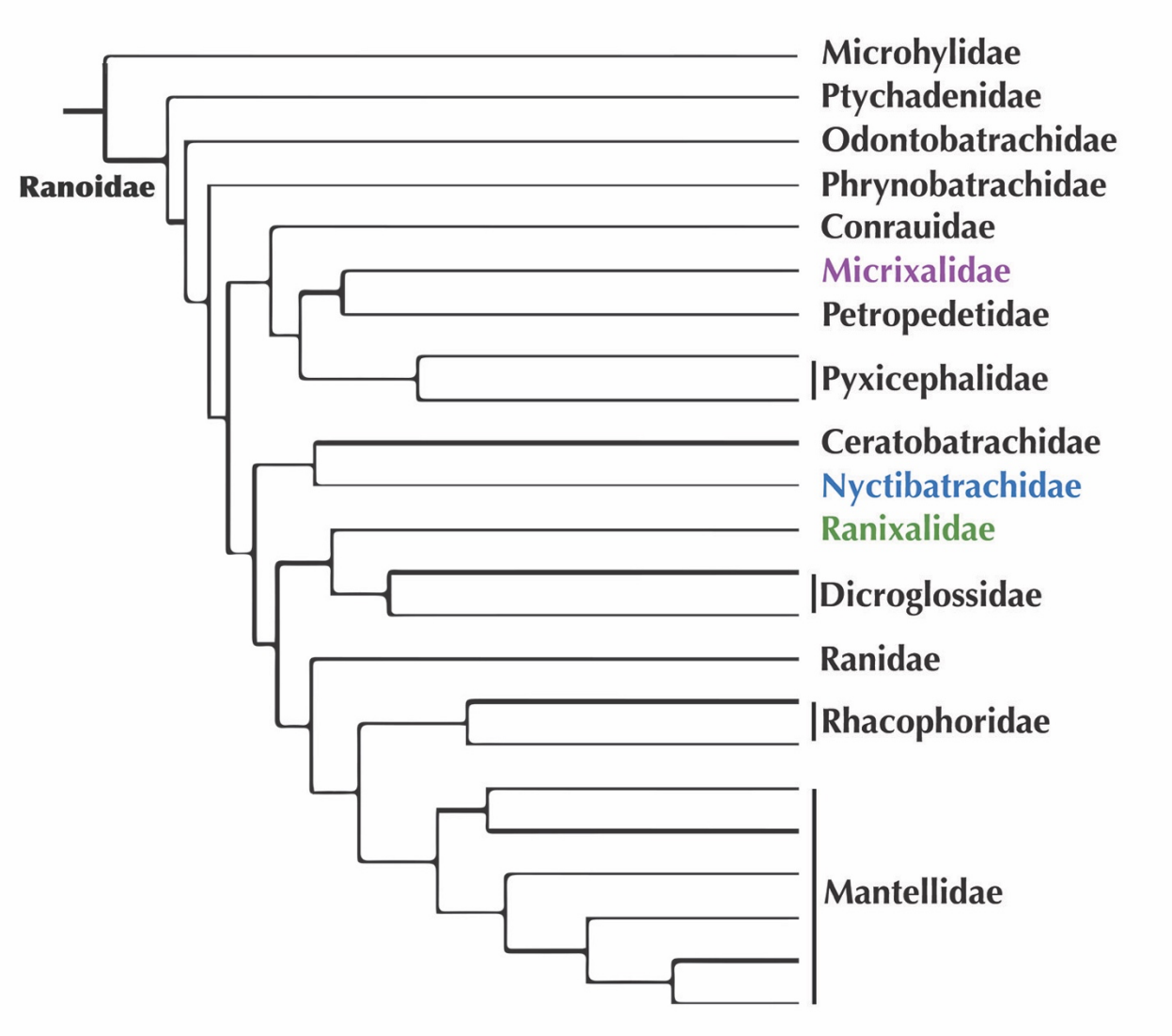

Supp. Fig. 6. Bayesian tree (376 Anchored Hybrid Enrichment loci) by Yuan et al. (2018)

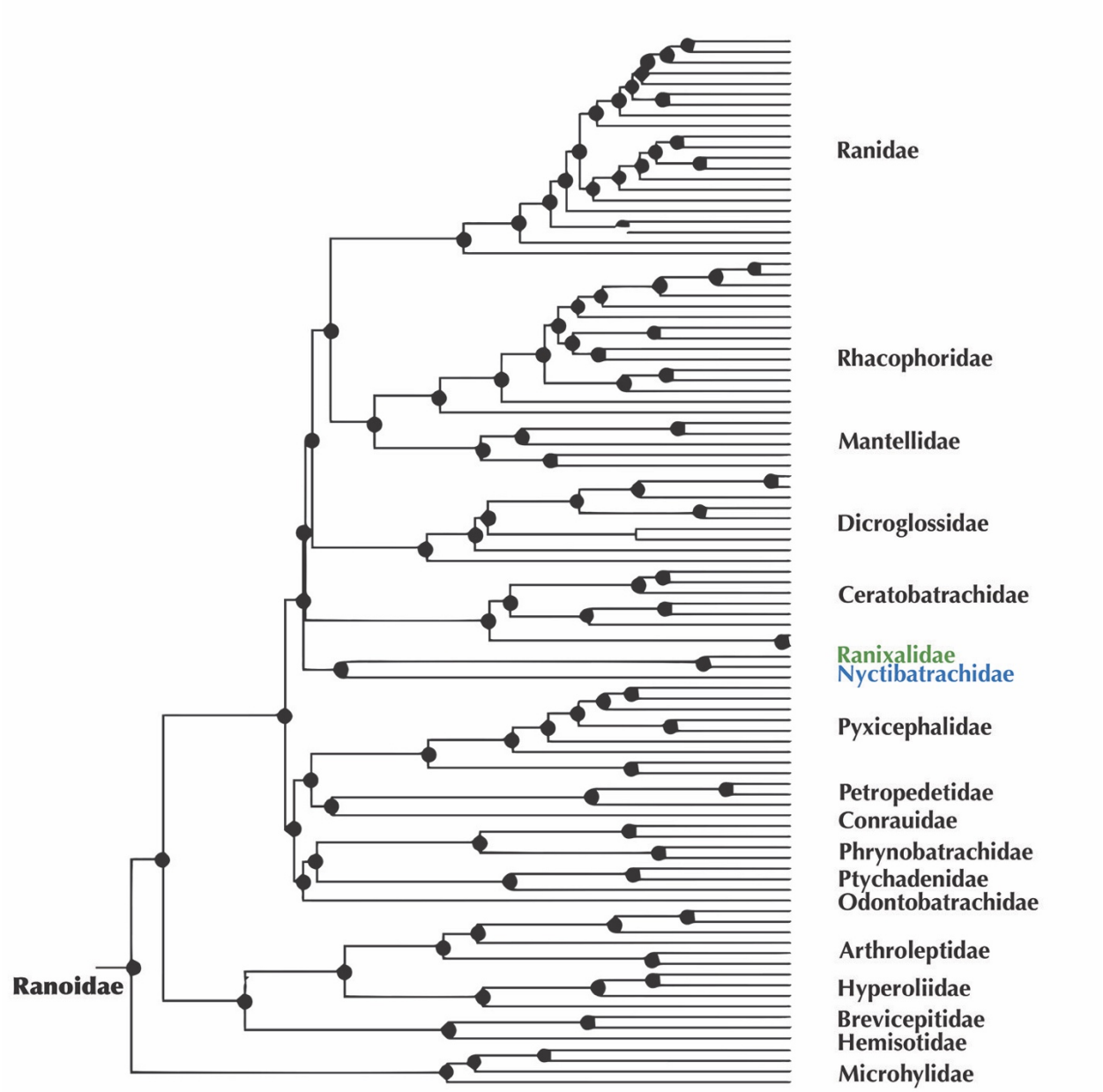

Supp. Fig. 7. Bayesian tree (220 Anchored Hybrid Enrichment) by Hime et al. (2020)

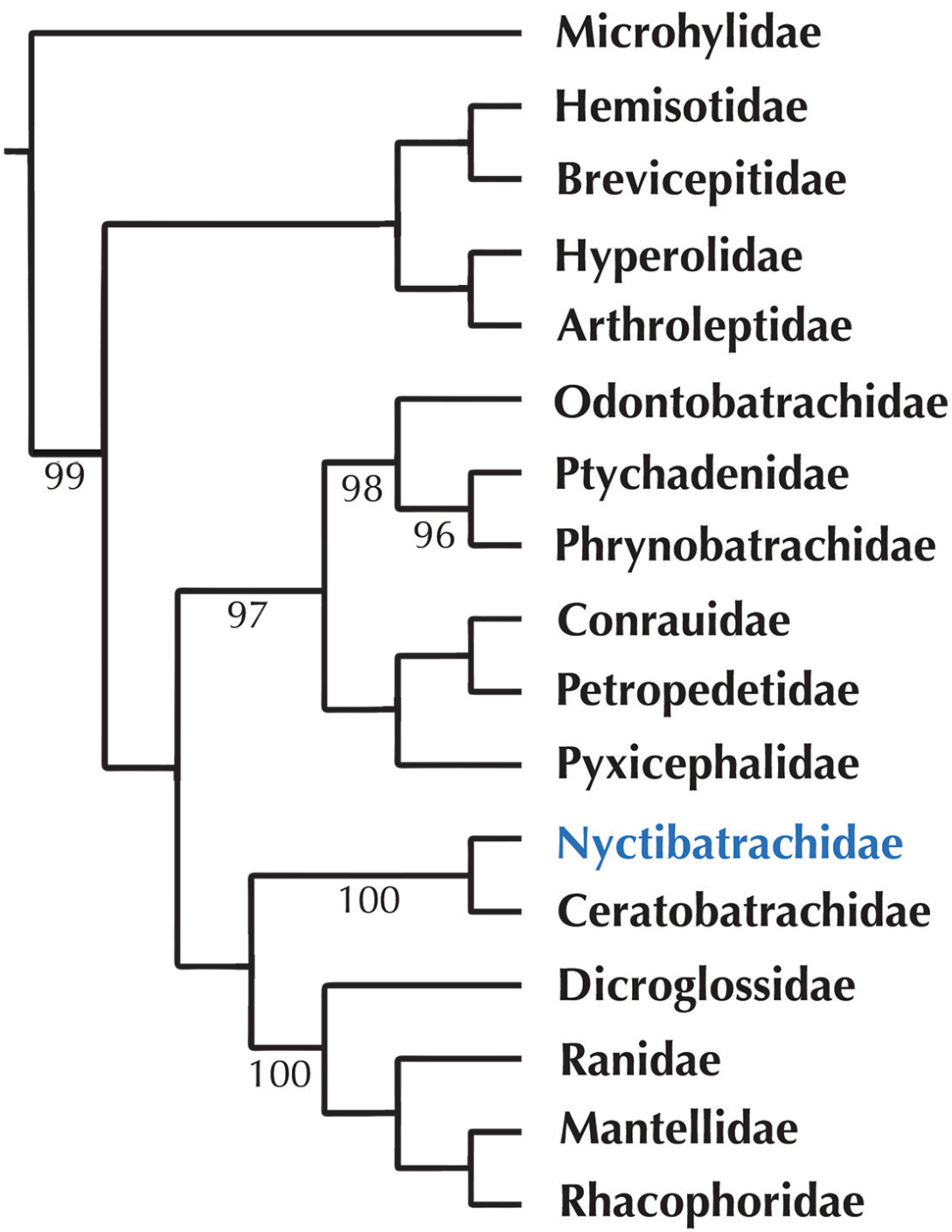

Conclusion

Species delimitation, and the identification of species boundaries, is a fundamental endeavour of biological sciences (von Humboldt, 1972; Darwin, 1859, Mayr, 1949, Simpson, 1951); the identification of operational taxonomic units we conceive as species is a "first-principles" discipline (Aristotle, Linnaeus), which is vital to our understanding of evolutionary and ecological processes (Jones et al., 2003; Jones & Taub, 2018; Lindberg & Shank, 2013; Mayr, 1982; Park et al., 2006; Toulmin, 1958). Because the manner and practice by which scientists recognize and describe biodiversity has shifted so substantially over the last several centuries (Linné, 1751; Günther, 1858; Dumeril & Bibron, 1844; Boulenger, 1898; Taylor, 1920; Inger, 1954; Leviton et al., 2018), reconsideration of those units, and the accumulated biodiversity, using powerful statistical approach to species delimitation (Carstens et al., 2013; De Queiroz, 2007), using data from across the genome, is both warranted and desirable. This work represents part of an exercise to explore species boundaries of currently-recognized species in two different insular systems; (1) the sky islands of India's Western Ghats, and (2) the Philippines archipelago in the Eastern Pacific Ocean. Both are heralded internationally as megadiverse biodiversity hotspots (Mittermeier et al., 2011), and both are badly overdue for objective, statistical reconsiderations of the resident vertebrate biodiversity—which is imperilled by a looming extinction crisis (Berridge et al., 2008; Zachos & Habel, 2011) but still misunderstood and under-studied (Bickford et al. 2007 vs Chan et al. 2020).

In this thesis, I demonstrate using different classes of data for these two different regions, in which currently-recognized species boundaries can be contested because of the piecemeal historical accumulation of species (AmphibiaWeb, 2020; Frost, 2020), differing taxonomic

practices and disparate systematic philosophies of the scientists who have worked on these faunas (Günther, 1858; Dumeril & Bibron, 1844; Boulenger, 1898; Taylor, 1920; Inger, 1954, Biju et al., 2011; Abraham et al., Chapters 1 and 2). As part of this exercise I have been able to perform a series of "Validation stage" analyses, which have the potential to redraw species boundaries in ways differing from historical demarcations (polytypic taxonomy; variable species concepts; biogeographical paradigm-based concepts) suggested by "Discovery stage" delimitation procedures or traditional taxonomy. Validation steps involved integrative approaches using phenotypic, ecological, larval, bioacoustics, and genomic (exploiting the data rich FrogCap protocol by Hutter et al. 2019) data. Among the Indian *Nyctibatrachus* frogs, for which 36 species had been formally described, this work has provided evidence that the number of species has been "taxonomically inflated" (Issac et al., 2014) by last-generation taxonomic practices, subjectivity, and taxonomic authority (opinion; Biju et al., 2011). I reject that notion that each sky island is host to isolated species; rather, my data demonstrate that each is part of a linear system, of continuous and connected populations of the same species. The group on which I focus is the *N. aliciae* clade, that comprises of four described species (Biju et al., 2011; Van Bocxlaer et al., 2012). I demonstrate that characters and their states, used by Biju et al (2011) to diagnose these taxa are subjective, overlapping in ranges, not at all discrete (but rather "binned" into subjective states/terms such as "small," medium," and "large"; Biju et al., 2011), and thus not truly diagnostic. I corroborate this initial finding with (1) comparable bioacoustic data from all proposed species in this clade, (2) comparable tadpole characters at a standardized Gosner Stage of development (Gosner, 1960), (3) amplectic reproductive behaviour, (4) additional genetic samples from intermediate geographical locations, and (5) similar environmental correlates.

For the Philippine archipelago, my evaluation of two different datasets, for two unrelated frog radiations revealed taxonomic inflation in one clade, but evidence for the existence of previously unrecognized diversity in another clade. The *Limnonectes magnus* group sensu lato of the Mindanao PAIC which included what was considered a high-elevation restricted species corresponding to the name *L. magnus* and a widespread low elevation undescribed species, in addition to two other species *L. diuatus* and *L. ferneri* restricted to other mountains on the island of Mindanao. My preliminary work involved an integration of Sanger sequencing derived phylogeny of four loci, a morphometric analysis for a densely sampled dataset of 161 specimens from multiple islands across the PAIC, and a reassessment of the taxonomy of the group, as part of a "Discovery-stage" analysis. This revealed the existence of two clades in a monophyletic arrangement; a lowland species across all the islands on the PAIC (true *L. magnus*) that exists as three haplogroups with shallow mitochondrial divergence (one of which is a haplotype clade restricted to the western island of Bohol), and a highland endemic *L. diuatus* (with *L. ferneri* being relegated a junior synonym of *L. diuatus*) with two haplogroups restricted to the mountains of Mindanao island. These two species clades were further substantiated by a concatenated mito+nucelar dataset of a subset of 18 specimens sampled from the larger dataset. However, the reassessment of the same subset of samples with genomic data as part of my "Validation-stage" genomic analysis confirmed the unique, isolated population of *L. magnus* on Bohol. Additionally, the two non-Bohol haplogroups recognized in the "Discovery-stage" procedure comprised of a non-admixed population restricted to the eastern islands of the PAIC and populations in the central and southern islands being the same genotype—albeit with a small proportion of admixture from the Bohol genotype. Also, I identified two separate genotype clusters in the *L. diuatus* clade, which conform to my results from morphometric analyses

(Abraham, Chapter 2). The distinct and isolated genotypes recovered in the validation step now warrant further investigation with additional morphological, acoustic, and larval traits, which could be utilized to assess their status as unique, species-level, biologically meaningful, independent evolutionary lineages.

For the Philippines *Pulchrana* dataset, I revisited the previously recognized pectinate topological arrangement of *P. grandocula* and *P. similis* of the eastern part of the archipelago with genomic data as a validation step. The resulting 14,000 loci data-based phylogeny reinforced the pectinate, nested relationship originally recognized by Brown & Siler's (2014) multilocus Sanger phylogeny, which attempted a preliminary validation step following Gunther (1873) and Taylor (1920)'s original descriptions of these two species. Additionally, two rare species *P. guttmani* (from southern Mindanao, which was described after the Brown & Siler (2014) phylogeny was published) and *P. melanomenta* (a species from Tawi-tawi island in the politically volatile Sulu archipelago, with few samples available) were also revisited with genomic data. Both taxa were found to be highly admixed in almost similar proportions, with admixture from other non-admixed *Pulchrana* species from both the Philippines and Borneo. This raises interesting questions as to whether these two entities are part of a single historically introgressed/admixed hybrid species, or if unstudied selective forces have allowed them to persist at high elevations in one case (*P. guttmani*) and as a small isolated island endemic in another (*P. melanomenta*).

Finally, I used a 12,824 loci dataset to construct a phylogeny for Asian frog families of the superfamily Ranoidea, which included the paleoendemic Indian family Micrixalidae (for which genomic data had never been published before). The resulting topology show for the first time that all three Indian paleoendemic families form a monophyletic clade, a finding contrary to all

previously published, non-genomic phylogenetic estimates that included all three Indian families. In addition, I also generated a phylogeny from the same FrogCap dataset sampled 31 out 36 described species, which agreed with published phylogenies (Van Bocxlaer et al., 2012; Garg et al., 2017). With this confirmation, my goal now is to densely sample across populations of each proposed sky island species, to perform phylogenomic analyses, which have the potential to reveal artifacts of admixture and introgression, reticulation, retained ancestral polymorphisms, or other early evolutionary events and processes, that may illuminate such phenomena on the endemic Indian taxa for the first time—while simultaneously excising subjectivity, opinion, and 1800 century traditions of "authority" from future studies characterizing biodiversity of the Indian Subcontinent.

References

AmphibiaWeb (2020). Electronic database accessible at: https://amphibiaweb.org (accessed 02 November 2020). University of California, Berkeley, CA, USA.

Berridge, R. J., Ramani, P., & Young, B. E. (2008). Threatened amphibians of the world. Lynx Editions.

Bickford, D., Lohman, D. J., Sodhi, N. S., Ng, P. K., Meier, R., Winker, K., Ingram, K.K., & Das, I. (2007). Cryptic species as a window on diversity and conservation. Trends in Ecology & Evolution, 22(3), 148-155.

Biju, S. D., I. Van Bocxlaer, S. Mahony, K. P. Dinesh, C. Radhakrishnan, A. Zachariah, V. Giri, & F. Bossuyt. (2011). A taxonomic review of the Night Frog genus *Nyctibatrachus* Boulenger, 1882 in the Western Ghats, India (Anura: Nyctibatrachidae) with description of twelve new species. Zootaxa 3029, 1-96.

Boulenger, G. A. (1898). Fourth Report on Additions to the Batrachian Collection in the Natural-History Museum 1. In Proceedings of the Zoological Society of London (Vol. 66, No. 3, pp. 473-482). Oxford, UK: Blackwell Publishing Ltd.

Brown, R. M., & Siler, C. D. (2014). Spotted stream frog diversification at the Australasian faunal zone interface, mainland versus island comparisons, and a test of the Philippine 'dual umbilicus' hypothesis. Journal of Biogeography, 41(1), 182-195.

Carstens, B. C., Pelletier, T. A., Reid, N. M., & Satler, J. D. (2013). How to fail at species delimitation. Molecular Ecology, 22(17), 4369-4383.

Chan, K. O., Hutter, C. R., Wood Jr, P. L., Grismer, L. L., Das, I., & Brown, R. M. (2020). Gene flow creates a mirage of cryptic species in a Southeast Asian spotted stream frog complex. Molecular Ecology, 29(20), 3970-3987.

Darwin, C. (1859). On the Origin of Species by Means of Natural Selection. London: John Murray.

De Queiroz, K. (2007). Species concepts and species delimitation. Systematic Biology, 56(6), 879-886.

Duméril, C., & Bibron, G. (1844). Erpétologie générale ou histoire naturelle complète des reptiles: comprenant l'histoire génerale des ophidiens, la description des genres et des espèces de serpents non venimeux. (Vol. 6). Imp. de Fain et Thunot.

Frost, D. R. 2020. Amphibian Species of the World: an Online Reference. Version 6.0. American 509 Museum of Natural History, New York, USA., Electronic Database accessible at 510 http://research.amnh.org/herpetology/amphibia/index.html.

Garg, S., Suyesh, R., Sukesan, S., & Biju, S. D. (2017). Seven new species of Night Frogs (Anura, Nyctibatrachidae) from the Western Ghats Biodiversity Hotspot of India, with remarkably high diversity of diminutive forms. PeerJ, 5, e3007.

Gosner, K. L. (1960). A simplified table for staging anuran embryos and larvae with notes on identification. Herpetologica, 16(3), 183-190.

Günther, A. C. (1858). Catalogue of the Batrachia Salientia in the Collection of the British Museum: By Albert CLG Günther. order of the Trustees.

Günther, A. C. L. G. (1873). Notes on some reptiles and batrachians obtained by Dr. Adolf Bernhard Meyer in Celebes and the Philippine Islands. Proceedings of the Zoological Society of London 1873, 165-172.

Hutter, C. R., Cobb, K. A., Portik, D., Travers, S. L., Wood, P. L., & Brown, R. M. (2019). FrogCap: A modular sequence capture probe set for phylogenomics and population genetics for all frogs, assessed across multiple phylogenetic scales. bioRxiv, 825307.

Inger, R. F. (1954). Systematics and zoogeography of Philippine Amphibia. Fieldiana Zoology, 33, 181-531.

Isaac, N. J., Mallet, J., & Mace, G. M. (2004). Taxonomic inflation: its influence on macroecology and conservation. Trends in Ecology & Evolution, 19(9), 464-469.

Jones, A., Shank, M. H., Bowler, P. J., Pickstone, J. V., & Livingstone, D. N. (2003). The Cambridge history of science: Volume 4, eighteenth-century science (Vol. 4). Cambridge University Press.

Jones, A., & Taub, L. (Eds.). (2018). The Cambridge History of Science: Volume 1, Ancient Science. Cambridge University Press.

Leviton, A. E., Siler, C. D., Weinell, J. L., & Brown, R. M. (2018). Synopsis of the snakes of the Philippines. Proceedings of the California Academy of Sciences, 64(14), 399-568.

Lindberg, D. C., & Shank, M. H. (2013). The Cambridge History of Science: Volume 2, Medieval Science. Cambridge University Press.

Linné, C. V. (1751). Philosophia botanica.

Mayr, E. (1949). The species concept: semantics versus semantics. Evolution, 3(4), 371-372.

Mayr, E. (1982). The growth of biological thought: Diversity, evolution, and inheritance. Harvard University Press.

Mittermeier, R. A., Turner, W. R., Larsen, F. W., Brooks, T. M., Gascon, C., Zachos, F. E., & Habel, J. C. (2011). Biodiversity hotspots: distribution and protection of conservation priority areas. Biodiversity Hotspots, 3-22.

Park, K., Daston, L., Lindberg, D. C., & Numbers, R. L. (2006). The Cambridge history of science (Vol. 3, p. 160). Cambridge: Cambridge University Press.

Simpson, G. G. (1951). The species concept. Evolution, 5(4), 285-298.

Taylor, E. H. (1920). Philippine Amphibia. Philippine Journal of Science 16, 213-359.

Toulmin, S. E. (1958). The philosophy of science (Vol. 14). Genesis Publishing Pvt Ltd.

Van Bocxlaer, I., Biju, S. D., Willaert, B., Giri, V. B., Shouche, Y. S., & Bossuyt, F. (2012). Mountain-associated clade endemism in an ancient frog family (Nyctibatrachidae) on the Indian subcontinent. Molecular Phylogenetics and Evolution, 62(3), 839-847.

Von Humboldt, A. (1872). Views of Nature: Or, Contemplations on the Sublime Phenomena of Creation. With Scientific Illustrations. G. Bell & Daldy.

Zachos, F. E., & Habel, J. C. (Eds.). (2011). Biodiversity hotspots: distribution and protection of conservation priority areas. Springer Science & Business Media.